Regulation of secondary compounds synthesis by photosynthetic organisms under stress

Parisa Heydarizadeh

Thèse de Doctorat

Parisa HEYDARIZADEH

Mémoire présenté en vue de l'obtention du
grade de Docteur de l'Université du Maine
sous le label de L'Université Nantes Angers Le Mans

École doctorale: *Végétal, Environnement, Nutrition, Alimentation, Mer*

Discipline: *Biologie des Organismes*
Spécialité: *Biologie, Biochimie Moléculaire et Cellulaire*
Unité de recherche: *Mer Molécules Santé*

Soutenue le *15 décembre 2015*
Thèse N: *(10)*

Regulation of secondary compounds synthesis by photosynthetic organisms under stress

JURY

Rapporteurs: **Fabrice FRANCK**, Professeur, Université de Liège
Jean-Paul CADORET, Managing Directeur, Greensea Biotechnologies

Examinateurs: **Marc-André SELOSSE,** Professeur, Muséum National d'Histoire Naturelle, Paris (Président du jury)
Soulaiman SAKR, Professeur, Agrocampus Ouest, Institut National d'Horticulture et de Paysage, Angers

Directeur de Thèse: **Benoît SCHOEFS**, Professeur, Université du Maine, Le Mans
Co-encadrantes: **Justine MARCHAND**, Maître de Conférences, Université du Maine, Le Mans
Véronique MARTIN-JEZEQUEL, Chargée de recherche, Centre National de la Recherche Scientifique à La Rochelle

Acknowledgments

I would like to thank my supervisor Professor Benoît Schoefs for his patient guidance, encouragement, support and expertise throughout my graduate experience. At many stages in the course of this research project I benefited from his advice, particularly so when exploring new ideas. His positive outlook and confidence in my research inspired me and gave me confidence. His careful editing contributed enormously to the production of this thesis.
I would also wish to sincere gratitude to my co-supervisor Dr. Justine Marchand for her constant support, guidance, motivation, advice and confidence. I would like to thank my second co-supervisor Dr. Véronique Martin-Jézéquel for her valuable helps and supports. It would never have been possible for me to take this work to completion without their support and encouragement.
I wish to appreciate the member of committee Dr. Jean-Paul Cadoret, Professor Fabrice Franck, Professor Soulaiman Sakr and Professor Marc-André Selosse for their careful editing and endurance. I thank again Dr. Jean-Paul Cadoret and Professor Fabrice Franck to accept to review my thesis.
During my Ph.D. work, I benefited greatly from many fruitful discussions with Brigitte Moreau. I cannot forget the valuable helps of her. I would like to thank Wafâa Boureba and Bing Huang for their help in the lab.
I have a special thank to Dr. Martine Bertrand and Professor Annick Morant-Manceau, who not only helped me in science, but because of the confidante and also good moments they offered to me. I also wish to thank Fanny Laude-Molina that without her helps my stay in France would not be possible.
I wish to say thank to the other people who worked in the lab to progress this thesis, Dr. Ewa Lukomska, Dr. Gaël Bougaran, Dr. Gaëlle Wielgosz and Dr. Aurélie Couzinet.
From Iran's side, I would like to thank my supervisor Dr. Morteza Zahedi for his patient, guidance and support. I would like to extend my sincerest thanks and appreciation to my two co-supervisors Dr. Hosein Zeinali and Dr. Farhad Rejali for their helps and encouragements.
I thank Dr. Mohammad reza Sabzalian and Dr. Ehsan Ataii for their help and supports. Furthermore, I appreciate the support of Isfahan University of Technology (IUT).
I wish to thank all of those people in both universities, Doctoral school VENAM, Région "Pays de la Loire", Pres LUNAM, Foreign Office of the Republic of France in which this thesis work could not have been done without their generous assistance and helps.

Finally, I wish to express my heartfelt gratitude and speciall thanks to my family specially my father and my mother, my life supporters.

Abbreviation

ΔpH	*pH* gradient across the thylakoid membrane
AM	*A*rbuscular *M*ycorrhiza
AMF	*A*rbuscular *M*ycorrhizal *F*ungi
ATP	*A*denosine *T*ri*P*hosphate
CA	*C*arbonic *A*nhydrase
cDNA	*C*omplementary *DNA*
CF	*C*oupling factor
Chl	*Chl*orophyll
CoA	*Co**E**n*zyme *A*
C*x*	molecules containing *x C*arbon atoms
Cytbf	*C*ytochrome*b6/f*
DHA	*D*ocosa*H*exaenoic *A*cid
DMAPP	*D*i*M*ethyl*A*llyl di*P*hos*P*hate
EO	*E*ssential *O*il
EPA	*E*icosa*P*entaenoic *A*cid
Fo	basic chlorophyll *F*luorescence level
Fm	*M*aximal chlorophyll *F*luorescence level
G6P	*G*lucose *6P*hosphate
GAP	*G*lycer*A*ldehyde3*P*
GES	*GE*raniol *S*ynthase
GGPP	*G*eranyl*G*eranyl di*P*hos*P*hate
GPP	*G*eranyl di*P*hos*P*hate
GPT	*G*6P *P*hosphate *T*ranslocator
IPP	*I*sopentenyl di*P*hos*P*hate
LED	*Light emitting D*iodes
LHC	*L*ight*H*arvesting *C*omplex
MEP	*M*ethyl*E*rythritol 4*P*hosphate
mRNA	*M*essenger *RNA*
NPQ	*Non-photochemical Q*uenching
NADPH	*N*icotinamide *A*denine *D*inucleotide *P*hosphate
Nudix	family of enzymes catalyzes the hydrolysis of a*NU*cleoside *D*iphosphate l*I*nked to another moiety X
OEC	*O*xygen *E*volving *C*omplex
PAR	*P*hotosynthetically *A*ctive *R*adiation
PEPC1	*P*hospho*EnolP*yruvate *C*arboxylase
PEP	*P*hospho*EnolP*yruvate
PGT	*P*eltate *G*landular *T*richomes
PSI	*P*hoto*S*ystem *I*
PSII	*P*hoto*S*ystem *II*
PUFA	*P*oly*U*nsaturated *F*atty *A*cids
PSY	*P*hytoene *SY*nthase
Q_A	*Q*uinone *A*

Q_B	*Q*uinone *B* or plastoquinone
RC	*R*eaction *C*enter
RhNUDX	*R*osa *x h*ybrida *N*UDi*X* hydrolase
TAG	*T*ri*A*cyl*G*lyceride

Chapter

1

General introduction

Since the neolithic revolution, some 15000 years ago, the importance of plants for the human societies never cessed to grow. Although they are used not only as sources for textiles, medicine and energy, but also they are mostly used as a source of food. Their success as source of food resides on the fact that they perform oxygenic photosynthesis, a process allowing them to build organic molecules using water, carbon dioxide and light as a source of energy. A waste of the process is molecular oxygen.

After a complex serie of biochemical reactions, the carbon atoms are combined to produce building block molecules *i.e.* fatty acids, amino acids and simple sugars such as sucrose that are in turn used as a source of energy or to synthesis more complex compounds such as lipids and proteins. The complex set of reactions involved in these syntheses is referred as the primary metabolism. It provides basic processes like photosynthesis, respiration, growth, development with building blocks, mostly carbohydrates, lipids and proteins. This metabolism is of great importance because it provides the living biomass from which the whole biosphere relies for growth and development.

Plants being mostly nonmotile organisms have to face with the modifications of their biotic and/or abiotic environmental factors. Good examples of these factors are appearance of pathogens, modifications of the growth temperature and/or light intensity. These modifications of the environmental constraints may have different timespan and therefore are susceptible to affect differently plant functioning depending on their duration. Along evolution, plants have acquired several defense mechanisms that can be activated to cope as a response to environmental changes. Among these mechanisms, the reorientation of the metabolism (Figure 1.1) toward the production of secondary metabolites such as phenolic compounds (*e.g.,* anthocyanins, tannins, lignin), nitrogenerated compounds (*e.g.*, alkaloids) and terpenes (*e.g.* essential oils, terpenoids, *etc*.) is very common (Ramawat et al. 2009).

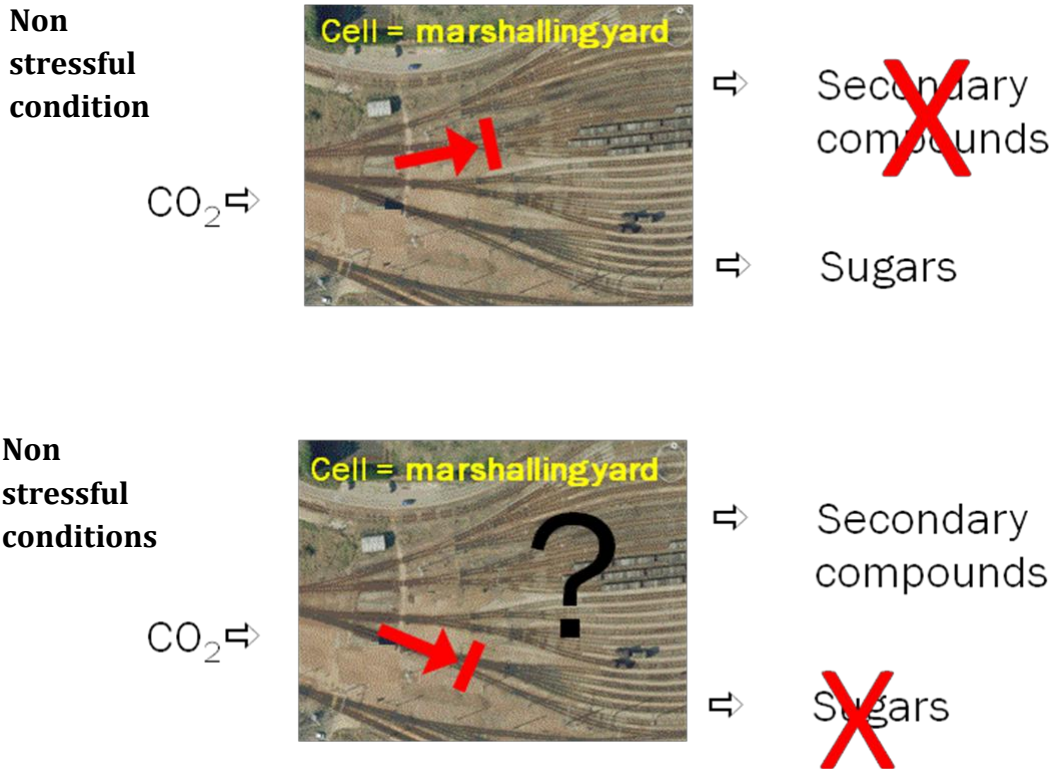

Figure 1.1. Scheme presenting the effects of a stress on the metabolism orientation in a cell (car: carotenoids).

By definition, secondary metabolites are compounds that are not necessary for cell but play important role in the interactions of the organisms with their environment (Gandhi et al. 2015). As primary metabolites, secondary metabolites have a considerable interest for human societies, serving as odoriferous, spices, colorants for food and textile and medicine (*e.g.*, Gandhi et al. 2015; Adolfsson et al. 2015). Healing with medicinal plants is as old as mankind itself. The oldest written evidence of medicinal plants usage for preparation of drugs has been found on a Sumerian clay slab from Nagpur (India), approximately 5000 years old (Kelly, 2009). Since this pioneer record, the pharmacopea greatly enriched and today, mint is one of the most important medicinal and aromatic plants that has been widely used in food, flavoring, traditional medicine, in cosmetics and pharmaceutical industries (Park et al. 2002; Bhat et al. 2002; Lange et al. 2011).

The clear separation between primary and secondary metabolism is vanishing when internal factors such as the concentration in phytohormones are considered and when secondary metabolites are produced by a restricted number of cells within a tissue producing only primary compounds. A good example is the peltate glandular trichomes

(PGT) of aromatic plants such as mint, the model plant used for my work, that produce essential oil (EO) by the direction of primary metabolites from mesophyll cells toward PGT. This is why in this manuscript I have chosen the term 'reorientation of the metabolism' instead of 'secondary production'.

Beside land plants, algae[1] are another type of organisms performing oxygenic photosynthesis. Plants and algae have originated through a primary endosymbiosis, a process where a non-photosynthetic eukaryote engulfed a cyanobacterium, thereby acquiring a photosynthetic apparatus that became housed within an organelle surrounded by two membranes and it conveniently explains the monophyletic origins of all plastids within eukaryotic cells (Facchinelli & Weber, 2011; Prihoda et al. 2012). This initial endosymbiotic event diverged in the green and red algal lineages, as well as to the Glaucophytes (Figure 1.2). Land plants arose following the evolution of multicellularity within the green algal lineage. In contrast with the evolution of land plants and green algae, the evolutionary history of diatoms is believed to have followed a rather different path. Generally, they have originated from a second non-photosynthetic eukaryote that engulfed a green or a red microalga through a secondary endosymbiosis, resulting a plastid surrounded by four membranes (Gould et al. 2008; Solymosi, 2012). It is believed that a single event is at the origin of the whole Chromalveolata super group, which comprises Heterokonts (also known as Stramenopiles, and to which the diatoms belong), Alveolates (Ciliates, Apicomplexans, and Dinoflagellates), Haptophytes, Cryptophytes, and perhaps also Rhizaria (Facchinelli & Weber, 2011; Prihoda et al. 2012; Kroth 2015). However the question about the number of secondary endosymbioses is still under debate (Keeling, 2013; Kroth, 2015). Regardless to this aspect of the evolution history diatoms, plants and green algae share many similarities at the biochemistry and cell physiology levels. For instance, land plants and diatoms are able to reoriente their metabolism toward the production of secondary metabolites of the terpenoid family, although of different natures. Plants from the Lamiaceae's botanical family produce essential oil composed by C_{10} monoterpenoids whereas diatoms accumulate C18-C22 polyunsaturated fatty acids (PUFAs) (Figure 1.3) (reviewed in Mimouni et al. 2012; see also chapter 4). Nevertheless, because land plants and diatoms evolutionary diverged rapidly, diatoms exhibit unique properties. Convincing evidences are the presence of several carbon concentration mechanisms, full urea cycle, unique pigments and/or lipid compositions and the presence of silica frustules.

Despite a long history of usage, the first written traces about the use of microalgae dates back 2000 years to the Chinese who used *Nostoc* to survive during famine. The role of microalgae in the biosphere as well as their potential remain rather confidential

[1] In this text, the term 'microalga' has been concidered to its broad sense, *i.e.* unicellular photosynthetic micro-organisms and therefore, includes cyanobacteria.

until recently (Borowitzka, 1999). Microalgae, especially diatoms (Bacillariophyceae), the second model used in this study, constitute strong oxygen emitter and are responsible for a large part (up to 41%–50%) of the CO_2 fixed in oceans (Field et al. 1998; Williams & Laurens, 2010).

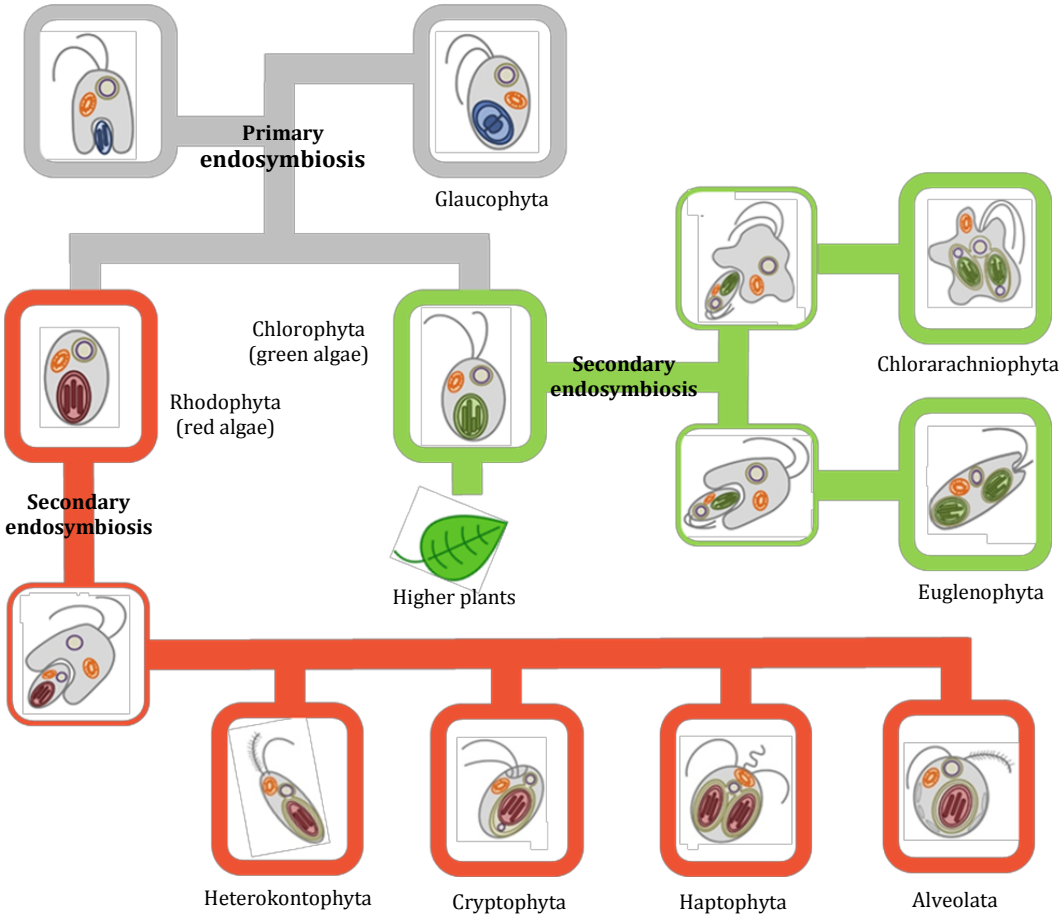

Figure 1.2. Schematic view of plastid evolution in the history of photosynthetic eukaryotes. The uptake of a cyanobacterium resulted in a photosynthetic plantae ancestor which subsequently gave rise to the three lineages containing primary plastids: the Chlorophytes (including green algae and the land plants), the Rhodophytes, and the Glaucophytes. The subsequent secondary endosymbioses of green and red algae engulfed by different hosts resulted in the Euglenophyta and Chlorarachniophyta (greens) and in the possibly monophyletic Chromalveolates (reds) that are devided into four major subgroup, *i.e.* Heterokontophyta/stramenopiles, Cryptophyta, Haptophyta and Alveolata (Facchinelli & Weber, 2011; Kroth, 2015).

In the past, microalgae played a crucial role in the formation of crude oil deposits in ocean floors, which are a rich natural source of fossil fuel (Shukla & Mohan, 2012). This contribution continues today because algae are responsible for a large fraction of the organic carbon being buried on continental margins (Smetacek, 1999).

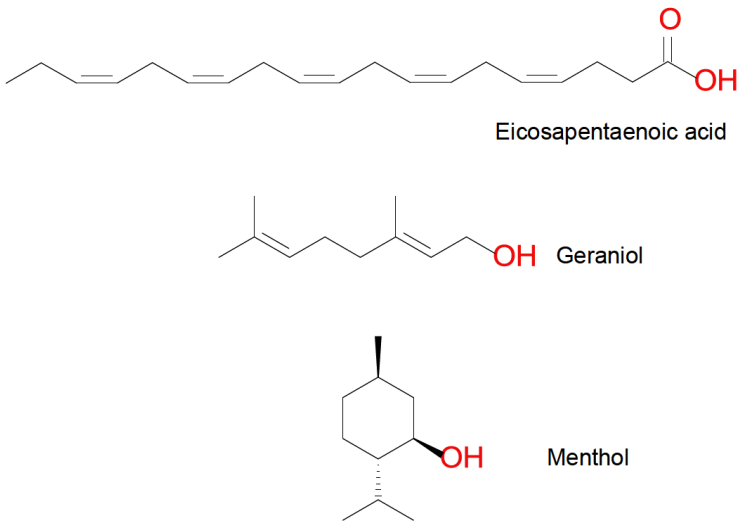

Figure 1.3. Chemical structure of eicosapentaenoic acid (EPA), geraniol and menthol.

Actually, the human population is up to 7.2 billion people alive today and is expected to coast upward to 9.6 billion by 2050 and 10.9 billion by 2100 (Sullivan, 2014). Several reasons including contribution of human to the acceleration of the depletion in natural resources (Alexandratos & Bruinsma, 2012), increasing the prices of raw materials based on these resources in markets and potentially change the Earth's climate have increased dramatically the interest for microalgae. This make them as many as major alternative sources of compounds such as polysaccharides, lipids, polyunsaturated fatty acids and pigments (Table 1.1) (land plants: Schoefs, 2002, 2005; microalgae: Cadoret et al. 2012; Mimouni et al. 2012; Hudek et al. 2014) and energy sources, including *via* genetic engineering and nanotechnology (Monica & Cremonini, 2009; Gordon & Seckbach, 2012; Mimouni et al. 2012; Carrier et al. 2014; Ge et al. 2014). Also their important applications for food, health, cosmetic, waste treatment, energy or pharmaceutical industries are considered (Schoefs, 2003; Gordon & Seckbach, 2012; Mimouni et al. 2012; Gandhi et al. 2015; Gateau et al. 2015).

The production of many of these compounds results from the reorientation of the carbon metabolism toward the production of secondary metabolites (Vinayak et al. 2015). As reflected by the dramatic increase of publications and patents presented in figure 1.4, the field of microalga has become very attractive and this development is strongly impacted the microalgal biotechnology as a topic that began to develop in the middle of the last century (Borowitzka, 1999). Commercial large-scale culture started in the early 1960's in Japan and the first aquaculture fields appeared in the 1970's (Muller Feuga, 1996; Pulz & Scheibenbogen, 1998; Borowitzka, 1999; Iwamoto, 2004).

Table 1.1 Main storage compounds and oil percentage of some microalgae (Vinayak et al. 2015).

Phylum	Class	Taxonomy	Oil Content (% d.w.)	High Value Molecules
Chlorophyta	Chlorodendrophyceae	*Tetraselmis suecica*	15–32	Carotenoids, chlorophyll, tocopherol, lipids
Chlorophyta	Chlorophyceae	*Ankistrodesmus* sp.	28–40	Mycosporinelike amino acids, polysaccharides
Chlorophyta	Chlorophyceae	*Dunaliella salina*	10	Carotenoid, β-carotene, mycosporinelike amino acids, sporopollenin
Chlorophyta	Chlorophyceae	*Dunaliella tertiolecta*	36–42	Carotenoid, β-carotene, mycosporinelike amino acids
Chlorophyta	Chlorophyceae	*Neochloris oleoabundans*	35–65	Fatty acids, starch
Chlorophyta	Trebouxiophyceae	*Botryococcus braunii*	29–75	Isobotryococcene, botryococcene, triterpenes
Chlorophyta	Trebouxiophyceae	*Chlorella vulgaris*	58	Neutral lipids
Chlorophyta	Trebouxiophyceae	*Chlorella emersonii*	34	Neutral lipids
Chlorophyta	Trebouxiophyceae	*Chlorella protothecoides*	15–55	EPA, ascorbic acid
Chlorophyta	Trebouxiophyceae	*Chlorella minutissima*	57	C16 and C18lipids
Heterokontophyta	Bacillariophyceae	*Nitzschia laevi*	28–69	EPA
Heterokontophyta	Coscinodiscophyceae	*Thalassiosira pseudonana*	21–31	Glycosylglycerides, neutral lipids, TAG
Heterokontophyta	Labrynthulomycetes	*Schizochytrium limacinum*	50–77	Docosahexaenoic acid (DHA)
Myzozoa	Peridinea	*Crypthecodinium cohnii*	20	DHA, Starch
Ochrophyta	Coscinodiscophyceae	*Cyclotella* sp.	42	Neutral lipids
Ochrophyta	Eustigmatophyceae	*Nannochloropsis* sp.	46–68	EPA, TAG, ω3 LCPUFA

Thus, in a short period of about 30 years, the microalgal biotechnology industry has grown and diversified significantly. Nowadays, the microalgal biomass market produces about 5000 T of dry matter/year but remains 'confidential' regarding to that of land plants in terms of production (10^6 times less than land plants) (Prof. Dussap, personal communication). Interestingly, the actual market generates a turnover of approximately US$ 125 million in 2004, US$ 271 million in 2010 and US$ 1.6 billion in 2015 (Pulz & Gross, 2004; http://www.biodieselmagazine.com/articles/8604/reportalgaebiofuels technologiesmarketat16bin2015). On the other hand, the global market for botanical and plantderived drugs has been increased from US$ 19.5 billion in 2008 to US$ 32.9 billion in 2013, with an annual growth rate of 11.0% (Trakranrungsie, 2011).

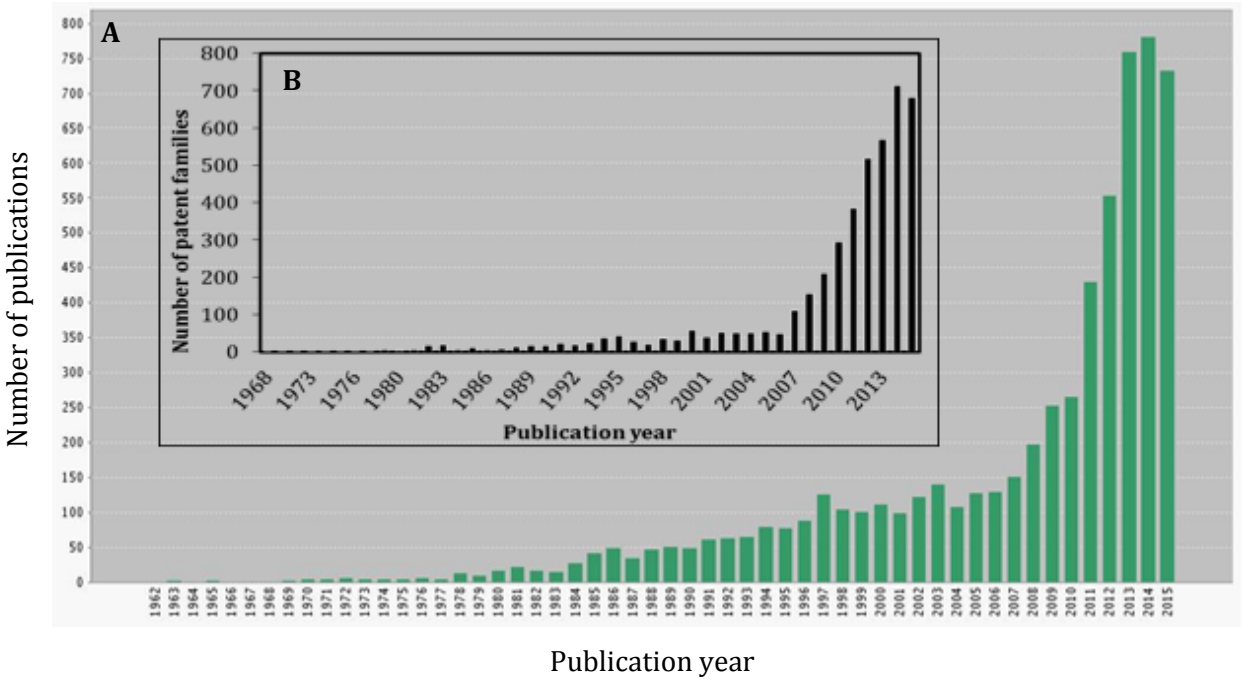

Figure 1.4. The time course of the occurrence of the term 'microalga*' in the title of publications (A) and patent families (B) (Source: web of science, core database, last consultation, 29.10.2015; https://www.webofknowledge.com.

1.1 The photosynthetic process in land plants and diatoms

Oxygenic photosynthesis is a biophysicochemical process that converts carbon dioxide into organic compounds using sunlight as a source of energy. In land plants, as in diatoms, photosynthesis takes place in the chloroplasts, and uses water as a source of electrons, releasing oxygen as a waste product (for a recent review, see Hohmann-Marriott & Blankenship, 2011). As mentioned above, the chloroplast in algae and plants has evolved from a cyanobacterial ancestor *via* endosymbiosis with a primitive eukaryotic host. The chloroplast is a highly compartmentalized organelle, with three membrane systems (outer envelope, inner envelope, and thylakoids) and three soluble spaces (intermembrane space, stroma, and thylakoid lumen) (Figure 1.5.A). A major difference between land plant and diatom chloroplasts resides in the presence of additional surrounding membranes outside the double envelope. They are generally termed periplastid membrane(s) or periplastid/chloroplast endoplasmic reticulum (Solymosi, 2012). The origin of these outer plastid enveloping membranes is still under debate (reviewed in Cavalier-Smith, 2003, 2007; Keeling, 2004; Solymosi, 2012).

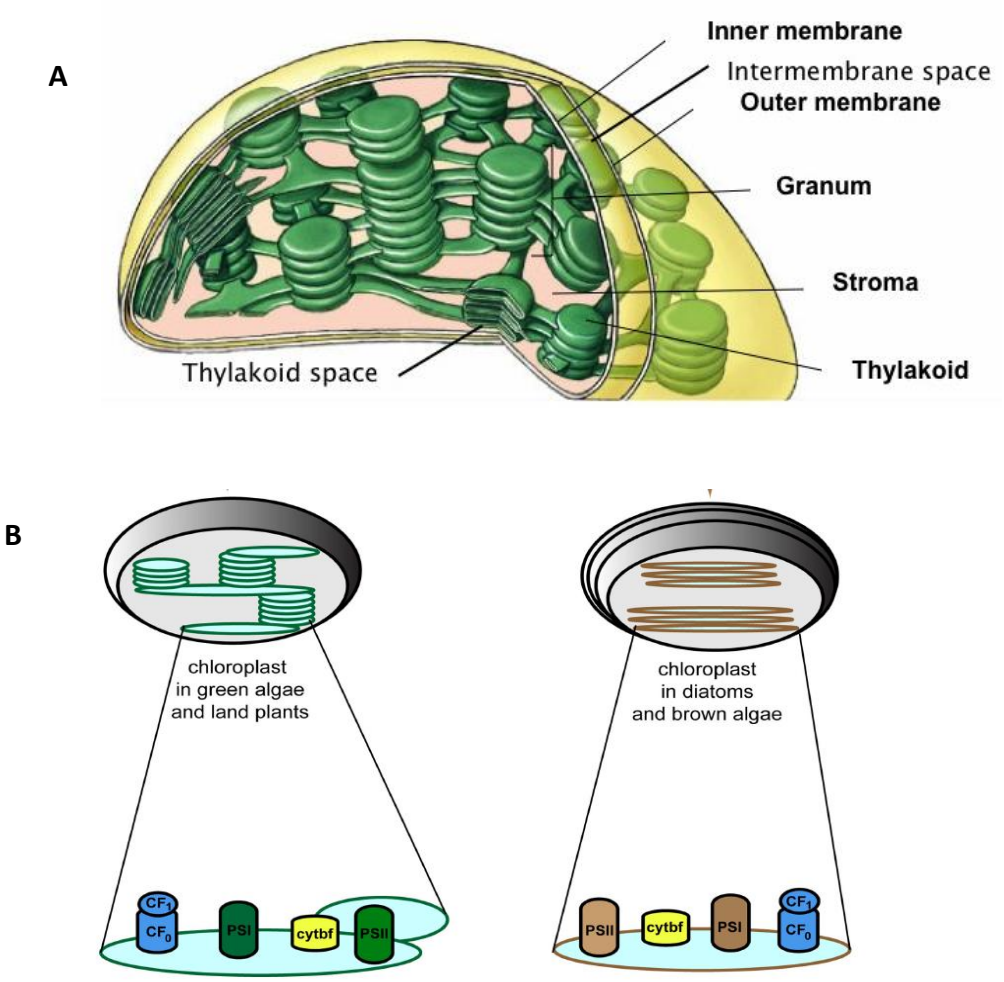

Figure 1.5 (A) Structure of chloroplast in land plants, (B) Comparison of the organization of the photosynthetic complexes within thylakoid membranes (Pfeil et al. 2014).
Thylakoid membranes in diatoms (shown in brown) are arranged in groups of three and contain fucoxanthin–chlorophyllprotein complexes for harvesting light (Bertrand, 2010). Note the fourlayer envelopes surrounding the chloroplast as compared to the types found in land plants. Thylakoid membranes in land plants (shown in green) are located inside the chloroplast. They are organized in grana stacks (5–20 vesicles) interconnected by stromaexposed lamellae, and contain chlorophyll–protein complexes for harvesting light (Mustárdy & Garab, 2003).
The photosynthetic apparatus is composed of four multisubunit complexes, namely the wateroxidizing photosystem II (PSII), cytochromeb6/f (cytbf), photosystem I (PSI), and the H^+-translocating ATP synthase (CF0F1) (Nelson & Ben Shem, 2004). These complexes are laterally distributed in land plants, whereas in diatoms, they display a more uniform distribution.

It is mentioned here because some important enzymes involved in the carbon metabolism, namely carbonic anhydrase (CA) and phospho*enol*pyruvate carboxylase (PEPC1), have been predicted to be localized in this unique compartment (Solymosi, 2012; Matsuda & Kroth, 2014; see chapter 3). The organization of the thylakoids also

differs in the two models. In land plants, these membranes are organized in highly stacked (appressed) regions, the so called grana. Grana are interconnected by stromaexposed (nonappressed) regions (Figure 1.5.B). In diatoms, the photosynthetic membranes display groups of 3 weakly stacked thylakoids (for details see Solymosi, 2012 and Figure 1.5).

The photosynthetic apparatus is composed of four macrocomplexes, namely the wateroxidizing PSII, cytbf, PSI, and the H^+-translocating ATP synthase (CF0F1) (Nelson & Ben Shem, 2004). They supply ATP and NADPH for the synthesis of many essential compounds, such as carbohydrates, for autotrophic growth. A PS is composed of a reaction center (RC) and a light harvesting complex (LHC). Two families of pigments are found in LHCs, namely tetrapyrroles and carotenoids. In all photosynthetic organisms, except for most cyanobacteria and red algae, Chlorophyll (Chl) *a* is aided in its task of harvesting light by accessory pigments, namely other types of Chl (Chl c in diatoms and Chl b in land plants) and carotenoids (Table 1.2). In diatoms, the major carotenoid is fucoxanthin, an allenic ketocarotenoid (Table 1.2). Other important carotenoids in diatoms are the diadinoxanthin and diatoxanthin due to their involvement in the xanthophyll cycle (Bertrand, 2010, Moulin et al. 2010) (Table 1.2). The xanthophyll cycle is a reaction of de-epoxidation triggered by the acidification of the thylakoid lumen.

In land plants, the major carotenoids are lutein and violaxanthin. Other important carotenoids are β-carotene, neoxanthin and zeaxanthin. This last one is involved with violaxanthin in the xanthophyll cycle. The purpose of accessory pigments is to enlarge the range of wavelengths collected by LHCs (Hohmann-Marriott & Blankenship, 2011). In addition to their role in harvesting light, carotenoids play crucial roles in thylakoid organization (Inwooda et al. 2008), in photoprotection of Chl molecules and dissipation of excess energy, for instance, through operation of the xanthophyll cycle (Bertrand, 2010; Goss & Jakob, 2010; Moulin et al. 2011).

Despite the distinct carotenoid composition of brown algae, diatoms and land plants (Table 1.2) they all share a role in photoprotection that includes the xanthophyll cycle (Moulin et al. 2010). Due to lack of space, a detailed comparison of the arrangement of pigments within PSI, PSII and associated LHCs will not be described here, but the interested reader will find relevant information in several recent reviews (Neilson & Durnford, 2010; Busch & Hippler, 2011; Hohmann-Marriott & Blankenship, 2011; Sozer et al. 2011).

It was held for a long time that the different macro-complexes comprising the photosynthetic apparatus were organized linearly along the thylakoid membranes. If this view is still valid for diatoms, (Grouneva et al. 2011) (Figure 1.6), it is no longer accepted for land plants since it has been established that these complexes are laterally

Table 1.2. Main chlorophyll and carotenoid types in the various taxons of photosynthetic organisms (Pfeil et al. 2014, Heydarizadeh et al. 2013).

Pigment type	Diatoms	Land plants	Chemical structure
Chl *a*	+	+	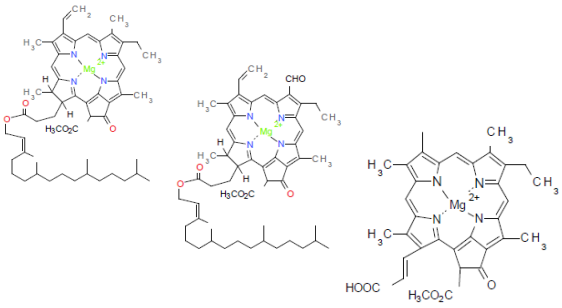
Chl *b*	-	+	
Chl *c*	+	-	
b-carotene	+	+	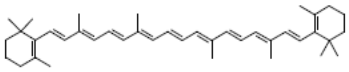
Fucoxanthin	+	-	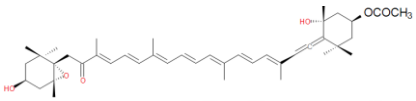
Diadinoxanthin	+	-	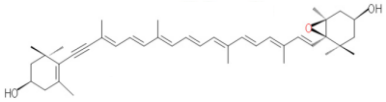
Diatoxanthin	+	-	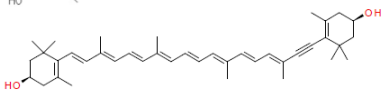
Violaxanthin	+	+	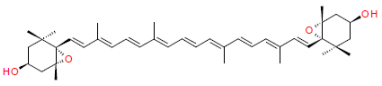
Lutein	-	+	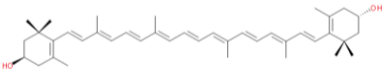
Zeaxanthin	Traces	+	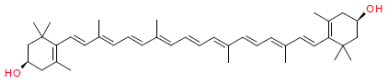
Xanthophyll cycle	+	+	

distributed, *i.e*. localized exclusively in the appressed membranes (PSII), exclusively in the stromaexposed thylakoids (PSI and ATP synthase) or in both types of membranes (cytbf; Anderson, 2002) (Figure1.6).

The differences in thylakoid membrane organization among diatoms and land plants may have implications for biogenesis and turnover of photosynthetic complexes. Because these aspects were not considered in this work, they are not detailed here and the interested reader is requested to consult specialized publications on that topic (Daum & Kühlbrandt, 2011; Austin & Staehelin, 2011).

From the functional point of view, the photons that are harvested by the LHC are directed to the RC of PSII. There, they trigger the release of one electron from one of the two Chl *a* molecules of the RC.

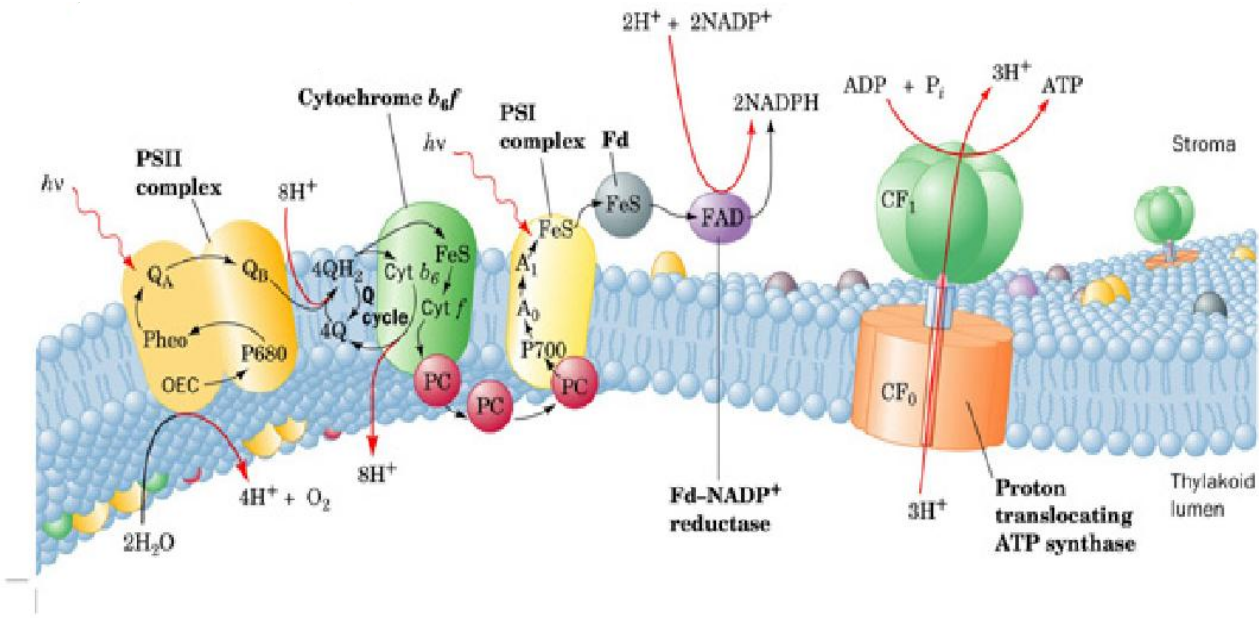

Figure 1.6. The ATP and NADPH that are generated along the photosynthetic apparatus are for CO2 fixation and transformation into organic compounds (Roháček et al. 2008).

This electron is first transferred to the primary acceptor Q_A (one electron acceptor) and then to the second electron acceptor Q_B (two electron acceptor). The changes in the redox state of Q_A are reflected by the intensity of the fluorescence emitted by the Chl molecules of the LHC (Duysens & Sweers, 1963): when Q_A is oxidized, the level of Chl fluorescence is minimum. This level is denoted F_0. When Q_A is reduced the Chl fluorescence is maximum. This level is denoted F_M. Using these values, the maximum quantum yield of PSII photochemistry can be calculated (for details, see chapter 3). The recording of these chlorophyll fluorescence levels in a sample containing billions of PSII require that all the Q_A are oxidized or reduced simultaneously (Roháček et al. 2008). This can be obtained by placing the samples in complete darkness for 15 min or by illuminating it with a saturating light, respectively. The electron gap at the RC is filled using an electron coming from the oxidation of a water molecules by the oxygen evolving complex (OEC) that releases oxygen molecules and protons in the thylakoid lumen (Figure 1.6). The rate of oxygen evolving thus reflects the photosynthesis activity.

Once Q_B^2 has accumulated two electrons, it leaves PSII to deliver the electrons to the cytbf. Because charged molecules are unable to cross hydrophobic media such a membrane, Q_B^2 binds 2 protons from the stroma and it is actually Q_BH_2 that it is crossing the thylakoids membranes until Q_BH_2 pocket of cytbf, located at the other side of the membrane. While the electrons are delivered, the cotransported protons are released to the lumen of the thylakoids. The electrons are then transferred to the PSI where they

are used for production of NADPH. The protons that are delivered in the lumen are transported back to the stroma through the activity of the ATP synthase (Figure 1.6). The biochemical reactions leading to these compounds are common or similar in land plants and diatoms and are described in details in chapter 3. Consequently, they will not be described here.

Under stressless condition, the rate of proton delivery into the lumen is in equilibrium with the rate of proton movement from the lumen to the stroma. In case of stress, for instance during an intense irradiation, the equilibrium is broken and protons accumulate in the lumen, creating a trans-thylakoidal pH gradient (ΔpH). Lumen acidification triggers the xanthophyll cycle, a molecular device aiming to dissipate the excess of energy. It consists in the reversible de-epoxidation of epoxy-xanthophylls (violaxanthin in land plants and diadinoxanthin in diatoms (Moulin et al. 2010)). To summarize, a proportion of the energy captured by the LHC is used to extract electron from the Chl molecules located in the RC. This proportion is called the photochemical quenching. The rest of the captured energy is dissipated into other mechanisms that are collectively referred as non-photochemical quenching (NPQ). After a continuous illumination, the NPQ relaxes. The analysis of the relaxation kinetic using a nonlinear regression procedure (Roháček, 2010; Roháček et al. 2014) revealed three main components with different shapes, constant rate and underlying mechanisms (Table 1.3). In both models the xanthophyll cycle is the main energy dissipation pathway under short term stress conditions (Roháček, 2010; Roháček et al. 2014).

The ATP and NADPH that are generated along the photosynthetic apparatus are used for CO_2 fixation and its transformation into building blocks molecules (Figure 1.7). In brief, storage carbohydrates (chrysolaminarin (polymer of β(1→3) and β(1→6) linked

Table 1.3. Characteristics of the three components composing the NPQ and revelead by the nonlinear regression analyses of the NPQ relaxation. From Roháček, 2010 and Roháček et al. 2014.

Component	**Fast**		**Medium**		**Slow**	
	Land plants	Diatoms	Land plants	Diatoms	Land plants	Diatoms
Constant rate	Of the order of s	Of the order of s	Of the order of min	Of the order of min	Of the order of several tens of min	Of the order of h
Shape	Exponential	Exponential	Exponential	Sigmoid	Exponential	Exponential
Mechanism	ΔpH and xanthophyll cycle	Fast conformational changes in the membranes	State transitions (does not exist in diatoms)	ΔpH and xanthophyll cycle	Photoinhibition	Photoinhibition and partial dissipation of the ΔpH

glucose units) in diatoms and starch (polymer of α(1→4) and α(1→6) linked glucose units) in land plants are one of the main sinks for carbon fixed during light periods, and it is also incorporated into glucans through gluconeogenesis (Myklestad & Granum, 2009). Another fraction of the fixed carbon is incorporated *via* pyruvate into fatty acids or *via* phospho*enol*pyruvate into aromatic compounds (Figure 1.7).

The complexity of studying carbon metabolism appears when the pathways are developed and replaced in their cellular context (Figure 1.8). Carbon metabolism is composed by a myriad of enzymatic reactions distributed between the different compartments of the cell *i.e.* chloroplast, cytoplasm, mitochondria and peroxisome. The complexity is essentially linked to the pathway duplication. A good example is the set of reactions catalyzing the transformation of glyceraldehyde 3-P (GAP) to phospho*enol* pyruvate that is present in the cytosol and chloroplast in land plants and also in the mitochondria in diatoms (Figure 1.8). The complexity is even increased by the fact that each reaction is enhanced by an enzyme that is encoded by several isogenes, which expression is differentially regulated by environmental factors. For these reasons, the study of carbon metabolism is very difficult at the biochemical level and inferences from modifications of the gene expression are usually preferred, with all the reservations that imply such reasoning (see chapter 3).

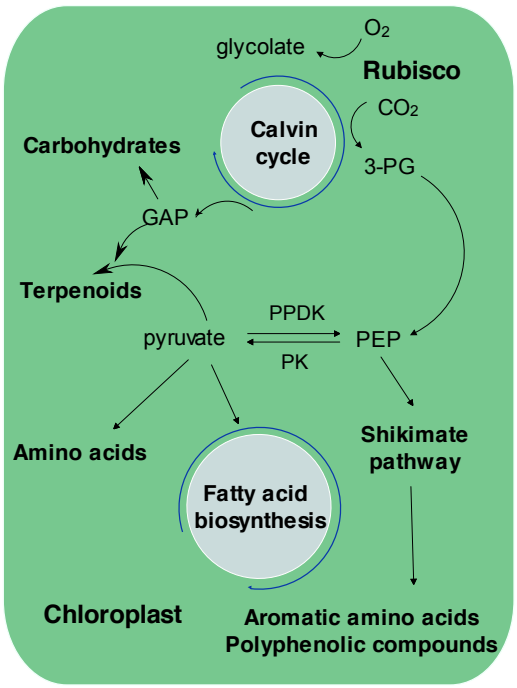

Figure 1.7. General scheme of fixed carbon transformation into building blocks molecules and final products.

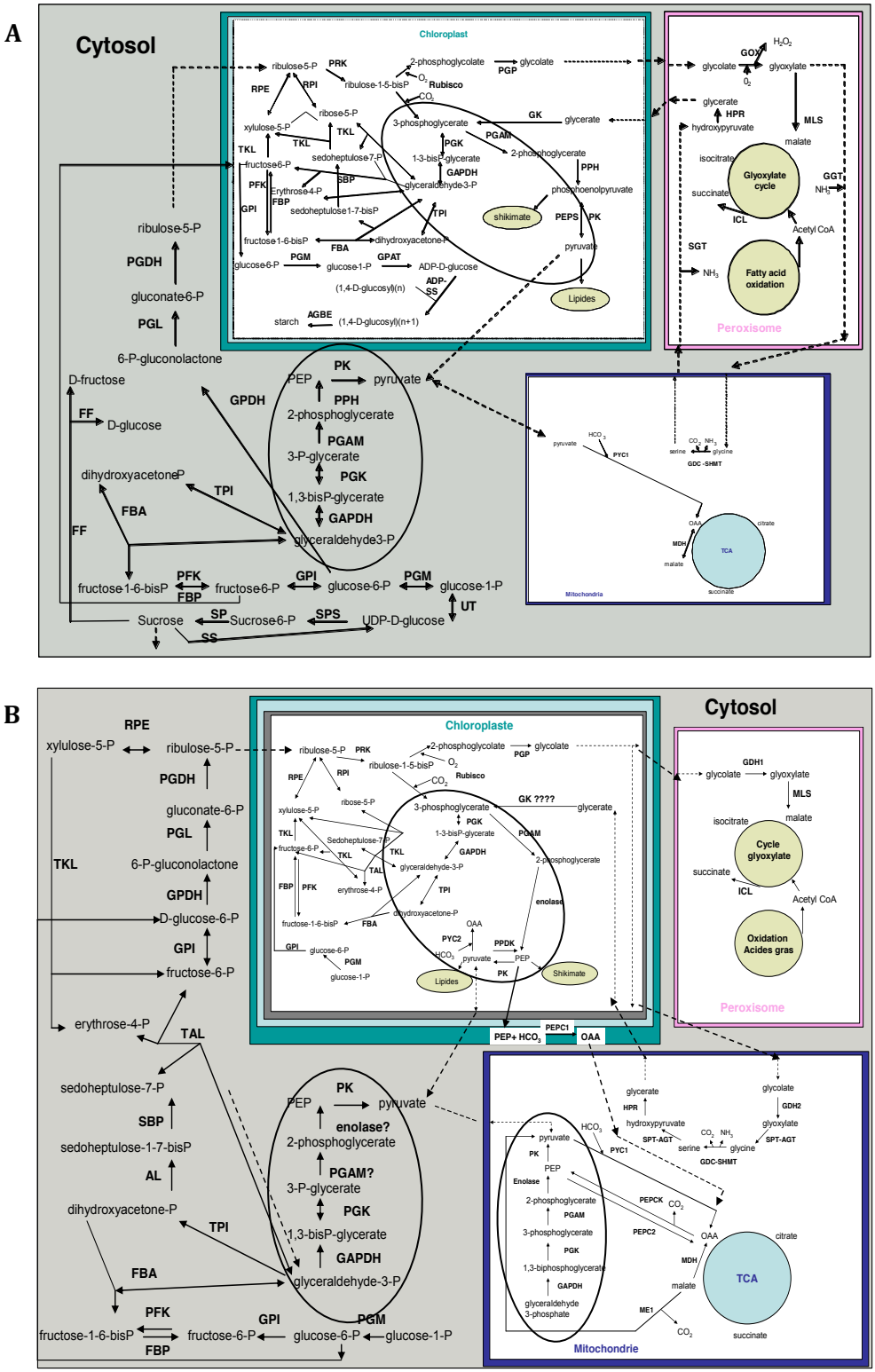

Figure 1.8. General scheme of central carbon metabolism in land plant (A) and diatom (B) (Martin-Jézéquel et al. 2012). Circles show second part of glycolysis pathway from glyceraldehyde 3-phosphate to pyruvate that exist in plastid and cytosol in land plants and also in mitochondria in diatom.

1.2 The reorientation of the carbon metabolism toward the production of secondary compounds

When photosynthetic organisms are growing in a non-stressful environment, the photosynthetically fixed carbon is mostly oriented toward the synthesis of carbohydrates. The metabolic reorientation consists in reducing the production of carbohydrates and concomitantly inject carbon in (an)other pathway(s) to produce the socalled secondary compounds. Chemically, secondary metabolites can be devided into three groups based on their chemical structure: terpenes, phenolic compounds and alkaloids (Wink, 1988)

Phenolics are a class of chemical compounds consisting of a hydroxyl group (—OH) bonded directly to an aromatic hydrocarbon group. Based on the number of phenol units in the molecule they are classified as simple phenols, *e.g.* phenolic acids or polyphenols such as flavonoids. Generally, their primary function is as protection against ultraviolet radiation and pathogens (Manach et al. 2004; Machu et al. 2015).

Alkaloids are a diverse group of low molecular weight, nitrogen containing compounds derived mostly from aromatic amino acids (made *via* shikimate pathway) including phenylalanine, tyrosine and tryptophan. These compounds are purported to associate with stress responses including herbivores and pathogens.

Owing to their potent biological activity, many of the approximately 12,000 known alkaloids have a wide range of pharmacological activities including antimalarial (*e.g.* quinine), anti-asthma (*e.g.* ephedrine), anti-cancer (*e.g.* homoharringtonine), analgesic (*e.g.* morphine), *etc*. (Wink, 2003; Sinatra et al. 2010; Kittakoop et al. 2014; Pedone-Bonfim et al. 2015).

Terpenoids are the largest class of plant secondary metabolites (Kawoosa et al. 2010; Akula & Ravishankar, 2011) and they derive from the C_5 alkene isoprene. They contain multiples of 5, 10, 15, 20 or more carbon atoms (Table 1.4) (Breitmaier, 2006; also see chapter 4). The terpenes are generally insoluble in water and synthesized by acetyl-CoA or glycolysis (Pedone-Bonfim et al. 2015). In plants, geranyl diphosphate (GPP), precursor of monoterpenes, is synthesized in plastids from dimethylallyl diphosphate (DMAPP) and isopentenyl diphosphate (IPP) supplied by the methylerythritol 4-phosphate pathway (MEP) (Rodríguez-Concepción & Boronat, 2002).

The monoterpenes in EO are produced through the activity of various monoterpene synthases (Chen et al. 2011). For example, geraniol synthase (GES) converts GPP into geraniol in basil (Iijima et al. 2004). Recently, Magnard et al. (2015) reported the presence of a cytosolic enzyme (RhNUDX1) taking action in the monoterpene alcohols pathway in roses. This discovery makes the basis for monoterpene biosynthesis even more obscure. Very interestingly, monoterpenes similar of those found in mint EO have been detected in the diatom *Thalassiosira (*Meskhidze et al. 2015).

Table 1.4. Diversity of terpenes in photosynthetic organisms.

Terpene type	Number of isoprene units	Number of carbon atoms	Examples
Monoterpene	2	10	Volatile compouds such as menthol, camphor, limonene, pinene, thujone, nerol (Meskhidze et al. 2015)
Sesquiterpene	3	15	Farnesol, carophyllene, αbergamotene (Ferriols et al. 2015)
Diterpene	4	20	Chlphytol
Sesterpene	5	25	haslenes (Rowland et al. 2001)
Triterpene	6	30	lanosterol, achilleol, rhizene (Belt et al. 2003)
Tetraterpene	8	40	β-carotene, fucoxanthine

The other branch in terpenoid biosynthesis is diterpene synthesis that requires geranylgeranyl diphosphate (GGPP) (see chapter 4). The first committed step in carotenoid biosynthesis is head to head condensation of the two C_{20} molecules of GGPP by phytoene synthase (PSY) to form phytoene. GGPP is also the precursor for several other groups of metabolites, including Chls. In diatom brown colour is due to the presence of high amounts of the xanthophylls fucoxanthin that masks the other carotenoids (*e.g.*, β-carotene, violaxanthin, diadinoxanthin and diatoxanthin and the chlorophyllous pigments). The absolute and/or relative amounts of individual pigments may differ according to the taxon and its ecology (Bertrand, 2010).

In unicellular organisms such as microalgae the metabolic reorientation *per se* concerns the whole organisms. In diatoms, modifications in the environmental factors such as nutrient depletion (Reitan et al. 1994; Breteler et al. 2005) or excess light energy (Norici et al. 2011) may increase cellular lipid content in diatoms. In multicellular organisms such as land plants, the metabolic reorientation is often restricted to a part of the organisms. This part could even be restricted to few cells as it is the case for EO production in mint (Bhat et al. 2002; Lange et al. 2011). EO is fabricated and stored in specialized anatomical structures, termed PGT, on leaf surfaces (Lange et al. 2011; Jin et al. 2014) (Figure 1.9. A.B).

The secretory cells of the oil glands responsible for EO biosynthesis can be isolated in high yield from leaves (Fig. 1.9.C) (Gershenzon et al. 1992). The isolated secretory cells from glandular trichomes are capable of *de novo* biosynthesis of monoterpenes from sucrose as primary carbohydrate precursor (Mc Caskill et al. 1992) and they have been shown to be highly enriched in the enzymes of monoterpene biosynthesis (Lange et al. 2000). Thus, in a first approximation, diatoms and secretory cells could be considered as single cells. However, the two models greatly differ when the carbon and energy sources are considered. Actually diatoms are autotrophs *i.e*; the photosynthetically fixed CO_2 is

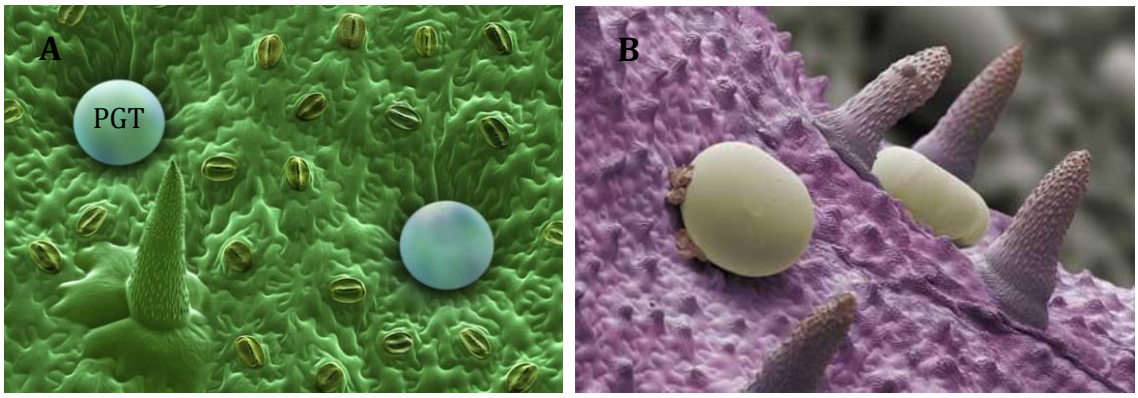

http://blog.wellcome.ac.uk/2014/07/11/imageoftheweekmint

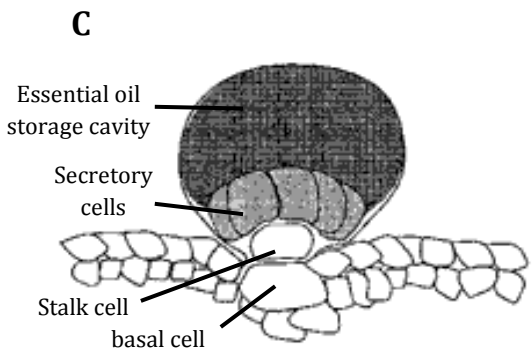

Figure 1.9. (A) and (B): Scanning electron microscope pictures of the surface of *Mentha piperita* leaf (B: Svoboda et al. 2001). PTG are oil glands responsible in which EO is synthesized and stored. It gives to mint its characteristic aroma. The spikes are small hairs (non glandular hairy trichome) on the leaf. The pictures have been colored using false colors. (C): Scheme of a transversal section of PGT of *Mentha piperita* (Mc Caskill & Croteau 1999).

used for further biosynthesis, including terpenoids, and the energy for biosynthesis is mostly arising from photosynthesis. In contrast, PGT are heterotrophic cells *i.e.* the energy needed for these syntheses does not come from photosynthesis because PGT of aromatic plants generally have non-green plastids while secreting terpenoids (Lange et al. 2013; Jin et al. 2014). Therefore, these cells rely on exogenous supply of sucrose from underlying leaf tissues, *i.e*. mesophyll, to use as carbon source for monoterpene production (Jin et al. 2014). Sturm & Tang (1999) found higher expression of genes encoding enzymes for sucrose catabolism in secretory cells, such as sucrose synthase, neutral and alkaline invertases that are important to transfer carbon from sucrose in non-photosynthetic tissues. These enzymes convert sucrose to hexose phosphates.

In most plants glucose 6-phosphate (G6P), which is synthesized from sucrose in the cytosol, seems to be the preferred hexose phosphate taken up by non-green plastids. The transporter proteins responsible for this import of carbon into plastids are known as G6P-phosphate translocator (GPT) and secretory cells are enriched in GPT (about 30 times more than green leaf cells) (Jin et al. 2014). Two genes coding for GPT, GPT_1 and GPT_2, have been described in the *Arabidopsis* genome, while GPT_2 is non-essential and generally expressed at lower levels than GPT_1 (Niewiadomski et al. 2005).

Regardless the model under consideration, the available data have revealed that triggering the metabolic reorientation involves a complex signaling network, the description of which is out of the scope of this general introduction. Among these factors light appears to be one of the most important and fundamental environmental factor affecting the orientation of the carbon metabolism (Bowler et al. 2010; Lemoine & Schoefs, 2010; Meitao Dong et al. 2012; Lan et al. 2013). Actually, light can affect the regulation of central carbon metabolism through its two characteristics *i.e.* wavelength and intensity (Fan et al. 2013; Li et al. 2013). The reorientation of the carbon metabolism toward the production of secondary metabolites is rather well understood when the final pathways are considered (*e.g.,* Lemoine & Schoefs, 2010) but little is known about the pathway used to carbon dispatch between the different pathways, especially under light stress in diatom and land plants (Rech et al. 2008; Vidoudez & Pohnert, 2012). In addition, it has become evident that the production of certain metabolites is highly dependent on the development of the cells and several ecological interactions are mediated by these strongly regulated metabolites (Barofsky et al. 2010; Barofsky et al. 2009, 2010; Vidoudez & Pohnert, 2008).

1.3 Influence of light on growth and reorientation of the carbon metabolism

Land plants and microalgae being photosynthetic organisms, the presence of light is mandatory for their growth and development. As mentioned above photons are harvested by pigments and the energy associated to the photons is used to drive photosynthesis (Chen & Blankenship, 2011). In nature, including outdoor cultures, sunlight is the continuous source of photons. *Per se,* indoor culture requires artificial lighting, that are typically outfitted with fluorescent and/or incandescent bulbs providing a general spectrum that is accommodating to the human eyes but not necessarily supportive to plant development (Folta et al. 2005; Li et al. 2013) (see chapters 6 and 7). The incandescent or fluorescent bulbs contain filaments that must be periodically replaced, consume a lot of electrical power and also generate heat, making impossible their use close to the canopy (Tennessen et al. 1994; Singh et al. 2015). Incandescent and fluorescent bulbs differ by their operational lifetime: around of 20,000 h for fluorescent bulbs whereas only 1000 h for incandescent bulbs (Barta et al. 1992; Tennessen et al. 1994). Beside these traditional lighting systems, another lighting source, the Light emitting diodes (LED), rapidly developed (Girón González, 2012). This lighting system has been used less than two decades to test plant responses to narrow wavelength irradiations and has shown to be a promising lighting technology for future because LED usage eliminated limitations of traditional lighting systems environments (Olvera-Gonzalez et al. 2013; Li et al. 2013).

LEDs have an extraordinary lifetime (about 100,000 h), require little maintenance, and they can be placed close to plants and can be configured to emit high light fluxes

even at high light intensities (Barta et al. 1992; Tennessen et al. 1994; Singh et al. 2015). The emergence of energy efficient LEDs has opened up a new methodology for conversion of photonic wavelengths to organic compounds in photosynthetic macro and microorganisms (Tan Nhut et al. 2005; Lan et al. 2013; Fan et al. 2013; Olvera-Gonzalez et al. 2013).

Because the photosynthetic activity is a light dependent process, it is usually thought that increasing the irradiance level is proportionally increasing the photosynthetic activity and thus growth. This is true until a certain level of irradiance (Terry et al. 1983) above which the photosynthetic activity is saturated (Nguyen-Deroche et al. 2012). When the irradiance levels exceed the electron transport capacity, the photosynthetic organisms are stressed and the photosynthetic machinery can be damaged. These damaged can lead to an arrest of photosynthesis (Ritchie, 2010). To avoid such a situation, defense mechanisms such as the xanthophyll cycle, state transition, chloroplast cycling and photoinhibition are activated to dissipate the excess of absorbed energy (Moulin et al. 2010; Allorent et al. 2013; de Marchin et al. 2014; Spetea et al. 2014). It is interesting to note that some of these mechanisms might not exist in some taxons. For instance state transition, which consists in changing the relative antenna size of PSII and PSI does not exist in diatoms. The energy invested in these defense mechanisms being not available for growth, the relation between growth rate and irradiance level reaches a stationary phase or even presents a decreasing phase (Geider et al. 1985). How the carbon metabolism is impacted by the growth light intensity in diatoms remain largely unknown. This is mostly due to the fact that the completion of the genome sequences of diatoms is very recent (*Phaeodactylum tricornutum*: Bowler et al., 2008; *Thalassiosira pseudonana*: Armburst et al. 2004) and the reconstitution of the cellular metabolism including prediction of enzyme localization even more fresh and still under discussion (Kroth et al. 2008; Fernie et al. 2012; Kroth, 2015). The transcriptome of *P. tricornutum* has been studied in a few contexts, such as silicon metabolism (Sapriel et al. 2009), short term light acclimation (Nymark et al. 2009), carbon fixation, storage and utilization (Chauton et al. 2013) and nitrogen stress (Levitan et al. 2015) but growth related modifications in gene expression induced by different light intensities in *P. tricornutum* are not yet described.

A similar study could not be started in mint because of a general lack of information at the genomic level. When this thesis was initiated, only one paper was reporting mRNA from isolated *M. piperita* and *M. spicata* secretory cells that were used to generate a cDNA library (Lange et al. 2000). Recently, next generation sequencing methods have been applied to mint and revealed a more complex metabolism than expected (Jin et al. 2014). Altogether, the knowledge about the development of PGT, terpene production and its regulation is very limited making it difficult a study on carbon reorientation toward the production of EO (Glas et al. 2012; Tissier, 2012).

In addition to be an energy shuttle for photosynthetic organisms, light provides information from the environment to the organisms. For instance, it has been shown that the presence of light has a positive impact on shoot branching (Djennane et al. 2014) and bud burst (Henry et al. 2011) are mechanisms regulated by light. These information are decoded by photoreceptors such as phytochrome (red/farred, blue light, UVB photoreceptors) (Lin, 2000; Rockwell et al. 2006; Heijde & Ulm, 2012). If the knowledge about photoreceptors is really advanced in land plants, it remains in its infancy in microalgae and especially in diatoms (Hegemann, 2008; Fortunato et al. 2015) and will not be treated here. Many studies over the last several decades have clearly shown that variation in light quality can affect growth and control developmental transitions of diatoms and land plants, including mint (diatoms: Mouget et al. 2004; Huysman et al. 2013; land plants; Urbonavičiūtė et al. 2008; Li et al. 2012; Tarakanov et al. 2012; Colquhoun et al. 2013; Bula et al. 1991; Duong et al. 2002, Duong & Nguyen, 2010; Kurilcik et al. 2008; Barisic et al. 2006; mint: Nishioka et al. 2008; Malayeri et al. 2011). Indeed, several results showed that LED light is more suitable for land plant growth than fluorescent lamps (Bula et al. 1991; Folta et al. 2005; Li et al. 2010; Olvera-Gonzalez et al. 2013). To the best of our knowledge, there is no report about the effect of different quality of LED light on plant growth and essential oil production in *Mentha* taxon, except the study performed in this Ph.D thesis (see chapter 7).

1.4 Reorientation of the carbon metabolism by biotic factors: the case of arbuscular mycorrhizal

As mentioned earlier, land plants and diatoms have emerged from first and secondary endosymbiosis, respectively. When Earth colonization by plants started, plants had only rudimentary xylem for conducting mineral sap (Gerrienne et al. 2011), probably making difficult mineral nutrition (Selosse & Le Tacon, 1998). Plants being rooted they were immobile and unable to move to capture nutrients from their immediate environment. To circumvent this difficulty, plants established a symbiotic associations with Glomalean fungi from the Glomeromycota, ancestors of modern arbuscular mycorrhizal fungi (AMF), about 460 million years ago (Simon et al. 1993; Taylor et al. 1995; Redecker et al. 2000). This is estimated to be some 300–400 million years before the appearance of root nodule symbioses with nitrogen fixing bacteria (Finlay, 2008). In this respect, symbiosis with AMF is the most ancient and widespread form of fungal symbiosis with plants. Indeed today, more than 74% of plant species and more than 90% of the cultivated species still acquire nutrients from soil using AMF, reflecting the evolutionary success of this mutualistic symbiosis (Wang & Qiu, 2006; Smith & Read, 2008; Heijden et al. 2015). These interactions between organisms pervade all ecosystems and strongly influence the structure of natural populations and

communities (Cairney, 2000). It is interesting to note that only 150–200 species of AMF have so far been distinguished on the basis of morphology, but DNAbased studies suggest the true diversity of these symbionts may be very much higher (Fitter, 2005; Soka & Ritchie, 2015).

From the functional point of view, the symbiosis is primarily seen as a trade contract between the two partners: the fungus provides the plants with water and mineral, especially phosphate. AMF being heterotrophs, they require an external source of carbon for energy and cellular synthesis that the plant is 'offering'. Thus, photosynthetic products under the form of glucose and fructose to the fungus, are converted to trehalose and lipids (Pfeffer et al. 1999; Doidy et al. 2012). Lipids translocate to the extraradical mycelium for further metabolism, as they are the major forms of carbon storage in AM fungal spores, hyphae, and vesicles (Cox et al. 1975). The trading of compounds occurs through the unique highly branched fungal structures, the so called arbuscule, which grow intracellularly without penetrating the host plasmalemma (Finlay, 2008) (Figure 1.10)

Depending on the AMF species, it is assumed that the total carbohydrate cost of the arbuscular mycorrhiza (AM) symbiosis can be up to 20% of the host plant photosynthetic production (Harrison, 1999; Kaschuk et al. 2009; Lendenmann et al. 2011; van der Heijden et al. 2015). Clearly, AMF constitutes additional carbon sinks that sources, the above ground part of plants, should feed.

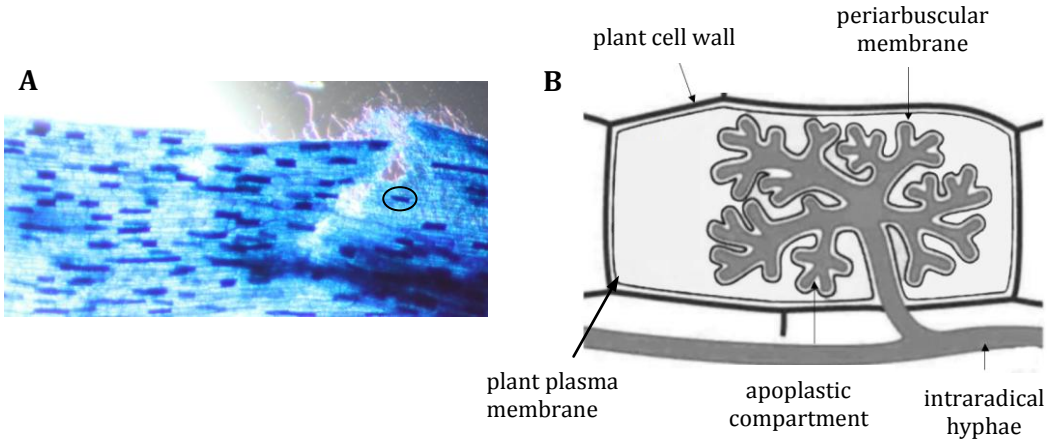

Figure 1.10. A) light microscopic image of *Mentha spicata* root with arbuscules inside root cells. The black circle represent an arbusculecontainig root cell that is explained by detailes in partB (picture B from Recorbet et al. 2008)

Consequently, the photosynthetic activity of mycorrhized plants is expected to be enhanced. Actually, many reports describe stimulatory effects of photosynthesis in

mycorrhizal plants (Louche-Tessandier et al. 1999; Valentine et al. 2001). Boldt et al. (2011) reported a decrease, and Parádi et al. (2003) and Adolfsson et al. (2015) found no effect of mycorrhization on Chl content and fluorescence. In contrast, Adolfsson et al. (2015) demonstrated that photosynthesis in *Medicago truncatula* was enhanced through branching enhancement. The reason for this discrepancy remains unclear as well as the mechanism by which AM could influence these photosynthetic parameters in plant leaves. Arbuscular mycorrhization also induces carbon reorientation. For instance, in the root, mycorrhization induces the synthesis of secondary carotenoids that eventually are used for the production of C_{13}/C_{14} apocarotenoids regulating the timelife of the arbuscules (Walter et al. 2015).

The activation of the carotenoid metabolism has likely additional function relevant for symbiosis due to plastid role in the biosynthesis of gibberellin, abscisic acid and strigolactone (Seddas et al. 2010; Walter et al. 2015; Takeda et al. 2015). In addition, the increased amounts of glutamate and aspartate in roots of AM plants (Lohse et al. 2005; Schliemann et al. 2008; Rivero et al. 2015) suggest a stimulation of amino acid biosynthetis and N assimilation in plastids upon mycorrhization. A mycorrhiza related activation of plastidic metabolism was also inferred from the increased abundance of some fatty acids (palmitic and oleic acids) in *M. truncatula* roots (Lohse et al. 2005; Schliemann et al. 2008), presumably reflecting the extension and *de novo* synthesis of the plasma membrane around the arbuscule, the so-called periarbuscular membrane (Figure 1.10) (Gaude et al. 2012a; b). Gutjahr et al. (2011) also showed that although starch is dispensable for mycorrhization, it can, when present, be used as a second energy source for AM symbiosis. Likewise, the comparison of the membrane proteome between mycorhizal and non-mycorrhizal roots of *M. truncatula* indicated a reduced abundance of plastidic proteins having role in carbon import to plastids, ammonium assimilation and glycolysis, thereby suggesting that part of carbon skeletons devoted to plastid metabolism might be highjacked to sustain the fungal development within host roots (Abdallah et al. 2014).

For the reasons explained earlier, much less is known about carbon reorientation in the photosynthetic cells of AM plants. This reorientation should occur at least in aromatic plants because a higher production of secondary metabolic is often recorded in AM plants (del Rosario Cappellari et al. 2015; Copetta et al. 2006; Khaosaad et al. 2006; Zeng et al. 2013; Kumar et al. 2014 a; b; Ratti et al. 2015). Last but not least, it is worth to mention that mycorrhization enhance plant fitness by increasing resistance or tolerance to biotic and abiotic stresses (Newsham et al. 1995; Auge, 2001; Aloui et al. 2011). How light intensity and light quality influence the carbon reorientation mechanisms in the photosynthetic tissue remains unknown, as to the best of our knowledge, there is no report showing the interaction between mycorrhizal symbiosis and different LED light quality on plant productivity.

1.5 Objectives

The main objective of this study was to evaluate the impact of modifications of the lighting environment on the carbon metabolism in diatom and land plant with the aim to decipher the modification of the carbon circuits triggered by these modifications. Working on this main frame light intensity and light quality alone or together with the presence of an additional biotic stress was tested. To perform this study, we have chosen two models: the diatom "*P. tricornutum"* and land plant "*Mentha* sp."

P. tricornutum was chosen because of

(i) its genome has been sequenced, facilitating genomic and transcriptomic studies (Bowler et al. 2008; Kroth et al. 2008; Saade & Bowler, 2009; Cadoret et al. 2012; Ji et al. 2013) as well as reverse genetics (*e.g.*, Cadoret et al. 2012; Ge et al. 2014);

(ii) its culture is rather easy and the cell are growing fast;

(iii) there is an abundant references about this alga;

(iv) under certain circumstances, such as light stress, the amount of triacyl glycerides (TAG) is increased making this alga an alternative source for the production and extraction of lipids;

(v) it doesn't need to form the characteristic frustules, suggesting that it can be grown in medium with less silicon (Francius et al. 2008; Shrestha et al. 2012; Zhao et al. 2014). This provides an experimental advantage when compounds such as pigment have to be extracted.

These special characteristics make *P. tricornutum* an ideal model to study the reorientation of the carbon metabolism toward the production of secondary metabolites.

and *Mentha* sp. was chosen because of

(i) very significant role in economy, not only for its application as food ingredient but also for its highly diversified industrial use in confectionary, cosmetics and pharmaceutical sectors.

(ii) its appropriate size for studying the growth inside incubator.

After a general introduction (Chapter 1), the thesis is organized in two parts. The first one (Chapters 2 and 3) is dedicated to the investigation in the diatom *P. tricornutum* cells under different irradiances (30-1000 µmol m^{-2} s^{-1}). As diatoms may respond to environmental stresses by accumulating high value components such as lipids, we determined how carbon participation changes from primary to secondary metabolite synthesis by changing the level of the light intensity. For this aim we studied the variations of the transcription activity of genes coding for key enzymes of the central carbon metabolism and also some genes related to secondary metabolite biosynthesis. This information may be of help to understand better the regulation of secondary metabolites not only in diatom, but also in *Mentha* species.

The second part (Chapters 4-8) is focused on the effects of light on the growth of several mint species and their EO production. First we report the natural occurrence of mycorrhized mint accessions[1] in different geographical regions of Iran distinct by their climate (Chapter 5). These accessions have been used to study the impact of different light qualities on growth and EO production (Chapter 7). The capacity to additionally enhance the growth and EO production by introducing an additional stress factors, a mycorrhizal fungus, in the plant environment has been then tested (Chapter 8).

The manuscript ends with a general conclusions and perspective in chapter 9. For the presentation of the results, we have decided to take advantage of the fact that part of our results have been published or submitted for publication (Chapters 3 and 8). Because we had the opportunity to participate to the writing of several review paper, we have used them to introduce more specifically research papers.

1.6 References

Abdallah C., Valot B. et al. (2014). The membrane proteome of *Medicago truncatula* roots displays qualitative and quantitative changes in response to arbuscular mycorrhizal symbiosis. J. Proteomics 108: 354–368.

Adolfsson L., Solymosi K., Andersson M.X., Keresztes Á., Uddling J., Schoefs B. & Spetea C. (2015). Mycorrhiza symbiosis increases the surface for sunlight capture in *Medicago truncatula* for better photosynthetic production. PLoS One 10: e0115314.

Akula R. & Ravishankar G.A. (2011). Influence of abiotic stress signals on secondary metabolites in plants. Plant Signal Behav. 6: 1720–1731.

Alexandratos N. & Bruinsma J. (2012). World agriculture towards 2030/2050: the 2012 revision. ESA Work. 3.

Allorent G., Tokutsu R. et al. (2013). A dual strategy to cope with high light in C*hlamydomonas reinhardtii.* Plant Cell 25: 545–557.

Aloui A., Recorbet G., Robert F., Schoefs B., Bertrand M., Henry C., GianinazziPearson V., DumasGaudot E. & AschiSmiti S. (2011). Arbuscular mycorrhizal symbiosis elicits shoot proteome modifications that are recruited during cadmium stress alleviation in *Medicago truncatula*. BMC Plant Biol. 11: 75.

Anderson J.M. (2002). Changing concepts about the distribution of photosystems I and II between granaappressed and stromaexposed thylakoid membranes. Photosynth. Res. 73: 157–164.

Armbrust E.V., Berges J.A., et al. (2004). The genome of the diatom *Thalassiosira pseudonana*: ecology, evolution, and metabolism. Science 306: 79–86.

Auge R.M. (2001). Water relations, drought and vesicular–arbuscular mycorrhizal symbiosis. Mycorrhiza 11: 3–42.

Austin J.R. & Staehelin L.A. (2011). Threedimensional architecture of grana and stroma thylakoids of higher plants as determined by electrontomography. Plant Physiol. 155: 1601–1611.

[1] The term accession refers to the collected plant material from their particular location. These plants are not commercially cultivated.

Barisic N., Stojkovic B. & Tarasjev A. (2006). Plastic responses to light intensity and planting density in three *Lamium* species. Plant Syst. Evol. 262: 25–36.
Barofsky A., Vidoudez C. & Pohnert G. (2009). Metabolic profiling reveals growth stage variability in diatom exudates. Limnology and Oceanography: Methods, 7: 382–390.
Barofsky A., Simonelli P. et al. (2010). Growth phase of the diatom *Skeletonema marinoi* influences the metabolic profile of the cells and the selective feeding of the copepod *Calanus spp*. J. Plankton Res. 32: 263–272.
Barta D.J., Tibbits T.W., Bula R.J. & Morrow R.C. (1992). Evaluation of light emitting diode characteristics for a spacebased plant irradiation source. Adv. Space Res. 12: 141–9.
Belt S.T., Massé G., Allard W.G., Robert J.M. & Rowland S.J. (2003). Novel monocyclic sesterand triterpenoids from the marine diatom, *Rhizosolenia setigera*. Tetrahedron lett. 44: 9103–9106.
Bertrand M. (2010). Carotenoid biosynthesis in diatoms. Photosynth. Res. 106: 89–102.
Bhat S., Maheshwari P., Kumar S. & Kumar A. (2002). *Mentha* species: *In vitro* regeneration and genetic transformation. Mol. Biol. Today 3: 11–23.
Boldt K., Pors Y. et al. (2011). Photochemical processes, carbon assimilation and RNA accumulation of sucrose transporter genes in tomato arbuscular mycorrhiza. J. Plant Physiol. 168: 1256–1263.
Borowitzka M.A (1999) Commercial production of microalgae: ponds, tanks, tubes and fermenters. J. Biotechnol. 70: 313–321.
Bowler C., Allen A.E. et al. (2008). The *Phaeodactylum* genome reveals the evolutionary history of diatom genomes. Nature 456: 239–244.
Bowler C., Vardi A. & Allen A.E. (2010). Oceanographic and biogeochemical insights from diatom genomes. Ann. Rev. Mar. Sci. 2: 333–363.
Breitmaier E. (2006). Terpenes: Flavors, Fragrances, Pharmaca, Pheromones, WileyVCH, Weinheim.
Breteler W.C.M.K., Schogt N. & Rampen S. (2005). Effect of diatom nutrient limitation on copepod development: role of essential lipids. Mar. Ecol. Prog. Ser. 291: 125–133.
Bula R.J., Morrow R.C., Tibbitts T.W., Barta D.J., Ignatius R.W. & Martin T.S. (1991). Light emitting diodes as a radiation source for plants. Hort. Sci. 26: 203–205.
Busch A. & Hippler M. (2011). The structure and function of eukaryotic photosystem I. Biochim. Biophys. Acta. 1807: 864–877.
Cadoret J.P., Garnier M. & SaintJean B. (2012). Microalgae, functional genomics and biotechnology. Adv. Bot. Res. 64: 285–341.
Cairney J.W.G. (2000). Evolution of mycorrhiza systems. Naturwissenschaften 87: 467–475.
Carrier G., Garnier M., Le Cunff L., Bougaran G., Probert I., De Vargas C., Corre E., Cadoret J.P. & SaintJean B. (2014). Comparative transcriptome of wild type and selected strains of the microalgae Tisochrysis lutea provides insights into the genetic basis, lipid metabolism and the life cycle. PLoS One 9(1).
Cavalier-Smith T. (2003). Genomic reduction and evolution of novel genetic membranes and proteintargeting machinery in eukaryote eukaryote chimaeras (metaalgae). Phil. Trans. R. Soc. Lond. B. 358: 109 The *Phaeodactylum* genome reveals the evolutionary history of diatom genomes. Nature 134.
Cavalier-Smith T. (2007). Unravelling the algae, the past, present and future of algal systematics. In: Brodie J. & Lewis J. (Eds.). The systematics association special volume series 75. Boca Raton, London, New York: CRC Press. 21–55.
Chauton M.S., Winge P., Brembu T., Vadstein O. & Bones A.M. (2013). Gene regulation of carbon fixation, storage, and utilization in the diatom *Phaeodactylum tricornutum* acclimated to light/dark cycles. Plant Physiol. 161: 1034–1048.

Chen F., Tholl D., Bohlmann J. & Pichersky E. (2011). The family of terpene synthases in plants: a mid-size family of genes for specialized metabolism that is highly diversified throughout the kingdom. Plant J. 66: 212-229.
Chen M. & Blankenship R.E. (2011). Expanding the solar spectrum used by photosynthesis. Trend. Plant Sci. 16: 427–431.
Colquhoun T.A., Schwieterman M.L., Gilbert J.L., Jaworski E.A., Langer K.M., Jones C.R., Rushing G.V., Hunter T.M., Olmstead J. & Clark D.G. (2013). Light modulation of volatile organic compounds from petunia flowers and select fruits. Postharvest Biol. Technol. 86: 37–44.
Copetta A., Lingua G. & Berta G. (2006). Effects of three AM fungi on growth, distribution of glandular hairs, and essential oil production in *Ocimum brasilicum* L. var. Genovese. Mycorrhiza 16: 485–494.
Cox G., Sanders F.E., Tinker P.B. & Wild J.A. (1975). Ultrastructural evidence relating to host endophyte transfer in vesiculararabuscular mycorrhizas. In: Sanders F.E, Morse B & Tinker P.B (Eds.). Endomycorrhizas. London: Academic Press. 297–312.
Daum B. & Kühlbrandt W. (2011). Electron tomography of plant thylakoid membranes. J. Exp. Bot. 62: 2393–2402.
del Rosario Cappellari L., Santoro M.V., Reinoso H., Travaglia C., Giordano W. & Banchio E. (2015). Anatomical, morphological, and phytochemical effects of inoculation with plant growthpromoting rhizobacteria on peppermint (*Mentha piperita*). J. chem. Ecol. 41: 149–158.
de Marchin T., Ghysels B., Nicolay S. & Franck F. (2014). Analysis of PSII antenna size heterogeneity of *Chlamydomonas reinhardtii* during state transitions. Biochim. Biophys. Acta Bioenerg. 1837: 121–130.
Djennane S., HibrandSaint Oyant L. et al. (2014). Impacts of light and temperature on shoot branching gradient and expression of strigolactone synthesis and signalling genes in rose. Plant Cell Environ. 37: 742–757.
Doidy J., Grace E., Kühn C., SimonPlas F., Casieri L. & Wipf D. (2012). Sugar transporters in plants and in their interactions with fungi. Trends Plant Sci. 17: 413–422.
Duong T.N., Hong L.T.A., Watanabe H., Goi M. & Tanaka M. (2002). Growth of banana plantlets cultured *in vitro* under red and blue Light emitting diode (LED) irradiation source. Act. Hortic. 575: 117–124.
Duong T.N. & Nguyen B.N. (2010). Light emitting diodes (LEDs): an artificial lighting source for biological studies. In: Proceedings of the 3rd International Conference on the Development of BME in, Vietnam, 133–138.
Duysens L.N.M. & Sweers H.E. (1963). Mechanisms of two photochemical reactions in algae as studied by means of fluorescence. In: Japanese Society of Plant Physiologists (ed) Studies on microalgae and photosynthetic bacteria, Special Issue of Plant and Cell Physiology. University of Tokyo Press, Tokyo. 353–372.
Facchinelli F. & Weber A.P. (2011). The metabolite transporters of the plastid envelope: an update. Front. Plant Sci. 2: 50.
Fan X.X., Xu Z.G., Liu X.Y., Tang C.M., Wang L.W. & Han X.L. (2013). Effects of light intensity on the growth and leaf development of young tomato plants grown under a combination of red and blue light. Scient. Hortic. 153: 50–55.
Fernie A.R., Obata T., Allen A.E., Araújo W. L. & Bowler C. (2012). Leveraging metabolomics for functional investigations in sequenced marine diatoms. Trends Plant Sci. 17: 395–403.
Ferriols V.M.E.N., Yaginuma R., Adachi M., Takada K., Matsunaga S. & Okada S. (2015). Cloning and characterization of farnesyl pyrophosphate synthase from the highly branched isoprenoid producing diatom *Rhizosolenia setigera*. Sci. Rep. 5.
Field C.B., Behrenfeld M.J., Randerson J.T. & Falkowski P. (1998). Primary production of the biosphere: Integrating terrestrial and oceanic components. Science 281: 237–240.

Finlay R.D. (2008). Ecological aspects of mycorrhizal symbiosis: with special emphasis on the functional diversity of interactions involving the extraradical mycelium. J. Exp. Bot. 59: 1115–1126.
Folta K.M., Koss L.L., McMorrow R., Kim H.H., Kenitz J.D., Wheeler R. & Sager J.C. (2005). Design and fabrication of adjustable redgreenblue LED light arrays for plant research. BMC Plant Biol. 5: 17.
Fortunato A.E., Annunziata R., Jaubert M., Bouly J.P. & Falciatore A. (2015). Dealing with light: the widespread and multitasking cryptochrome/photolyase family in photosynthetic organisms. J. Plant Physiol. 172: 42–54.
Francius G., Tesson B., Dague E., Martin-Jézéquel V. & Dufrêne Y.F. (2008). Nanostructure and nanomechanics of live *Phaeodactylum tricornutum* morphotypes. Environ. Microbiol. 10: 1344–1356.
Gandhi S.G., Mahajan V. & Bedi Y.S. (2015). Changing trends in biotechnology of secondary metabolism in medicinal and aromatic plants. Planta. 241: 303–317.
Gateau H., Marchand J. & Schoefs B. (2015). Carotenoids of microalgae used in food industry and medicine. Mini Rev. Med. Chem. (submitted).
Gaude N., Bortfeld S., Duensing N., Lohse M. & Krajinski F. (2012a). Arbusculecontaining and noncolonized cortical cells of mycorrhizal roots undergo extensive and specific reprogramming during arbuscular mycorrhizal development. Plant J. 69: 510–528.
Gaude N., Schulze W.X., Franken P. & Krajinski F. (2012b). Cell typespecific protein and transcription profiles implicate periarbuscular membrane synthesis as an important carbon sink in the mycorrhizal symbiosis. Plant Signal. Behav. 7: 461–464.
Ge F., Huang W., Chen Z., Zhang C., Xiong Q., Bowler C., Yang J., Xu J. & Hu H. (2014). MethylcrotonylCoA carboxylase regulates triacylglycerol accumulation in the model diatom *Phaeodactylum tricornutum*. Plant Cell 26: 1681–1697.
Geider R.J., Osborne B.A. & Raven J.A. (1985). Light dependence of growth and photosynthesis in *Phaeodactylum tricornutum* (Baccilariophyceae). J. Phycol. 21: 609–619.
Gerrienne P., Gensel P.G., StrulluDerrien C., Lardeux H., Steemans P. & Prestianni C. (2011). A simple type of wood in two early eevonian plants. Science 333: 837.
Gershenzon J., Mc Caskill D., Rajaonarivony J.I.M., Mihaliak C., Karp F. & Croteau C. (1992). Isolation of secretory cells from plant glandular trichomes and their use in biosynthetic studies of monoterpenes and other gland products. Anal. Biochem. 200: 130–138.
Girón González E. (2012). LEDs for general and horticultural lighting. AALTO University. School of Electrical Engineering.
Glas J.J., Schimmel B.C., Alba J.M., EscobarBravo R., Schuurink R.C. & Kant M.R. (2012). Plant glandular trichomes as targets for breeding or engineering of resistance to herbivores. Int. J. Mol. Sci. 13: 17077–17103.
Gordon R. & Seckbach, J. (2012). The science of algal fuels: phycology, geology, biophotonics, genomics and nanotechnology. Springer: Dordrecht, The Netherlands.
Goss R. & Jakob T. (2010). Regulation and function of xanthophylls cycledependent photoprotection in algae. Photosynth. Res. 106: 103–122.
Gould S.B., Waller R.F. & McFadden G.I. (2008). Plastid evolution. Annu. Rev. Plant Biol. 59: 491–517.
Grouneva I., Rokka A. & Aro E.M. (2011). The thylakoid membrane proteome of two marine diatoms outlines both diatomspecific and speciesspecific features of the photosynthetic machinery. J. Prot. Res. 10: 5338–5353.
Gutjahr C., Novero M., Welham T., Wang T. & Bonfante P. (2011). Root starch accumulation in response to arbuscular mycorrhizal colonization differs among *Lotus japonicus* starch mutants. Planta 234: 639–646.

Harrison M.J. (1999). Biotrophic interfaces and nutrient transport in plant fungal symbioses. J Exp. Bot. 50: 1013–1022.
Hegemann P. (2008). Algal sensory photoreceptors. Annu. Rev. Plant Biol. 59: 167–89.
Heijde M. & Ulm R (2012) UVB photoreceptormediated signalling in plants. Trend. Plant Sci. 17: 230–237.
Heijden M.G., Martin F.M., Selosse M.A. & Sanders I.R. (2015). Mycorrhizal ecology and evolution: the past, the present, and the future. New Phytol. 205: 1406–1423.
Henry, C., Rabot, A. et al. (2011). Regulation of RhSUC2, a sucrose transporter, is correlated with the light control of bud burst in *Rosa* sp. Plant Cell Environ. 34: 1776–1789.
Heydarizadeh P., Poirier I., Loizeau D., Ulmann L., Mimouni V., Schoefs B. & Bertrand M. (2013). Plastids of marine phytoplankton produce bioactive pigments and lipids. Mar. Drugs 11: 3425–3471.
Hohmann-Marriott M.F. & Blankenship R.E. (2011). Evolution of photosynthesis. Annu.Rev.Plant Biol. 62: 515–548.
Hudek K., Davis L.C., Ibbini J. & Erickson L. (2014). Commercial products from algae. In Algal biorefineries. Springer Netherlands. 275–295.
Huysman M.J., Fortunato A.E. et al. (2013). AUREOCHROME1amediated induction of the diatomspecific cyclin dsCYC2 controls the onset of cell division in diatoms (Phaeodactylum tricornutum). Plant Cell 25: 215–228.
Iijima Y., Gang D.R., Fridman E., Lewinsohn E. & Pichersky E. (2004). Characterization of geraniol synthase from the peltate glands of sweet basil. Plant Physiol. 134: 370–379.
Inwooda W., Yoshiharaa C., Zalpurib R., Kima K.S. & Kustua S. (2008). The ultrastructure of a *Chlamydomonas reinhardtii* mutant strain lacking phytoene synthase resembles that of a colorless alga. Mol Plant 1: 925–937.
Iwamoto H. (2004). Industrial production of microalgal cellmassand secondary products major industrial species Chlorella. Handbook of microalgal culture. Blackwell, Oxford. Richmond A (Ed.). 255–263.
Ji C., Huang A., Liu W., Pan G. & Wang G. (2013). Identification and bioinformatics analysis of pseudogenes from whole genome sequence of *Phaeodactylum tricornutum*. 58: 10101017.
Jin J., Panicker D., Wang Q., Kim M.J., Liu J., Yin J.L., Wong L., Jang I.C., Chua N.H. & Sarojam R. (2014). Next generation sequencing unravels the biosynthetic ability of Spearmint (*Mentha spicata*) peltate glandular trichomes through comparative transcriptomics. BMC Plant Biol. 14: 292.
Kaschuk G., Kuyper T.W., Leffelaar P.A., Hungria M. & Giller K.E. (2009). Are the rates of photosynthesis stimulated by the carbon sink strength of rhizobial and arbuscular mycorrhizal symbioses? Soil Biol. Biochem. 41: 1233–1244.
Kawoosa T., Singh H., Kumar A., Sharma S.K., Devi K., Dutt S., Kumar Vats S., Sharma M., Singh Ahuja P. & Kumar S. (2010). Light and temperature regulated terpene biosynthesis: hepatoprotective monoterpene picroside accumulation in *Picrorhiza kurrooa*. Funct. Integr. Genomic. 10: 393–404.
Keeling P.J. (2004). Diversity and evolutionary history of plastids and their hosts. Am. J. Bot. 91: 1481–1493.
Keeling P.J. (2013). The number, speed, and impact of plastid endosymbioses in eukaryotic evolution. Annu. Rev. Plant Biol. 64: 583–607.
Kelly K. (2009). History of medicine. New York: Facts on file. 29–50.
Khaosaad T., Vierheiling H., Nell M., ZitterlEglsser K. & Novak J. (2006). Arbuscular mycorrhiza alter the concentration of essential oils in oregano (*Origanum* sp., Lamiaceae). Mycorrhiza 16: 443–446.

Kittakoop P., Mahidol C. & Ruchirawat S. (2014). Alkaloids as important scaffolds in therapeutic drugs for the treatments of cancer, tuberculosis, and smoking cessation. Curr. Top. Med. Chem. 14: 239–252.

Kroth P., Chiovitti A., Gruber A., MartinJezequel V., Mock T., Parker M., Stanley M., Kaplan A., Caron L.,WeberT., Maheswari U., Armbrust V. & Bowler C. (2008). A model for carbohydrate metabolism in the diatom *Phaeodactylum tricornutum* deduced from comparative whole genome analysis. PLoS One 3: e1426.

Kroth P.G. (2015). The biodiversity of carbon assimilation. J. plant physiol. 172: 76–81.

Kumar A., Sengar R.S. & Sahi S.V. (2014a). Acclimation and adaptation of plants to different environmental abiotic stresses. Climate Change Effect on Crop Productivity.329.

Kumar A., Mangla C., Aggarwal A. & Srivastava V. (2014b). Rhizospheric effect of endophytic mycorrhiza and trichoderma viride on physiological parameters of *Mentha spicata* linn. Asian J. Adv. Basic Sci. 2: 99–104.

Kurilcik A., MiklusyteCanova R., Dapkuniene S., Zilinskaite S., Kurilcik G., Tamulaitis G., Duchovskis P. & Zukauskas A. (2008). *In vitro* culture of *chrysanthemum plantlets* using light emitting diodes. Cent. Eur. J. Biol. 3: 161–167.

Lan J.C.W., Raman K., Huang C.M. & Chang C.M. (2013). The impact of monochromatic blue and red LED light upon performance of photo microbial fuel cells (PMFCs) using *Chlamydomonas reinhardtii* transformation as biocatalyst. Biochem. Engin. J. 78: 39–43.

Lange B.M., Wildung M.R., Stauber E.J., Sanchez C., Pouchnik D. & Croteau R. (2000). Probing essential oil biosynthesis and secretion by functional evaluation of expressed sequence tags from mint glandular trichomes. Proc. Nati. Acad. Sci. 97: 2934–2939.

Lange B.M., Mahmoud S.S., Wildung M.R., Turner G.W., Davis E.M., Lange I., Baker R.C., Boydston R.A. & Croteau R.B. (2011). Improving peppermint essential oil yield and composition by metabolic engineering. Proc. Nat. Acad. Sci. USA. 108: 16944–16949.

Lange B.M., Lange I., Turner G.W. & Herron B.K. (2013). Utility of Aromatic Plants for the Biotechnological Production of Sustainable Chemical and Pharmaceutical Feedstocks. Med. Aromat. Plants.

Lemoine Y. & Schoefs B. (2010). Secondary ketocarotenoid astaxanthin biosynthesis in algae: a multifunctional response to stress. Photosynth. Res. 106: 155–177.

Lendenmann M., Thonar C., Barnard R.L., Salmon Y., Werner R.A., Frossard E. & Jansa j. (2011). Symbiont identity matters: carbon and phosphorus fluxes between *Medicago truncatula* and different arbuscular mycorrhizal fungi. Mycorrhiza 21: 689–702.

Levitan O., Dinamarca J., Zelzion E., Lun D.S., Guerra L.T., Kim M.K., Kim J., AS Van Mooy B., Bhattacharya D. & Falkowski P.G. (2015). Remodeling of intermediate metabolism in the diatom *Phaeodactylum tricornutum* under nitrogen stress. Proc. Natl. Acad. Sci. 112: 412–417.

Li H.M., Xu Z.G. & Tang C.M. (2010). Effect of Light emitting diodes on growth and morphogenesis of upland cotton (*Gossypium hirsutum* L.) plantlets *in vitro*. Plant Cell Tiss. Organ Cult. 103: 155–163.

Li Y., Zhou W., Hu B., Min M., Chen P. & Ruanb R.R. (2012). Effect of light intensity on algal biomass accumulation and biodiesel production for mixotrophic strains *Chlorella kessleri* and *Chlorella protothecoide* cultivated in highly concentrated municipal wastewater. Biotechnol. Bioeng. 109: 2222–2229.

Li H., Tang C. & Xu Z. (2013). The effects of different light qualities on rapeseed (*Brassica napus* L.) plantlet growth and morphogenesis *in vitro*. Scient. Hortic. 150: 117–124.

Lin C. (2000). Plant bluelight receptors. Trends Plant Sci. 5: 337–342.

Lohse S., Schliemann W., Ammer C., Kopka J., Strack D. & Fester T. (2005). Organization and metabolism of plastids and mitochondria in arbuscular mycorrhizal roots of *Medicago truncatula.* Plant Physiol. 139: 329–340.

Louche-Tessandier D., Samson G., Hernandez-Sebastia C., Chagvardieff P. & Desjardins Y. (1999). Importance of light and CO_2 on the effects of endomycorrhizal colonization on growth and photosynthesis of potato plantlets (*Solanum tuberosum*) in an *in vitro* tripartite system. New Phytol. 142: 539–550.

Machu L., Misurcova L., Vavra Ambrozova J., Orsavova J., Mlcek J., Sochor J. & Jurikova T. (2015). Phenolic content and antioxidant capacity in algal food products. Molecules 20: 11181133.

Magnard J.L., Roccia A. et al. (2015). Biosynthesis of monoterpene scent compounds in roses. Science 349: 81–83.

Malayeri S.H., Hikosaka S., Ishigami Y. & Goto E. (2011). Growth and photosynthetic rate of Japanese mint (*Mentha arvensis*) grown under controlled environment. Acta. Hort. 907:73–79.

Manach C., Scalbert A., Morand C., Rémésy C. & Jiménez L. (2004). Polyphenols: Food sources and bioavailability. Am. J. Clin. Nutr. 79*:* 727–747.

Martin-Jézéquel V., Schoefs B. & Heydarizadeh P. (2012). Diatom's genome: which carbon's pathway and for what use? Book of abstracts of the '6èmes journées scientifiques du réseau français de métabolomique et fluxomique' (RFMF), Nantes. 78

Matsuda Y. & Kroth P.G. (2014). Carbon fixation in diatoms. In the structural basis of biological energy generation. Springer Netherlands. 335**–**362.

Mc Caskill D., Gershenzon J. & Croteau R. (1992). Morphology and monoterpene biosynthetic capabilities of secretory cell clusters isolated from glandular trichomes of peppermint (*Mentha piperita* L.). Planta 187: 445–454.

Mc Caskill D. & Croteau R. (1999). Strategies for bioengineering the development and metabolism of glandular tissues in plants. Nat. Biotech. 17: 31–36.

Meitao Dong M., Zhang X., Zhuang Z., Zou J., Ye N., Xu D., Mou S., Liang C. & Wang W. (2012). Characterization of the LhcSR gene under light and temperature stress in the green alga *Ulva linza.* Plant Mol. Biol. Rep. 30: 10–16.

Meskhidze N., Sabolis A., Reed R. & Kamykowski D. (2015). Quantifying environmental stressinduced emissions of algal isoprene and monoterpenes using laboratory measurements. Biogeo Sci. 12: 637**–**651.

Mimouni V., Ulmann L., Pasquet V., Mathieu M., Picot L., Bougaran G., Cadoret J.P., Morant-Manceau A. & Schoefs B. (2012). The potential of microalgae for the production of bioactive molecules of pharmaceutical interest. Curr. Pharm. Biotech. 13: 2733–2750.

Monica R.C. & Cremonini R. (2009). Nanoparticles and higher plants. Caryologia 62: 161–165.

Mouget J.L., Rosa P. & Tremblin G. (2004). Acclimation of Haslea ostrearia to light of different spectral qualities–confirmation ofchromatic adaptation in diatoms. J. Photochem. Photobiol. B: Biol. 75: 111.

Moulin P., Lemoine Y. & Schoefs B. (2011). Carotenoids and stress in higher plants and algae. In: Pessarakli M. (ed.). Handbook of plant and crop stress. Taylor and Francis, New York, 407–433.

Moulin P., Lemoine Y. & Schoefs B. (2010). Modification of the carotenoid metabolism in plastids: A response to stress conditions. In Handbook of Plant and Crop Stress. Pessarakli M. (Ed.). 407–433. Boca Raton. CRC Press.

Muller Feuga A. (1996). Microalgues marines. Les enjeux de la recherche. Institut Français de Recherche pour l'Exploitation de la Mer, Plouzané.

Mustárdy L. & Garab G. (2003). Granum revisited. A threedimensional model–where things fall into place. Trends Plant Sci. 8: 117–122.

Myklestad S. & Granum E. (2009). Biology of (1,3) β-glucans and related glucans in protozoans and chromistans. Chemistry, biochemistry, and biology of (1,3) β-glucans and related polysaccharides. Academic Press, Boston. 353–385.

Neilson J.A. & Durnford D.G. (2010). Structural and functional diversification of the lightharvesting complexes in photosynthetic eukaryotes. Photosynth. Res. 106: 57–71.
Nelson N. & Ben Shem A. (2004). The complex architecture of oxygenic photosynthesis. Nature Rev. Mol. Cell Biol. 5:.971–982.
Newsham K.K., Fitter A.H. & Watkinson A.R. (1995). Arbuscular mycorrhiza protect an annual grass from root pathogenic fungi in the field. J. Ecol. 83: 991–1000.
Nguyen-Deroche T.L.N., Caruso A., Trung Le T., Viet Bui T.V., Schoefs B., Tremblin G. & Morant-Manceau A. (2012). Zinc affects differently growth, photosynthesis, antioxidant enzyme activities and phytochelatin synthase expression of four Marine Diatoms. Sci. World J. 15.
Niewiadomski P., Knappe S., Geimer S., Fischer K., Schulz B., Unte U.S., Rosso M.G., Ache P., Flugge U.I. & Schneider A. (2005). The Arabidopsis plastidic glucose 6phosphate/phosphate translocator GPT1 is essential for pollen maturation and embryo sac development. Plant Cell 17: 760–775.
Nishioka N., Nishimura T., Ohyama K., Sumino M., Malayeri S.H., Goto E., Inagaki N. & Morota T. (2008). Light quality affected growth and contents of essential oil components of Japanese mint plants. Acta Hortic. 797.
Norici A., Bazzoni A.M., Pugnetti A., Raven J.A. & Giordano M. (2011). Impact of irradiance on the C allocation in the coastal marine diatom *Skeletonema marinoi Sarno* and Zingone. Plant Cell Environ. 34: 1666–1677.
Nymark M., Valle K., Brembu T., Hancke K., Winge P., Andresen K., Johnsen G. & Bones A. (2009). An integrated analysis of molecular acclimation to high light in the marine diatom *Phaeodactylum tricornutum*. PLoS One 4: e7743.
Olvera-Gonzalez E., Alaniz-Lumbreras D., Ivanov-Tsonchev R., Villa-Hernández J., Olvera-Olvera C., González-Ramírez E., Araiza-Esquivel M., Torres-Argüelles V. & Castaño V. (2013). Intelligent lighting system for plant growth and development. Comput. Electron. Agr. 92: 48–53.
Parádi I., Bratek Z. & Láng F. (2003). Influence of arbuscular mycorrhiza and phosphorus supply on polyamine content, growth and photosynthesis of *Plantago lanceolata*. Biol. Plant 46: 563–569.
Park K.J., Vohnikova Z. & Brod F.P.R. (2002). Evaluation of drying parameters and desorption isotherms of garden mint leaves (*Mentha crispa* L.). J. Food Eng. 51: 193–199.
Pedone-Bonfim M.V.L., da Silva F.S.B. & Maia L.C. (2015). Production of secondary metabolites by mycorrhizal plants with medicinal or nutritional potential. Acta. Physiol. Plant. 37: 112.
Pfeffer P.E., Douds D.D., Becard G. & ShacharHill Y. (1999). Carbon uptake and the metabolism and transport of lipids in an arbuscular mycorrhiza. Plant Physiol. 120: 587–598.
Pfeil B., Schoefs B. & Spetea C. (2014). Function and evolution of channels and transporters in photosynthetic membranes. Cell. Mol. Life Sci. 71: 979–998.
Prihoda J., Tanaka A., Paula W.B.M., Allen J.F., Tirichine L. & Bowler C. (2012) Chloroplastmitochondria crosstalk in diatoms. J. Exp. Bot. 63: 1543–1557.
Pulz O. & Scheibenbogen K. (1998). Photobioreactors: designand performance with respect to light energy input. Adv. Biochem. Eng. Biotechnol. 59: 123–151.
Pulz O. & Gross W. (2004). Valuable products from biotechnology of microalgae. Appl. Microbiol. Biotechnol. 65: 635–648.
Ramawat K.G., Dass S. & Mathur M. (2009). The chemical diversity of bioactive molecules and therapeutic potential of medicinal plants. In Herbal drugs: ethnomedicine to modern medicine Springer Berlin Heidelberg. 732.
Ratti N., Khaliq A., Shukla P.K., Haseeb A. & Janardhanan K.K. (2015). Effect of *Glomus mosseae* (Nicol. and Gerd.) Gerdemann and Trappe on rootknot disease of menthol mint (*Mentha arvensis* sub sp. haplocalyx Briquet) caused by Meloidogyne incognita (Kofoid and White) Chitwood. J. Spices Aromat. Crops. 9(2).

Rech M., Morant-Manceau A. & Tremblin G. (2008). Carbon fixation and carbonic anhydrase activity in *Haslea ostrearia* (Bacillariophyceae) in relation to growth irradiance. Photosynthetica 46: 56–62.
Recorbet G., Valot B., & DumasGaudot E. (2008). Plasma membrane proteins in arbuscular mycorrhiza. In: Plant Cell Compartments Selected Topics, Research Signpost. Schoefs B (Ed.). Kerala, India. 367–384.
Redecker D., Kodner R. & Graham L.E. (2000). Glomalean fungi from the Ordovician. Science 289: 1920–1921.
Reitan K.I., Rainuzzo J.R. & Olsen Y. (1994). Effect of nutrient limitation on fatty acid and lipid content of marine microalgae. J. Phycol. 30: 972–979.
Ritchie R.J. (2010). Modelling photosynthetic photon flux flux density and maximum potential gross photosynthesis. Photosynthetica 48: 596–609.
Rivero J., Gamir J., Aroca R., Pozo M.J. & Flors V. (2015). Metabolic transition in mycorrhizal roots. Front. Microbiol. 6: 598.
Rockwell N.C., Su Y.S. & Lagarias J.C. (2006). Phytochrome structure and signaling mechanisms. Annu. Rev. Plant Biol. 57:837–878.
Rodríguez-Concepción M. & Boronat A. (2002). Elucidation of the methylerythritol phosphate pathway for isoprenoid biosynthesis in bacteria and plastids. A metabolic milestone achieved through genomics. Plant physiol. 130: 1079–1089.
Roháček K., Soukupová J. & Barták M. (2008). Chlorophyll fluorescence: A wonderful tool to study plant physiology and plant stress. In Plant Cell Compartments. Selected Topics. Schoefs B. (Ed.). Research Signpost, Kerala, India. 41–104.
Rohácek K. (2010). Method for resolution and quantification of components of the non-photochemical quenching (qN). Photosynth. Res. 105: 101–113.
Rohácek K., Bertrand M., Moreau B., Jacquette J., Caplat C., Morant-Manceau A. & Schoefs B. (2014). Relaxation of the non-photochemical Chlorophyll fluorescence quenching in diatoms: kinetics, components and mechanisms. Phil. Trans. R. Soc. 369: 20130241.
Rowland S.J., Belt S.T., Wraige E.J., Massé G., Roussakis C. & Robert J. M. (2001). Effects of temperature on polyunsaturation in cytostatic lipids of *Haslea ostrearia*. Phytochem. 56: 597–602.
Saade A. & Bowler C. (2009). Molecular tools for discovering the secrets of diatoms. BioScience 59: 757–765.
Sapriel G., Quinet M., Heijde M., Jourdren L., Tanty V., Luo G., Le Crom S. & Lopez P.J. (2009). Genomewide transcriptome analyses of silicon metabolism in *Phaeodactylum tricornutum* reveal the multilevel regulation of silicic acid transporters. PLoS One 4: e7458.
Schliemann W., Ammer C. & Strack D. (2008). Metabolite profiling of mycorrhizal roots of *Medicago truncatula*. Phytochemistry 69: 112–146.
Schoefs B. (2002). Chlorophyll and carotenoid analysis in food products. Properties of the pigments and methods of analysis. Trends Food Sci. Tech. 13: 361–371.
Schoefs B. (2003). Chlorophyll and carotenoid analysis in food products. A practical casebycase view. TrAC Trends Anal. Chem. 22: 335–339.
Schoefs B. (2005). Plant pigments: properties, analysis, degradation. Adv. Food Nutr. Res. 49: 42–92.
Seddas P., GianinazziPearson V., Schoefs B., Küster H. & Wipf D. (2009). Communication and signaling in the plantfungus symbiosis: the mycorrhiza. Dans: PlantEnvironment Interactions. Baluska F (Ed.). Springer Verlag. 45–71.
Selosse M.A. & Le Tacon F. (1998). The land flora: a phototrophfungus partnership?. Trend. Ecol. Evol. 13: 15–20.
Shukla S.K. & Mohan R. (2012). The contribution of diatoms to worldwide crude oil deposits. In the science of algal fuels: phycology, geology, biophotonics, genomics and nanotechnology,

Gordon R. & Seckbach J. (Eds.). Springer, Dordrecht, The Netherlands. 355–382.
Shrestha R.P., Tesson B., NordenKrichmar T., Federowicz S., Hildebrand M. & Allen A.E. (2012). Whole transcriptome analysis of the silicon response of the diatom *Thalassiosira pseudonana.* BMC Genomics 13: 499.
Simon L., Bousquet J., Lévesque R.C. & Lalonde M. (1993). Origin and diversification of endomycorrhizal fungi and coincidence with vascular land plants. Nature. 363: 67–69.
Sinatra R.S., Jahr J.S. & WatkinsPitchford J.M. (2010). The essence of analgesia and analgesics. Cambridge University Press. 82–90.
Singh D., Basu C., MeinhardtWollweber M. & Roth B. (2015). LEDs for energy efficient greenhouse lighting. Renew. Sust. Energ. Rev. 49: 139–147.
Smetacek V. (1999). Diatoms and the ocean carbon cycle. Protist 150: 25–32.
Smith S.E. & Read D.J. (2008). Mycorrhizal symbiosis. Cambridge UK: Academic Press.
Soka G. & Ritchie M. (2015). Arbuscular mycorrhizal symbiosis, ecosystem, processes and environmental changes in tropical soils. Appl. Ecol. Environ. Res. 13: 229–245.
Solymosi K. (2012). Plastid structure, diversification and interconversions in algae. Curr. Chem. Biol. 6:167–186.
Sozer O., Kis M., Gombos Z. & Ughy B. (2011). Proteins, glycerolipids and carotenoids in the functional photosystem II architecture. Front. Bio. Sci. 16: 619–643.
Spetea C., Rintamäki E. & Schoefs B. (2014). Changing the light environment: chloroplast signalling and response mechanisms. Phil. Trans. R. Soc. B. 369: 20130220
Sturm A. & Tang G.Q. (1999). The sucrosecleaving enzymes of plants are crucial for development, growth and carbon partitioning. Trends Plant Sci. 4: 401–407.
Sullivan C. (2014). Human population growth creeps back up. Scientific American. http://www. scientificamerican. com/article/humanpopulationgrowthcreepsbackup/>. Accessed, 11.
Svoboda K.P., Svoboda T.G. & Syred A.D. (2001). A closer look: secretory structures of aromatic and medicinal plants. HerbalGram 53: 34–43.
Takeda N., Handa Y., Tsuzuki S., Kojima M., Sakakibara H. & Kawaguchi M. (2015). Gibberellins interfere with symbiosis signaling and gene expression and alter colonization by arbuscular mycorrhizal fungi in *Lotus japonicus.* Plant Physiol. 167: 545–557.
Tan Nhut D., Takamura T., Watanabe H. & Tanaka M. (2005). Artificial light source using Light emitting Diodes (LEDs) in the efficient micropropagation of *Spathiphyllum* plantlets. Acta Hort. 692: 137–142.
Tarakanov I., Yakovleva O., Konovalova I., Paliutina G. & Anisimov A. (2012). Light emitting diodes: on the way to combinatorial lighting technologies for basic research and crop production. In VII international symposium on light in horticultural systems. 956: 171–178.
Taylor T.N., Remy W., Hass H. & Kerp H. (1995). Fossil arbuscular mycorrhizae from the Early Devonian. Mycologia. 87: 560–573.
Tissier A (2012). Glandular trichomes: what comes after expressed sequence tags? Plant J. 70: 51–68.
Tennessen D.J., Singsaas E.L. & Sharkey T.D. (1994). Light emitting diodes as a light source for photosynthesis research. Photosynth. Res. 39: 85–92.
Terry K.L., Hirata J. & Laws E.A. (1983) Lightlimited growth of two strains of the marine diatom *Phaeodactylum tricornutum* Bohlin: chemical composition, carbon partitioning and the diel periodicity of physiological processes. J. Exp. Mar. Biol. Ecol. 68: 209–227.
Trakranrungsie N. (2011). Plant derived antifungal trends and potential applications in veterinary medicine: A minireview. Science against microbial pathogens: communicating current research and technological advances. Formatex. 1195–1204.
Urbonavičiūtė A., Samuolienė G., Brazaitytė A., Ulinskaitė R., Jankauskienė J., Duchovskis P. & Zukauskas A. (2008). The possibility to control the metabolism of green vegetables and sprouts using light emitting diode illumination. Sodininkystė ir Daržininkystė. 27: 83–92.

Valentine A.J., Osborne B.A. & Mitchell D.T. (2001). Interactions between phosphorus supply and total nutrient availability on mycorrhizal colonization, growth and photosynthesis of cucumber. Sci. Hortic. 88: 177–189.
van der Heijden M.G., de Bruin S., Luckerhoff L., van Logtestijn R.S. & Schlaeppi K. (2015). A widespread plantfungalbacterial symbiosis promotes plant biodiversity, plant nutrition and seedling recruitment. ISME J. 111.
Vinayak V., Manoylov K.M., Gateau H., Blanckaert V., Hérault J., Pencréaćh G., Marchand J., Gordon R. & Schoefs B. (2015). Diatom milking: a review and new approaches. Marine drugs 13: 2629–2665.
Vidoudez C. & Pohnert G. (2008). Growth phase specific release of polyunsaturated aldehydes by the diatom Skeletonema marinoi. J. Plankton Res. 30: 1305–1313.
Vidoudez C. & Pohnert G. (2012). Comparative metabolomics of the diatom *Skeletonema marinoi* in different growth phases. Metabolomics 8: 654–669.
Walter M.H., Stauder R. & Tissier A. (2015). Evolution of rootspecific carotenoid precursor pathways for apocarotenoid signal biogenesis. Plant Sci. 233: 110.
Wang B. & Qiu Y.L. (2006). Phylogenetic distribution and evolution of mycorrhizas in land plants. Mycorrhiza. 16: 299–363.
Williams P.J.L.B. & Laurens L.M. (2010). Microalgae as biodiesel & biomass feedstocks: Review & analysis of the biochemistry, energetics & economics. Energy Environ. Sci. 3: 554–590.
Wink M. (1988). Plant breeding importance of plant secondary metabolites for protection against pathogens and herbivores. Theor. Appl. Genet. 75: 14322242.
Wink M. (2003). Evolution of secondary metabolites from an ecological and molecular phylogenetic perspective. Phytochem. 64: 319.
Zeng Y., Gu L.P., Che D.B., Hao Z.P., Wang J.Y., Huang L.Q., Yang G., Cui X.M., Yang L., Wu Z.X., Chen M.L. & Zhang Y. (2013). Arbuscular mycorrhizal symbiosys and active ingredients of medicinal plants: current research status and prospectives. Mycorrhiza 23: 253–265.
Zhao P., Gu W., Wu S., Huang A., He L., Xie X., Gao S., Zhang B., Niu J., Lin A.P. & Wang G. (2014). Silicon enhances the growth of *Phaeodactylum tricornutum* Bohlin under green light and low temperature. Sci. rep. 4.

Part I

Regulation of secondary metabolites production in *Phaeodactylum tricornutum* under different light intensities

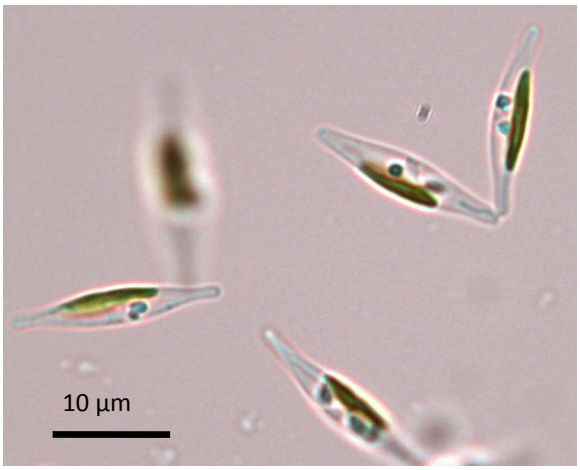

These last years, the interest for microalgae, including diatoms has been increased as these organisms start to accumulate high value compounds such as pigments, fatty acids, xanthophylls, astaxanthin, *β-carotene*, fucoxanthin and biofuels, when facing abiotic stresses. Despite the efforts made in microalgae engineering, the culture systems are still not as efficient as they should do to satisfy the demand. We believe that it is mainly due to the wide gaps between the knowledge of microalgae like diatom biochemistry and physiology, especially when responses to stress conditions are concerned (Chapter 2). Therefore, deciphering the complex interactions of diatoms and their metabolic responses in their natural environment first requires a better understanding of the metabolic responses in simple and controlled environment. One possibility to reach this goal consists to more efficiently and effectively leverage large-scale genomewide databases to address contemporary issues such as improving algal lipid yields for algal applications. *P. tricornutum* is a very good candidate producing numerous bioactive molecules of interest for health such as lipid rich in omega-3 fatty acids including EPA and carotenoids (*e.g.* fucoxanthin). As the complete genome sequence of the diatom has become available, it has been intensively studied at the genomic and transcriptomic levels and studies on cell physiology and metabolism during stress have been developed recently. Physiological reactions of the cells to different light intensities during the growth have been studied in the past, but the molecular mechanisms, especially those involving in carbon metabolism, has not been reported yet. This theme constitutes the core of this part of the manuscript. It starts with an introductory chapter (chapter 2) explaining why the understanding of cell functioning requires complementary approaches and diatoms are used as examples. Following this guidelines, we used bioinformatic tools to develop a model of central carbon metabolism in the diatom *P. tricornutum*. Cells were then grown under different light intensities and their responses observed at the molecular, biochemical and physiological levels. The metabolic pathway model was used to analyze transcriptome data to address questions with regard to the regulation of secondary metabolites (Chapter 3).

Chapter 2

Functional investigations in diatoms need more than a transcriptomic approach

Parisa Heydarizadeh[a,b], Justine Marchand[a], Benoit Chenais[a], Mohammad R. Sabzalian[b], Morteza Zahedi[b], Brigitte Moreau[a] and Benoît Schoefs[a*]

[a] MicroMar, Mer Molécules Santé, LUNAM, IUMLFR 3473 CNRS, University of Le Mans, Le Mans, France
[b] Department of Agronomy and Plant Breeding, College of Agriculture, Isfahan University of Technology, Isfahan, Iran

* Corresponding author
email: benoit.schoefs@univ-lemans.fr
Tel: +33 2 43 83 37 72
fax: +33 2 43 83 39 17

Diatom research (2014). 29 (1): 75-89.

2.1 Abstract

The particular gene complement in diatoms, inherited from various types of organisms, has contributed to the development of metabolic networks that contrast with those found in other photosynthetic organisms. To understand these networks and how they are linked, transcriptomic, proteomic and metabolomic approaches have been used over the last decade. Understanding how these networks developed and interact remains a major goal for physiologists. Metabolic compartmentalization and fluxes between compartments are still poorly known, requiring: (1) the localization of proteins and biological activities, as well as potential protein isoforms and (2) relating metabolite measurements to pathway fluxes. Moreover, when considering metabolism, the identification of transcription factors, which are largely unknown for diatoms, is necessary. Integration of the results from these different approaches will complete our understanding of cell functioning and how differences impact metabolic reorientation.

Keywords: diatom, microalgae, transcriptomic, proteomic, metabolomic, metabolism, network, regulation

2.2 Introduction

Since the appearance of the first agricultural practices, humans have tried to improve plants to produce food, animal feed and highvalue compounds. These practices, which have supported the development of human communities all over the world, would not have been possible without a petroleum-based economy producing fuels, materials, such as plastic and chemicals, such as fertilizers. This economy has at least three major consequences: (1) a shortage of natural resources, (2) a competition for land to produce energy and food, and (3) a rise in the atmospheric CO_2 concentration (Feely et al. 2008). For example, Dukes (2003) reported that the total fossil fuels consumed per year release 44 × 1018 g of carbon into the atmosphere, *i.e*. 400-fold the amount fixed by photosynthesis. This large difference between carbon release in the atmosphere and carbon fixation results in a carbon accumulation in the atmosphere, which has a strong ecological impact known as global warming. Consequently, the petroleum-based economy does not appear to be sustainable for much longer.

The increase in atmospheric CO_2 also has an impact on the oceans because atmospheric CO_2 dissolves in water to form $HCO_3^- + H^+$, which ultimately decreases the pH and carbonate ion concentration in seawater (Orr et al. 2005; Wu et al. 2010). Acidification of the ocean may have pleiotropic effects on living organisms because it can perturb respiration and photosynthetic activities (Crawley et al. 2010; Wu et al. 2010), disturb the calcification processes of diverse organisms (for a review, see Doney et al. 2012) and modify the vertical stratification of water, a phenomenon that modifies sound absorption (Hester et al. 2008) and isolates plankton from nutrient sources. The production of biomass from phototrophic macro and/or microorganisms is one type of CO_2 mitigation technology (Benemann, 1997) aimed at reducing these negative effects. Among the algae, diatoms constitute the most abundant group of marine eukaryotic organisms, contributing ~20–40% of the organic matter produced in the ocean, which is more than all terrestrial rainforests combined (Field et al. 1998; Granum et al. 2005; Bowler et al. 2010). In addition, diatoms are very promising biotechnological tools because they are capable of producing many highvalue compounds such as polysaccharides, lipids, polyunsaturated fatty acids, pigments and biofuels (Cadoret et al. 2012; Mimouni et al. 2012; Heydarizadeh et al. 2013). Last, but not least, diatoms are promising subjects for the preparation of nanotechnological tools (Kroger & Poulsen, 2008).

Despite the important progress made in microalgal bioreactor technology (Cogne et al. 2011; Vasseur et al. 2012), the use of algae as cell factories remains in its infancy.We believe that the major reason for this is that the gaps in the knowledge of diatom biochemistry and physiology are still tremendous, especially where responses to stress conditions are concerned. A deep knowledge of algal stress physiology is of particular importance for biotechnology because the production of highvalue compounds often

results from metabolic shifts that are induced by stressful conditions. For example, blue light triggers accumulation of the blue pigment mareninne, typical of *Haslea ostrearia* (Bory) Simonsen (Mouget et al. 2005). Elucidation of the regulatory mechanisms involved in the incorporation of carbon atoms fixed by photosynthesis into biomass and/or highvalue compounds is crucial. The cellular metabolism of an autotrophic cell can be illustrated using a marshalling yard, in which each railroad represents a biosynthetic pathway ending with the production of particular compounds.

The entry of carbon is achieved through the fixation of CO_2 via ribulose1,5-bisphosphate carboxylase/oxygenase (RubisCo) or phospho*enol*pyruvate carboxylase (PEPCK; Raven, 1993). Under nonstressful conditions, the carbon is mostly used to produce carbohydrates through primary metabolism. Stress conditions trigger modifications of the metabolic switches, changing the flow of the carbon toward new compounds (*e.g*. Lemoine & Schoefs, 2010).

Which biochemical pathways are used to drive the carbon atoms for the synthesis of stressinduced compounds? What are the regulatory elements involved in the control of the switches? En route toward answering these questions, the first goal has been to establish a list of the potential proteins involved in cell functioning. The first part of this article (Genome sequencing: towards the system's part list) briefly explains what wholegenome sequencing has provided. With genomics data in hand, the second goal is to draw metabolic schemes, taking into account the compartmentalization of enzymatic activities.

Genome sequencing allows the development of further global (omics) approaches, which, when combined, permit an understanding of the interplay between the major players, *e.g.* genes (genomics), RNA (transcriptomics), proteins (proteomics) and metabolites in a cell. The need to combine different global approaches is explained (Combining several 'omics' to generate cell models) and finally the control of metabolic networks by transcription factors is considered.

2.3 Genome sequencing: towards the system's part list

One of the major goals of modern biology is to elucidate the mechanisms that allow organisms to modulate their functioning according to changing environmental conditions.

To reach this goal, it became obvious that the identity of the players involved in the systems, *i.e.* the system's 'parts list' should be established. Until data from genome sequencing became available, the system's part list was progressively built up using biochemical studies, such as enzyme isolation or radioactive tracers. For example, using radiolabelled carbon ($NaH_{14}CO_3$), Rech et al. (2008) studied carbon allocation between C_3 and C_4like carbon acquisition metabolism in the diatom *H. ostrearia*, grown under different light conditions. Under blue light, more carbon was allocated to the C_4-like

pathway than the C_3 pathway, whereas the opposite occurred under green light. In addition to the typical metabolites of the C_3 and C_4 pathways, some unusual compounds, such as sucrose and glycerol were labelled, suggesting that adaptation to green light conditions requires a specific enzyme set. However, how frequently such particularities appear remains difficult to estimate.

The 'one gene–one protein' hypothesis (Beadle & Tatum, 1941) introduced the idea that determining all the coding sequences in a genome would at least furnish the system's parts list. For technical reasons, it took ~30 years before the first genome was sequenced (Fiers et al. 1976) and another 20 years before genomesequencing techniques were available to the scientific community. The first diatom genome sequenced was that of *Thalassiosira pseudonana* (Hustedt) Hasle & Heimdal (Armbrust et al. 2004).

Since then, several other sequenced genomes have either been published or completed, or are close to completion (Table 2.1). Genome analyses have revealed that significant horizontal gene transfer from bacteria has occurred (Bowler et al. 2008; Keeling & Palmer, 2008), with at least 587 genes (~5% of the total genome) of putative bacterial origin in the *Phaeodactylum tricornutum* Bohlin genome (Bowler et al. 2008). This is a much higher proportion than in other eukaryotes, and includes bacterial genes derived from different lineages (proteobacteria, cyanobacteria and archaea; Bowler et al. 2008). A large number of these genes are involved in organic carbon and nitrogen utilization processes. Examples include the cytosolic NAD(P)H-dependent nitrite reductase that is homologous to nirB of bacteria and fungi, and a mitochondrial glutamine synthase III. None of these enzymes could be found in green algae or land plants (Robertson & Alberte, 1996; Armbrust et al. 2004; Allen et al. 2006; Siaut et al. 2007). Diatoms also have many animal genomelike features. For instance, 806 deduced protein sequences (~7% of the total proteome) of *T. pseudonana* present homologies with mouse, but not land plant or red algal genes (Armbrust et al. 2004). Recent genomic analyses also suggested that many diatom genes actually have a green algal origin (reviewed in Archibald, 2012; Deschamps & Moreira, 2012; Mock & Medlin, 2012).

Thus, genomic data have revealed the mosaic character of diatom genomes. Genes originating from widely diverse sources have contributed to produce organisms with unique properties, such as the presence of four envelopes around the chloroplast and the absence of grana stacks (reviewed in Solymosi, 2012), a periplastid endoplasmic reticulum (Palmer & Delwiche, 1998), unique pigment composition (reviewed in Bertrand, 2010; Heydarizadeh et al. 2013) and biochemical pathways such as a full urea cycle (Armbrust et al. 2004; Bowler et al. 2008; Allen et al. 2011). Genomic data have also revealed new pathways or the particular cell localization of pathways (Kroth et al. 2008; Allen et al. 2011; Fernie et al. 2012) (see below) and have contributed to a more comprehensive understanding of the metabolic networks in diatoms. They have also

revealed the existence of putative proteins with unknown functions (Armbrust et al. 2004; Bowler et al. 2008; Hanson et al. 2010), for which functional studies should be performed to determine their physiological role.

2.4 From the genome to the biochemical model, or who is connected with whom?

The basis of cell functioning is the metabolic network, composed of interconnected individual reactions along which substrates are converted to products. Most individual reactions are catalysed by enzyme(s) although a few are spontaneous (*e.g*. Daher et al. 2010). Our current understanding of diatom metabolic networks lags significantly behind that for green algae or higher plants and, accordingly, knowledge from the latter models was often transferred to diatoms.

For instance, when the first experimental evidence of a C_4 mechanism for CO_2 fixation in diatoms became available, this was interpreted in the context of higher plant and green algal metabolism (Beardall et al. 1976). Reconstruction of diatom metabolic networks based on genome sequencing has revealed numerous unique features of their metabolism that differentiate them from Plantae (for a review, see Fernie et al. 2012).

The deduced amino acid sequence of proteins contains information about the cellular localization and function of proteins. The presence of conserved protein domains (*e.g*. ATPase, DNA binding) and the similarity to sequences of proteins/genes for which function has been established can inform functional annotation. However, similar sequences may encode proteins that catalyse different reactions (Hanson et al. 2010). Therefore, functional annotation based only on sequence analysis should be interpreted with caution; only demonstration of biochemical activity can confirm annotation. For instance, similarity based annotation revealed the presence of six putative carbonic anhydrase (CA) genes in the *P. tricornutum* genome, although the active site in four of these lacked a conserved histidine residue (Tachibana et al. 2011). Two *β*CAs have already been identified as active in the chloroplast (Satoh et al. 2001; Tanaka et al. 2005). Whether these four putative CA genes also encode active CAs remains an open question that should be addressed at the functional level (Tachibana et al. 2011).

Draft metabolic networks reconstructed from genomic information are provided by KEGG (http://www.genome.jp/kegg/pathway.html) or Diatomcyc (http://Diatomcyc.org/) (Fabris et al. 2012). It is important to recognize that these schemes are only a starting point for understanding diatom metabolism. Often they do not provide information about the compartment in which the pathways function (see below) or about the direction of metabolite flux under different ecophysiological conditions. This information is difficult to predict because biochemical reactions are formally reversible, but forward and reverse reactions are often catalysed by different enzymes. The duplication of pathways in different compartments may result in opposite metabolic

flows. For instance, the plastidial Calvin–Benson cycle and the cytoplasmic oxidative pentose phosphate pathway mediate net carbon flux in opposite directions. Consequently, the activities of the associated enzymes are tightly regulated, for instance, through co and/or post-translational modifications (Baiet et al. 2011; MathieuRivet et al. 2013). Thus, understanding metabolic adjustments in response to environmental stimuli involves several aspects that are not covered by information extracted from genome sequences.

2.5 Physiology requires an integrated model taking into account the cellular compartmentalization of the biochemical activities

Eukaryotic metabolism is strongly compartmentalized, *i.e.* different pathways or reactions occur only in particular organelles. Compartmentalization is a result of endosymbiosis and/or the presence of a membrane for enzymatic activity (Palmer & Delwiche, 1998; Schoefs, 2008; Curtis et al. 2012; Gould, 2012; Spetea et al. 2012). For instance, the biosynthetic pathway leading to photosynthetic pigment production is only located in chloroplasts (for reviews, see Bertrand, 2010; Heydarizadeh et al. 2013). The concept of microcompartments emerged from the observation that the biochemical activities in an organelle are not homogeneously distributed within it, but are located in specialized areas (for a review, see Sweetlove & Fernie, 2013).

For instance, plant membranes contain microdomains and rafts that can influence the spatiotemporal organization of protein complexes, thereby conferring specialization on these microdomains (for a review, see Malinsky et al. 2013). To our knowledge, the only report on the presence of rafts in microalgae was obtained from the green alga *Chlorella kessleri*, whose hexose–proton symporter HUP1 showed a spotty distribution on the plasma membrane of the yeast *Saccharomyces cerevisiae* (Grossmann et al. 2006).

Gierasch & Gershenson (2009) consider that few (if any) enzymes occur free in solution. There are many reasons (pH optimum, inhibition by metabolic intermediates, *etc*.) why particular pathways occur in separate compartments.

For instance, the xanthophyll de-epoxidation step of the xanthophyll cycle requires considerable acidification of the thylakoid lumen (pH~4.5) that would be incompatible with the activity of enzymes in the stroma (pH~6.8) for a review, see Bertrand, 2010). Thus, full understanding of cell functioning requires the composition and structure of both organelles and microcompartments to be determined.

In turn, this requires the isolation of cell compartments combined with assays to detect the presence and activity of selected enzymes. Isolation of highly enriched fractions of intact diatom organelles remains difficult (for a review, see Kroth, 2007). To our knowledge, only plasma membrane (Sullivan et al. 1974), thylakoid membranes

Table 2.1. List of the diatom genomes or transcriptomes sequenced or close to completion.

Type of diatom	Name	Ecology	Sequenced	Genome size (Mb)	Number of predicted genes	Core genes	Diatom-specific genes	Unique genes	Ref
Centric	*Thalassiosira pseudonana*	Marine, pelagic	Yes	32.4	11 776	4332	1407	3912	Armbrust et al. (2004)
	Thalassiosira oceanica(Hasle)	Marine, planktonic							Lommer et al. (2012)
Pennate	*Phaeodactylum tricornutum*	Marine, benthic	Yes	27.4	10 402	3523	1328	4366	Bowler et al. (2008)
Pennate	*Fragilariopsis cylindrus*(Grunow)	Marine, psychrophilic	Yes	80.5	27 137				These sequence data were produced by the US Department of Energy Joint Genome Institute http://www.jgi.doe.gov/ in collaboration with the user community
Pennate	*Pseudonitzschia multiseries*(Hasle) Hasle	Marine, producing domoic acid	Yes	219 (draft)					http://genome.jgi.doe.gov/genome-projects/pages/projects.jsf, Parker et al. (2013)
	Seminavis robusta	Marine, benthic	Yes						http://genome.jgi.doe.gov/genome-projects/pages/projects.jsf
	Danielidis & D. G. Mann	Marine, benthic							
	Fistulifera sp.	Oleaginous	Yes	49.9 (draft)	20 455 ORF				
	Thalassiosira rotula 1647 (Meunier)	Marine, planktonic	Transcriptome	(http://genome.jgi.doe.gov/genome-projects/pages/projects.jsf)					
	Haslea ostrearia	Marine, benthic, producing the blue pigment marennine							Gastineau et al. (2013)
	Cyclotella meneghiniana (Kützing)	Freshwater, planktonic	Abandonned	(http://genome.jgi.doe.gov/genome-projects/pages/projects.jsf)					GOLD
	Odontella sinensis	Marine,	Chloroplast	http://chloroplast.ocean.washington.edu/					

Table 2.2. Examples of antibodies used for subcellular protein localization in diatoms.

Protein targeted	Taxon used	Usage	Antibody origin	References
Mn-superoxide dismutase	*Thalassosira pseudonana*	Subcellular localization	Native	Wolfe-Simon et al. (2006)
Fucoxanthin Chl *a*/*c* binding polypeptides Fcp2, Fcp4 and Fcp6	*Cyclotella cryptica* (Reimann, Lewin & Guillard)	Subcellular localization	Synthetic	Becker & Rhiel (2006)
Nitrate reductase	*Skeletonema costatum* (Grev.) A. Cleve 1878	Flow cytometry	Synthetic	Jochem et al. (2000)
Tubulin	*Stephanopyxis turris*	Subcellular localization	Sea urchin tubulin	Wordeman et al. (1986)

(*Chaetoceros gracilis*: Nagao et al. 2007; *P. tricornutum* and *T. pseudonana*: Grouneva et al. 2011) and mitochondria (Bartulos et al. 2013) have been purified to any extent.

The protein content of enriched cell fractions can be determined using proteomic tools. Such an approach, combined with 2D bluenative SDS–PAGE electrophoresis and optimized for the separation of thylakoid protein complexes (Sirpio et al. 2011) was used to obtain the protein map of photosynthetic membranes of *P. tricornutum* and *T. pseudonana.* This revealed the presence of diatomspecific proteins, PGR5 (proton gradient regulator)/GPRL (PGR-like), associated with photosystem I (Grouneva et al. 2011). Because of the inevitable contaminations of purified fractions, and also to the fact that proteins could have dual localization, protein localization based on proteomics should be complemented by other methods (Beebo et al. 2013; Pfeil et al. 2013). Of these, immunocytochemistry is the method of choice but this requires that the protein of interest can be targeted by an antibody. Wolfe-Simon et al. (2006) used this to demonstrate that Mnsuperoxide dismutase (MnSOD) is localized in the chloroplast in *T. pseudonana*, whereas it is found exclusively in the mitochondria in other photoautotrophs (del Rio et al. 2003).

Unfortunately, antibodies prepared against diatom proteins are not always available. To overcome this difficulty, antibodies against synthetic C or Ntermini (Becker & Rhiel, 2006) or against homologous proteins of other organisms can be used (Table 2.2). For instance, Wordeman et al. (1986) used an antibody against sea urchin tubulin to follow the distribution of cytoplasmic microtubules during the cell cycle of *Stephanopyxis turris* (Greville) Ralfs.

More recently, the development of genetic transformation combined with the availability of more protein reporters (Remington, 2011) has allowed the localization of proteins in living cells (Poulsen & Kröger, 2005; Tachibana et al. 2011; Curnow et al. 2012; Muto et al. 2012). Methods for localizing metabolites are also available, but are more complex than for proteins (Stitt et al. 1980; Chaudhuri et al. 2011) and have not yet been applied to diatoms. In many cases, a single biochemical pathway requires

cooperation between several compartments, for example, the C_2 oxidative photosynthetic cycle. RubisCo, the primary enzyme for carbon fixation, has a single active site with a high affinity for both CO_2 and O_2 (for a review, see Sage et al. 2012). The C_2 oxidative photosynthetic cycle occurs when O_2 out-competes CO_2 at the RubisCo active site. O_2 utilization leads to the formation of a twocarbon molecule, 2-phosphoglycolate that cannot enter the Benson–Calvin cycle. Instead, it enters the C_2 oxidative photosynthetic cycle. In higher plants and green algae, this cycle involves organic carbon and nitrogen compounds, including glycolate, glycine and serine, ending with the formation of 3-phosphoglycerate, which can enter the Benson–Calvin cycle. The C_2 oxidative photosynthetic cycle requires the cooperation of three cell compartments, namely chloroplast, peroxisome and mitochondria (Figure 2.1). This pathway is also called photorespiration because it consumes O_2, and one of every four C atoms entering the C_2 oxidative photosynthetic cycle pathway is used to produce CO_2.

By contrast, the conversion of glycine to serine results in the formation of NH_3 (Keys et al. 1978), which can enter the urea cycle (for a review, see Fernie et al. 2012). Homologues to genes coding the C_2 oxidative photosynthetic cycle enzymes in other eukaryotes have been found for *P. tricornutum* and *T. pseudonana*, except for glycerate kinase, which catalyses the conversion of glycerate to 3-phosphoglycerate (Kroth et al. 2008). This absence leaves the C2 oxidative photosynthetic cycle pathway open in diatoms (Figure 2.1). Additional studies on the role of the C_2 oxidative cycle are needed, especially in relation to the C_4 CO2-fixation mode (see above) because this can be enhanced under certain light wavelengths (Rech et al. 2008). It is also clear that intimate cooperation between different cell compartments is required for this process to occur because the enzymes involved have unique cellular localizations. Although some organelles have their own genomes, many proteins are translated on cytoplasmic ribosomes and targeted to another compartment. In diatoms, as in other eukaryotes, the main molecular tools for targeting proteins to specific compartments are *N*-glycosylation and transit peptides. *N*-glycosylation is usually used to orientate proteins to the Golgi apparatus, cell wall and extracellular medium. Despite its importance for basic and applied science, little is known about post-translational modification for intracellular protein trafficking in microalgae.

Using an *in silico* approach and functional heterologous complementation experiments, Baiet et al. (2011) reconstituted the *N*-glycosylation pathway in *P. tricornutum* and demonstrated the involvement of an *N*-acetylglucosamine transferase I. Transit peptides are mostly used to target proteins to the chloroplast, mitochondria, endoplasmic reticulum and peroxisomes (Liaud et al. 2000; Bruce, 2001; Kroger & Poulsen, 2008; Gonzalez et al. 2011). The need to target peptides originates from gene transfer from the endosymbiont genome to the host nucleus during evolution, while maintaining the unique biochemical properties of the resulting organelle, e.g. respiration in mitochondria, photosynthesis in chloroplasts. This gene migration has

resulted in the highly reduced organelle genomes observed today, and in the necessity to import hundreds of proteins into the organelles to ensure their biochemical activity (Timmis et al. 2004).

To predict the subcellular localization of proteins based on the presence of targeting sequences, several *in silico* methods have been developed (Table 2.3). These are mostly based on analysis of the presence of single or multiple targeting signals that are required to cross the membrane *in situ* (Lang et al. 1998; Schwartzbach et al. 1998). Although none of these prediction algorithms is specific to diatoms, most postgenomic studies on diatoms use them to predict protein localization. For instance, glycine decarboxylase (Figure 2.1), an enzyme of the photorespiration pathway, has been hypothesized to be targeted to mitochondria, based on the fact that its sequence contains an N-terminus enriched in positively charged and nonpolar residues (Schnitzler-Parker et al. 2005), characteristic of mitochondrial presequences in higher plants (Chaumont & Boutry, 1995) and diatoms (Liaud et al. 2000). It is also clear that targeting signals show different degrees of evolutionary conservation, and thus, sequencebased detection of targeting sequences using models developed for other organisms has limited accuracy when applied to diatoms. *In silico* analyses of the targeting signal of translated sequences led to the discovery of an atypical cellular localization of proteins in diatoms compared to green algae or higher plants. For instance, in green algae, both the Calvin–Benson cycle and the oxidative pentose pathway are localized in the chloroplast.

In diatoms, the former pathway is localized in the chloroplast, but the latter is located in the cytoplasm (Kroth et al. 2008). In some diatoms, such as *P. tricornutum*, an incomplete oxidative pentose phosphate is also found in the chloroplast (Michels et al. 2005; Kroth et al. 2008).

These different localizations would induce different physiological strategies. There is an urgent need to confirm these protein localizations and their related biological activities using reporter genes, fluorescence-tagged proteins, *in situ* hybridization or immunolocalization. This has been done in *P. tricornutum*, using 5D timelapse confocal imaging of the protein EB1, a marker for microtubule dynamics, and along the microtubules in YFP (Yellow Fluorescent Protein) expressing transgenic cells (De Martino et al. 2009).

An additional difficulty is that parts of the biochemical networks in diatoms are redundant with respect to metabolite usage and also in enzyme isoforms. This is especially true for the central metabolism. For example, several copies of the genes encoding the Calvin–Benson cycle enzymes fructose 1,6-bisphosphatase aldolase (FBA) and fructose 1,6-bisphosphatase (FBP) are present in the *P. tricornutum* genome. Three of the predicted FBA proteins are targeted to the plastids and two to the cytosol. Four FBPases have been identified in the plastid while only one has been described in the cytosol (Kroth et al. 2008). This isoenzyme redundancy may in part reflect the evolution

of diatoms by secondary endocytobiosis (Patron et al. 2004). Duplication may contribute to the protection of essential processes by functional compensation in the event of genetic mutation (Zhang, 2012). To our knowledge, this has not been shown in diatoms, but is well established in higher plants (*e.g*. Beebo et al. 2009). However, different isoforms might respond to different (stress) situations, but we currently know very little about the function, localization and differentiation of diatom isoenzymes.

2.6 Combining several 'omics' to generate cell models

During their evolutionary history, diatoms inherited genes from various sources (see 'Introduction') resulting in a unique combination of networks, supporting a variety of defence mechanisms. This makes diatoms very different from other photosynthetic organisms, such as green algae and land plants (Fernie et al. 2012, see also above), and very successful in a dynamic environment. To uncover the different networks, and to understand how they are linked together, omics approaches have been developed.

With respect to transcriptomics, differential gene expression (Maheswari et al. 2005; 2009; Montsant et al. 2005), digital gene expression databases (Maheswari et al. 2010), microarrays (Allen et al. 2008; Mock et al. 2008) and transcriptome sequencing have been used (Valenzuela et al. 2012). Two different approaches, i.e. '*a priori*' and 'global' may be employed, and both are still widely, and successfully, used to reveal key aspects of the physiological state of cells, particularly carbon partitioning (Parker & Armbrust, 2005; Allen et al. 2008; Nymark et al. 2009; Valenzuela et al. 2012).

The '*a priori*' strategy targets genes for which the sequence is known (from genome web databases). Variations in the transcripts can be investigated in a few genes by northern blot or quantitative PCR (qPCR) or simultaneously on large numbers of genes using microarrays. For example, Parker & Armbrust (2005) studied the effects of nitrogen sources, temperature and light on transcript abundances of five key genes from three carbon and nitrogen metabolism pathways in *T. pseudonana*. Each gene was chosen based on its specificity to a pathway: nitrate reductase (NR) and glutamine synthetase II (GSII) are both required for nitrate consumption, phosphoglycolate phosphatase (PGP) and glycine decarboxylase Tprotein (GDCT, see Figure 2.1) for photorespiration, and sedoheptulose 1,7-biphosphatase (SBP) for carbon fixation through the Calvin cycle.

The data were used to build a hypothetical model explaining the patterns of transcript accumulation and demonstrating the complex interaction between carbon and nitrogen metabolism (Parker & Armbrust, 2005). When sequence information is available, this approach provides a straight-forward and relatively rapid method for assessing potential metabolic changes. Allen et al. (2008) employed a microarray combined with a range of physiological measurements and gas chromatography-mass spectroscopy (GC-MS)-aided non-targeted metabolomic analysis to explore the different

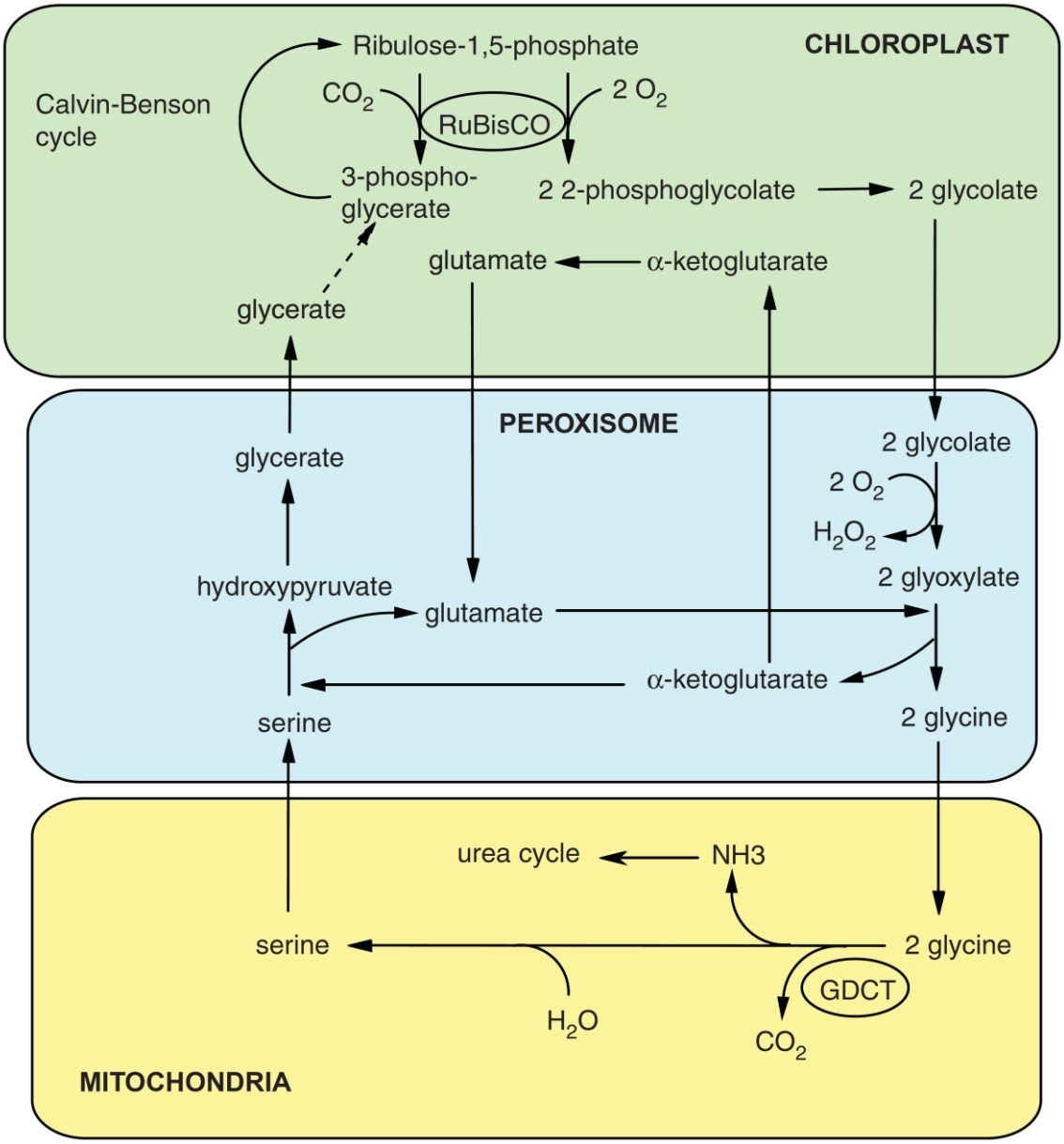

Figure 2.1. The main reaction of the photorespiratory pathway in diatoms. Operation of the C_2 oxidative photosynthetic cycle involves the cooperation of three cell compartments, i.e. the chloroplast (in green), the peroxisome (in blue) and the mitochondria (in yellow), underlying the crucial role of transporters in cell functioning. Two molecules of glycolate are transported from the chloroplast to the peroxisome where they are converted to glycine, which in turn, is exported to the mitochondria where it is respired, resulting in the release of CO_2 and NH_3. Serine is transported from mitochondria to the peroxisome where it is transformed to glycerate, which flows to the chloroplast. Glycerate kinase seems to be absent from diatom genomes, rendering the C_2 oxidative photosynthetic cycle incomplete. It is possible that glycine, serine and other intermediates of the pathways are used in other reactions such as glutathione synthesis (Raven & Beardall, 1981) or glyoxylate metabolism (Paul & Volcani, 1976).

Table 2.3. Examples of reporter protein used to elucidate proteins subcellular localization in diatoms.

Protein family	Taxon	Proteins	Reporter	Localization	Confirmed	References
β-CA	*Phaeodactylum tricornutum*	PtCA1 & PtCA2	GFP	Central part of the chloroplast (Pyrenoid)	Immunocyto-chemistry	Tachibana et al. (2011)
α-CA	*Phaeodactylum tricornutum*		GFP	Chloroplast	No	Tachibana et al. (2011)
γ-CA	*Phaeodactylum tricornutum*	CA-IX	GFP	?	No	Tachibana et al. (2011)
		CA-VIII		Mitochondria	Fluorescent dye (mitotracker)	
γ-CA	*Thalassosira pseudonana*	CA8 CA9 CA13	GFP	Mitochondria		Tachibana et al. (2011)

strategies of *P. tricornutum* at growth limiting levels of dissolved iron. The study identified 212 induced and 26 down-regulated genes. Processes such as photosynthesis, mitochondrial electron transport and nitrate assimilation were down-regulated, resulting in a reduced income in C and N atoms.

This was compensated for by nitrogen and carbon reallocation from protein and carbohydrate degradation, and adaptation to chlorophyll biosynthesis and pigment metabolism, with differential responses to oxidative stress.

To understand the functioning of metabolic networks it is important to know the direction of atoms and/or metabolite flux. This can be estimated by comparing transcript and protein levels. For instance, in *T. pseudonana* experiencing nitrogen starvation, protein, phosphoglycerate mutase, enolase and fructose1,6-bisphosphate aldolase increase (Hockin et al. 2012), whereas transcripts coding for pyruvate kinase decrease (Mock et al. 2008), suggesting that either gluconeogenesis or glycolysis is promoted under these conditions. The increase in transcript levels of phosphofructokinase and two pyruvate kinases, and the decrease in pyruvate kinase suggest that carbon flow was primarily oriented in the direction of glycolysis. However, large discrepancies between transcript level, protein level and biological functions are repeatedly reported.

They are explained by the existence of at least two regulation levels (*i.e.* transcriptional and translational) during protein production. Therefore, more traditional approaches, such as the use of radiolabelled tracers should be used to determine metabolic fluxes. For instance, Guiheneuf et al. (2011) used [^{14}C] sodium bicarbonate and [1-^{14}C] sodium acetate to investigate the pathways involved in the biosynthesis of longchain polyunsaturated fatty acids in the prymnesiophyte *Pavlova lutheri* (Droop) J.C. Green during photosynthesis in relation to light intensity. In this alga, lipid production, including galacto-lipids and phospholipids, increased with light intensity when the cells were incubated with [^{14}C] bicarbonate (inorganic carbon), but was less sensitive to differences in light intensity when incubated with [1-^{14}C] acetate, a

heterotrophic carbon source that stimulates the synthesis of monounsaturated fatty acids.

This suggests that *P. lutheri* has two distinct enzyme pools involved in long chain poly unsaturated fatty acids synthesis. The pool that is regulated by light intensity would be localized within the chloroplasts, whereas the second would be extra chloroplastidic and independent of light intensity (Guiheneuf et al. 2011). This study also underlines the need to correlate biochemical data with the localization of the enzymatic activities. Unfortunately, radio labelling is not appropriate for metabolomic investigations.

Genome sequencing and metabolic network reconstitution have revealed that thousands of gene products interact within a cell. The number of putative interactions increases exponentially with the number of partners, and the complexity of the metabolic network(s) rapidly becomes difficult to investigate from gene expression or protein abundance. Combining transcriptomics and proteomic investigations with metabolomic approaches is thus a major goal for physiology today. The need for metabolomic data is emphasized by the chemicophysical properties and biological activities of metabolites, which allow a large range of different combinations. There is much more complexity than that deduced from transcripts or protein profiles alone. Moreover, the general assumption that biological activity varies in accordance with transcripts or protein abundance more often fails because of enzymes kinetic, thermodynamic and stoichiometry constraints.

The complexity of physiological regulation is greater because metabolite fluxes are not obligatorily linked to enzyme levels. Moreover, even if genotypetophenotype relationships have been described for many organisms, numerous protein coding genes remain functionally uncharacterized.

Using sequence homology, only ~ 50% of diatom genes have been assigned to a known function. This is partly due to the lack of information on transcriptomes from other organisms taxonomically close to diatoms (Maheswari et al. 2009), and reflects the rapid evolution of diatoms (Bowler et al. 2008). Proteins with obscure functions (POFs) account for 44% of the putative proteome of *P. tricornutum* (Maheswari et al. 2010). By contrast, most of the proteins with defined functions (PDFs) in *T. pseudonana* have orthologues in other Heterokonts, and have also been found in Viridiplantae and Opisthokonta. Maheswari et al. (2010) also pointed out that under specific growth conditions, diatoms can express novel transcripts not predicted by conventional tools or homology methods, and therefore of unknown function. Another challenge to assigning functional roles to proteins is when low similarities between proteins require biochemical control, even if *in silico* comparison with known sequences can be made. For example, for the CA enzymes in *P. tricornutum*, seven CAs have been predicted by conserved domains, but need biochemical investigation to be formally identified (Kroth et al. 2008).

Another difficulty to inferring physiological regulation is that multiple genes can encode the same biochemical function. This is the case for the enzymes involved in carbon pathways in *P. tricornutum*, where it was proposed that both PEPCK and malate dehydrogenase/malic enzyme decarboxylate oxaloacetate C_4-acid reside in mitochondria (Kroth et al. 2008). It is therefore very important to relate metabolite concentration to pathway flux, and knowing entrypoint substrates or products and their flux regulation, relies on transcription, protein abundance and activity, and biological response information. Faced with this complexity, novel approaches have recently been developed to decipher biological networks.

Metabolic network reconstruction is now one of the best tools to quantify genotype–phenotype relationships. This requires the identification of missing reactions in the metabolic network, and genomescale metabolic network models such as constraint-based modeling (CBM) have been used to predict the phenotypes of various microorganisms (Oberhardt et al. 2009). More recently, the association of genes with network reactions has been developed. In this approach, named MIRAGE (metabolic reconstruction via functional genomics), missing reactions whose presence is supported by functional genomic data are sought (Vitkin & Shlomi, 2012). Another recent approach using protein–protein interactions, the socalled Interactome Map, has also been used to clarify how genotype-phenotype relationships are mediated in organisms. This methodology was developed in several organisms, such as *Arabidopsis thaliana* (L.) Heynh. (*Arabidopsi*s Interactome Mapping Consortium, 2012), and has improved the understanding of biological processes and global organization, as well as generating new hypotheses on the functional links between proteins and pathways.

A similar approach would be ideal for deciphering diatom physiology and helping us to understand the biological complexity of these organisms. To date, decoding all biological reactions has not been an easy task because of the huge numbers of metabolites present in an organism, even unicellular ones. Current estimations give from 4000 to 25 000 compounds per organism, and the plant kingdom alone probably contains more than 100 000 metabolites (Trethewey, 2004). Most often, studies only consider metabolites corresponding to a few percent of the existing components, even when new technologies allowing the extraction of ~1000 compounds from *Arabidopsis*, for instance are used (Giavalisco et al. 2008; Iijima et al. 2008; May et al. 2008; Krall et al. 2009). In addition, the turnover time for most metabolites is less than 1 s, much shorter than the protein turnover times, rendering metabolomic analyses very complicated (Arrivault et al. 2009). Moreover, metabolite isolation procedures have still to be refined to avoid artifacts. The use of highend machines (resonance-MS, orbitrap-MS, *etc.*) will probably expand the list of detected metabolites (Fernie & Schauer, 2009). Another challenge is understanding metabolic compartmentalization and the fluxes between the compartments, a crucial key to closing the gap between proteomic and metabolomic approaches.

2.7 Towards the understanding of metabolic control

Variation in environmental constraints and intracellular demands modulate metabolic activity (*e.g*. longterm: Falkowski et al. 2004; shortterm: Nguyen-Deroche et al. 2009). For instance, when the metal concentration increases in the environment, photosynthesis is impaired and defence mechanisms are activated (Bertrand et al. 2001; Nguyen-Deroche et al. 2012; for reviews, see Solymosi & Bertrand, 2012). It is beyond the scope of this article to review the different regulation possibilities and we will only insist on one crucial aspect, *i.e*. the role of transcription factors (TFs). Regulation of gene expression is central to all organisms and provides a complex control mechanism by which organisms modulate developmental processes and metabolic pathways and respond to stresses. This regulation is coordinated by a number of mechanisms that involve DNA methylation, chromatin organization, dimerization and sequencespecific binding of TFs (Maniatis & Reed, 2002). In addition to recognizing specific DNA motifs in gene regulatory regions, TFs can activate or repress transcription, possibly by interaction with other proteins. A significant proportion of protein encoded genes are dedicated to the control of gene expression (for example, 6% of the ~27 500 protein coding genes of *Arabidopsis*; Feller et al. 2011). The function of a few TFs has remained conserved between plants and animals, such as E2F family members, which control core cellcycle functions (Inze & De Veylder, 2006). However, most of the TFs have diverged significantly in function but keep conserved DNA-binding domains. Based on similarities in the DNAbinding domain, TFs have been categorized into families or super-families, several of which are composed of 100 or more members (Pabo & Sauer, 1992). For example, the MYB super-family is one of the largest and most diverse families of sequence specific TFs, particularly represented in plants with 100–200 MYB family members commonly found in individual plant species (Prouse & Campbell, 2012).

Genome-wide analyses of *P. tricornutum* and *T. pseudonana* diatoms reveal the presence of numbers of transcription factors families, the most represented being heat shock factors (HSF) and MYB proteins, then basic leucine zipper (bZIP) and various type of zincfinger transcription factors (Rayko et al. 2010). However, little is known about the specific transcription factors involved in any defined pathway.

Harada's team has identified CO_2–cAMP responsive elements (CCREs) in the promoter of the intracellular (chloroplastic) pyrenoidal *β*-CA of *P. tricornutum* (*ptca1*) that act as sensor of CO_2 conditions and repress the *ptca1* promoter under elevated CO_2 concentration (Harada et al. 2005; Harada et al. 2006). These CCREs *cis* elements are thought to bind bZIP transcription factors and at least one candidate, PtbZIP11, was identified in *P. tricornutum* (Ohno et al. 2012).

The cryptochrome/photolyase1 of *P. tricornutum* (PtCPF_1) was shown to be involved in both DNA 6–4 photoproduct repair and transcriptional repression of the circadian clock in a heterologous mammalian cell system (Coesel et al. 2009).

Furthermore, PtCPF_1 seems to have a wide role in blue-light-regulated gene expression in diatoms. Indeed PtCPF1 overexpression in *P. tricornutum* results in the up-regulation of genes encoding the tetrapyrrole biosynthetic enzymes, whereas genes of the carotenoid biosynthesis pathway and nitrogen metabolism were down-regulated (Coesel et al. 2009). These results indicate that CPF1 may act as a blue-light-sensitive transcription factor.

A CPF1 protein is present in both diatoms *P. tricornutum* and *T. pseudonana* (Takahashi et al. 2007; Coesel et al. 2009). Surprisingly, this CPF1 protein is phylogenetically closer to the animal cryptochrome/6–4 photolyase, but neither diatom taxon contains an orthologue of plant cryptochromes (Coesel et al. 2009). Recently, the transcriptional induction of the diatom specific cyclin (dsCYC2), which controls the onset of cell division, was shown to be triggered by blue light in a fluence ratedependent manner.

Consistent with this, dsCYC2 is a transcriptional target of the blue light sensor AUREOCHROME1a, which functions synergistically with the bZIP transcription factor bZIP10 to induce dsCYC2 transcription (Huysman et al. 2013).

Apart from these few examples, the transcription factors involved in gene regulation in diatoms remain largely unknown. The identification of transcription factors and characterization of their role may help to understand the molecular and cellular mechanisms of metabolism reorientation in diatoms. In particular, the role of Myb transcription factor in development and response to biotic and abiotic stresses is largely studied in higher plants (Prouse & Campbell, 2012), for example, the transcription factors involved in jasmonate-elicited secondary metabolisms have been recently reviewed by De Geyter et al. (2012).

2.8 Conclusions and future perspectives

The turbulent evolutionary history of diatoms has resulted in microorganisms presenting unique cytological, physiological and biochemical properties. From the genomic data, the metabolic and regulatory networks can be reconstituted and hypotheses on their interactions and/or regulation can be proposed (Fernie et al. 2012). Their functioning can be studied at several levels, *i.e.* transcription (transcriptomics), presence of proteins/enzymes (global and/or subcellular proteomics) and quantification of metabolites (metabolomics). Although the complement of metabolic pathways that contribute to energy management in diatom cells has been identified, the direct responses of the different pathways, their contributive flow and their integration with one another are not well enough known, yet are central and fundamental to maintain a healthy organism (Hibberd & Weber, 2012). Few studies have used different 'omics' side by side and therefore a comparative assessment of transcriptomic, proteomic, metabolomic and modelling analysis is still required. Moreover, vital

information on the cellular localization of the cell activities as well as on the various possibilities for metabolites transport across membranes is missing (Beebo et al. 2013; Pfeil et al. 2013). The general lack of knowledge about intracellular transporters is a major problem when it comes to building structural models of metabolic and regulatory networks. Actually, the presence or absence of transporters for given metabolites affect cooperation between the cell compartments, and possible routes through the metabolic networks. Within the frame of biotechnological applications, the addition of adequate transporters through genetic engineering have possibly resulted to dramatic increase of the resistance to stress.

For instance, in tomato transgenic plants over-expressing a vacuolar Na^+/H^+ antiport were able to grow, flower, and produce fruit in the presence of 200 mM sodium chloride whereas the control plant died under this condition (Zhang & Blumwald, 2001). To our knowledge, such a possibility was not yet tested in diatom. The dynamics of metabolite pools and its control constitutes data needed to understand the physiological responses.

The identification of the transcription factors mediating the metabolism orientation in response to stresses is obviously crucial, especially as diatoms may trigger specific and original metabolic and/or regulatory pathways while reaching a new equilibrium. These data are also needed for the development of efficient blue technologies, especially where microalgal engineering is concerned (Cadoret et al. 2012). Actually, this knowledge could be used to select the adequate step(s) of the metabolic or regulatory network that has (have) to be engineered. For instance, placing the entire metabolic pathway in one organelle rather than within two compartments significantly increased the biofuel production yield of yeasts (Avalos et al. 2013; DeLoache & Dueber, 2013). Our ability to obtain and integrate all these information into models will open new avenues about the understanding on the plasticity of the cellular life and how deviation impacts the maintaining a healthy organism.

2.9 Acknowledgment

The authors are very grateful to the Associate Editor and Editor-in-Chief of *Diatom Research* for their help in preparing the final version of this manuscript.

2.10 References

Allen A.E., Vardi A. & Bowler C. (2006). An ecological and evolutionary context for integrated nitrogen metabolism and related signalling pathways in marine diatoms. Curr. Opin. Plant Biol. 9: 264–273.

Allen A., Laroche J., Maheswari U., Lommer M., Schauer N., Lopez P., Finazzi G., Fernie A. & Bowler C. (2008). Wholecell response of the pennate diatom *Phaeodactylum tricornutum* to iron starvation. Proc Natl Acad Sci. U.S.A. 105: 10438–10443.

Allen A.W., Dupont C.L., Obornik M., Horak A., NunesNesi A., McCrow J.P., Zheng H., Johnson D.A., Fernie A.R. & Bowler C. (2011). Evolution and metabolic significance of the urea cycle in photosynthetic diatoms. Nature 473: 203–207.

Arabidopsis Interactome Mapping Consortium. (2011). Evidence for network evolution in an Arabidopsis interactome map. Science 333: 601–607.

Archibald J.M. (2012). The evolution of algae by secondary and tertiary endosymbiosis. Adv. Botanic. Res. 64: 87–118.

Armbrust E.V., Berges J.A. et al. (2004). The genome of the diatom *Thalassiosira pseudonana*: ecology, evolution, and metabolism. Science 306: 79–86.

Arrivault S., Guenther M., Ivakov A., Feil R., Vosloh D., Van Dongen J.T., Sulpice R. & Stitt M. (2009). Use of reversephase liquid chromatography, linked to tandem mass spectrometry, to profile the Calvin–Benson cycle and other metabolic intermediates in *Arabidopsis* rosettes at different carbon dioxide concentrations. Plant J. 59: 826–839.

Avalos J.L., Fink G.R. & Stephanopoulos G. (2013). Compartmentalization of metabolic pathways in yeast mitochondria improves the production of branchedchain alcohols. Nat. Biotechnol. 31: 335–341.

Baiet B., Burel C., SaintJean B., Louvet R., MenuBouaouiche L., KieferMeyer M.C., MathieuRivet E., Lefebvre T., Castel H., Carlier A., Cadoret J.P., Lerouge P. & Bardor M. (2011). *N*glycans of *Phaeodactylum tricornutum* diatom and functional characterization of its *N*acetylglucosaminyltransferase I enzyme. J. Biol. Chem. 286: 6152–6164.

Bartulos C.R., Scherer A.S. & Kroth P.G. (2013). Isolation of mitochondria from diatoms. Book of abstracts of the EMBO Workshop 'The Molecular Life of Diatoms'. 69.

Beadle G.W. & Tatum E.L. (1941). Genetic control of biochemical reactions in Neurospora. Proc Natl Acad Sci. U27: 499–506.

Beardall J., Mukerji D., Glover H.E. & Morris I. (1976). The path of carbon in photosynthesis by marine phytoplankton. J. Phycol. 12: 409–417.

Becker F. & Rhiel E. (2006). Immunoelectron microscopic quantification of the fucoxanthin chlorophyll a/c binding polypeptides Fcp2, Fcp4, and Fcp6 of *Cyclotella cryptic* grown under low and highlight intensities. Internation. Microbiol. 9: 29–36.

Beebo A., Thomas D., Der C., Sanchez L., LeborgneCastel N., Marty F., Schoefs B. & Bouhidel K. (2009). Life with and without AtTIP1;1, an aquaporin preferentially localized in the apposing tonoplasts of adjacent vacuoles. Plant Molecul. Biol. 70: 193–209.

Beebo A., Schoefs B. & Spetea C. (2013). Assessment of the requirement for aquaporins in the thylakoid membrane of plant chloroplasts to sustain photosynthetic water oxidation. FEBS Lett. 587: 2083–2089.

Benemann J.R. (1997). CO_2 mitigation with microalgae systems. Energ. Convers. Manage. 38: 475–479.

Bertrand M. (2010). Carotenoid biosynthesis in diatoms. Photosynth. Res. 106: 89–102.

Bertrand M., Schoefs B., Siffel P., RoháčekK. & Molnar I. (2001). Cadmium inhibits epoxidation of diatoxanthin to diadinoxanthin in the xanthophyll cycle of the marine diatom *Phaeodactylum tricornutum*. FEBS Lett. 508: 153–156.

Bowler C., Allen A.E. et al. (2008). The *Phaeodactylum* genome reveals the evolutionary history of diatom genomes. Nature 456: 239–244.

Bowler C.,Vardi A.& Allen A.E. (2010). Oceanographic and biogeochemical insights from diatom genomes. Ann. Rev. Marine Sci. 2: 333–363.

Bruce B.D. (2001). The paradox of plastid transit peptides: conservation of function despite divergence in primary structure. Biochim. Biophys. Acta 1541: 2–21.

Cadoret J.P., Garnier M. & SaintJean B. (2012). Microalgae, functional genomics and biotechnology. Adv. Botanic. Res. 64: 285–341.

Chaudhuri B., Hormann F. & Frommer W.B. (2011). Dynamic imaging of glucose flux impedance using Fret sensors in wildtype *Arabidopsis* plants. J. Exp. Botany 62: 2411–2417.
Chaumont F. & Boutry M. (1995). Protein import into plant mitochondria. In: The molecular biology of plant mitochondria (Ed. by C.S. Levings & I.K. Vasil), 207–235. Kluwer Academic Publishers, Dordrecht, The Netherlands.
Coesel S., Mangogna M., Ishikawa T., Heijde M., Rogato A., Finazzi G., Todo T., Bowler C. & Falciatore A. (2009). Diatom PtCPF1 is a new cryptochrome/photolyase family member with DNA repair and transcription regulation activity. EMBO rep. 10: 655–661.
Cogne G., Rugen M., Bockmayr A., Titica M., Dussap C.G., Cornet J.F. & Legrand J. (2011). A modelbased method for investigating bioenergetic processes in autotrophically growing eukaryotic microalgae: application to the green algae *Chlamydomonas reinhardtii*. Biotechnol. Prog. 27: 631–640.
Crawley A. Kline D.I., Dunn S., Anthony K. & Dove S. (2010). The effect of ocean acidification on symbiont photorespiration and productivity in *Acrophora formosa*. Glob. Change Biol. 16: 851–863.
Curnow P., Senior L., Knight M.J., Thamatrakoln K., Hildebrand M. & Booth P.J. (2012). Expression, purification, and reconstitution of a diatom silicon transporter. Biochemist. 51: 3776–3785.
Curtis B.A., Tanifuji G. et al. (2012). Algal genomes reveal evolutionary mosaicism and the fate of nucleomorphs. Nature 492: 59–65.
Daher Z., Recorbet G., Valot B., Robert F., Balliau T., Potin S., Schoefs B.& DumasGaudot E. (2010). A first root plastid proteome survey identifying novel putative plastidic proteins candidates as plant cell guards in the model legume *Medicago truncatula*. Proteomics 10: 2123–2137.
De Geyter N., Gholami A., Goormachtig S. & Goosens A. (2012). Transcriptional machineries in jasmonateelicited plant secondary metabolism. Trends Plant Sci. 17: 349–359.
Deloache W.C. & Dueber J.E. (2013). Compartmentalizing metabolic pathways inorganelle. Nat. Biotechnol. 31: 320–321.
Del Rio L.A., Sandalio L.M., Altomare D.A.& Zilinskas B.A. (2003). Mitochondrial and peroxisomal manganese superoxide dismutase: differential expression during leaf senescence. J. Exp. Botany 54: 923–933.
De Martino A., Amato A. & Bowler C. (2009). Mitosis in diatoms: rediscovering an old model for cell division. BioEssays 31: 874–884.
Deschamps P. & Moreira D. (2012). Reevaluating the green contribution to diatom genomes. Genome Biol. Evol. 4: 795–800.
Doney S.C., Ruckelshaus M., Duffy J.E., Barry J.P., Chan F., English C.A., Galindo H.M., Grebmeier J.M., Hollowed A.B., Knowlton N., Polovina J., Rabalais N.N., Sydeman W.J. & Talley L.D. (2012). Climate change impacts on marine ecosystems. Ann. Rev. Marine Sci. 4: 11–37.
Dukes J.S. (2003). Burning buried sunshine: human consumption of ancient solar energy. Clim. Change 61: 31–44.
Fabris M., Matthijs M., Rombauts S., Vyverman W., Goossens A. & Baart G.J. (2012). The metabolic blueprint of *Phaeodactylum tricornutum* reveals a eukaryotic Entner-Doudoroff glycolytic pathway. Plant J. 70: 1004–1014.
Falkowski P.G., Matz M.E., Knoll A.H., Quigg A., Raven J.A., Schofield O. & Taylor F.J.R. (2004). The evolution of modern eukaryotic phytoplankton. Science 305: 354–360.
Feely R.A., Sabine C.L., HernbandezAyon J.M., Ianson D. & Hales B. (2008). Evidence for upwelling of corrosive 'acidified' water onto the continental shelf. Science 320: 1490–1492.
Feller A., Machemer K., Braun E.L. & Grotewold E. (2011). Evolutionary and comparative analysis of MYB and Bhlh plant transcription factors. Plant J. 66: 94–116.
Fernie A. & Schauer N. (2009). Metabolomicsassisted breeding: a viable option for crop improvement? Trends Genet. 25: 39–48.

Fernie A.R., Obata T., Allen A.E., Araujo W.L. & Bowler C. (2012). Leveraging metabolomics for functional investigations in sequenced marine diatoms. Trends Plant Sci. 17: 395–403.
Field C.B., Behrenfeld M.J., Randerson J.T. & Falkowski P.G. (1998). Primary production of the biosphere: integrating terrestrial and oceanic components. Science 281: 237–240.
FiersW., Contreras R., Duerinck F., Haegeman G., Iserentant D., Merregaert J., Min JouW., Molemans F., Raeymaekers A., Van Den Berghe A., Volckaert G. & Isebaert M. (1976). Complete nucleotide sequence of bacteriophage MS2 RNA: primary and secondary structure of the replicase gene. Nature 260: 500–507.
Gastineau R., Carrier G., Hermann D., Maumus F., Jacquette B., Hardivillier Y., Leignel V., Cariso A., Casse N., Kaczmarsk I., Davidovich N., Meleder V., SaintJean B., Cadoret J.P. & Mouget J.M. (2013). Book of abstracts of the EMBO Workshop 'The Molecular Life of Diatoms'. 74.
Giavalisco P., Hummel J., Lisec J., Inostroza A.C., Catchpole G. & Willmitzer L. (2008). Highresolution direct infusionbased mass spectrometry in combination with whole 13C metabolome isotope labeling allows unambiguously assignment of chemical sum formulas. Analytic. Chem. 80: 9417–9425.
Gierasch L.M. & Gershenson A. (2009). Postreductionist protein science, or putting Humpty Dumpty back together again. Nature Chem. Biol. 5: 774–777.
Gonzalez N.H., Felsner G., Schramm F.D., Klingl A., Maier U.G. & Bolte K. (2011). A single peroxisomal targeting signal mediated matrix protein import in diatoms. PlosOne 6(9): e25316.
Gould S.B. (2012). Algae's complex origins. Nature 492: 46–48.
Granum E., Raven J.A. & Leegood R.C. (2005). How do marine diatoms fix 10 bilion tons of inorganic carbon per year. Can. J. Bot. 83: 898–908.
Grossmann G., Opekarova M., Novakova L., Stolz J. & Tanner W. (2006). Lipid raftbased membrane compartmentation of a plant transport protein expressed in *Saccharomyces cerevisiae*. Eukaryot. Cell 5: 945–953.
Grouneva I., Rokka A. & Aro E.M. (2011). The thylakoid membrane proteome of two marine diatoms outlines both diatomspecific and speciesspecific features of the photosynthetic machinery. J. Proteome Res. 10: 5338–5353.
Guiheneuf F., Ulmann L., Tremblin G. & Mimouni V. (2011). Lightdependent utilization of two radiolabelled carbon sources, sodium bicarbonate and sodium acetate, and relationships with long chain polyunsaturated fatty acid synthesis in the microalga *Pavlova lutheri* (Haptophyta). Eur. J. Phycol. 46: 143–152.
Hanson A.D., Pribat A., Waller J.C. & de CrécyLagard V. (2010). 'Unknown' proteins and 'orphan' enzymes: the missing half of the engineering parts list – and how to find it. Biochem. J. 425: 1–11.
Harada H., Nakatsuma D., Ishida M. & Matsuda Y. (2005). Regulation of the expression of intracellular β-carbonic anhydrase in response to CO_2 and light in the marine diatom *Phaeodactylum tricornutum*. Plant Physiol. 139: 1041–1050.
Harada H., Nakajima K., Sakaue K. & Matsuda Y. (2006). CO_2 sensing at ocean surface mediated by cAMP in marine diatom. Plant Physiol. 142: 1318–1328.
Hester K.C., Peltzer E.T., Kirkwood W.J. & Brewer P.G. (2008). Unanticipated consequences of ocean acidification: a noisier ocean at lower pH. Geophysic. Res. Lett. 35: L19601.
Heydarizadeh P., Poirier I., Loizeau D., Ulmann L., Mimounii V., Schoefs B.& Bertrand M. (2013). Plastids of marine phytoplankton produce bioactive pigments and lipids. Mar. Drugs 11: 3425–3471.
Hibberd J. & Weber A. (2012). Plant metabolism and physiology. Curr. Opin. Plant Biol. 15: 225–227.

Hockin N.L., Mock T., Mulholland F., Kopriva S. & Malin G. (2012). The response of diatom central carbon metabolism to nitrogen starvation is different from that of green algae and higher plants. Plant Physiol. 158: 299–312.

Huysman M.J., Fortunato A.E., Matthijs M., Costa B.S., Vanderhaeghen R., Van Den Daele H., Sachse M., Inze D., Bowler C., Kroth P.G., Wilhelm C., Falciatore A., VyvermanW.& DeVeylder L. (2013). AUREOCHROME1amediated induction of the diatomspecific cyclin dsCYC2 controls the onset of cell division in diatoms (*Phaeodactylum tricornutum*). Plant Cell 25: 215–228.

IijimaY., NakamuraY., OgataY., Tanaka K., Sakurai N., Suda K., Suzuki T., Suzuki H., Okazaki K., Kitajima M. Kanaya S., Aoki K.& Shibata D. (2008). Metabolite annotations based on the integration of mass spectral information. Plant J. 54: 949–962.

Inze D. & de Veylder L. (2006). Cell cycle regulation in plant development. Ann. Rev. Genet. 40: 77–105.

Jochem F.J., Smith G.J., Gao Y., Zimmerman R.C., CabelloPasini A., Kohrs D.G. & Alberte R.S. (2000). Cytometric quantification of nitrate reductase by immunolabeling in the marine diatom *Skeletonema costatum*. Cytometry 39: 173–178.

Keeling P.J. & Palmer J.D. (2008). Horizontal gene transfer in eukaryotic evolution. Nat. Rev. Genet. 9: 605–618.

Keys A.J., Bird I.F., Cornelius M.J., Lea P.J.,Wallsgrove R.M. & Miflin B.J. (1978). Photorespiratory nitrogen cycle. Nature 275: 741–743.

Krall L., Huege J., Catchpole G., Steinhauser D. & Willmitzer L. (2009). Assessment of sampling strategies for gas chromatographymass spectrometry (GCMS) based metabolomics of cyanobacteria. J. Chromatogr. 877B: 2952–2960.

Kroger N. & Poulsen N. (2008). Diatoms – from cell wall biogenesis to nanotechnology. Ann. Rev. Genet. 42: 83–107.

Kroth P.G. (2007). Genetic transformation : a tool to study protein targeting in diatoms. Methods Mol. Biol. 390: 257–267.

Kroth P., Chiovitti A., Gruber A., MartinJezequel V., Mock T., Parker M., Stanley M., Kaplan A., Caron L.,WeberT., Maheswari U., Armbrust V. & Bowler C. (2008). A model for carbohydrate metabolism in the diatom *Phaeodactylum tricornutum* deduced from comparative whole genome analysis. PLoS One 3: e1426.

Lang M., Apt K.E. & Kroth P. (1998). Protein transport into 'complex' diatom plastids utilizes two different targeting signals. J. Biol. Chem. 273: 30973–30978.

Lemoine Y. & Schoefs B. (2010). Secondary ketocarotenoid astaxanthin biosynthesis in algae: a multifunctional response to stress. Photosynth. Res. 106: 155–177.

Liaud M.F., Lichtle C., Apt K., Martin W. & Cerff R. (2000). Compartmentspecific isoforms of TP1 and GAPDH are imported into diatom mitochondria as a fusion protein: evidence in favor of a mitochondrial origin of the eukaryotic glycolytic pathway. Mol. Biol. Evol. 17: 213–223.

Lommer M., Specht M. et al. (2012). Genome and lowiron response of an oceanic diatom adapted to chronic iron limitation. Genome Biol. 13: R66.

Maheswari U., Montsant A., Goll J., Krishnasamy S., Rajyashri K.R., PatelV.M. & Bowler C. (2005). The diatom EST database. Nuc. Acids Res. 33: D344–347.

Maheswari U., Mock T., Armbrust E.V. & Bowler C. (2009). Update of the Diatom EST Database:a new tool for digital transcriptomics. Nuc. Acids Res. 37: D1001–1005.

Maheswari U., Jabbari K. et al. (2010). Digital expression profiling of novel diatom transcripts provides insight into their biological functions. Genome Biol. 11: R85.

Malinsky J., Opekarová M., Grossmann G. & Tanner W. (2013). Membrane microdomains, rafts, and detergentresistant membranes in plants and fungi. Ann. Rev. Plant Biol. 64: 501–529.

Maniatis T. & Reed R. (2002). An extensive network of coupling among gene expression machines. Nature 416: 499–506.

MathieuRivet E., Scholz M. et al. (2013). Exploring the *N*-glycosylation pathway in *Chlamydomonas reinhardtii* unravels novel complex structures. Mol. Cell Proteomics, 12: 3160–3163.

May P., Wienkoop S., Kempa S., Usadel B., Christian N., Rupprecht J., Weiss J., RecuencoMunoz L., Ebenhöh O., Weckwerth W. & Walther D. (2008). Metabolomicsand proteomicsassisted genome annotation and analysis of the draft metabolic network of *Chlamydomonas reinhardtii*. Genetics 179: 157–166.

Mc-Ginn P.J. & Morel F.M. (2008). Expression and inhibition of the carboxylating and decarboxylating enzymes in the photosynthetic C4 pathway of marine diatoms. Plant Physiol. 146: 300-309.

Michels A., Wedel N. & Kroth P. (2005). Diatom plastids possess a phosphoribulokinase with an altered regulation and no oxidative pentose phosphate pathway. Plant Physiol. 137: 911–920.

Mimouni V., Ulmann L., Pasquet V., Mathieu M., Picot L., Bougaran G., Cadoret J.P., Morant-Manceau A. & Schoefs B. (2012). The potential of microalgae for the production of bioactive molecules of pharmaceutical interest. Curr. Pharm. Biotechno. 13: 2733–2750.

Mock T.& Medlin L.K. (2012). Genomics and genetics of diatoms. Adv. Botanic. Res. 64: 245–284.

Mock T., Manoj Pratim S. et al. (2008). Wholegenome expression profiling of the marine diatom *Thalassiosira pseudonana* identifies genes involved in silicon bioprocesses. Proc. Natl. Acad. Sci. U.S.A. 105: 1579–1584.

Montsant A., Jabbari K., Maheswari U. & Bowler C. (2005). Comparative genomics of the diatom Phaeodactylum tricornutum. Plant Physiol. 137: 500–513.

Mouget J.L., Rosa P., Vachoux C. & Tremblin G. (2005). Enhancement of marennine production by blue light in the diatom *Haslea ostrearia*. J. Appl. Phycol. 17: 437–445.

Muto M., Fukuda Y., Nemoto M., Yoshino T., Matsunaga T. & Tanaka T. (2012). Establishment of a genetic transformation system for the marine pennate diatom *Fistulifera* sp. Strain JPCC DA0580 – A high triglyceride producer. Mar. Biotechnol. 15: 4855.

Nagao R., Ishii A., Tada O., Suzuki T., Dohmae N., Okumura A., Iwai M., Takahashi T., Kashino Y. & Enami I. (2007). Isolation and characterization of oxygenevolving thylakoid membranes and photosystem II particles from a marine diatom *Chaetoceros gracilis*. Biochim. Biophys. Acta 1767: 1353–1362.

Nguyen-Deroche T.L.N., Le T.T., Bui T.V., Rince Y., Tremblin G. & Morant-Manceau A. (2009). Effects of copper on growth and photosynthesis in marine diatoms: a comparison between species from two different geographical areas. Cryptogamie Algol. 30: 97–109.

Nguyen-Deroche T.L.N., Caruso A., Le T.T., Bui T.V., Schoefs B., Tremblin G. & Morant-Manceau A. (2012). Zinc affects differently growth, photosynthesis, antioxidant enzyme activities and phytochelatin synthase expression of four marine diatoms. Sci. World J. ID 982957, 15.

Nymark M., Valle K., Brembu T., Hancke K., Winge P., Andresen K., Johnsen G. & Bones A. (2009). An integrated analysis of molecular acclimation to high light in the marine diatom *Phaeodactylum tricornutum*. PLoS One 4: e7743.

Oberhardt M.A., Palsson B.Ø. & Papin J.A. (2009). Applications of genomescale metabolic reconstructions. Mole. Syst. Biol. 5: 320.

Ohno N., Inoue T., Yamashiki R., Nakajima K., Kitahara Y., Ishibashi M. & Matsuda Y. (2012). CO_2cAMPresponsive ciselements targeted by a transcription factor with CREB/ATFlike basic zipper domain in the marine diatom *Phaeodactylum tricornutum*. Plant Physiol. 158: 499–513.

Orr J.C., Fabry V.J. et al. (2005). Anthropogenic ocean acidification over the twentyfirst century and its impact on calcifying organisms. Nature 437: 681–686.

Pabo C.O. & Sauer R.T. (1992). Transcription factors: structural families and principles of DNA recognition. Ann. Rev. Biochem. 61: 1053–1095.

Palmer J.D. & Delwiche C.F. (1998). The origin and evolution of plastids and their genomes. In: *Molecular systematics in plants: DNA sequencing.* Soltis D.E., Soltis P.S. & Doyle J.J. (Eds). 375–409. Kluwer Academic Publishers, Boston, USA.

Parker M. & Armbrust V. (2005). Synergistic effects of light, temperature, and nitrogen source on transcription of genes for carbon and nitrogen metabolism in the centric diatom *Thalassiosira pseudonana* (Bacillariophyceae). J. Phycol. 41: 1142–1153.

Parker M.S., Maumus F. & Armbrust E.V. (2013). *PseudoNitzschia multiseries*: a coastal bloomforming diatom with a fat genome. Book of abstracts of the EMBO Workshop 'The Molecular Life of Diatoms'. 24.

Patron N., Rogers M. & Keeling P. (2004). Gene replacement of fructose 1,6bisphosphate aldolase supports the hypothesis of a single photosynthetic ancestor of chromatoalveolates. Eukaryot. Cell 3: 1169–1175.

Paul J.S. & Volcani B.E. (1976). Photorespiration in diatoms. 4. 2 pathways of glycolate metabolism in synchronized cultures of *Cylindrotheca fusiformis*. Arch. Microbiol. 110: 247–252.

Pfeil B., Schoefs B. & Spetea C. (2013). Function and evolution of channels and transporters in photosynthetic membranes. Cell. Mol. Life Sci. 71: 979–998.

Poulsen N. & Kröger N. (2005). A new molecular tool for transgenic diatoms: control of mRNA and protein biosynthesis by an inducible promoterterminator cassette. FEBS J. 272: 3413–3423.

Prouse M.B. & Campbell M.M. (2012). The interaction between MYB proteins and their target DNA binding sites. Biochim. Biophys. Acta, Gene Regul. Mech. 1819: 67–77.

Raven J.A. (1993). Limits on growth rates. Nature 361: 209–210.

Raven J.A. & Beardall J. (1981). Respiration and photorespiration. Can. B. Fish. Aquat. Sci. 210: 55–82.

Rayko E., Maumus F., Maheswari U., Jabbari K. & Bowler C. (2010). Transcription factor families inferred from genome sequences of photosynthetic stramenopiles. New Phytol. 188: 52–66.

Rech M., Morant-Manceau A. & Tremblin G. (2008). Carbon fixation and carbonic anhydrase activity in *Haslea ostrearia* (Bacillariophyceae) in relation to growth irradiance. Photosynthetica 46: 56–62.

Remington S.J. (2011). Green fluorescent protein: a perspective. Protein Sci. 20: 1509–1519.

Robertson D.L. & Alberte R.S. (1996). Isolation and characterization of glutamine synthase from the marine diatom Skeletonema costatum. Plant Physiol. 111: 1169–1175.

Sage R.F., Sage T.L. & Kocacinar F. (2012). Photorespiration and the evolution of C_4 photosynthesis. Ann. Rev. Plant Biol. 63: 19–47.

Satoh D., Hiraoka Y., Colman B. & Matsuda Y. (2001). Physiological and molecular biological characterization of intracellular carbonic anhydrase from the marine diatom *Phaeodactylum tricornutum*. Plant Physiol. 126: 1459–1470.

Schnitzler-Parker M.S., Armbrust E.V., PioviaScott J. & Veil R.G. (2005). Synergistic effects of light, temperature, and nitrogen source on transcription of genes for carbon and nitrogen metabolism in the centric diatom *Thalassiosira pseudonana* (Bacillariophyceae). J. Phycol. 41: 1142–1153.

Schoefs B. (2008). Plant Cell Compartments – Selected Topics. Research Signpost: Kerala, India. 450.

Schwartzbach S.D., Osafune T. & Loffelhardt W. (1998). Protein import into cyanelles and complex chloroplasts. Plant Mol. Biol. 38: 247–263.

Siaut M., Heijde M., Mangogna M., Montsant A., Coesel S., Allen A., Manfredonia A., Falciatore A. & Bowler C. (2007). Molecular toolbox for studying diatom biology in *Phaeodactylum tricornutum*. Gene 406: 23–35.

Sirpio S., Suorsa M., Paakharinen V. & Aro E.M. (2011). Optimized native gel systems for separating thylakoid protein complexes: novel super and megacomplexes. Biochem. J. 439: 207–214.
Solymosi K. (2012). Plastid Structure, Diversification and Interconversions I. Algae. Curr. Chem. Biol. 6: 167–186 (Special issue: Plastids: a family of crucial actors in plant physiology. Schoefs, B. Ed).
Solymosi K. & Bertrand M. (2012). Soil metals, chloroplasts, and secure crop production: a review. Agron. Sustain. Environ. 32: 245–272.
Spetea C., Pfeil B.E. & Schoefs B. (2012). Phylogenetic analysis of the thylakoid ATP/ADP carrier reveals new insights into its function restricted to green plants. Front. Plant Sci. 2: 110.
Stitt M.,WirtzW.&Heldt H.W. (1980). Metabolite levels during induction in the chloroplast and extrachloroplast compartments of spinach protoplasts. Biochim. Biophys. Acta 593: 85–102.
SullivanC.W., Volcani B.E., LumD. & Chiappin M.L. (1974). Isolation and characterization of plasma and smooth membranes of marine diatom *Nitzschia alba*. Arch. Biochem. Biophys. 163: 29–45.
Sweetlove L.J. & Fernie A.R. (2013). The spatial organization of metabolism within plant cell. Ann. Rev. Plant Biol. 64: 723–746.
Tachibana M., Allen A.E., Kikutani S., Endo Y., Bowler C. & Matsuda Y. (2011). Localization of putative carbonic anhydrases in two marine diatoms, *Phaeodactylum tricornutum* and *Thalassiosira pseudonana*. Photosynth. Res. 109: 205–221.
Takahashi F., Yamagata D., Ishikawa M., Fukumatsu Y., Ogura Y., Kasahara M., Kiyosue T., Kikuyama M.,Wada M. & Kataoka H. (2007). Aureochrome, a photoreceptor required for photomorphogenesis in stramenopiles. Proc Natl Acad Sci. U.S.A. 104: 19625–19630.
Tanaka Y., Nakatsuma D., Harada H., Ishida M. & Matsuda Y. (2005). Localization of soluble betacarbonic anhydrase in the marine diatom *Phaeodactylum tricornutum*. Sorting to the chloroplast and cluster formation on the girdle lamellae. Plant Physiol. 138: 207–217.
Timmis J.N., Ayliffe M.A., Huang C.Y. & Martin W. (2004). Endosymbiotic gene transfer: organelle genomes forge eukaryotic chromosomes. Nat. Rev. Genet. 5: 13–135.
Trethewey R. (2004). Metabolite profiling as an aid to metabolic engineering in plants. Curr. Opin. Plant Biol. 7: 196–201.
Valenzuela J., Mazurie A., Carlson R., Gerlach R., Cooksey K., Peyton B. & Fields M. (2012). Potential role of multiple carbon fixation pathways during lipid accumulation in *Phaeodactylum tricornutum.* Biotechnol. Biofuels 5: 40.
Vasseur C., Bougaran G., Garnier M., Hamelin J., Leboulanger C., Le Chevanton M., Mostajir B., Sialve B., Steyer J.P. & Fouilland E. (2012). Carbon conversion efficiency and population dynamics of a marine algaebacteria consortium growing on simplified synthetic digestate: first step in a bioprocess coupling algal production and anaerobic digestion. Bioresour. Technol. 119: 79–87.
Vitkin E. & Shlomi T. (2012). MIRAGE: a functional genomicsbased approach for metabolic network model reconstruction and its application to cyanobacteria networks. Genome Biol. 13: R111.
Wolfe-Simon F., Starovoytov V., Reinfelder J.R., Schofield O. & Falkowski P.G. (2006). Localization and role of manganese superoxide dismutase in a marine diatom. Plant Physiol. 142: 1701–1709.
Wordeman L., Mcdonald K.L. & Cande W.Z. (1986). The distribution of cytoplasmic microtubules throughout the cell cycle of the centric diatom *Stephanopyxis turris*: their role in nuclear migration and positioning the mitotic spindle during cytokinesis. J. Cell Biol. 102: 1688–1698.

Wu Y., Gao K. & Riebesell U. (2010). CO_2induced seawater acidification effects physiological performance of the marine diatom *Phaeodactylum tricornutum*. Biogeosciences 7: 2915–2923.
Zhang J. (2012). Genetic redundancies and their evolutionary maintenance. Adv. Exp. Med. Biol. 751: 279–300.
Zhang H.X. & Blumwald E. (2001). Transgenic salttolerant tomato plants accumulate salt in foliage but not in fruit. Nat. Biotechnol. 19: 765–768.

Chapter 3

Phaeodactylum metabolism converges to pyruvate/phospho*enol*pyruvate formation during growth under different light conditions

Parisa Heydarizadeh[a,b], Wafaa Boureba[a], Brigitte Moreau[a], Ewa Lukomska[c], Véronique Martin-Jézéquel[d], Gaëlle Wielgosz[e], Aurélie Couzinet[e], Morteza Zahedi[b], Gaël Bougaran[a], Justine Marchand[a], Benoît Schoefs[a*]

[a] MicroMar, Mer Molécules Santé, LUNAM, IUMLFR 3473 CNRS, University of Le Mans, Le Mans, France
[b] Department of Agronomy and Plant Breeding, College of Agriculture, Isfahan University of Technology, Isfahan, 8415683111, Iran
[c] IFREMER, Physiology and Biotechnology of Algae Laboratory, rue de l'Ile d'Yeu, 44311 Nantes, France
[d] UMR 6250CNRS LIENSs, Université de La Rochelle, 2 rue Olympe de Gouge, 17000, La Rochelle
[e] ChimiMar, Mer Molécule Santé, University of Nantes, IUML FR 3473 CNRS, France

* Corresponding author
email: benoit.schoefs@univ-lemans.fr
Tel: +33 2 43 83 37 72
fax: +33 2 43 83 39 17

(to be submitted)

3.1 Abstract

Photosynthetic diatoms adapt to changing irradiance in a very efficient way, as they are exposed to rapid changes in light intensity in their nature, and must be able to acclimate their light harvesting systems to varying light conditions. Molecular mechanisms behind light acclimation in diatoms are largely unknown. In this work we report the differences in physiological, biological and molecular mechanisms of different light acclimation (LL, ML, HL) in *Phaeodactylum tricornutum* using a set of experiments including transcriptom. Molecular, biological and physiological responses were studied at three growth phases (lag, exponential, plateau). The integrated results indicate that the impact of ML and HL on diatom cells were similar but quite different from LL. In addition of light, growth phase and aging of the culture could affect pigments concentration and primary metabolites. The trend of gene expression coding enzymes in

central carbon metabolism pathways differed under LL, but the orientation of the metabolisms was toward pyruvate formation in all three light intensities. LL provided a condition for cells to accumulate chrysolaminarin and lipid, while ML mostly stimulated lipid synthesis. A significant increase in the amount of protein was observed under HL. We concluded that pyruvate is a key intermediate in diatom cell to synthesis valuable compounds and serves as precursor of PEP that is also a key point for the synthesis of valuable compounds such as aromatic amino acids and polyphenolics.

3.2 Introduction

Microalgae denote a wide variety of waterliving photosynthetic microorganisms capable of a high productivity per unit area when compared to other photosynthetic organisms as higher plants (Gordon & Polle, 2007). Among the microalgae, diatoms constitute the most abundant group of marine eukaryotic organisms with more than 200 genera and approximately 100,000 species, and many have still to be discovered (*e.g.*, Heydarizadeh et al. 2014; Bork et al. 2015). Altogether, diatoms contribute to 20–40% to the primary productivity of the ocean, which is more than all terrestrial rainforests combined (Hasle et al. 1996; Field et al. 1998; Granum et al. 2005; Bowler et al. 2010). Diatoms are able to adapt to a broad range of environmental conditions including light irradiances (Gordon & Polle, 2007; Spetea et al. 2014) through adjustment of their physiology and biochemical activity (Obata et al. 2013; Spetea et al. 2014; Fortunato et al. 2015; Roháček et al. 2014), and maintaining high growth rates and a high efficiency of carbon incorporation into different organic metabolites (Falkowski & Laroche, 1991; Lavaud et al. 2003; Nymark et al. 2009). Yet, excessive or insufficient incident light constrains diatom optimal performance in terms of biomass and biomass composition *i.e.* metabolites (Goldman, 1980; Vidoudez & Pohnert, 2008; Barofsky et al. 2009; Barofsky et al. 2010; Carvalho et al. 2011). Metabolites are generated along biochemical pathways, including carbon metabolism that appeared to be tightly regulated by light (Dron et al. 2012).

These responses occur through a number of mechanisms including photoacclimation (physiological acclimation) and photoadaptation (genetic adaptation) (Nymark et al. 2009). Both mechanisms are linked and may work together to maximize the coupling between light regulation and cell cycle progression (Nymark et al. 2009; Depauw et al. 2012). Since the sequencing of diatom genomes (Armburst et al. 2004; Bowler et al. 2008), many progresses have been made in the elucidation and the understanding of diatom metabolism and physiology (Roberts et al. 2007; Nymark et al. 2009; Valenzuela et al. 2012; Herbstová et al. 2015). However little is still known about carbon flux direction inside the cell, partition between the different pathways and molecular mechanisms behind light acclimation in diatoms. One way to follow these mechanisms consists in exploring genes coding proteins associated with the pathways because the

level of gene expression may affect enzyme amount and, thus, flux distribution (Depauw et al. 2012; Heydarizadeh et al. 2014).

The marine diatom *Phaeodactylum tricornutum* belongs to Bacillariophyta, a phylum comprising one-third of all known marine phytoplankton. The recent completion of the genome sequence of this diatom (Bowler et al. 2008) made *P. tricornutum* a 'model' diatom for genomic, biochemical and physiological studies (Ge et al. 2014; Zhang & Hu, 2014). The transcriptome of *P. tricornutum* has been studied in a few contexts, such as silicon metabolism (Sapriel et al. 2009), short-term light acclimation (Nymark et al. 2009), carbon fixation, storage and utilization (Chauton et al. 2013) and nitrogen stress (Levitan et al. 2015). Molecular mechanisms behind light acclimation during diatom growth remain largely unknown. For instance, growth-related modifications in gene expression induced by different light intensities in *P. tricornutum* are not yet described. In this study, we investigate the mechanisms of light acclimation in *P. tricornutum* along diatom growth and its consequence of diatom physiology. We examined how *P. tricornutum* is capable of efficient execution of photoprotective mechanisms, changes in the composition of the photosynthetic machinery and remodels intermediates of central carbon metabolism that enable the diatom to respond different levels of received light energy.

3.3 Material and methods

3.3.1 *Phaeodactylum tricornutum*

Empire: Eucaryota
Kingdom: Chromalveolata
Phylum : Heterokontophyta
Classe: Bacillariophyceae
Order: Naviculales
Family: Phaeodactylaceae
Genus: *Phaeodactylum*
Species: *P. tricornutum*
Binomiale name: *Phaeodactylum tricornutum* (Bohlin, 1897)

P. tricornutum is a marine phytoplankton and the only species in the genus *Phaeodactylum*. The diatom can be in different morphotypes: oval (8µm×3µm), fusiform or triradiate ranging in size from 25 to 35 µm long, with arms slightly bent (Lewin, 1958) (Figure 3.1). Recently, *P. tricornutum* cruciform morphotype was observed by He et al. (2014). Cell morphotype changes can be stimulated by environmental conditions (De Martino et al. 2011). The organization and structure of the cytoplasmic organelles is similar in all the first three morphotypes, except that the vacuoles occupy the extra volume created by the arms of the fusiform and triradiate cells. The frustule in fusiform and triradiate cells is organic; in the oval type it may be organic or one of the valves may have a silica frustule surrounded by an organic wall. In all cells, the organic cell wall has up to 10 silica bands (13 nm wide) embedded in its surface in the girdle region, lacks

girdle bands, and has an outer corrugated cell wall layer, except in the girdle region (Borowitzka, 1999). In higher plants, it has been reported, relative to organic cell walls, silica frustules require less energy to synthesize that might be a significant saving on the overall cell energy budget (Raven, 1983). In diatoms, Milligan & Morel (2002) have suggested that the biogenic silica in diatom cell walls acts as an effective PH buffering agent, facilitating the conversion of bicarbonate to dissolved CO_2.

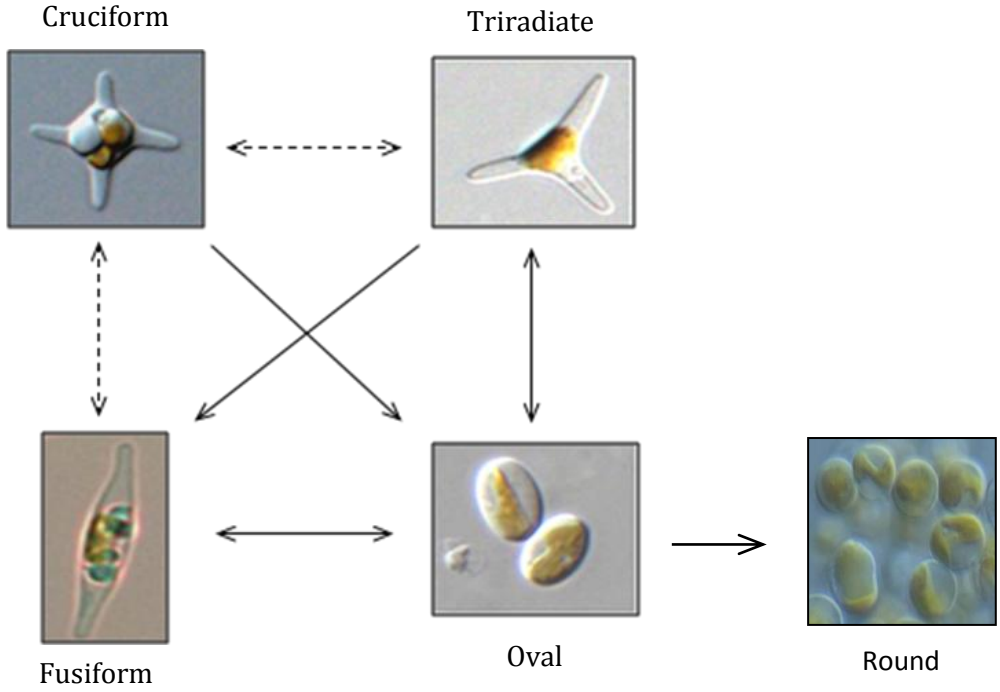

Figure 3.1. Light micrographs of (clockwise from top right) triradiate, round, oval, fusiform ((UTEX 646) performed in the laboratory using optical microscopy (GX 400)) and cruciform *Phaeodactylum tricornutum* (He et al. 2014).

3.3.2 Experiment strategy and sampling

Approximately 10^5 cells mL^{-1} of axenic culture of *Phaeodactylum tricornutum* Bohlin (UTEX 646) available in MicroMar team, Laboratoire de Biologie Marine of the University of Le Mans (France) were batch cultured in 200 mL of f/2 prepared with artificial seawater (Guillard & Ryther, 1962) in three biological replications. Cells were irradiated at a photon flux density of 30, 300 and 1000 µmol m^{-2} s^{-1} as low light (LL), medium light (ML) and high light (HL), respectively, using cool-white fluorescent tubes (Philips Master TLD 90 DE luxe 58W/965 and Osram L58/77 FLUORA). These levels of irradiance were choosen according to the value of E_k parameters obtained for *P. tricornutum* grown under 300 µmol m^{-2} s^{-1}. The value of E_k was measured as explained

in Supplemental data 3.5 and Supplemental Table 3.5. While 300 µmol m^{-2} s^{-1} was close to the optimum irradiance level, 30 and 1000 µmol m^{-2} s^{-1} where much below and higher this level, providing stress conditions.

The photon flux densities were measured using a 4π waterproof light probe (Walz, Germany) connected to a LiCor 189 quantum meter (Tremblin et al. 2000). In all cases a 12/12 h light/dark cycle and 21°C were applied. Once the axenic cultures reached sufficient cell densities in phase 1, 2 and 3 (Supplemental Figure 3.1) cells were harvested for following measurements.

3.3.3 Growth determination of microalgae

Cell counting was carried out regularly using a Neubauer hemocytometer. Growth rate was obtained after fitting growth kinetics with the sigmoid equation using the freeware CurveExpert 1.4 software (http://www.curveexpert.net/). For short time interval, the growth rate μ_{sti} was estimated using equation 1

$$\mu_{sti} \text{ (cell } d^{-1}) = [\ln (N_t) - \ln (N_{t-1})]/\Delta t \quad \text{(Eq. 1)}$$

with N_t and N_{t-1} are the number of cells at time t and t^{-1}

3.3.4 Pigment extraction

Chlorophyll and carotenoids were measured according to the methods described by Jeffrey et al. (1997). Briefly, an aliquot of diatom culture (2 mL) was centrifuged (16100 × *g*, 5 min, 5°C) (Eppendorf Centrifuge 5415R, Beckman). The supernatant was discarded and the pellet containing biomass was mixed in 2 mL of a 95.5% acetone and the mixture was homogenized by grinding in a mortar and was placed in the dark at 4°C for at least 4 h. Cell debris was removed by centrifugation under the same conditions and supernatant was used for the assay.

Chlorophyll *a* = 11.77 (A665nm - A750nm) - 0.82 (A650nm - A750nm) (Eq. 2)
Chlorophyll c = 26.27 (A650nm - A750nm) - 3.52 (A665nm - A750nm) (Eq. 3)
Carotenoids = [(A443nm-A750nm) - (21.5 10^{-3}*Chl *a*) - (369.1 10^{-3}*Chl c)]/(166.0 10^{-3}) (Eq. 4)

3.3.5 Photosynthetic and respiratory activity, PI-curve

Rates of oxygen evolution were measured at 21°C in the light and in the dark-using a fiber optic oxygen meter (Pyroscience® FireSting O_2, Germany) using a diatom suspen - sion (1.5 mL). For phase characterization, the cells were illuminated with the different growth light, except for PI-curves for which the cells were irradiated with different

photon flux densities ranging from 0 to 2500 µmol m^{-2} s^{-1}. For respiration, the cells were maintained in darkness for the whole measurement. Gross photosynthesis was calculated as net photosynthesis plus respiration, assuming that respiration was the same in light and in darkness. Calculated values were normalized for cell density or chlorophyll *a* amount.

To derive the values of E_k, α^B and P^B_{max} the PI-curves were fitted using the model of Eilers & Peeters (1988) using the CurveExpert freeware (Supplemental data 3.5).

3.3.6 Chlorophyll fluorescence yield measurement

Chlorophyll fluorescence yield was monitored at the growth temperature using a fluorimeter FMS1 (Hansatech®) after a dark adaptation period (15 min) (Roháček et al. 2014). Briefly, F_0 was recorded under a weak modulated light (less than 15 µmol m^{-2} s^{-1}, 800 Hz). NPQ was induced during a 7 min non-saturating white actinic radiation (photon flux density 800 µmol m^{-2} s^{-1}, KL 1500; H. Walz, Germany). At the end of the actinic illumination, the dark relaxation of the Chlorophyll fluorescence yield was recorded in order to allow quenching analysis. For each sample, the minimum (F_0, F'_0, F''_0), maximum (F_M, F'_M, F''_M) and maximum variable (F_V, F'_V, F''_V) Chlorophyll fluorescence yields in a dark-adapted state, in a light-adapted state and during the dark relaxation were measured, respectively (Roháček et al. 2014) (for representative recording, see Supplemental Figure 3.4.

The measurements were performed by using 2 mL of culture according to the protocol published by Roháček et al. (2014). It is divided into three phases: dark adaptation state, light adaptation state and dark relaxation of the non-photochemical quenching. To avoid CO_2 shortage during measurements, the cultures were provided with $NaHCO_3$ (final, 4 mM/stock, 0.2 M). Fluorescence parameters were calculated using the described equations in Supplemental data 3.4.

The analysis of the qN relaxation kinetic into its components qNi, qNf and qNs was performed as explained in Roháček et al. (2014). The quality of the regression procedure was assessed using two parameters: (1) the values of qN_1 = qNf + qNi + qNs were compared to the experimental values of qN and (2) coefficient of determination of the fitting (R^2) was taken as a measure of how well observed outcomes are replicated by the regression model (Steel & Torrie, 1960). In this work a regression was considered as good when $R^2 \geq 0.90$.

3.3.7 Quantification of intracellular carbon and nitrogen, cellular carbon and nitrogen quotas, C and N uptake rate

Cell nitrogen and carbon quota (Q_N and Q_C) were determined for each growth phase (see Supplemental Figure 3.1) using a CHN elemental analyser (EAGER 300, Thermo

Scientific). Samples were filtered through precombusted Whatman GF/C glass filters under gentle vaccum (50 mm Hg) and dried at 70°C for 48h. The volume of solution filtered was adjusted to have either 0.1 or 0.3 10^{-8} cells per filter (Marchetti et al. 2012). The C (ρ_C) and N uptake rate (ρ_N) were estimated according to Marchetti et al. (2012) using equations 5 and 6:

ρ_C (pg cell^{-1} d^{-1}) = μ_{sti} Q_C (Eq. 5)

ρ_N (pg cell^{-1} d^{-1}) = μ_{sti} Q_N (Eq. 6)

Total amount of C immobilized (pg) = Q_C $N_{phase\ 3}$ (Eq. 7)

Total amount of N immobilized (pg) = QN $N_{phase\ 3}$ (Eq. 8)

3.3.8 Determination of protein content

To isolate total proteins, cell cultures were centrifuged (5000×*g*, 5 min, 4°C). Harvested cells were overlaid in 2 mM EDTA (Ethylene Diamine Tetra Acetic Acid) and were homogenized using Ultra Turrax® (IKAAnalysentechnik GmbH) for 10 min. After centrifugation of the mixture (13000×*g*, 5 min, 4°C), the supernatant was taken and protein amount was measured using spectrophotometer at 595 nm. Bradford assay was routinely used to determine the concentration of protein in the samples (Bradford, 1976).

3.3.9 Determination of lipid content

For lipid extraction, 10^8-10^9 cells were harvested as explained above. The lipid content was determined by the gravimetric method (Mettler Toledo M5 25-60C) and the content pg cell^{-1} (Kendel et al. 2013).

3.3.10 Determination of chrysolaminarin content

Cellular β-1,3-glucan was extracted according to the method explained by Granum & Myklestad (2002) with some modifications. Briefly, 10^7 cells were harvested as explained above. Each filter was transferred directly to a glass vial, and stored at 20 ˚C until analysis. The cellular β-1,3-glucans were extracted by H_2SO_4 (50 mM) at 60 ˚C for 10 min using a water bath. The extract was centrifuged at 14000 rpm for 10 min (4°C). The resulting supernatant was collected and transferred into a new tube and dried at 60 ˚C. 25 µL of 3% aqueous phenol and 2.5 ml concentrated H_2SO_4 were added to 2 mL sample in a test tube and the mixture was immediately vortexed. The tubes was allowed to stand for 30 min, and then cooled with running water. Absorbance at 485 nm was measured. The amount of reducing sugar was calculated using glucose (stock concentration: 50 µg mL^{-1}) as a standard.

3.3.11 Primer design

A total of 33 enzymes involved in carbon metabolism pathways from the diatom *P. tricornutum* were selected and the corresponding genes (74) coding for each enzymes (Supplemental Table 3.6) were searched in genomic data published by Kroth et al. (2008) (diatomcyc: http://www.diatomcyc.org; JGI portal: http://genome.jgipsf.org/ Phatr2 /Phatr2.home. html; BLAST: http://blast.ncbi.nlm.nih.gov/Blast.cgi). Primers were designed using Primer Express version 2.0 (Applied Biosystems, Foster City, CA) (primer sequences of genes and housekeeping genes are shown in Supplemental Table 3.6.

3.3.12 mRNA sampling and extraction

mRNA extractions were done at phase 1, 2 and 3 by filtration in order to have 1.5 10^8 cells per filter (see above for details). The filters were immediately flash frozen in liquid nitrogen and stored in −80 °C until RNA extraction. Total RNA was extracted following the Spectrum Total RNA kit (Sigma Aldrich) protocol with on-column DNase digestion as suggested by the manufacturer and RNA concentration of samples were determined by UV absorption at 280/260 nm (Nanodrop).

3.3.13 Real-time quantitative PCR and analyses

One microgram of total RNA was reverse transcribed into cDNA using the MMLV reverse transcriptase (Promega) following the manufacturer's protocoleReal time PCR reactions were performed using a Step One plus appartus (Applied Biosystems) with the Gotaq QPCR Master Mix (Promega) and specific primers described in Supplemental Table 3.6. The threshold cycle (Ct) was determined by the Step One plus version 2.1 software. The efficiency of the PCR reaction was calculated for each gene using the Ct slope method, which involves generating a dilution series of the target template and determining the Ct value for each dilution. A plot of Ct versus log (concentration) was constructed and efficiency (E) expressed as $E= 10^{(-1/slope)}$. Efficiencies calculated for all genes ($90 \leq E \leq 110$) indicated correct PCR reactions without inhibition (Gašparič et al. 2008).
Amplified products of the expected sizes were excised from agarose gel and purified using the QIAEX II gel extraction kit (Qiagen), then cloned into pGEMT plasmid vector (Promega) and sequenced by Beckman Coulter Genomics (Sanger sequencing). BLAST analysis confirmed the sequence identification.
Out of the 12 housekeeping gene (HKG) candidates, the most stable (tbp, ubi and rps) were selected due to high Ct standard deviation (>1) and weak pairwise correlations ($p>0.05$) compared to the 9 others ($p<0.001$). The selected housekeeping genes were used as the endogenous control genes to normalize the expression of the 74 target

genes, using the Bestkeeper Software (Pfaffl et al. 2004). This software determines the optimal housekeeping genes employing pairwise correlations and calculates the geometric mean of the best suited ones for accurate normalization of the target genes (TG). The calculation of the relative expression (RE) was based on the comparative Ct method (Livak & Schmittgen, 2001):
$RE = ((E_{TG})^{\Delta Ct\text{-}TG})/(E_{HKG})^{\Delta Ct\text{-}HKG}$ with $\Delta Ct = Ct_{Calibrator}\text{-}Ct_{sample}$ (Pfaffl et al., 2004).
PCA analyses were performed by SPSS (Statistical Package for the Social Sciences) and Heatmaps performed using Netwalker 1.0. Statistical analyses for physiological data were performed by *t*-test and $p \leq 0.05$ was considered statistically significant.

3.4 Results

3.4.1 Effect of light intensity on the growth of *Phaeodactylum tricornutum*

Light is a major factor regulating the development of microalga (Spetea et al. 2014; see also chapter 6). Light regime, including short terms and long-terms intensity fluctuations, are major factors affecting growth and biochemical composition of microalgae (Wahidin et al. 2013). Regardless the growth irradiance intensity, the growth curve of *P. tricornutum* could be fitted using a logistic law. The curves presented typical phases *i.e.* lag, exponential and plateau phases. In the rest of the manuscript, we will refer to these different phases as phase 1, phase 2 and phase 3, respectively (Supplemental Figure 3.1). No significant difference ($p<0.05$) between the growth curves of *P. tricornutum* under medium light (ML) and high light (HL) was observed. Cell density under low light (LL) was significantly lower ($p<0.05$) than under ML and HL and growth phases were delayed in LL. Accordingly, growth rate 'μ' and duplication time 'G', were similar under ML and HL, whereas these values were lower under LL (Table 3.1).

Table 3.1. Impact of the light intensity on culture growth rate and generation time of *Phaeodactylum tricornutum*. The growth rates (μ) and duplication times (G) were calculated from the curves of Figure 3.1 using the equation indicated in the 'Material and method' section. Under LL, the rate of cell division was *circa* 30% less than under ML and HL. Mean values ± SE (n= 3–5). Significant different data are indicated by an asterisk (Tukey Test, $p \leq 0.05$).

Irradiance (μmol m^{-2} s^{-1})	30 (LL)	300 (ML)	1000 (HL)
μ (day^{1})	0.340 ± 0.003*	0.873 ± 0.009	0.865 ± 0.010
d (day)	2.039 ± 0.048*	0.797 ± 0.008	0.806 ± 0.009

Altogether, the results demonstrated that *P. tricornutum* was able to grow well under the three light conditions. Because cell physiology is not independent of growth

conditions (Klumpp et al. 2009; Scott et al. 2010; Regenberg et al. 2006; Brauer et al. 2008), the elucidation of the underlying mechanisms requires comparing samples being in close physiological state. To fulfill this condition, the time-course of the daily division rate (μ_{ddr}) along the growth period was calculated for each light intensity (data not shown). Regardless the light intensity, the time courses present a bell-shape peaking at the middle of the exponential phase and zeroing in lag and plateau phases (data not shown). Sampling times were chosen when time-courses were reaching its maximum and were close to zero. These events are indicated in Supplemental Figure 3.1, by arrows.

3.4.2 N and C fluxes to lipid, carbohydrate and protein

Because the primary metabolism and physiological activities primarily rely on the C and N availability and cell uptake, the cellular N and C quota (Q_N and Q_C , respectively) were recorded. The time-courses of Q_N and Q_C were different according to the irradiance level: under LL, Q_N and Q_C decreased from phase 1 to phase 2 and increased from phase 2 to phase 3. Under ML, Q_N and Q_C decreased continuously whereas under HL, the decrease occurred only between phase 2 and phase 3 (Figures 3.2.A and 3.2.B). From these data, the N and C uptake rates could be estimated using equation 5 and 6. As expected the uptake was the most intense in phase 2 and much reduced in phase 3 (Figure 3.2.C and 3.2.D). When expressed relatively to Q_N, Q_C, varied only significantly in phase 3 in function of the growth light intensity: it increased from LL to HL (data not shown).

Having determined Q_N and Q_C as well as the amount of cells present in phase 3, the total amounts of N and C immobilized in the algae were estimated (see equations 7 and 8 in the Material and method section). The yield of C fixation ranged between 73 (LL and ML) and 78% (HL) whereas the yield of N fixation was around 10 %, regardless of the light intensity (Table 3.2). Altogether, the results indicate that the synergism between N and C metabolisms was almost not disrupted at any moment of the growth in our condition.

The fixed N and C are used for the synthesis of cellular building blocks including lipids, proteins and carbohydrates. Modification(s) of the chemical or physical environmental stimuli, including light intensity may change the orientation of the fixed C into the different pathways (Hu et al. 2008; Sharma et al. 2012). Growth phase and aging of the culture can also affect TAG content and fatty acid composition (Fidalgo et al. 1998; Hu et al. 2008). To evaluate if shifts in C and N orientation occurred, total amount of lipids, proteins and carbohydrates (LPC) were measured in the culture media and in the cells. None of these compounds could be detected in the culture media (data not shown) showing that export of such material was low under our conditions. We cannot

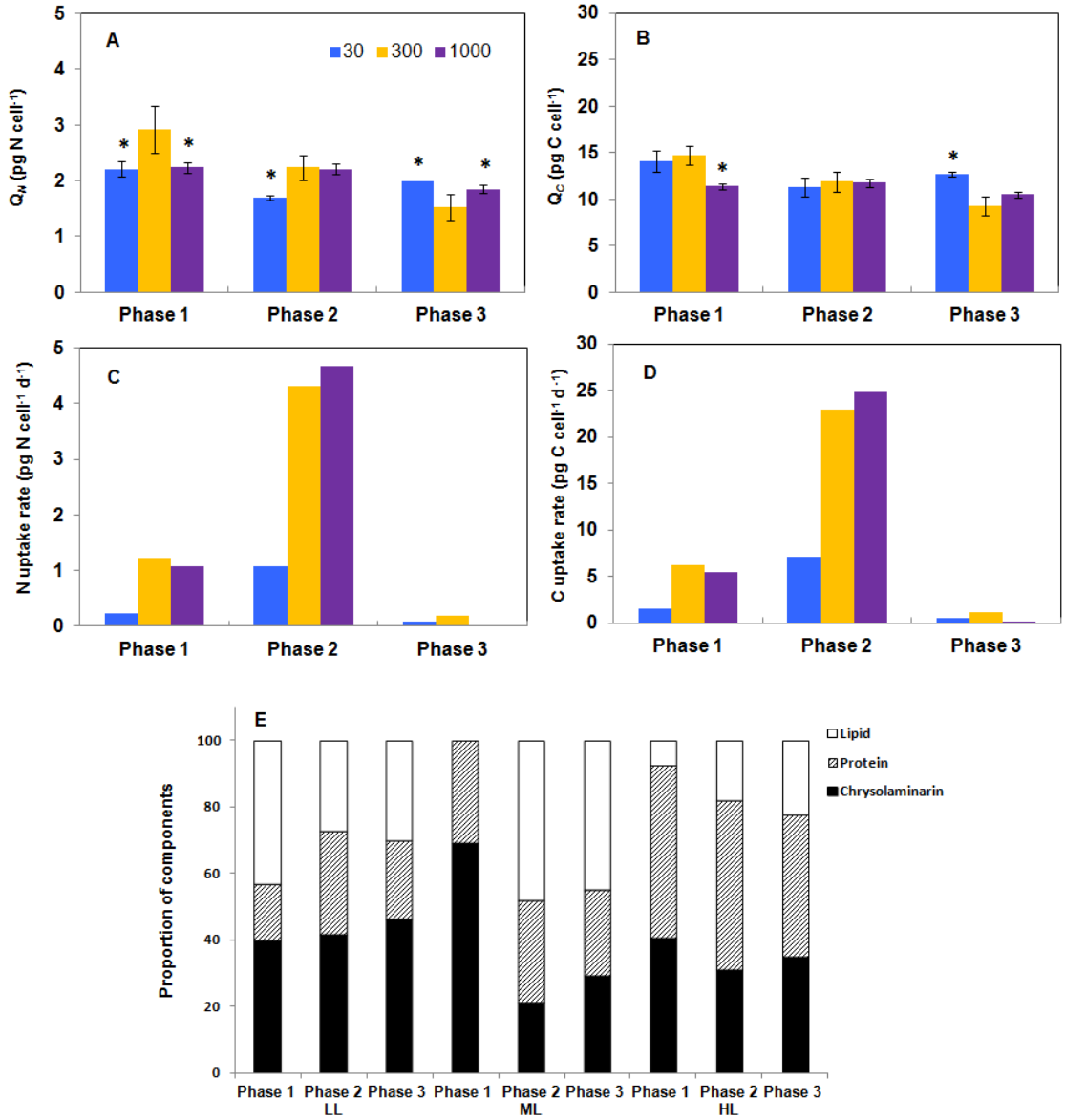

Figure 3.2. Modifications of the carbon, nitrogen, total carbohydrate, protein and lipid content of *Phaeodactylum tricornutum* during growth under different photon flux densities. Under LL, Q_N and Q_C decreased from phase 1 to phase 2 and increased from phase 2 to phase 3 whereas under ML, Q_N and Q_C decreased continuously. Under HL, the decrease occurred only between phase 2 and phase 3 (panels A and B). The rate of C and N uptake were the most intense in phase 2 and very reduced in phases 1 and 3 (panels C and D). The relative amount of LPC was greatly impacted by the photon flux density. Lipids were the most abundant in phase 1 under LL whereas under ML and HL, they were barely detectable (panel E). Under LL, the relative abundance of lipids decreased during the transition from phase 1 to phase 2 and then remained constant until phase 3. This contrast with ML and HL for which the lipid proportion increased until phase 2 (ML) or phase 3 (HL) (Panel E).

however exclude that the presence of such compounds in the culture medium but then under the detection limits.

The relative amount of LPC was greatly impacted by the light intensity. For instance, in phase 1 and under LL, lipids represent more than 60% of the total cellular mass of LPC whereas under ML and HL, lipids were barely detectable at that stage of growth (Figure 3.2.E). Under LL, the relative abundance of lipids decreased during the transition from phase 1 to phase 2 and then remained constant until phase 3. This contrast with ML and HL for which the lipid proportion increased until phase 2 (ML) or phase 3 (HL) (Figure 3.2.E).

The relative abundance of carbohydrates was the highest (70%) in phase 1 under ML. It dramatically decreased during the transition to phase 2 whereas under LL and HL it did not changed by more than 8%. The relative amount of proteins was the highest (55%) under HL. Under this growth irradiance, it decreased only from phase 2 to phase 3 by circa 10% (Figure 3.2.E).

When normalized to the Chl amount, the Q_C/Chl a between phase 1 and phase 2 changed according to the growth light intensity: under LL, it slightly decreased, remained constant under ML and increased in HL. In phase 3, the values were similarly small for each condition (data not shown).

Table 3.2. Quantitative and relative amounts of C and N immobilized in the cells in phase 3. At the end of the studied period, approximately the same proportion of the initial carbon content has been consumed. The cells differ by the amount of C accumulated within the cells. The total amount of C within the cells is the highest in cells grown under ML suggesting that the conditions were the most favourable for C storage. The oxygen evolution measurements suggest that the lower level of carbon accumulation is due to an increase of the respiratory and/or photorespiration activity under LL and the HL.

	LL	**ML**	**HL**
Total C amount (mg)	197	167	199
Relative amount of the initial C consumed (%)	73	73	78
Total N amount (mg)	3.0	2.3	2.8
Relative amount of the initial N consumed (%)	10	8	9

3.4.3 Pigment content

Chlorophyll *a* (Chl *a*), chlorophyll c (Chl c) and fucoxanthin are the major light harvesting pigments in diatoms (Jeffrey et al. 1997; Nguyen-Deroche et al. 2012). Changing growth irradiance altered the concentrations of these components. To characterize further these changes during growth, the amount of pigments were expressed relatively to the value reached in the corresponding phase 2 (Table 3.3).

Table 3.3. Impacts of growth phase and photon flux density on the relative amount of photosynthetic cells in different growth phases grown under different light intensities. Each growth phase of LL and HL has been compared to phase 2 of each light condition, separately. Generally, the proportion of pigments is the largest in phase 3.

Light intensity	**L**			**M**			**H**		
Growth phase	1	2	3	1	2	3	1	2	3
Total pigments	95	100	128	126	100	278	187	100	304
Chl *a*	98	100	129	112	100	271	198	100	343
Chl c	292	100	233	26	100	85	94	100	252
Carotenoids	62	100	112	338	100	612	202	100	270

Cells grown under LL contained always more pigments compared to the other treatments (Figure 3.3). This result agrees with those obtained with other diatoms (*P. tricornutum*: Geider et al. 1985; *Thalassiosira weisflogii*: Post et al. 1984, 1985; *Haslea ostrearia*: Mouget et al. 1999).

The time-course of Chl *a* and carotenoids accumulations were very similar under ML and HL: both decreased during the transition between phase 1 to phase 2 and significantly increased in phase 3 (Supplemental Figure 3.2.A and C). This increase was around 271% and 343% for Chl *a* and 612% and 217% for carotenoids under ML and HL, respectively (Table 3.3). Under LL, the level of individual pigments increased from phase 1 to phase 3 except Chl c that decreased by 33% between phase 1 and phase 2 and then increase by 233% in phase 3 (Table 3.3 and Supplemental Figure 3.2). During phase 1 and phase 3, Chl c content was higher under LL than under ML or HL (Supplemental Figure 3.2.B).

The variation of the Chl *a*/Chl c ratio is used as a proxy of the size of the light harvesting antenna complex (Lamote et al. 2003; Nguyen-Deroche et al. 2012). It varied in opposite under LL and ML/HL, respectively. Under LL, the ratio increased from phase 1 to phase 2 and then decreased until phase 3 (Supplemental Figure 3.2.D). At the end of

phase 3 the ratio was similar for all conditions. Interestingly, carotenoids mostly followed the Chl *a*/Chl c ratio except during phase 2 to phase 3 transition under LL (Supplemental Figure 3.2.D).

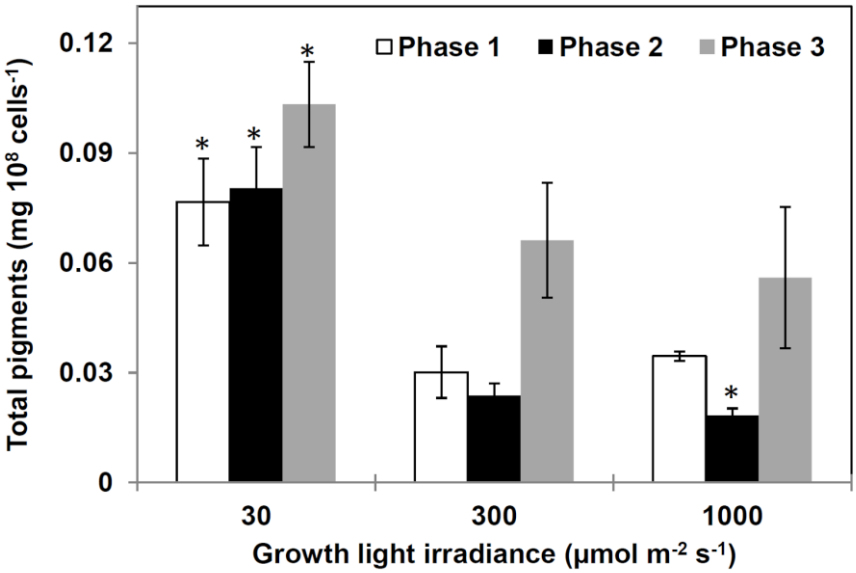

Figure 3.3. Total pigments in *Phaeodactylum tricornutum* grown under different light intensities. The content in Chl *a*, Chl c and fucoxanthin is altered by growth irradiance. Under LL, diatom cells contained always more pigments than under other light intensities. Under ML and HL, Chl *a* and fucoxanthin decreased during the transition between phase 1 to phase 2 and significantly increased in phase 3. Data are mean values ± SE (n = 3) and error bars represent SD. Means followed by asterisks are significantly different from the corresponding value in ML ($p < 0.05$).

3.4.4 Photosynthetic and respiratory activities

The photosynthetic activity was measured as the capacity of the algae to emit oxygen under an illumination. Because the value of the compensation point increased with the photon flux density (Supplemental Table 3.5), we concluded that the respiration activity (R_d) is impacted by the light intensity (see Figure 3.4.B). Consequently, R_d was measured in the dark immediately after each measurement of photosynthesis.

Net photosynthesis (A_{max}) expressed relatively to the cell number (Figure 3.3.A) or to the Chl *a* amount (Supplemental Figure 3.2.A) present the same trends. Regardless the growth phase, the net oxygen emission was significantly higher under ML and HL than under LL.

As shown earlier, R_d was impacted by the growth irradiance: it was higher under ML and HL than under LL except during phase 3 (Figure 3.4.B and Supplemental Figure

3.3.B). However, when taken individually, neither R_d nor A_{max} were significantly affected by the irradiance value during phase 1 and phase 2. The view is less clear in phase 3: under ML and HL both activities were reduced suggesting a strong reduction of the metabolic activities (Figure 3.4 and Supplemental Figure 3.3).

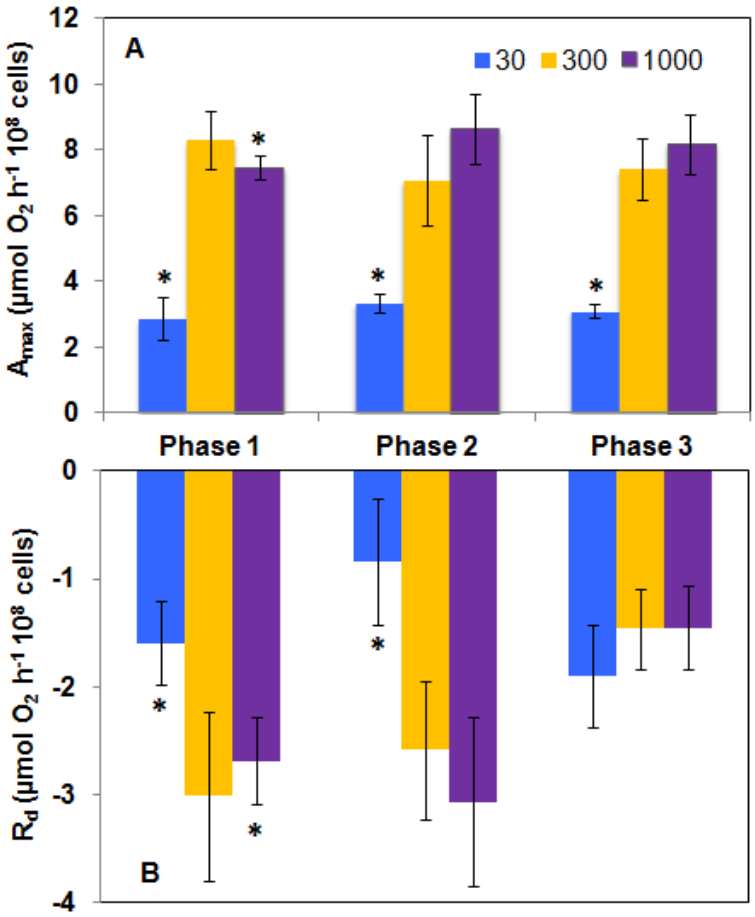

Figure 3.4. Net photosynthesis (A_{max}) and respiration (R_d) activities in *Phaeodactylum tricornutum* grown under different light intensities. A_{max} and R_d were significantly higher under ML and HL than under LL. However, their values did not change along the growth at any of the grown photon flux densities. Under LL, A_{max} was reduced while respiration was high, staying however below. Values represent the mean ± SE (n = 3) and error bars represent SD. Means followed by different letters and asterisks are significantly different in each light intensity and each growth phase, respectively ($p < 0.05$).

Under LL, R_d increased, staying however under A_{max} value when related to the cell amount (Figure 3.4.B). Due to the change of Chl *a* occurring in phase 3, an inverse relationship was found when R_d and A_{max} were related to the Chl *a* amount (Supplemental Figure 3.3.B).

3.4.5 Photochemical and non-photochemical quenching analysis

To determine whether the modifications in the pigment content reported above were affecting the management of the incoming energy, the variations of the Chl *a* fluorescence yield were recorded during an actinic illumination equal to the growth irradiance. Typical recording are presented in Supplemental Figure 3.4. Figure 3.5 compares the variations of photochemical and non-photochemical processes using characteristic parameters (photochemical: ΦP0, ΦII, qP, 1-qP; non-photochemical: (q_0, qN) during growth under the different light intensities. The meaning of the parameters and the equations used for calculations are presented in Supplemental Table 3.4. The maximum quantum yield of photosystem II (PSII) photochemistry (ΦP0) in cells grown under different light condition and different growth phases was constant (almost 0.6) (Figure 3.5), being consistent with that previously reported in *P. tricornutum* (Bertrand et al. 2001; Roháček et al. 2014) for non stressed diatoms, suggesting that cells were healthy. This result contrasts with the effective quantum yield of photochemical energy conversion in PSII, which progressively reduced from LL to HL. When compared to ML, ΦII was higher about 60, 53 and 125% (phase 1, 2 and 3, respectively) in cells grown under LL.

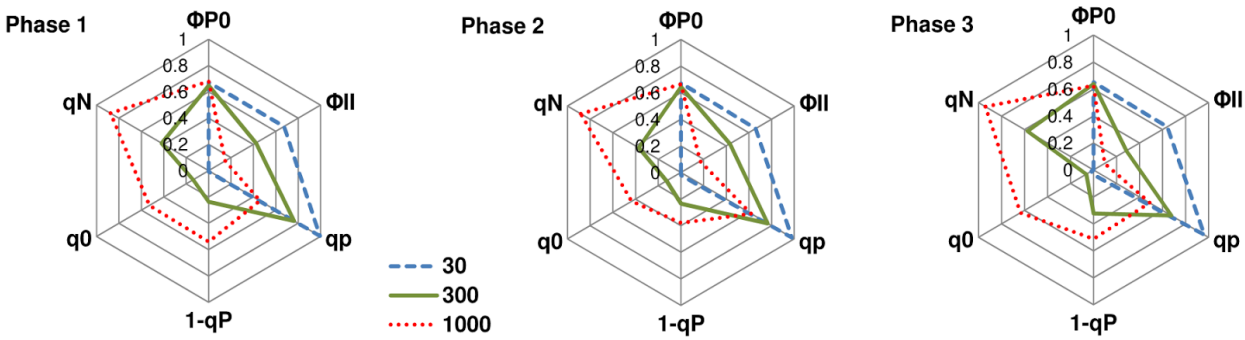

Figure 3.5. Variations of fluorescence kinetic parameters of *Phaeodactylum tricornutum* grown under different light intensities and during different growth phases. The maximum quantum yield of PSII photochemistry (ΦP0) in cells grown under different light condition and different growth phases was constant (almost 0.6), suggesting that cells were healthy. This result contrasts with the effective quantum yield of photochemical energy conversion in PSII, which progressively reduced from LL to HL. The photochemical quenching (qP) that quantifies the actual fraction of PSII reaction centers staying open during the illumination. qP values decreased as the light intensity increased in an antiparallel manner with 1-qP, that quantifies the fraction of closed reaction centers.
The non-photochemical quenching parameters qN and q0 reflect the excess radiation converted to heat during the actinic radiation. Under LL, qN and q0 are close to zero, indicating that under this lighting condition, there was no excess of absorbed energy. The intensity of these parameters was higher under ML and HL, suggesting that under these photon flux densities, part of the incoming energy needed to be dissipated as heat.

The photochemical quenching (qP) quantifies the actual fraction of PSII reaction centers staying open under either light intensity (Roháček et al. 2008). No significant change of qP was observed during different growth phases under either light intensity showing that diatoms were well adapted to the growth conditions. However, the qP values decreased as the light intensity increased. Under HL, qP values were approximately 50% of the values under LL (Figure 3.5).

The values of 1-qP, that quantifies the fraction of closed reaction centers varied accordingly (Figure 3.5). The absorption of an excess of photon triggers mechanisms of energy dissipation as heat (Roháček et al. 2008; Roháček, 2010; Stirbet et al. 2014). These mechanisms are collectively referred to as the non-photochemical quenching (NPQ or qN) because they are lowering the Chl fluorescence yield (Roháček et al. 2008; Roháček, 2010; Stirbet et al. 2014).

The related parameters qN and q0 reflect the excess radiation converted to heat during the actinic radiation. According to the figure 3.5, these parameters increased with increasing the light intensity. Under LL, they were close to zero, indicating that under this lighting condition, there was no excess of absorbed energy. This was not the case when cells were growing under ML and HL. To decipher the mechanisms contributing to the dissipation of the excess of energy, the kinetic of the relaxation of the non-photochemical quenching was recorded according to Roháček et al. (2014). When adapted to the light conditions (Fs phase) cells were placed in the dark, non-photochemical quenching gradually relaxed (Supplemental Figure 3.4). The mathematical analyses could only be performed on the relaxation kinetics recorded with samples illuminated with actinic light equal to ML or HL.

In agreement with Roháček et al. (2014) three individual components were found in both cases (data not shown). The mathematical analyses revealed that regardless the growth phase and the growth light the less intense component was qNf while the most intense component was qNi (for a detailed explanation of the meaning of these components, see the discussion and the Supplemental Figure 3.4). The amplitude of qNf remains at the basic levels except in phase 3 under ML. The intensity of qNi and qNs were always larger in cells grown under HL than in cell grown under ML whereas the intensity of qNf was always larger in cell grown under ML than under HL, except in phase 2 in which the values were not significantly different one from each other. The proportion of qNi increased from phase 1 to phase 3 (Figure 3.6). qNs was the second mostly intense components. Its amplitude slightly decreased from phase 1 to phase 3 under HL while it remained constant under ML.

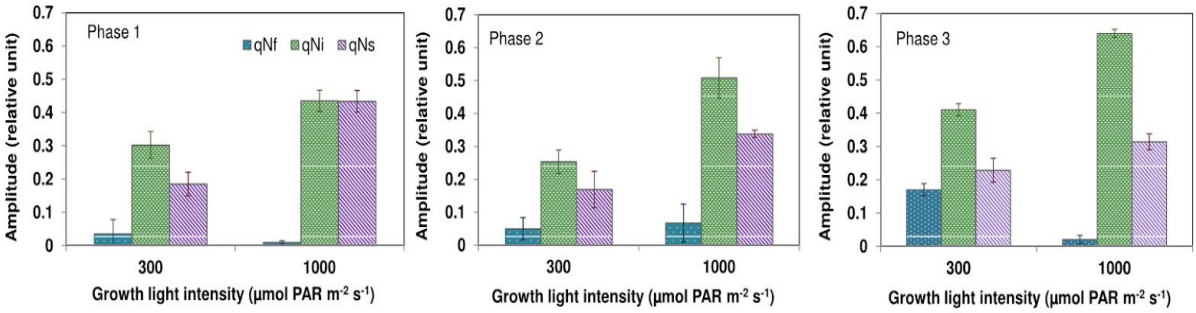

Figure 3.6. Variations of the intensity of the components qNf, qNi and qNs during the relaxation of the non-photochemical quenching recorded after an actinic illumination of *Phaeodactylum tricornutum*. When light adapted cells were placed in the dark, the light induced non-photochemical quenching gradually relaxed (Supplemental Figure 3.4). The mathematical analyses of the relaxation kinetic allowed the determination of three individual components that are denoted qNs, qNi and qNf. The intensity of qNi and qNs were always the largest in cells grown under HL whereas the intensity of qNf was the largest under ML, except in phase 2 in which the values were not significantly different. The proportion of qNi increased from phase 1 to phase 3. qNs was the second mostly intense components. Its amplitude decreased from phase 1 to phase 3 under HL while it remained constant under ML.

3.4.6 *In silico* reconstruction of *Phaeodactylum tricornutum* central carbon metabolism

3.4.6.1. Central metabolism

To retrieve the set of genes putatively encoding the biosynthetic key enzymes involved in central carbon metabolism of *P. tricornutum,* DiatomCyc, JGI, BLAST and Kroth et al. (2008) data were mined. The key enzymes distributed among the different compartments and their related gene/isogene(s) and primers are listed in the Supplemental Table 3.6. To get a clear view on central carbon metabolism pathways, a simplified overview of the most important metabolites and reactions between pathways is briefly described in Supplemental Figure 3.7. More details of each pathway with the number of isoforms for each enzyme are shown in Figure 3.7.

The Calvin–Benson cycle plays a central role in the global carbon cycle: CO_2 is assimilated by RubisCo and processed into triose phosphate (TP) including glyceraldehyde 3phosphate (GAP) and dihydroxyacetone phosphate (DHAP) that occur as intermediate in several central metabolic pathways (Kroth et al. 2008; Obata et al. 2013). Kroth et al. (2008) have identified various Calvin–Benson cycle enzymes in up to five isoforms, distributed between plastids, mitochondria and cytosol. Although most of the Calvin–Benson cycle enzymes in diatoms are very similar to those of land plants, they might be differently regulated by light (Wilhelm et al. 2006). RubisCo is an enzyme

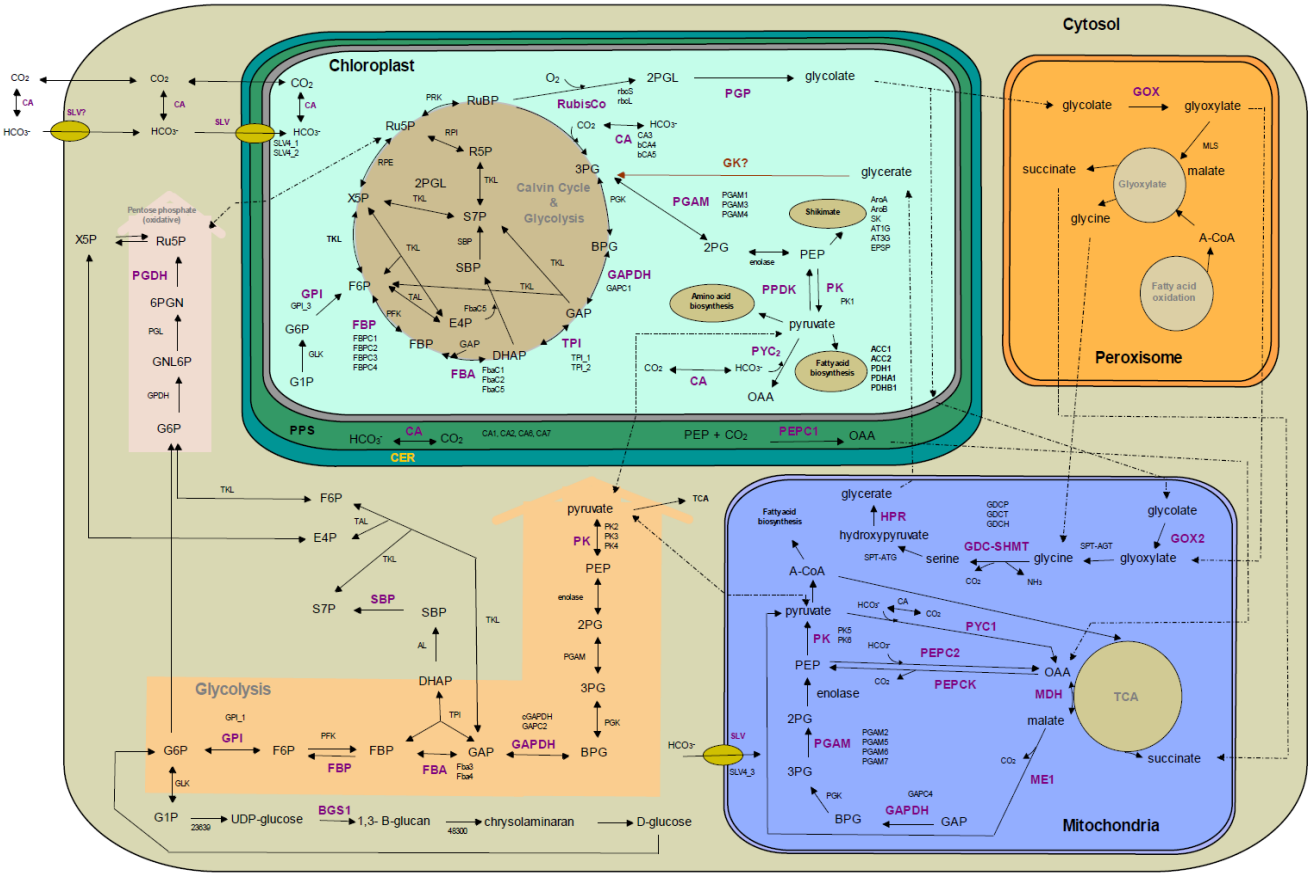

Figure 3.7. Cellular pathways and processes of central carbon metabolism in *Phaeodactylum tricornutum*. All red depicted enzymes are the key enzymes and their related gene/isogenes are listed beside.

Abbreviations: RUBP: D-ribulose-1,5-bisphosphate; 3PG: 3-phospho-*D*-glycerate; BPG: 1,3-diphosphateglycerate; GAP: D-glyceraldehyde-3-phosphate; DHAP: dihydroxyacetone phosphate; FBAC: chloroplastic fructose-1,6-bisphosphate aldolase; FBP: fructose-1,6-bisphosphate; F6P: D-fructose-6-phosphate; X5P: D-xylulose-5-phosphate; Ru5P: D-ribulose-5-phosphate; SBP: D-sedoheptulose-1,7-bisphosphate; S7P: D-sedoheptulose-7-phosphate; R5P: D-ribose-5-phosphate; E4P: D-erythrose-4-phosphate; 2PGL: 2-phosphoglycolate; 2PG: 2-phosphoglycerate; PEP: phospho*enol*pyruvate; OAA: oxaloacetate; A-CoA: acetyl-CoA; G1P: D-glucose 1-phosphate; G6P: D-glucose-6-phosphate; GNL6P: D-glucono-δ-lactone-6-phosphate; 6PGN: 6-phospho-D-gluconate; PPS: periplasmic space; ER: endoplasmic reticulum (chloroplastic); ACC1, ACC2: Acetyl-CoA-carboxylase; PDH1, PDHA1, PDHB: pyruvate dehydrogenase E1; BGS1: glycosyl transferase

composed of eight large (rbcL) and eight small subunits (rbcS) (Joshi et al. 2015). When O_2 out-competes CO_2 for binding acceptor ribulose D-ribulose-1,5-bisphosphate (RuBP), photorespiration occurs, leading to the formation of a two carbon molecules, 2-phosphoglycolate (2PGL), the first product of oxygenation reaction by RubisCo (Nishimura et al. 2008), known to inhibit the Calvin–Benson cycle enzyme triosephosphate isomerase (TPI) (Husic et al. 1987) (Figure 3.7). 2PGL is then dephosphorylated to glycolate by 2-phosphoglycolate phosphatase (PGP).

Although a large fraction of the produced glycolate is released by marine phytoplankton into the water body, resulting in carbon loss (Leboulanger et al. 1997), the remaining portion of the chloroplastic glycolate pool is reclyed through photorespiratory pathway (Parker & Armbrust, 2004). In diatoms, photorespiration utilizes enzymes present in the plastid, mitochondria and also peroxisome (Kroth et al. 2008; Figure 3.7). In addition to glycolate shunt from chloroplast to peroxisome to form glyoxylate in a reaction catalyzed by a glycolate-oxidising enzyme (GOX) (more probably a dehydrogenase than an oxidase), glycolate is also exported into mitochondria where the formation of glyoxylate is followed by transamination to produce glycine. Alternatively, glyoxylate can be directly exported from peroxisome to mitochondria where it is transformed to glycine. To summarize, photorespiration results in a succession of organic compounds including glycolate, glycine, and serine (see Figure 3.7). Serine is further metabolized to glycerate. Generally, but not in diatoms, glycerate may then enter the Calvin–Benson cycle in the chloroplast after phosphorylation by glycerate kinase (GK). So far, no evidence for a gene coding a chloroplastic GK was identified in the genome of *P. tricornutum* or in *T. pseudonana* (Kroth et al. 2008; Fabris et al. 2012). Nevertheless, a gene encoding a mitochondrial GK has been identified in *P. tricornutum* by Fabris et al. (2012). Smith et al. (2012) suggested that if a mitochondrial GK exists, the photorespiration by-product could then directly enter mitochondrial glycolysis and the tricarboxylic acid (TCA) cycle and be used to either drive energy generation or to replenish TCA cycle intermediates (not presented in Figure 3.7). Another hypothesis claims that all the glycine and serine may be shunted to other pathways such as the formation of the antioxidant glutathione (Raven & Beardall, 1981; Kroth et al. 2008). In contrast, Matsuda & Kroth (2014) have reported the photorespiration is the major pathway to recycle 2PGL in diatoms to produce glycine and serine, suggesting that photorespiration might not be involved in recycling of 3PG. The fate of glycerate and more generally the role of the photorespiration remain open questions in diatoms.

Glycolysis is an energy generating pathway (Smith et al. 2012) that is closely linked to the other carbon metabolic pathways (Figure 3.7). Glycolysis pathway is divided into two main phases with an ATP consuming upper part (first phase) from glucokinase (GLK) to triose phosphate isomerase (TPI) and an ATP producing lowerpart (second phase) from glyceraldehyde 3-phosphate dehydrogenase (GAPDH) to pyruvate kinase

(PK) (Figure 3.7) (Smith et al. 2012). Glucose produced by degradation of chrysolaminarin is metabolized via glycolysis to provide the cell with energy (ATP and NADH) as well as the metabolic intermediates required to supply either the TCA cycle or fatty acid biosynthesis (Obata et al. 2013). Investigating the genome of *Thalassiosira pseudonana* allowed to identify genes coding enzymes for the complete cytosolic glycolysis (Armbrust et al. 2004) and analysis of the genome of *P. tricornutum* suggested that this pathway, is duplicated in diatom plastids (Kroth et al. 2008). On the basis of *in silico* analyses, Kroth et al. (2008) predicted the additional location of isozymes corresponding to the complete lower half of glycolysis (GAPDH, TPI to PK) in the mitochondria. Of the six identified GAPDH genes in *P. tricornutum*, GAPC4 and the fusion protein TPI/GAPC3 are predicted to be targeted in the mitochondria (Liaud et al. 2000; Kroth et al. 2008; Chauton et al. 2013). Other GAPC genes encode enzymes localized in the cytosol and in the chloroplasts (Gruber et al. 2009; Liaud et al. 2000). Most of the enzymes involved in these pathways can function bi-directionally. The direction of the flux of the pathways tends to be regulated by mass action, allostery, or post-translational modification(s) (Smith et al. 2012).

It is worth mentioning that in *P. tricornutum,* Fabris et al. (2012) highlighted the presence of a functional Entner-Doudoroff pathway (EDP), which converts glucose-6-phosphate (G6P) to pyruvate and GAP in the mitochondria (not shown in Figure 3.7). The role of the EDP may be to feed TCA cycle with pyruvate early after the transition from dark to light *i.e.* when pyruvate production through the "classic" glycolytic pathway is weak, resulting in a deficiency of ATP generation (Shtaida et al. 2015) that could not be compensated by photosynthesis that is resuming (for more details see Fabris et al. 2012; Chauton et al. 2013).

3.4.6.2 CO_2 supply

In addition to inorganic carbon acquisition through CO_2 diffusion, the majority of microalgae aid RubisCo to capture efficiently CO_2 by activating carbon concentration mechanisms (CCMs). Two types of CCM have been described.

The first type is known as the biochemical CCM. It involves the fixation of HCO_3^- into C_4 compounds in the manner of C_4 plants (Roberts et al. 2007; Matsuda et al. 2011; Nakajima et al. 2013). However, and in contrast with C_4 plants, *in silico* analyses of the subcellular localization of the relevant enzymes predicted a scrambled C_4 metabolism. Phospho*enol*pyruvate carboxylase 1 (PEPC1) is predicted to be targeted either in the endoplasmic reticulum (ER) (chloroplastic ER) or in the periplasmic space (PPS) between the second and third membranes of the four plastid membrane of diatom (for a detailled description of the chloroplast envelops in diatoms, see Solymosi, 2012). PEPC2, PEP carboxykinase (PEPCK), malate dehydrogenase (MDH), malic enzyme (ME) and pyruvate carboxylase (PYC1) are all predicted to be localized in the mitochondria,

whereas pyruvate phosphate dikinase (PPDK) and PYC2 are predicted to be plastidtargeted (Figure 3.7) (Kroth et al. 2008; Chauton et al. 2013; Haimovich-Dayan et al. 2013).

The second mechanism of CCM is denoted as the biophysical CCM. This mechanism involves the transport of CO_2 and HCO_3^- as inorganic forms by transporters located in the plasma membrane and chloroplasts envelopes (SLVs) and carbonic anhydrases (CAs). There are numerous carbonic anhydrases (CAs) within the matrix of the layered plastidic membranes, strongly suggesting large interconversion activity between CO_2 and HCO_3^- within the chloroplast envelope (Matsuda & Kroth, 2014). The alkaline stromal pH is very important for the conversion between CO_2 and HCO_3^- (Figure 3.7) (Wang et al. 2011). HCO_3^- enters the thylakoid lumen through an anion channel (still controversial) by the light-powered proton pump, which generates both an electrical potential difference and a pH difference across the thylakoid membrane (Raven et al. 2014).

The pyrenoid is a crystallike proteinaceous undefined cellular micro-compartement that may play important role in CCMs. These structures are in the chloroplast in which most of the RubisCo are located, and it is here that CO_2 is concentrated around RubisCo (Moroney & Ynalvez, 2007; Matsuda & Kroth, 2014). It has been reported that thylakoid and pyrenoid are closely associated to each other and form a so-termed thylakoid-pyrenoid complex allowing the enzyme to operate at a higher efficiency than when dispersed throughout the chloroplast. Carbonic anhydrases accelerate the equilibration of HCO_3^- and CO_2. CA3 has been reported to be active in the chloroplast endoplasmic reticulum (CER) (Samukawa et al. 2014) and in the thylakoid-pyrenoid complex. Pyrenoid also contains bCA4 and bCA5 (for more details see Raven et al. 2014). Although, the presence of a pyrenoid does not necessarily mean that the cells possess a CCM (Ratti et al. 2007; Genkov et al. 2010), there is the possibility that the pyrenoid functions as a focal point of the CCM, specially with the presence of bCA4 and bCA5 (Figure 3.7) (for more details see Matsuda & Kroth, 2014; Samukawa et al. 2014; Holtz et al. 2015).

In addition to CAs involved in the biophysical CCM, there are several HCO_3^- transporters acting in CO_2 acquisition in diatom forming the SLV family of transporters. Within the 10 SLV families identified in *P. tricornutum,* 7 genes, forming the SLV4 family, were found to encode bicarbonate, CO_3^{2-} or HCO_3^- transporters across membranes (Romero et al. 2004; Nakajima et al. 2013). In the study performed by Chauton et al. (2013), SLV4 transporters were strongly down-regulated at dark. While Reinfelder et al. (2000) reported higher transcriptional activity late in the day and during the night in SLV4 and putative CA1 and CA2. In addition to participate in CCM, plastidic bicarbonate transporters play an important role in excess light energy dissipation by consuming ATP for a carbon cycling through a fast efflux of CO_2 across the plasmalemma (Tchernov et al. 2003).

3.4.6.3 The fate of photosynthetically fixed CO_2

Under stress or unfavorable environmental conditions, many algal species produce substantial amounts of neutral lipids (20-50% dry cell weight), mainly in the form of triacylglycerols (TAGs) that serve as a storage form of carbon and energy for cell (Hu et al. 2008; Lemoine & Schoefs, 2010; Sharma et al. 2012; Mimouni et al. 2012; Heydarizadeh et al. 2013; Nogueira et al. 2015). The accumulation of fatty acids requires the continuous provision of acetyl-CoA (A-CoA) as an essential precursor for fatty acid synthesis as well as a sufficient supply of NAD(P)H in the cytosol, that primarily is produced by malic enzyme (ME). This enzyme has a key role in the regulation of lipid accumulation process in oleaginous microorganisms (Liang & Jiang, 2015). Overexpression or down-expression of ME can increase or decrease lipid content, respectively, inside the cell (Kendrick & Ratledge, 1992; Li et al. 2013).

GAPDH is an important enzyme for lipid biosynthesis that converts D-glyceraldehyde-3-phosphate (GAP) (formed from dihydroxyacetone phosphate (DHAP)) to bisphosphate glycerate (BPG) through glycolytic pathway (Figure 3.7). Over expression of this enzyme can promote the conversion of DHAP to GAP, resulting in an increase of neutral lipid content (Yao et al. 2014).

Diatoms, like other autotrophs, synthesize a whole range of amino acids, including aromatic amino acids. Tryptophane, phenylalanine and tyrosine serve also as precursors of other aromatic compounds such as such as phenylpropanoids and flavonoids (Rico et al. 2013). The synthesis of aromatic compounds starts with chorismate biosynthesis in the shikimate pathway. It is the only known biosynthetic route for synthesis of aromatic compounds. The carbon skeletons of amino acids are derived from central carbon metabolism, including the major photosynthetic pathways (light-dependent reactions and the Calvin cycle) and other associated pathways *e.g.* glycolysis (pyruvate as an important intermediate for amino acid synthesis and phospho*enol*pyruvate (PEP) as a precursor for aromatic amino acid synthesis, oxidative pentose phosphate pathway, photorespiration and TCA cycle (for more details see Bromke, 2013).

3.4.7 Changes in selected gene expression during growth

Enzyme localization and diel gene expression pattern are important to understand the role(s) of different enzyme/isoenzymes, including gene compensation mechanisms, in the physiological response of diatoms (Chauton et al. 2013). To reach this goal, 74 genes coding 33 enzymes involved in the central carbon metabolism were studied. A global view (heatmap) of the changes in the expression of the 74 genes of *P. tricornutum*

based on growth phases (Supplemental Figure 3.8) under the three light intensities. Out of the 74 genes, only 34 showed a particular profile with respect to growth phase and or/light levels (Figures 3.8 and 3.9). The analysis revealed that for several genes, the mRNA expression pattern was similar regardless the light condition with respect to the growth of the culture with a particularly high up-regulation of PEPCK, FbaC5 and PPDK and a down-regulation for others (PGP, GOX2, PYC2, GAPC1, PK2, CA7 and TPI_2) (Figure 3.8 and Supplemental Figure 3.8). To emphasize gene expression variations and find out the strong patterns in our complex data set, principle component analysis (PCA) was performed (Figure 3.9). The two first components (61% of explained variance on the data) were selected as the most representative principal components according to their discriminative power and resulted in clear separation of the three different light conditions and growth phases (Figure 3.9). In the score plots, expression of genes under LL completely separated from those under ML and HL while the expression level under ML was more similar to that of HL than LL grown cells (Figure 3.9). Indeed, four groups (circles) of correlated parameters ($p<0.05$, Pearson's test) appeared according to their location relative to the 2 first axes of the PCA (Figure 3.9).

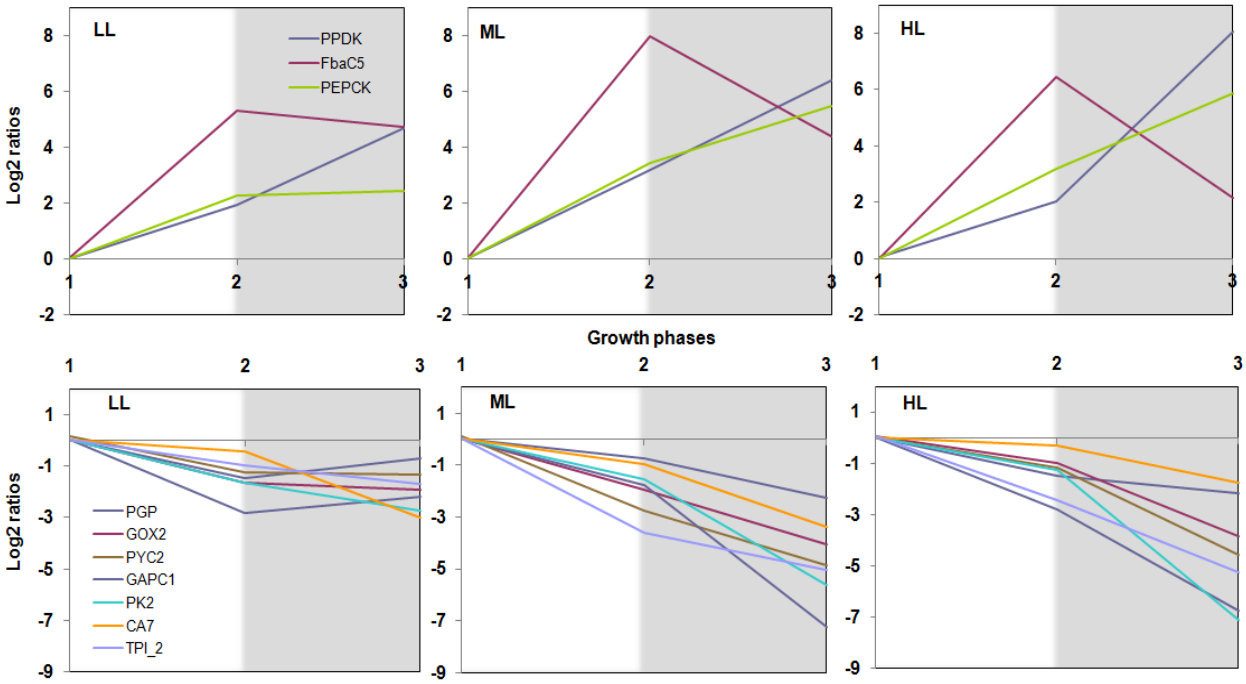

Figure 3.8. mRNA profiles of genes either up- or down-regulated during three growth phases under three light conditions. In all conditions phase 1 of each light is used as calibrator.

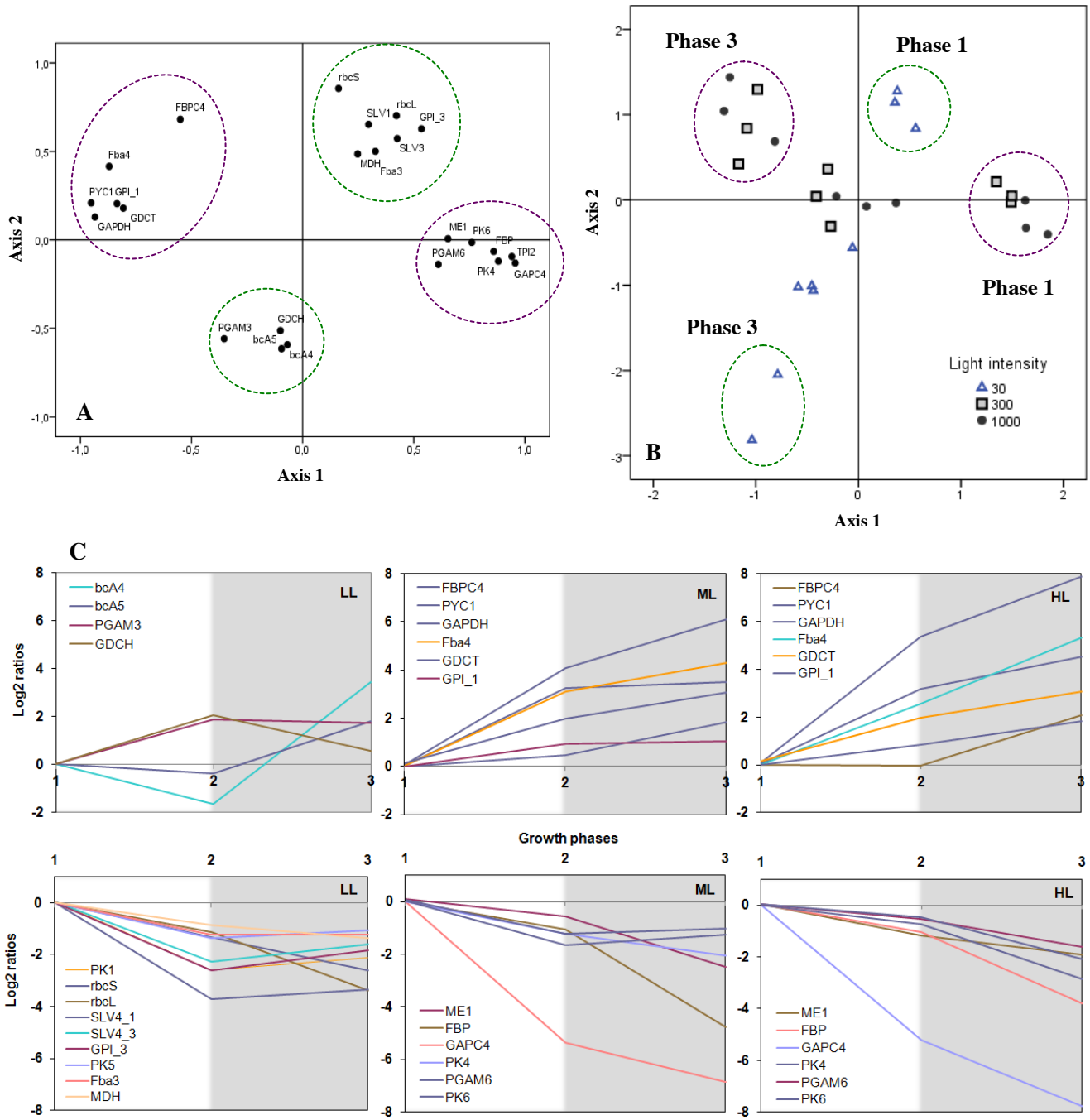

Figure 3.9. A) PCA labeling of differentially up- or down-regulated genes under different light intensities defined as group inside ovals, green: low light (LL), violet: medium (ML) and high light (HL); **B**) Projection of the samples (3 replicates per condition) on the 2 first axis (62 % of the variance explained by the 2 first axis); **C**) log2 mRNA expression ratios in the 3 conditions over growth phases using phase 1 as calibrator.

The analysis revealed that under LL, genes located at the top of the PCA (green circle group) were particularly down-regulated during the growth of the culture as shown in panel A (Figure 3.9). It includes the genes encoding: (1) the HCO_3^- transporters SLV4_1 and SLV4_3 involved in the biophysical CCM (up to 10 and 3 fold the expression of this gene in phase 1, respectively); (2) the plastidic rbcL and rbcS encoding two subunits of the RubisCo from the Calvin cycle, particularly in phase 3 (respectively 22 and 11 fold the expression of phase 1); and (3) most of the genes (GPI_3, PK1, PK5, and Fba3) coding enzymes of glycolysis in the three cell compartments in which glycolysis occurs (Figure 3.9). Still under LL, the genes found at the bottom of the PCA encoding the two carbonic anhydrases (bCA4 and bCA5) were highly up-regulated in phase 3 (10 and 3.5 fold the expression of these genes in phase 1), and to a lesser extend the genes encoding PGAM3 and GDCH (3 and 4 fold respectively in phase 2 compare to phase 1) (Figure 3.9).

The group found on the left of the factorial map (violet circle) was composed of genes that were significantly up-regulated during the growth of the culture for ML and HL. It included particularly the genes encoding PYC1, Fba4, GDCT, GPI_1, GAPDH and FBPC4 (Figure 3.9). The group found on the right of the factorial map (violet circle) was composed of genes that were significantly down-regulated in phase 2 and/or phase 3 compared to phase 1 (Figure 3.9). It included the genes encoding: (1) the single mitochondrial GAPC4 involved in glycolysis, reaching for ML (45 and 200 fold respectively in phase 2 and 3 the expression of this gene in phase 1) and HL (45 and 240 fold respectively); (2) FBP and PK4 both involved in the cytosolic glycolysis; and (3) ME1 under ML.

3.4.7.1 Light intensity influenced expression of genes in different growth phases

To determine how gene expression can be regulated under different light intensities mRNA levels in the three growth phases under LL and HL were compared to that reached under ML (Figure 3.10). The differences in mRNA levels between LL and ML were the strongest in phase 1 and 3, whilst they did not differ sharply under HL (compared to ML). Also, in phase 2, mostly down-expression of genes was observed in different pathways in both LL and HL, except some slight increase of expression in some genes (Figure 3.10). LL stimulated the expression of mitochondrial genes encoding PYC1 and PEPCK from biochemical CCM (12 and 67 fold, respectively), more than ML in phase 1, whilst these genes were down expressed almost 4 and 2 fold, respectively, under HL, and their expression decreased during phase 2 and 3 in both LL and HL (Figure 3.10). During phase 2, genes coding enzymes of the biophysical CCM were downexpressed with some exceptions, including CA7 and CA1 under LL and HL (compared to ML).

Figure 3.10. Dysregulated heatmap showing the expression pattern of 74 genes related to carbon metabolic pathways, with the greatest differences in expression (red: high, green: low). Columns represent three growth phases under low light (LL) and high light (HL). In each growth phase ML is used as calibrator.

Putative bCA4 and bCA5 were highly expressed (32 and 8 fold, respectively) during phase 3 under LL while some genes slightly up-expressed (mostly 4 fold in CA1) under HL. Among the 14 studied genes involved in the Calvin–Benson cycle under LL, 11 genes were over expressed in phase 1, mostly plastidic FbaC5 (7 fold) (Figure 3.8). Under HL a slight higher expression of two genes, FbaC1 (2 fold) and FbaC5 (3 fold) was observed.

Thereafter their regulation did not change strongly in phase 2 compare to ML but decreased drastically for some genes in phase 3 under LL especially for plastidic rbcS and rbcL (13 and 25 fold, respectively), and increased in FbaC5 and TPI_1 (7 and 5 fold, respectively) compared to ML and HL. Interestingly, modifications in the photorespiration was observed during phase 2 to phase 3 transition under LL: the mitochondrial GDCP was down-expressed (8 fold) followed by up-regulation of this gene (8 fold) in phase 3. These changes were accompanied by the overexpression of GOX2 and PGP (7 and 6 fold, respectively). In general, the expression of genes in photorespiration was higher under LL than under ML and LL, especially in phase 3.
Out of the 10 cytosolic studied genes in glycolysis, seven were expressed higher under LL phase 1, mostly Fba4 (9 fold), PK3 and GAPDH (both 6 fold), than under ML (Figure 3.10). The expression of these three genes decreased, especially Fba4 in phase 3 (4 fold). Putative GAPC1 had the highest expression in phase 3 under LL, around 60 fold more than under ML, while in phase 1 and 2 did not show significant differential expression compare to ML. No sharp modifications in the expression of genes coding enzymes involved in glycolysis under HL, compare to ML and it was the same for expression of genes in shikimate pathway, under LL and HL.

3.5 Discussion

Diatoms adapt to changing light intensities in a very efficient way (Wagner et al. 2006) and the molecular mechanisms involved in regulating diatom light responses are so far not completely elucidated (Bailleul et al. 2010). In this study, we have compared the impacts of three photon flux densities on *P. tricornutum* using physiological, biochemical and molecular tools with the aim how the partitioning of carbon among its potential sinks is impacted.

3.5.1 Growth

The effects of environmental factors on cell development, physiology and regulation mechanisms depend on cell status (Jia et al. 2015). Therefore, a careful study on the effects of growth light intensity requires comparing cells from cells at the similar developmental stages. To fulfil this requirement, the actual growth rate was calculated and the samples were prepared when the actual growth rate was at either maximum or minimum. The comparison of growth rate ’μ‘ and generation time ’G‘ values revealed that under LL, the mitosis frequency was circa three times lower than under ML or HL (Table 3.1), suggesting under LL, the low abundance of photons constituted a limiting factor for growth of *P. tricornutum*. The values reported in Table 3.1 are lower than those reported by Geider et al. (1985) for *P. tricornutum* grown under the same nominal irradiances. These differences arise probably from the difference of light sensor used for

measurements (Geider et al. (1985) used a planar (2π) sensor whereas a spheric (4π) was used in this study). It is well established that the nominal irradiance measured with spheric sensor is higher than with planar ones. Both studies however agree on the fact that increasing the irradiance from 30 to 300 μmol m^{-2} s^{-1} increased growth rate (Table 3.1). However, HL intensity did not promote growth rate suggesting that under HL, the additional energy was not used to promote growth. Altogether, these results agreed with those already published on this topic (Beardall & Morris, 1976; Bailleul et al. 2010; Marchetti et al. 2012; Xiang et al. 2015).

Among nutrient elements, C and N, above all else, are absolutely required for growth and the synthesis of biomolecules. The total C consumed by the culture was high (over 70%) whereas the total N decreased only by 10%. Therefore, one can assume that the reduction of C availability is mostly responsible for the stationary phase. In this work, we found that the variation of C and N uptake between phase 1 and phase 2 uptake followed the rule observed by Marchetti et al. (2012) with *Isochrysis* affinis *galbana i.e.* uptake decreases when growth rate increases but this was not true during the transition between phase 2 and phase 3, suggesting that other factors are involved in the control of the transition to the stationary phase.

The photosynthetically fixed C is mostly used to synthesize lipids, proteins and carbohydrates. Interestingly, under each lighting condition, the major compound was different in phase 1: under HL, the most abundant type of compound was proteins whereas under ML and LL, it was lipids and carbohydrates, respectively. To explain this result, it is enough to realize that growth conditions under LL, phase 1, recall some conditions favoring lipid accumulation in diatoms: elevated amount of available C and reduced cell division rate (Nogueira et al. 2015). Under ML and HL, the division rate increased rapidly after the start of the culture. To sustain this growth, most of the C was incorporated into simple carbohydrates that are used to generate the ATP needed to sustain the growth rate. Lipids started to accumulate in phase 2 and phase 3 but the accumulation was limited because of the progressive lack of C in the growth medium. The importance of high biomass production rate in enhancing algal lipid production was reported by Sukenik (1991). A positive correlation between lipid production (polyunsaturated fatty acids (PUFAs)) and cell concentration in *P. tricornutum* has also been observed by Yongmanitchai & Ward (1991). However, other studies have reported the decrease of total lipid production by the increase of light intensity and increase of algal growth rate (Terry et al. 1983; Spectorova et al. 1986; Sukenik et al. 1989; Tedesco & Duerr, 1989; Harrison et al. 1990; Thompson et al. 1990; Renaud et al. 1991). Consequently, increasing algal productivity by increasing irradiance might reduce the algal lipid productivity. Recently, in the study performed by Nogueira et al. (2015) in *P. tricornutum,* an increase of TAG content was observed by increasing the irradiance values (50, 300 and 600 μmol m^{-2} s^{-1}).

Analysis of central carbon metabolism transcript levels first highlighted genes coding for enzymes that may have important flux roles regardless light intensity conditions. First of all, no particular regulation of the genes coding the subunits of the RubisCo was observed except under LL for which a reduction was observed along growth. This confirms earlier reports on higher plants and phytoplankton communities showing that carbon fixation is regulated at early stage of development by transcriptional control of RubisCo synthesis and at the later phase at other biochemical levels (Loza-Tavera et al. 1990; Pichard et al. 1996). Besides, the expression of several genes coding for enzymes of the Calvin–Benson cycle were affected by the growth conditions. During phase 1 to phase 2 transitions, the rate of cell division increased and the reconstitution of daughter cells need of building blocks was very high. Because those are mostly made from photosynthetically fixed carbon, one should expect FbaC5 gene to be up-regulated in all three conditions, especially in the phase 2 (Figure 3.8). The localization of FbaC5 in the pyrenoid of *P. tricornutum* is indicative of a linkage between some components of the Calvin–Benson cycle and the CCM (Tachibana et al. 2011). In the vascular plant *Arabidopsis thaliana*, FBA is one of the three Calvin–Benson cycle enzymes that was most sensitive to biological perturbations and found to have an important ratelimiting role in regulating the carbon assimilation flux of the Calvin–Benson cycle (Sun et al. 2003). This is presumably what is happening in our cultures in the phase 2 during which photosynthesis is particularly active (Figure 3.4).

Regardless the irradiance intensity, the FbaC5 gene expression fell from phase 2 to phase 3 but remained much higher than in phase 1 (Figure 3.8). The up-regulation of FbaC5 is accompanied by a significant down-regulation of TPI_2 and GAPC1 both involved in the reverse reaction that produce back trioses (Allen et al. 2012). Altogether, this change in gene expression could be interpreted as a lack of DHAP formation in the Calvin cycle. To feed the putative sink in DHAP created by the overexpression of FbaC5, one can postulate an import of this component from the cytosol using triose phosphate translocator (TPT) (Batz et al. 1992; Heber, 1974). This DHAP would be transformed in Ru5P through the non-oxidative pentose-phosphate pathway or the Calvin–Benson cycle (Figure 3.7).

Up-regulation of FBPC2 and FBPC4 genes under ML and HL, phase 3 suggests the use of the Calvin–Benson cycle (for C5 regeneration) along the growth of the cultures (Supplemental Figure 3.8). The Ru5P can then serve as substrate for RubisCo for binding CO_2. In case of CO_2 shortage *e.g.* during the transition from phase 2 to phase 3, Ru5P could be exported to the cytosol (Heber, 1974) and metabolized through the oxidative pentose phosphate pathway after isomerisation to X5P (Figure 3.7). The increase in the expression of the gene coding cytosolic PGDH, the last enzyme of this pathway agreed with this reasoning (Supplemental Figure 3.8). The resulting Ru5P would be reimported in the chloroplast stroma (Matsuda & Kroth, 2014) through the X5P/phosphate translocator (Facchinelli & Weber, 2011) to maintain/restore the

chloroplastic pool of this compound. Importantly, the reaction from 6-phospho-D-gluconate (6PGN) to Ru5P catalyze by PGDH, generates CO_2 that can potentially increase the CO_2 concentration in PPS. Thus, the fixed CO_2 is mostly used to form 3PG that is then transformed to 2PG. If we hypothesize that the flux of C is directed to the formation of 2PG, then one should expect that the genes coding for the enzyme catalyzing the transformation of 3PG to 2PG (PGAM) are up-regulated. This was indeed the case for PGAM3 in phase 2 (> 2 fold) under the three light intensities (Supplemental Figure 3.8).

2PG is the substrate of enolase to form PEP, that, in turn, serves as a precursor of the Shikimate pathway or to produce pyruvate (Figure 3.7). The gene coding PPDK, the enzyme converting pyruvate into PEP, was one of the highest up-regulated genes in phase 3 (13, 84 and 229 fold) under LL, ML and HL, respectively (Supplemental Figure 3.8). This result, with the mostly down expression of PK genes, strongly suggested that PEP was mainly oriented toward the Shikimate pathway *i.e*. the formation of aromatic amino acids and derivatives. These aromatic compounds are unlikely used in protein synthesis as the protein amount in cells grown in HL is not significantly modified during growth. This contrast with the LL and ML conditions in which protein amount increased (Figure 3.2). Alternatively, PEP serves as acceptor for CO_2/HCO_3^- fixation by PEPC in the C_4 route (Figure 3.7). The enzymes PEPC1 and PEPC2 are localized in the chloroplast (PPS) and mitochondria, respectively. The expression of PEPC1 and PEPC2 did not varied significantly as already observed by Mc-Ginn & Morel (2008) and Valenzuela et al. (2012) in *P. tricornutum* under low CO_2 conditions. In mitochondria, OAA formation occurs through the carboxylation of PEP or pyruvate by PEPC2 and PYC1, respectively (Figure 3.7). The much higher over-expression of PYC1 than PEPC2 suggested that HCO_3 was preferentially fixed through the latter enzyme. This conclusion is in line with the suggestion by Valuenzela et al. (2012). In addition, Chauton et al. (2013) have proposed that activation of PEP and pyruvate carboxylations are more involved in the dissipation of excess light energy and pH homeostasis than to the CCM. In our conditions, this was however unlikely because non-photochemical quenching measurements suggested that the capacity to dissipate the excess absorbed light energy was far to be exhausted (Figure 3.6). Instead, we prefer to favor the hypothesis according to which CCM was progressively activated to supply the cell with C. However, we cannot exclude that both roles occurred simultaneously. This conclusion reinforces the proposal by Roberts et al. (2007) and Reinfelder (2011) on this regulation aspect.

It is well recognized that O_2 and CO_2 are in competition for RubisCo active site. When the gas partial pressure in the surrounding of RubisCo is in favor of O_2, RuBP enters in the photo-respiration pathway of which the first step consists in the oxidation of RuBP to 2PGL by RubisCo (Figure 3.7) (Beardall, 1989; Spreitzer, 1999; Ogren & Bowes, 1971; Sage & Stata, 2015). This pathway was found to be down-regulated in this study. The gene coding PGP, the enzyme catalyzing the formation of glycolate from 2PGL was down-regulated in LL, ML and HL in phases 2 and 3 compared to phase 1 (Supplemental

Figure 3.8). These changes were accompanied by the down-regulation of the expression of two other photorespiratory genes coding the mitochondrial GOX2 (3, 17 and 17 in phase 3 for LL, ML and HL, respectively) and GDCP (3, 12 and 7 for LL, ML and HL, respectively) (Supplemental Figure 3.8). Beside its role in diverting carbon atoms, photorespiration plays a critical role in nitrogen metabolism in diatom cell and a role in excess energy dissipation under stress conditions (Parker & Armbrust, 2005; Kroth et al. 2008). The former role was probably easily filled as the N of the medium remained high whereas the latter one is unlikely as the capacity to dissipate the excess of energy through the non-photochemical quenching was not exhausted. Altogether, our results highlight that photorespiration is not particularly enhanced, even under HL, since no differential of expression was found for photo-respiration genes under HL or LL compared to ML.

3.5.2 The stationary phase: adaptation to carbon deficiency conditions

The stationary phase is characterized by a very low, close to zero, cell division rate and a reduced respiration rate (Figure 3.4 and Supplemental Figure 3.1). It is currently admitted that the establishment of a stationary phase results from the occurrence of a deficiency in at least one growth factor, including photon availability. The reasoning presented above suggests that C-deficiency was mostly responsible for the occurrence of stationary phase. The fact that under ML and HL, the amount of Chl *a* and carotenoids were higher in phase 3 than phase 2 suggested that cellular shading effect might also be partly responsible of the occurrence of the stationary phase. The additional pigments are used to maintain the photosynthetic activity during this phase. This change was less intense under LL probably because the pigment cellular quota was already almost at its maximum. This data in itself constitutes interesting information for biotechnological applications aiming to produce high added value pigments that can be used in many industries, including food coloring and health (Mimouni et al. 2012; Heydarizadeh et al. 2013; Leu & Boussiba, 2014; Adolfsson et al. 2015). The slight increase in the qN values observed in phase 3 suggests that energy production and energy expenditure were somehow more unbalanced than during phase 2 (Figure 3.5).

In the preceding section, we have hypothesized that the flux of C is directed to the formation of 2PG, which is ultimately used to produce PEP. Accordingly, an up-regulation of PPDK gene under the three growth light intensities was recorded. A similar conclusion can be reached for the mitochondria. Actually, PYC1 and PEPCK were highly up-regulated in phase 3 under ML (69 and 42 fold the expression in phase 1, respectively) and, HL (227 and 56 fold) (Supplemental Figure 3.8) suggesting the orientation of the utilization of pyruvate for PEP formation with OAA as an intermediate. Thus, if we hypothesize that the change in gene expression reflects

somehow the enzyme amount, one can predict that under ML and HL, a large proportion of the OAA pool is used to synthesize PEP whereas under LL, a significant part of it enters the TCA cycle to be respirated. Indeed the respiratory activity was higher under this light condition (Figure 3.4). Pyruvate can also be produced by mitochondrial ME1 from malate. ME1 supplies both carbon and reducing equivalents in the form of NADPH for *de novo* fatty acid production (kroth et al. 2008; Xue et al. 2015). Little is known about the role of ME in fatty acid and TAG biosynthesis in microalgae (Shtaida et al. 2015) but it has been reported previously (Yang et al. 2013; Xue et al. 2015) that under N depletion, ME encoding genes may stimulate lipid production. In this study, no N deprivation was observed and accordingly, ME1 was down-regulated under LL, ML and HL, mostly in phase 3 (2.5, 6.0, 3.7 fold, respectively) (Supplemental Figure 3.8) suggesting that this possibility is unlikely. One hypothesis could be the shunt of malate from mitochondria to plastid and up-regulation of plastidial ME2 (it is not studied in this experiment) that could provide the precursur of A-CoA, *i.e.* pyruvate, for fatty acid biosynthesis (Ge et al. 2014). This would be consistent with the involvement of the mitochondrial pool of pyruvate in CCM to produce PEP that might be exported in other cell compartments. PEP can be used for (1) cytosolic gluconeogenesis to produce glucose. Several genes coding enzymes localized in the cytosol, particularly in the glycolysis pathway, were differentially regulated. The genes coding the cytosolic GPI_1, Fba4 and GAPDH (function in both glycolysis and gluconeogenesis pathways) were up-regulated in phase 2 and 3 under ML and HL (Supplemental Figure 3.8). The gene coding the cytosolic FBP in the opposite direction, *i.e*. gluconeogenesis (Figure 3.7) was on the contrary down-regulated (8, 28 and 14 fold its expression in phase 1 under ML for respectively phase 3 of LL, ML and HL) (2) transformed into pyruvate by a PK enzyme. This last possibility seems limited because the expression of the mitochondrial, chloroplastic and cytosolic PKs either did not changed or were down-regulated and/or (3) translocated in the plastid using transporters, where it may serves as building blocks *e.g.* aromatic amino acids and lipids.

For aromatic amino acids, the expression of 6 genes coding enzymes involved in the Shikimate pathway was studied. AroB and SK were slightly down-regulated in the 3 conditions, leading us to hypothesize that this is not the direction of carbon flux (Supplemental Figure 3.8).

It is usually reported that phase 3 is characterized by lipid accumulation (Valenzuela et al. 2012; Mus et al. 2013; Wu et al. 2015). A moderate lipid accumulation was also observed in this study under ML and HL (Figure 3.2). The origin of the lipid biosynthesis, *i.e.* PEP or pyruvate, is still under debate. Some authors have assumed that lipid biosynthesis branch from PEP (Kroth et al. 2008; Mus et al. 2013), while some others revealed that it goes through pyruvate (Ge et al. 2014; Radakovits et al. 2010; Schwender et al. 2014; Yang et al. 2013; Ma et al. 2014).

The pyruvate dehydrogenase complex (PDC) is an important enzyme of lipid metabolism. Three isoforms of pyruvate dehydrogenase, namelly PDH1, PDHB1 and PDHA1, were found in the *P. tricornutum* genome (Chauton et al. 2013). PDH1 was the most expressed in phase 1 for the 3 conditions but its mRNA expression decreased in phase 2 and 3 while the expression of the PDHA1 increased. PDHB1 level did not change significantly (Supplemental Figure 3.8). Moreover, the mRNA expression of the 2 isoforms of A-CoA carboxylase (ACC1 and ACC2), which catalyze the conversion of A-CoA into malonylCoA for fatty acid production, indicated a singuliar pattern: a higher expression of both genes in LL (up to 2 fold the expression of ML) and an up-regulation of ACC2 in phase 3 (though not significant for HL) were found. It seems higher expression of these genes during phase 3 under LL, speed up the conversion of pyruvate to malonyl-CoA. This compound is a key cofactor of the fatty acid biosynthesis.

These results support the results of lipid quantification that showed an increase in the lipid amount in phase 1 under LL and under phase 2 and/or 3 under LL and ML . Lipid production promoted by physical environmental stimuli and light intensity is one of the main physiological cues of diatoms (Hu et al. 2008; Sharma et al. 2012). Also, growth phase and aging of the culture have already been shown to affect TAG content and fatty acid composition (Fidalgo et al. 1998; Hu et al. 2008). The importance of high biomass production rate in enhancing algal lipid production was reported by Sukenik (1991). A positive correlation between lipid production (PUFAs) and cell concentration in *P. tricornutum* has also been observed by Yongmanitchai & Ward (1991). However, other studies have reported the reduce of total lipid production by the increase of light intensity and increase of algal growth rate (Terry et al. 1983; Spectorova et al. 1986; Sukenik et al. 1989; Tedesco & Duerr, 1989; Harrison et al. 1990; Thompson et al. 1990; Renaud et al. 1991). Consequently, increasing algal productivity by increasing irradiance might reduce the algal lipid productivity. From the qualitative point of view, the results presented here are in line with those published by Nogueira et al. (2015), which showed an increase of TAG content of *P. tricornutum,* was observed by increasing the irradiance values from LL (50 µmol m^{-2} s^{-1}) to ML (300 µmol m^{-2} s^{-1}) while decreasing under HL (600 µmol m^{-2} s^{-1}).

In this study, several CAs were found to be differentially regulated both by the growth of the culture and by the light intensity (see above). The CA protein family is composed of proteins, which have different cellular sublocations (*e.g*. chloroplast, periplasm, cytosol) (Tachibana et al. 2011), a factor that will contribute to define their role in the cell physiology. CAs catalyze the reversible reaction of CO_2 hydratation and thus their physiological function deeply relies on the local pH of the compartments in which the enzymes are present. Interestingly, and only for LL, the two bCAs (bCA4/PtCA1 and bCA5/PtCA2; Tachibana et al. 2011) were highly up-regulated in phase 3, reaching 16 and 8 according to the data I have is 32 and 8 fold their expression in phase 1 ML (Figure 3.10). Recent investigations revealed that RubisCo and btype CAs

(bCA4 and bCA5) are located in the pyrenoid of *P. tricornutum* and that these CAs are induced remarkably at low CO_2 concentrations to efficiently bring CO_2 at the proximity of RubisCo (Harada & Matsuda, 2005; Harada et al. 2005; Tachibana et al. 2011). bCAs were previously reported by several authors to change in mRNA accumulation under different growth conditions (Harada et al. 2005; Harada & Matsuda, 2005; Tachibana et al. 2011). Higher expression of these genes under LL in phase 3 may show the lower efficiency of RubisCo, consistent with the decrease of mRNA expression in phase 3 LL of rbcS and rbcL (13 and 25 fold, respectively) (Figure 3.9), providing thus more CO_2 around this enzyme. Accordingly, we postulate that under LL, the increase in the pigment content (Figure 3.3) is a way to compensate for the lower expression of genes encoding RubisCo. Also, down-regulation of 2 out of the 3 HCO_3^- transporters SLV (SLV4_1 and SLV4_3) was observed in this same phase under LL (1.6 and 1.4 fold, respectively).

In *P. tricornutum* putative CA1, CA2, CA6 (except CA7) seems to be transcriptionally active and expressed independently of light and CO_2 conditions, and thus appear to be synthesized constitutively. (Tachibana et al. 2011). The gene coding CA7, that is located in PPS, was down-regulated in the 3 conditions compared to phase 1 (9, 10 and 4 fold respectively for LL, ML and HL in phase 3; Supplemental Figure 3.8). The genes coding for CA2, CA6 (and CA1 but to a lesser extend because of its low expression in phase 3 under ML), were up-regulated in phases 2 and phase 3 in ML (between 1 and 3 fold) and in HL (between 1 and 3 fold) while down-regulated in LL (between 1 and 2 fold). Among several CCM related genes, Winck et al. (2013) suggested that some CAs may function on determining the structure of the pyrenoid while not essential to the CCM process itself. CCM mechanisms together allow cells to increase inorganic carbon uptake and to keep high photosynthetic rates under low CO_2 environmental conditions. Based on our finding the expression of CA genes was light and also growth phase dependent (Supplemental Figure 3.8). However, due to the lack of studies published in similar conditions than those used in here, direct conclusions are complicated. In general, the nature of the CCM operating in diatoms is not clear and the extent of its expression may be species-specific and strongly affected by growth conditions (Roberts et al. 2007; Reinfelder, 2011). Altogether, this study highlighted the activation of different pathways toward PEP and pyruvate synthesis. These two precursors are the key branch points early in the partitioning of carbon in some pathways including protein and lipid biosynthesis. Also they important intermediates in gluconeogenesis (the opposite direction of glycolysis) to produce energy (ATP), glucose and also storage (as chrysolaminarin) for the cell.

3.5.3 Adapting to low light condition

The pigment concentration under LL was higher than the other conditions, while A_{max} was lower (Figures 3.3 and 3.4), demonstrating that the low photosynthetic activity was due to low irradiance level. This is also demonstrated by the high values of qP (Figure 3.5) and the absence of activation of mechanism for excess energy dissipation. It has been reported that the photosynthetic capacity of *P. tricornutum* cells, can vary greatly depending on growth conditions (Griffiths, 1973). Compare to photosynthesis, respiration of diatom cells under LL condition was high (Figure 3.4), suggesting that increase of cell division rate in diatoms required another source of energy than the one made through photosynthesis. Actually, algae tried to increase this production by accumulating more photosynthetic pigments (Chl *a*, Chl c, carotenoids) than the cells growing under ML or HL (Figure 3.3). This acclimation mechanism started very early as it was already observed after three days of growth. These pigments are integrated in functional photosynthetic pigments as indicated by the typical value of the maximum quantum yield of photosystem II (Fv/Fm) that did not decreased. Actually, it has been shown that samples containing non-integrated Chl molecules are characterized by a low Fv/Fm ratio linked to a higher F_0 value (higher plants: Schoefs & Franck 1991; Schoefs et al. 1992; algae: Lamote et al. 2003). Indeed, these additional pigment molecules are used to form very large light harvesting antennae as indicated by the low values of the Chl *a*/Chl c ratio, a proxy of the LHC size (Lamote et al. 2003; Nguyen-Deroche et al. 2012). This interpretation is line with previous results (*Isochrysis* sp.: Marchetti et al. 2013; *P. tricornutum*: Beardall & Morris, 1976; *Skeletonema costatum*: Anning et al. 2000). From the biosynthetic poitn of view, the decrease of the Chl *a*/Chl c ratio, combined with the large increase of the total amount of Chl under LL suggest a strong activation of the Chl biosynthetic pathway and a channelling of the precursors toward Chl c formation. In the absence of data about the Chl c biosynthetic pathway and its regulation, this point is difficult to discuss (Beale 1999; Tanaka & Tanaka, 2007). Therefore, only some elements are given here to stimulate further experimentations. First of all, from the chemical point of view, Chl c is not a Chl but a protochlorophyllide (Schoefs, 2002) *i.e.* a molecule that is well known to serve as regular Chl precursor (Schoefs, 2001; Schoefs & Franck, 2003). Thus to explain our result, one should imagine that the pool of divinyl (DV)-protochlorophyllide is funnel preferentially toward Chl c formation. In the absence of gene candidate for this conversion, it is not possible to determine whether the increase of Chl c would require control of gene expression and/or a regulation at another level.

One of the aim of the increase of the light harvesting capacity is the allocation of energy in the carbon concentrating mechanism (CCM) operation, especially for the LL grown cells, which need more energy for operation of CCMs (Li et al. 2014). Thus, in

conditions for which the demand for operation of CCM is lower, the energy saved can be invested for growth.

Because, the assembly of functional LHC requires adequate pigment amount, the carotenoid pathway is also activated to generate the fucoxanthin molecules required for the assembly of functional LHC (Dambek et al. 2012). Alternatively, and not exclusively, carotenoids are needed to quench ROS that could have been formed by the nonintegrated Chl molecules (Franck et al. 1995; Schoefs & Franck, 2003). It has been reported that the Chl and Car biosynthetic pathways are usually coupled (Schoefs et al. 2001; Bidigare et al. 2014). Despite of the larger amount of pigments, the photosynthetic activity remained weak (Figure 3.4) and very close to the respiration activity. Thus, LL intensity used in this work for growing the cells provides conditions closed to the compensation point. In these conditions, the PSII reaction centers remained permanently open and the non-photochemical quenching was absent (Figure 3.5).

Under LL Q_C values were either close or higher than under ML and HL, while C uptake was significantly lower under LL than in two other conditions (Figure 3.2). This is not completely unexpected as growth rate was the lowest under LL (Table 3.1) and therefore the need for C import was low. The comparison of Q_C values reached in the different phases suggests that in LL conditions, the photon deficiency triggers a decrease of *Qc* along growth. This conclusion is in line with that reached with the diatom *Thalassiosira fluviatilis* (Laws & Bannister, 1980) and the Prymnesiophyceae *Isochrysis* sp. (Marchetti et al. 2013) grown in continuous culture under LL conditions.

3.5.4 High light adaptation

Cells growing under HL conditions received 30 times more than under LL and three times more energy than those grown under control condition (ML). The additional energy brought by HL conditions did not result in an increase of growth rate when compared to ML (Table 3.1) because photosynthesis performed only slightly better – but not significantly – in this condition than in ML (Figure 3.4). This interpretation is confirmed by the reduced amount of pigments present in diatom cells grown in these conditions and by the reduced LHC size (Supplemental Figure 3.2) (Janssen et al. 2001; Perry et al. 1981). In addition, under ML and HL, the growth rate was the fastest and the amount of pigments was the lowest. This suggests a coregulation of the cell cycle and cell development. Alternatively, the cell division rate could be faster than the rate of pigment biosynthesis.

Under HL, diatoms received more photons and the excess light energy could trigger the production of reactive oxygen species (ROS) and/or damage photosystems. To overcome the consequences of excess energy dissipation mechanisms are activated (Depauw et al. 2012; Bertrand et al. 2001). Under HL, 50% of the PSII were closed

permanently whereas the excess of absorbed energy was dissipated through the establishment of non-photochemical quenching (qN) (Figure 3.6), which may involve in diatoms several mechanisms: dissipation by the establishement of the proton gradient (ΔpH relaxation) and the xanthophyll cycle, diatoxanthin (Dtx) de-epoxidation fast conformational changes in the vicinity of the PSII complexes and/or photoinhibition (Roháček et al. 2014). The analysis of the qN relaxation kinetics demonstrated that the energy was mostly dissipated through the operation of the xanthophyll cycle, which in diatoms consists in the reversible conversion of diadinoxanthin to diatoxanthin (Moulin et al. 2010; Bertrand 2010; Goss & Jakob, 2010)

Under HL, the dissipation of the excess was mostly performed by means of the establishment of the proton gradient (ΔpH relaxation) and the xanthophyll cycle and photoinhibition. The involvement of this process is confirmed by the increase of P^B_{max} level under HL (Suppemental Table 3.5). The extent of photo-inhibition (qNs) (Figure 3.6) remained approximately constant along growth but contributed more intensively in phase 1 under HL *i.e.* when the photon/Chl ratio was the highest. During this phase, carbon uptake was low and one can hypothesized that the ROS formed within the chloroplasts have constituted the signal leading to the decrease of the pigment content during the transition to phase 2. It was reported that increasing the irradiance level triggered an increase of the *Qc* of the diatom *Thalassiosira pseudonana* (Taraldsvik & Myklesad, 2000) and in *Isochrysis* affinis *galbana* (Sukenik & Wahon, 1991). Our measurements do not confirm this conclusion because in this study we have compared cells that are approximately in the same physiological state (see above) whereas in other studies, the cells are compared according to the time basis. It is interesting to note that in phase 2 the pH of the medium (8.7) is more alkaline than in phase 1 (8.2) (data not shown). In *Skeletonema costatum,* such an increase favors CO_2 uptake and the accumulation of amino acids (Taraldsvik & Myklesad, 2000). On the other hand, the increase in irradiance triggered favored the accumulation of carbohydrates and neutral lipids in *Isochrysis* affinis *galbana* (Sukenik & Wahon, 1991). In our conditions, *Phaeodactylum tricornutum* accumulated protein under HL while carbohydrates under LL.

3.5.5 Influence of light intensity on the regulation of different pathways

Altogether, physiological and molecular data revealed in this study showed that ML and HL impacted the diatom very similar and quite differently from the LL. Indeed, growth rate, photosynthesis and respiration and mRNA expressions were not significantly different between the two conditions, suggesting different adaptations with particular enzymes that may have important flux roles with respect to light intensity.

Under LL, the cellular energy was limited. To generate more energy for carbon fixation diatom cells increased their capacity to harvest more photons as possible

(Nymark et al. 2009). However under LL conditions, the available energy remained low. Remarkably, the cells managed to fix similar carbon amount than under ML and HL intensity. This could not be possible without the activation of CCM mechanisms as well as the mobilisation of main energy generating pathways (Calvin cycle, glycolysis, CCM, photorespiration). This was especially evident during phase 1 during which the gene expression was higher than under HL.

One of the main results of this study was the orientation of the metabolism toward pyruvate formation. Pyruvate may be used for gluconeogenesis to produce glucose that, in turn, can be assembled into high molecular weight carbohydrates as chrysolaminarin. The relative amount of chrysolaminarin was found to increase only under LL. Indeed, mRNAs of the first enzyme of the chrysolaminarin synthesis, BGS1 (β-1,3-glucane glycosyl-transferase) was found to be slightly overexpressed (2 fold) under LL compared to ML and HL and tend to decrease in phase 2 and phase 3. Another interesting feature revealed by this study was that mRNA profiles differ in the activity of the biophysical CCM that seems to be particularly different with lower mRNA content of key genes (PPDK, CAs and SLV, GDCP under LL and HL (compared to ML). This could mean that the cells are provided by other CO_2 source(s) such as lipid degradation or simply regulate their income of CO_2 according to the available energy.

Compared to ML, genes encoding FbaC5, TPI_1 and TPI_2 were up-regulated under LL, phase 3, while the expression of the other genes in the Calvin–Benson cycle decreased, dramatically in the case of RubisCo (Figure 3.10). This movement was accompanied by an up-regulation of photorespiratory genes. The question was how storage of cell *i.e*. chrysolaminarin was increased under LL, especially in phase 3 (Figure 3.2) while carbon fixation was decreased by less expression of RubisCo genes. According to the hypothesis of Kroth et al. (2008) that synthesized glycerate in photorespiration may back to the Calvin–Benson cycle by the activation of glycerate kinase (GK) (see Figure 3.7). We concluded more expression of key enzymes of this pathway may lead to enter more synthesized glycerate in the Calvin–Benson cycle that may contribute for chrysolaminarin accumulation, as it is described before. Indeed, photorespiratory pathway plays a critical role in carbon and nitrogen metabolism in diatom (Parker & Armbrust, 2005). HL condition, high concentrations of O_2 and poor performance of RubisCo enzyme type, are known as major reasons to enhance photorespiration in marine algae (Beardall, 1989; Spreitzer, 1999; Ogren & Bowes, 1971; Sage & Stata, 2015). Under our growing conditions, the gene coding the peroxisomal MS enzyme was down-regulated under LL and HL (except in phase 3) suggesting that the direct shunt of glycolate from plastid to mitochondria would be stronger than its shunt to peroxisome.

One particularity of phase 3 was the up-regulation of genes coding proteins involved in the biophysical CCM. Under LL, it was essentially the bCAs that were up-regulated whereas under HL it was PPDK, SLVs and CAs that were overexpressed (Figure 3.10). bCA4 and bCA5 were previously shown to be CO_2 responsive and changing in

accumulation of their mRNAs consistent with those reported previously by several authors under different growth conditions (Harada et al. 2005; Harada & Matsuda, 2005; Tachibana et al. 2011). Higher expression of 'CCM genes' in phase 3 is consistent with the low CO_2 available at this growth phase. It is interesting that the different gene set were induced according to the growth light intensity. .

3.6 Acknowledgments

The authors are grateful to the Bing Huang, Vincent Blanckaert, French Ministry for Education and Scientific Research and the University of Le Mans, Collège doctoral of the University of Le Mans, Ministery of Forein Office and Isfahan University of Technology (IUT) for their help and support in preparing this manuscript.

3.7 References

Adolfsson L., Solymosi K., Andersson M.X., Keresztes Á., Uddling J., Schoefs B. & Spetea C. (2015). Mycorrhiza symbiosis increases the surface for sunlight capture in *Medicago truncatula* for better photosynthetic production. PLoS One 10: e0115314.

Allen A.E., Moustafa A., Montsant A., Eckert A., Kroth P.G. & Bowler C. (2012). Evolution and functional diversification of fructose bisphosphate aldolase genes in photosynthetic marine diatoms. Mol. Biol. Evol. 29: 367–379.

Anning T., MacIntyre H.L., Pratt S.M., Sammes P.J., Gibb S. & Geider R.J. (2000). Photoacclimation in the marine diatom Skeletonema costatum. Limnol. Oceanogr. 45: 1807-1817.

Armbrust E.V., Berges J.A. et al. (2004). The genome of the diatom *Thalassiosira pseudonana*: ecology, evolution, and metabolism. Science 306: 79–86.

Bailleul B., Rogato A., Martino A., Coesel S., Cardol P., Bowler C., Falciator A. & Finazzi G. (2010). An atypical member of the LightHarvesting Complex stress related protein family modulated diatom response to light. Proc. Natl. Acad. 107: 18214–18219.

Barofsky A., Vidoudez C. & Pohnert G. (2009). Metabolic profiling reveals growth stage variability in diatom exudates. Limnol. Oceanogr. Methods 7: 382–390.

Barofsky A., Simonelli P., Vidoudez V., Troedsson C., Nejstgaard J.C., Jakobsen H.H. & Pohnert G. (2010). Growth phase of the diatom *Skeletonema marinoi* influences the metabolic profile of the cells and the selective feeding of the copepod *Calanus* spp. J. Plankton Res. 32: 263–272.

Batz O., Scheibe R. & Neuhaus H.E. (1992). Transport processes and corresponding changes in metabolite levels in relation to starch synthesis in barley (*Hordeum vulgare* L.) etioplasts. Plant physiol. 100: 184–190.

Beale S.I. (1999). Enzymes of chlorophyll biosynthesis. Photosynth. Res. 60: 4373.

Beardall J. & Morris I. (1976). The concept of light intensity adaptation in marine phytoplankton: Some Experiments with *Phaeodactylum tricomutum*. Mar. Biol. 37: 377–387.

Beardall J. (1989). Photosynthesis and photorespiration in marine phytoplankton. Aquat. Bot. 34: 105–130.

Bertrand M., Schoefs B., Siffel P., Rohácek K. & Molnar I. (2001) Cadmium inhibits epoxidation of diatoxanthine to diadinoxanthine in the xanthophylls cycle of the marine diatom *Phaeodactylum tricornutum.* FEBS Lett. 508: 153–156.

Bidigare R.R., Buttler F.R., Christensen S.J., Barone B., Karl D.M. & Wilson S.T. (2014). Evaluation of the utility of xanthophyll cycle pigment dynamics for assessing upper ocean mixing processes at Station ALOHA. J. Plankton Res. 36: 1423-1433.

Bork P., Bowler C., de Vargas C., Gorsky G., Karsenti E. & Wincker, P. (2015). Tara Oceans studies plankton at planetary scale. Science 348: 873–873.

Bradford M.M. (1976). A rapid and sensitive method for the quantitation of microgram quantities of protein utilizing the principle of proteindye binding. Anal. Biochem. 72: 248–254.

Brauer M.J., Huttenhower C., Airoldi E.M., Rosenstein R., Matese J.C., Gresham D., Boer V.M., Troyanskaya O.G. & Botstein D. (2008). Coordination of growth rate, cell cycle, stress response, and metabolic activity in yeast. Mol. biol. cell. 19: 352–367.

Bromke M.A. (2013). Amino acid biosynthesis pathways in diatoms. Metabolites 3: 294–311.

Bohlin K.H. (1897). Zur morphologie und biologie einzelliger Algen.

Bowler C., Allen A.E. et al. (2008). The *Phaeodactylum* genome reveals the evolutionary history of diatom genomes. Nature 456: 239–244.

Bowler C., Vardi A. & Allen A.E. (2010). Oceanographic and biogeochemical insights from diatom genomes. Annu. Rev. Mar. Sci. 2: 333–363.

Carvalho A.P., Silva S.O., Baptista J.M. & Malcata F.X. (2011). Light requirements in microalgal photobioreactors: an overview of biophotonic aspects. Appl. Microbiol. Biotechnol. 89: 1275–1288.

Chauton M.S., Winge P., Brembu T., Vadstein O. & Bones A.M. (2013). Gene regulation of carbon fixation, storage, and utilization in the diatom *Phaeodactylum tricornutum* acclimated to light/dark cycles. Plant Physiol. 161: 1034–1048.

Dambek M., Eilers U., Breitenbach J., Steiger S., Büchel C. & Sandmann G. (2012). Biosynthesis of fucoxanthin and diadinoxanthin and function of initial pathway genes in *Phaeodactylum tricornutum*. J Exp. Bot.

De Martino A., Bartual A., Willis A., Meichenin A., Villazán B., Maheswari U. & Bowler C. (2011). Physiological and molecular evidence that environmental changes elicit morphological interconversion in the model diatom *Phaeodactylum tricornutum*. Protist. 162: 462–481.

Depauw F.A., Rogato A., Alcalá M.R. & Falciatore A. (2012). Exploring the molecular basis of responses to light in marine diatoms. J. Exp. Bot. 63: 1575–1591.

Dron A., Rabouille S., Claquin P., Le Roy B., Talec A. & Sciandra A. (2012). Lightdark (12:12) cycle of carbon and nitrogen metabolism in *Crocosphaera watsonii* WH8501: relation to the cell cycle. Environ. Microbiol. 14: 967–981.

Fabris M., Matthijs M., Rombauts S., Vyverman W., Goossens A. & Baart G.J. (2012). The metabolic blueprint of *Phaeodactylum tricornutum* reveals a eukaryotic Entner-Doudoroff glycolytic pathway. Plant J. 70: 1004–1014.

Facchinelli F. & Weber A.P. (2011). The metabolite transporters of the plastid envelope: an update. Front. Plant Sci. 2.

Falkowski P.G. & Laroche J. *(*1991). Acclimatation to spectral irradiance in algae. J. Phycol. 27: 8–14.

Fidalgo J.P., Cid A., Torres E., Sukenik A. & Herrero C. (1998). Effects of nitrogen source and growth phase on proximate biochemical composition, lipid classes and fatty acid profile of the marine microalga *Isochrysis galbana*. Aquacult. 166: 105–116.

Field C.B., Behrenfeld M.J., Randerson J.T. & Falkowski P.G. (1998). Primary production of the biosphere: integrating terrestrial and oceanic components. Science 281: 237–240.

Fortunato A.E., Annunziata R., Jaubert M., Bouly J.P. & Falciatore A. (2015). Dealing with light: The widespread and multitasking cryptochrome/photolyase family in photosynthetic organisms. J. plant physiol. 172: 42–54.

Franck F., Schoefs B., Barthélemy X., MysliwaKurdziel B., Strzalka K. & Popovic R. (1995). Protection of native chlorophyll(ide) forms and of photosystem II against photodamage during early stages of chloroplast differentiation. Acta Physiol. Planta. 17: 123–132.

Gašparič M.B., Cankar K., Žel J. & Gruden K. (2008). Comparison of different realtime PCR chemistries and their suitability for detection and quantification of genetically modified organisms. BMC biotechnol. 8: 26.

Ge F., Huang W., Chen Z., Zhang C., Xiong Q., Bowler C., Yang J., Xu J. & Hu H. (2014). MethylcrotonylCoA carboxylase regulates triacylglycerol accumulation in the model diatom *Phaeodactylum tricornutum*. Plant Cell 26: 1681–1697.

Geider R.J., Osborne B.A. & Raven J.A. (1985). Light dependence of growth and photosynthesis in *Phaeodactylum tricornutum* (Bacillariophyceae). J. Phycol. 21: 609–619.

Genkov T., Meyer M., Griffiths H. & Spreitzer R.J. (2010). Functional hybrid RubisCo enzymes with plant small subunits and algal large subunits: engineered rbcS cDNA for expression in *Chlamydomonas* .J. Biol. Chem. 285: 19833–19841.

Goldman J.C. (1980). Physiological aspects in algal mass cultures. In: Shelef G, Soeder CJ (eds) Algae biomass. Elsevier/NorthHolland Biomedical Press, Amsterdam 343–359.

Gordon J.M. & Polle J.E.W. (2007). Ultrahigh bioproductivity from algae. Appl. Microbiol. Biotechnol. 76: 969–975.

Goss R. & Jakob T. (2010). Regulation and function of xanthophyll cycledependent photoprotection in algae. Photosynth. res. 106: 103–122.

Granum E. & Myklestad S.M. (2002). A simple combined method for determination of β-1, 3-glucan and cell wall polysaccharides in diatoms. Hydrobiologia 477: 155-161.

Granum E., Raven J.A. & Leegood, R.C. (2005). How do marine diatoms fix 10 billion tons of inorganic carbon per year. Can. J. Bot. 83: 898–908.

Griffiths D.J. (1973). Factors affecting photosynthetic capacity of laboratory cultures of diatom *Phaeodactylum tricornutum*. Mar. Biol. 21: 91–97.

Gruber A., Weber T., Bártulos C.R., Vugrinec S. & Kroth P.G. (2009). Intracellular distribution of the reductive and oxidative pentose phosphate pathways in two diatoms. J. Basic Microbiol. 49: 58–72.

Guillard R.R. & Ryther J.H. (1962). Studies of marine planktonic diatoms: I. *Cyclotella nana* and Detonula confervacea (cleve). Can. J. Microbiol. 8: 229-239.

Haimovich-Dayan M., Garfinkel N., Ewe D., Marcus Y., Gruber A., Wagner H., Kroth P.G. & Kaplan A. (2013). The role of C_4 metabolism in the marine diatom *Phaeodactylum tricornutum*. New Phytol. 191: 175–188.

Harada H., Nakatsuma D., Ishida M. & Matsuda Y. (2005). Regulation of the expression of intracellular β-carbonic anhydrase in response to CO_2 and light in the marine diatom *Phaeodactylum tricornutum*. Plant Physiol. 139: 1041–1050.

Harada H. & Matsuda Y. (2005). Identification and characterization of a new carbonic anhydrase in the marine diatom *Phaeodactylum tricornutum*. Can. J. Bot. 83: 909-916.

Harrison P.J., Thompson P.A. & Calderwood G.S. (1990). Effects of nutrient and light limitation on the biochemical composition of phytoplankton. J. appl. Phycol. 2: 45–56.

Hasle G.R. & Syvertsen E.E. (1996). Marine diatoms. in identifying marine diatoms and dinoflagellates. Elsevier: Amsterdam, The Netherland.

He L., Han X. & Yu Z. (2014). A rare *Phaeodactylum tricornutum* cruciform morphotype: culture conditions, transformation and unique fatty acid characteristics. PLoS One 9: e93922.

Herbstová, M., Bína, D., Koník, P., Gardian, Z., Vácha, F., and Litvín, R. (2015). Molecular basis of chromatic adaptation in pennate diatom *Phaeodactylum tricornutum.* Biochim. Biophys. Acta 1847: 534–543.

Holtz L.M., WolfGladrow D. & Thoms S. (2015). Numerical cell model investigating cellular carbon fluxes in *Emiliania huxleyi*. J. Theor. Biol. 364: 305–315.

Hu Q., Sommerfeld M., Jarvis E., Ghirardi M., Posewitz M., Seibert M. & Darzins A. (2008). Microalgal triacylglycerols as feedstocks for biofuel production: perspectives and advances. Plant J. 54: 621–639.

Husic D.W., Husic H.D., Tolbert N.E. & Black Jr C.C. (1987). The oxidative photosynthetic carbon cycle or C_2 cycle. Crit. Rev. Plant Sci. 5: 45–100.

Janssen M., Bathke L., Marquardt J., Krumbein W.E. & Rhiel E. (2001). Changes in the photosynthetic apparatus of diatoms in response to low and high light intensities. Int. Microbiol. 4: 27–33.

Jeffrey S.W. & Humphrey G.F. (1997). Application of pigment methods to oceanography. 127-66.

Jia J., Han D., Gerken H.G., Li Y., Sommerfeld M., Hu Q. & Xu J. (2015). Molecular mechanisms for photosynthetic carbon partitioning into storage neutral lipids in *Nannochloropsis oceanica* under nitrogendepletion conditions. Algal Res. 7: 66–77.

Joshi J., MuellerCajar O., Tsai Y.C.C., Hartl F.U. & HayerHartl M. (2015). Role of small subunit in mediating assembly of redtype form I RubisCo. J. Biol. Chem. 290: 1066–1074.

Kendel M., CouzinetMossion A., Viau M., Fleurence J., Barnathan G. & WielgoszCollin G. (2013). Seasonal composition of lipids, fatty acids, and sterols in the edible red alga *Grateloupia turuturu*. J. Appl. Phycol. 25l: 425432.

Kendrick A. & Ratledge C. (1992). Desaturation of polyunsaturated fatty acids in Mucor circinelloides and the involvement of a novel membrane-bound malic enzyme. Eur. J. Biochem. 209: 667–673.

Klumpp S., Zhang Z. & Hwa T. (2009) Growth ratedependent global effects on gene expression in bacteria. Cell 139: 1366–1375.

Kroth P.G., Chiovitti A. et al. (2008). A model for carbohydrate metabolism in the diatom *Phaeodactylum tricornutum* deduced from comparative whole genome analysis. PLoS One 3: e1426.

Lamote M., Darko E., Schoefs B. & Lemoine Y. (2003). Assembly of the photosynthetic apparatus in embryos from *Fucus serratus* L. Photosynth. Res. 77: 45–52.

Lavaud J., Rousseau B. & Etienne A.L. (2003). Enrichment of the lightharvesting complex in diadinoxanthin and implications for the non-photochemical fluorescence quenching in diatoms. Biochemistry 42: 5802–5808.

Laws E.A. & Bannister T.T. (1980). Nutrient-and light-limited growth of *Thalassiosira fluviatilis* in continuous culture, with implications for phytoplankton growth in the ocean. Limnol. Oceanogr. 25: 457–473.

Leboulanger C., Oriol L., Jupin H. & DescolasGros C. (1997). Diel variability of glycolate in the eastern tropical Atlantic Ocean. DeepSea Res. 44: 2131–2139.

Lemoine Y. & Schoefs B. (2010). Secondary ketocarotenoid astaxanthin biosynthesis in algae: A multifunctional response to stress. Photosynth. Res. 106: 155–177.

Leu S. & Boussiba S. (2014). Advances in the production of high-value products by microalgae. Ind. Biotechnol. 10: 169-183.

Levitan O., Dinamarca J., Zelzion E., Lun D.S., Guerra L.T., Kim M.K., Kim J., AS Van Mooy B., Bhattacharya D. & Falkowski P.G. (2015). Remodeling of intermediate metabolism in the diatom *Phaeodactylum tricornutum* under nitrogen stress. Proc. Natl. Acad. Sci. 112: 412–417.

Lewin J.C. (1958). The taxonomic position of *Phaeodactylum tricornutum*. J. Gen. Microbiol. 18: 427–432.

Li H., Tang C. & Xu Z. (2013). The effects of different light qualities on rapeseed (*Brassica napus* L.) plantlet growth and morphogenesis in vitro. Sci. Hortic. 150: 117–124.

Li Y., Xu J. & Gao K. (2014). Light modulated responses of growth and photosynthetic performance to ocean acidification in the model diatom *Phaeodactylum tricornutum*. PLoS One 9: e96173.

Liang Y.J. & Jiang J.G. (2015). Characterization of malic enzyme and the regulation of its activity and metabolic engineering on lipid production. RSC. Advances. 5: 45558–45570.
Liaud M., Lichtl C., Apt K., Martin W. & Cerff R. (2000). Compartmentspecific isoforms of TPI and GAPDH are imported into diatom mitochondria as a fusion protein: evidence in favor of a mitochondrial origin of the eukaryotic glycolytic pathway. Mol. Biol. Evol. 17: 213–223.
Livak K.J. & Schmittgen T.D. (2001). Analysis of relative gene expression data using real time quantitative PCR and the 2Ct method. Methods 25: 402–408.
Loza-Tavera H., Martínez-Barajas E. & Sánchez-de-Jiménez E. (1990). Regulation of ribulose-1, 5-bisphosphate carboxylase expression in second leaves of maize seedlings from low and high yield populations. Plant Physiol. 93: 541–548.
Ma Y.H., Wang X., Niu Y.F., Yang Z.K., Zhang M.H., Wang Z.M., Yang W.D., Liu J.S. & Li H.Y. (2014). Antisense knockdown of pyruvate dehydrogenase kinase promotes the neutral lipid accumulation in the diatom *Phaeodactylum tricornutum.* Microb. cell fact. 13: 100.
Marchetti A., Schruth D.M., Durkin C.A., Parker M.S., Kodner R.B., Berthiaume C.T., Morales R., Allen A.E. & Armbrust E.V. (2012). Comparative metatranscriptomics identifies molecular bases for the physiological responses of phytoplankton to varying iron availability. Proc. Natl. Acad. Sci. 109: E317–E325.
Marchetti J., Bougaran G., Jauffrais T., Lefebvre S., Rouxel C., SaintJean B., Lukomska E., Robert R. & Cadoret J.P. (2013). Effects of blue light on the biochemical composition and photosynthetic activity of *Isochrysis* sp.(Tiso). J. Appl. Phycol. 25: 109–119.
Matsuda Y., Nakajima K. & Tachibana M. (2011). Recent progresses on the genetic basis of the regulation of CO_2 acquisition systems in response to CO_2 concentration. Photosynth. Res. 109: 191–203.
Matsuda Y. & Kroth P.G. (2014). Carbon fixation in diatoms. In the structural basis of biological energy generation. Springer Netherlands 335–362.
Milligan A.J. & Morel F.M.M. (2002). A proton buffering role for silica in diatoms. Science 297: 1848–1850.
Mimouni V., Ulmann L. & Pasquet V. (2012). The potential of microalgae for the production of bioactive molecules of pharmaceutical interest. Curr. Pharm. Biotechnol. 13: 2733–2750.
Moroney J.V. & Ynalvez R.A. (2007). Proposed carbon dioxide concentrating mechanism in *Chlamydomonas reinhardtii*. Eukaryot Cell 6: 1251–1259.
Mouget J.L., Tremblin G., Morant-Manceau A., Morancais M. & Robert J.M. (1999). Longterm photoacclimation of *Haslea ostrearia* (Bacillariophyta): effect of irradiance on growth rates, pigment content and photosynthesis. Eur. J. Phycol. 34: 109–115.
Moulin P., Lemoine Y. & Schoefs B. (2010). Modification of the carotenoid metabolism in plastids: A response to stress conditions. In Handbook of Plant and Crop Stress. Pessarakli M. (Ed.). 407–433. Boca Raton, FL: CRC Press
Müller P., Li X.P. & Niyogi K.K. (2001). Non-photochemical quenching. A response to excess light energy. Plant Physiol. 125: 1558–1566.
Mus F., Toussaint J.P., Cooksey K.E., Fields M.W., Gerlach R., Peyton B.M. & Carlson R.P. (2013). Physiological and molecular analysis of carbon source supplementation and pH stressinduced lipid accumulation in the marine diatom *Phaeodactylum tricornutum*. Appl. Microbiol. Biotechnol. 97: 3625–3642.
Nakajima K., Tanaka A. & Matsuda Y. (2013). SLV4 family transporters in a marine diatom directly pump bicarbonate from seawater. *Proceedings of the National Academy of Sciences*, 110: 1767–1772.
Nguyen-Deroche T.L.N.N., Caruso A., Le T.T., Viet Bui T., Schoefs B., Tremblin G. & Morant-Manceau A. (2012). Zinc affects differently growth, photosynthesis, antioxydant enzyme activities and phytochelatin synthase expression of four marine diatoms. Sc. World Journal. 15. ID 982957.

Nishimura T., Takahashi Y., Yamaguchi O., Suzuki H., Maeda S. & Omata T. (2008). Mechanism of low CO_2induced activation of the cmp bicarbonate transporter operon by a LysR family protein in the cyanobacterium *Synechococcus elongatus* strain PCC 7942. Mol. Microbiol. 68: 98–109.

Nogueira D.P.K., Silva A.F., Araújo O.Q. & Chaloub R.M. (2015). Impact of temperature and light intensity on triacylglycerol accumulation in marine microalgae. Biomass Bioenerg. 72: 280–287.

Nymark M., Valle K.C., Brembu T., Hancke K., Winge P., Andresen K., Johnsen G. & Bones A.M. (2009). An integrated analysis of molecular acclimation to high light in the marine diatom *Phaeodactylum tricornutum*. PLoS One 4: e7743.

Obata T., Fernie A.R. & NunesNesi A. (2013). The central carbon and energy metabolism of marine diatoms. Metabolites 3: 325–346.

Ogren W.L. & Bowes G. (1971). Ribulose diphosphate carboxylase regulates soybean photorespiration. Nat. New Biol. 230: 159–160.

Parker M.S. & Armbrust E.V. (2004). Induction of photorespiration by light in the centric diatom *Thalassiosira weissflogii* (Bacillariophyceae): molecular characterization and physiological concequences. J. Phycol. 40: 557–567.

Parker M. & Armbrust V. (2005). Synergistic effects of light, temperature, and nitrogen source on transcription of genes for carbon and nitrogen metabolism in the centric diatom *Thalassiosira pseudonana* (Bacillariophyceae). J. Phycol. 41: 1142–1153.

Perry M.J., Talbot M.C. & Alberte R.S. (1981). Photoadaption in marine phytoplankton: response of the photosynthetic unit. Mar. Biol. 62: 91–101.

Pfaffl M.W., Tichopad A., Prgomet C. & Neuvians T.P. (2004). Determination of stable housekeeping genes, differentially regulated target genes and sample integrity: BestKeeperExcelbased tool using pairwise correlations. Biotechnol. Lett. 26: 509–515.

Pichard S.L., Campbell L., Kang J.B., Tabita F.R. & Paul J.H. (1996). Regulation of ribulose bisphosphate carboxylase gene expression in natural phytoplankton communities. 1. Diel rhythms. Mar. Ecol. Prog. Ser. 139: 257.

Post A.F., Dubinsky Z., Wyman K. & Falkowski P.G. (1984). Kinetics of lightintensity adaptation in a marine planktonic diatom. Mar. Biol. 83: 231–238.

Post A.F., Dubinsky Z., Wyman K. & Falkowski P.G. (1985). Physiological responses of a marine planktonic diatom to transitions in growth irradiance. Mar. Ecol. Prog. Ser. 25: 141–149.

Radakovits R., Jinkerson R.E., Darzins A. & Posewitz M.C. (2010). Genetic engineering of algae for enhanced biofuel production. Eukaryotic cell 9: 486501.

Ratti S., Giordano M. & Morse D. (2007). CO_2 concentrating mechanisms of the potentially toxic dinoflagellate *Protoceratium reticulatum* (Dinophyceae, Gonyaulacales). J Phycol. 43: 693–701.

Raven J.A. & Beardall J. (1981). Respiration and photorespiration. Physiological bases of phytoplankton ecology. Platt, editor. Can. Bull. Fish Aquat. Sci. 210: 55–82.

Raven J.A. (1983). The transport and function of silicon in plants. Biol. Rev. 58: 179–207.

Raven J.A., Beardall J. & Giordano M. (2014). Energy costs of carbon dioxide concentrating mechanisms in aquatic organisms. Photosynth. Res. 121: 111–124.

Regenberg B., Grotkjær T., Winther O., Fausbøll A., Åkesson M., Bro C., Hansen L.K., Brunak S. & Nielsen J. (2006). Growthrate regulated genes have profound impact on interpretation of transcriptome profiling in Saccharomyces cerevisiae. Genome biology 7: R107.

Renaud S.M., Parry D.L., Thinh L.V., Kuo C., Padovan A. & Sammy N. (1991) Effect of light intensity on the proximate biochemical and fatty acid composition of *Isochrysis* sp. And *Nannochloropsis oculata* for use in tropical aquaculture. J. appl. Phycol. 3: 43–53.

Reinfelder J.R., Kraepiel A.M. & Morel F.M. (2000) Unicellular C_4 photosynthesis in a marine diatom. Nature 407: 996–999.

Reinfelder J.R. (2011). Carbon concentrating mechanisms in eukaryotic marine phytoplankton. Ann. Rev. Mar. Sci. 3: 291–315.
Rico M., López A., SantanaCasiano J.M., Gonzàlez A.G. & GonzálezDávila M. (2013). Variability of the phenolic profile in the diatom *Phaeodactylum tricornutum* growing under copper and iron stress. Limno. Oceanogr. 58: 144–152.
Roberts K., Granum E., Leegood R.C. & Raven J.A. (2007). Carbon acquisition by diatoms. Photosynth. Res. 93: 79–88.
Roberts K., Granum E., Leegood R.C. & Raven J.A. (2007). C_3 and C_4 pathways of photosynthetic carbon assimilation in marine diatoms are under genetic, not environmental, control. Plant Physiol. 145: 230–235.
Roháček K., Soukupová J. & Barták M. (2008). Chlorophyll fluorescence: A wonderful tool to study plant physiology and plant stress. Research Signpost 661: 41–104.
Roháček K. (2010). Method for resolution and quantification of components of the non-photochemical extinction (qN). Photosynth. Res. 105: 101–113.
Rohácek k., Bertrand M., Moreau B., Jacquette j., Caplat C., Morant-Manceau A. & Schoefs B. (2014). Relaxation of the non-photochemical Chlorophyll fluorescence quenching in diatoms: kinetics, components and mechanisms. Phil. Trans. R. Soc. 369: 20130241.
Romero M.F., Fulton C.M. & Boron W.F. (2004). The SLV4 family of HCO_3^- transporters. Pflügers Archiv 447: 495–509.
Sage R.F. & Stata M. (2015). Photosynthetic diversity meets biodiversity: the C_4 plant example. J. Plant Physiol. 172: 104–119.
Samukawa M., Shen C., Hopkinson B.M. & Matsuda Y. (2014). Localization of putative carbonic anhydrases in the marine diatom, *Thalassiosira pseudonana*. Photosynth. Res. 121: 235–249.
Sapriel G., Quinet M., Heijde M., Jourdren L., Tanty V., Luo G., Le Crom S. & Lopez P.J. (2009). Genomewide transcriptome analyses of silicon metabolism in *Phaeodactylum tricornutum* reveal the multilevel regulation of silicic acid transporters. PLoS One 4: e7458.
Schoefs B., Bertran M. & Franc F. (1992). Plant greening-Biogenesis of photosynthetic apparatus in bean leaves irradiated shortly after germination. Photosynthetica 27(4).
Schoefs B., Darko E. & Rodermel S. (2001). Photosynthetic pigments, photosynthesis and plastid ultrastructure in RbcS antisense DNA mutants of tobacco (*Nicotiana tabacum*). Zeitschrift für Naturforschung 56: 1067–1074.
Schoefs B. (2002). Chlorophyll and carotenoid analysis in food products. Properties of the pigments and methods of analysis. Trends Food Sci. Technol. 13: 361–371.
Schoefs B. & Franck F. (2003). Protochlorophyllide reduction: Mechanisms and evolution. Photochem. Photobiol. 78: 543–557.
Schwender J., König C. et al. (2014). Transcript abundance on its own cannot be used to infer fluxes in central metabolism. Front. Plant Sci. 5.
Scott M., Gunderson C.W., Mateescu E.M., Zhang Z. & Hwa T. (2010). Interdependence of cell growth and gene expression: Origins and consequences. Science 330: 1099–1102.
Sharma K.K., Schuhmann H. & Schenk P.M. (2012). High lipid induction in microalgae for biodiesel production. Energies. 5: 1532–1553.
Shtaida N., KhozinGoldberg I. & Boussiba S. (2015). The role of pyruvate hub enzymes in supplying carbon precursors for fatty acid synthesis in photosynthetic microalgae. Photosynth. Res. 116.
Smith S.R., Abbriano R.M. & Hildebrand M. (2012). Comparative analysis of diatom genomes reveals substantial differences in the organization of carbon partitioning pathways. Algal Res. 1: 216.
Solymosi K. (2012). Plastid structure, diversification and interconversions I. Algae. Curr. Chem. Biol. 6: 167–186.

Spectorova L.V., Nosova L.P., Goronkova O.I., Albitskaya O.N. & Filippovskij Y.N. (1986) Highdensity culture of marine microalgae promising items for mariculture II. Determination of optimal light regime for *Chlorella sp. f marina* under highdensity culture conditions. Aquacult. 55: 221–229.

Spetea C., Rintamäki E. & Schoefs B. (2014). Changing the light environment: chloroplast signalling and response mechanisms. Phil. Trans. R. Soc. B. 369: 20130220

Spreitzer R.J. (1999). Questions about the complexity of chloroplast ribulose 1,5bisphosphate carboxylase/oxygenase. Photosynth. Res. 60: 29–42.

Steel R.G. & Torrie J.H. (1960). Principles and procedures of statistics. Principles and procedures of statistics.

Stirbet A., Riznichenko G.Y. & Rubin A.B. (2014). Modeling Chlorophylla fluorescence transient: Relation to photosynthesis. Biochemistry (Moscow) 79: 291–323.

Sukenik A., Carmeli Y. & Berner T. (1989). Regulation of fatty acid composition by irradiance level in the Eustigmatophyte *Nannochloropsis* sp. J. Phycol. 25: 686–692.

Sukenik A. (1991). Ecophysiological considerations in the optimization of eicosapentaenoic acid production by *Nannochloropsis* sp. (Eustigmatophyceae). Bioresource Technol. 35: 263–269.

Sukenik A. & Wahnon R. (1991). Biochemical quality of marine unicellular algae with special emphasis on lipid composition. I. *Isochrysis galbana*. Aquacult. 97: 61–72.

Sun N., Ma L., Pan D., Zhao H. & Deng X.W. (2003). Evaluation of light regulatory potential of Calvin–Benson cycle steps based on large-scale gene expression profiling data. Plant Mol. Biol. 53: 467–478.

Tachibana M., Allen A., Kikutani S., Endo Y., Bowler C. & Matsuda Y. (2011). Localization of putative carbonic anhydrases in two marine diatoms, *Phaeodactylum tricornutum* and *Thalassiosira pseudonana*. Photosynth. Res. 109: 205–221.

Tanaka R. & Tanaka A. (2007). Tetrapyrrole biosynthesis in higher plants. Annu. Rev. Plant Biol. 58: 321–346.

Taraldsvik M. & Myklestad S.M. (2000). The effect of pH on growth rate, biochemical composition and extracellular carbohydrate production of the marine diatom *Skeletonema costatum*. Eur. J. Phycol. 35: 189-194.

Tchernov D., Silverman J., Luz B., Reinhold L. & Kaplan A. (2003). Massive lightdependent cycling of inorganic carbon between oxygenic photosynthetic microorganisms and their surroundings. Photosynth. Res. 77:95–103.

Tedesco M.A. & Duerr E.O. (1989). Light, temperature and nitrogen starvation effects on the total lipid and fatty acid content and composition of *Spirulina platensis* UTEX1928. J. appl. Phycol. 1: 201–209.

Terry K.L., Hirata J. & Laws E.A. (1983). Lightlimited growth of two strains of the marine diatom *Phaeodactylum tricornutum* Bohlin: Chemical composition, carbon partitioning and the diel periodicity of physiological processes. J. exp. mar. Biol. Ecol. 68: 209–227.

Thompson P.A., Harrison P.J. & Whyte J.N.C. (1990). Influence of irradiance on the fatty acid composition of phytoplankton. J. Phycol. 26: 278–288.

Tremblin G., Cannuel R., Mouget J.L., Rech M. & Robert J.M. (2000). Change in light quality due to a bluegreen pigment marenine, released in oysterponds: effect on growth and photosynthesis in two diatoms, *Haslea ostrearia* and *Skeletonema costatum*. J. App. Phycol. 12: 557-566.

Valenzuela J., Mazurie A., Carlson R.P., Gerlach R., Cooksey K.E., Peyton B.M. & Fields M.W. (2012). Potential role of multiple carbon fixation pathways during lipid accumulation in *Phaeodactylum tricornutum*. Biotechnol. Biofuels. 5: 40.

Vidoudez C. & Pohnert G. (2008). Growth phase specific release of polyunsaturated aldehydes by the diatom *Skeletonema marinoi*. J. Plankton Res. 30: 1305–1313.

Wahidin S., Idris A. & Shaleh S.R.M. (2013). The influence of light intensity and photoperiod on the growth and lipid content of microalgae *Nannochloropsis* sp. Bioresour. Technol. 129: 7-11.

Wang Y., Duanmu D. & Spalding M.H. (2011). Carbon dioxide concentrating mechanism in *Chlamydomonas reinhardtii*: inorganic carbon transport and CO_2 recapture. Photosynth. Res. 109: 115–122.

Wagner H., Jakob T. & Wilhelm C. (2006). Balancing the energy flow from captured light to biomass under fluctuating light conditions. New Phytol. 169: 95–108.

Wilhelm C., Büchel C. et al. (2006). The regulation of carbon and nutrient assimilation in diatoms is significantly different from green algae. Protist 157: 91–124.

Winck F.V., Arvidsson S., Riaño-Pachón D.M., Hempel S., Koseska A., Nikoloski Z., Gomez D.A.U., Rupprecht J. & Mueller-Roeber B. (2013). Genome-wide identification of regulatory elements and reconstruction of gene regulatory networks of the green alga *Chlamydomonas reinhardtii* under carbon deprivation. e79909

Wu S., Huang A. et al. (2015). Enzyme activity highlights the importance of the oxidative pentose phosphate pathway in lipid accumulation and growth of *Phaeodactylum tricornutum* under CO_2 concentration. Biotechnol. Biofuel. 8: 78.

Xiang T., Nelson W., Rodriguez J., Tolleter D. & Grossman A.R. (2015). Symbiodinium transcriptome and global responses of cells to immediate changes in light intensity when grown under autotrophic or mixotrophic conditions. Plant J. 82: 67-80.

Xue J., Niu Y.F., Huang T., Yang W.D., Liu J.S. & Li H.Y. (2015). Genetic improvement of the microalga *Phaeodactylum tricornutum* for boosting neutral lipid accumulation. Metabol. Engin. 27: 19.

Yang Z.K., Niu Y.F., Ma Y.H., Xue J., Zhang M.H., Yang W.D., Liu J.S., Lu S.H., Guan Y. & Li H.Y. (2013). Molecular and cellular mechanisms of neutral lipid accumulation in diatom following nitrogen deprivation. Biotechnol. Biofuels. 6: 67.

Yao Y., Lu Y., Peng K.T., Huang T., Niu Y.F., Xie W.H., Yang W.D., Liu J.S. & Li H.Y. (2014). Glycerol and neutral lipid production in the oleaginous marine diatom promoted by overexpression of glycerol3phosphate dehydrogenase. Biotechnol. Biofuels. 1: 19.

Yongmanitchai W. & Ward O.P. (1991). Growth of and omega-3 fatty acid production by *Phaeodactylum tricornutum* under different culture conditions. Appl. Envir. Microbiol. 57: 419–425.

Zhang C. & Hu H. (2014). Highefficiency nuclear transformation of the diatom *Phaeodactylum tricornutum* by electroporation. Mar. Genomics. 16: 63–66.

3.8 Supplemental data

Supplemental data 3.1: *Phaeodactylum tricornutum* growth curve

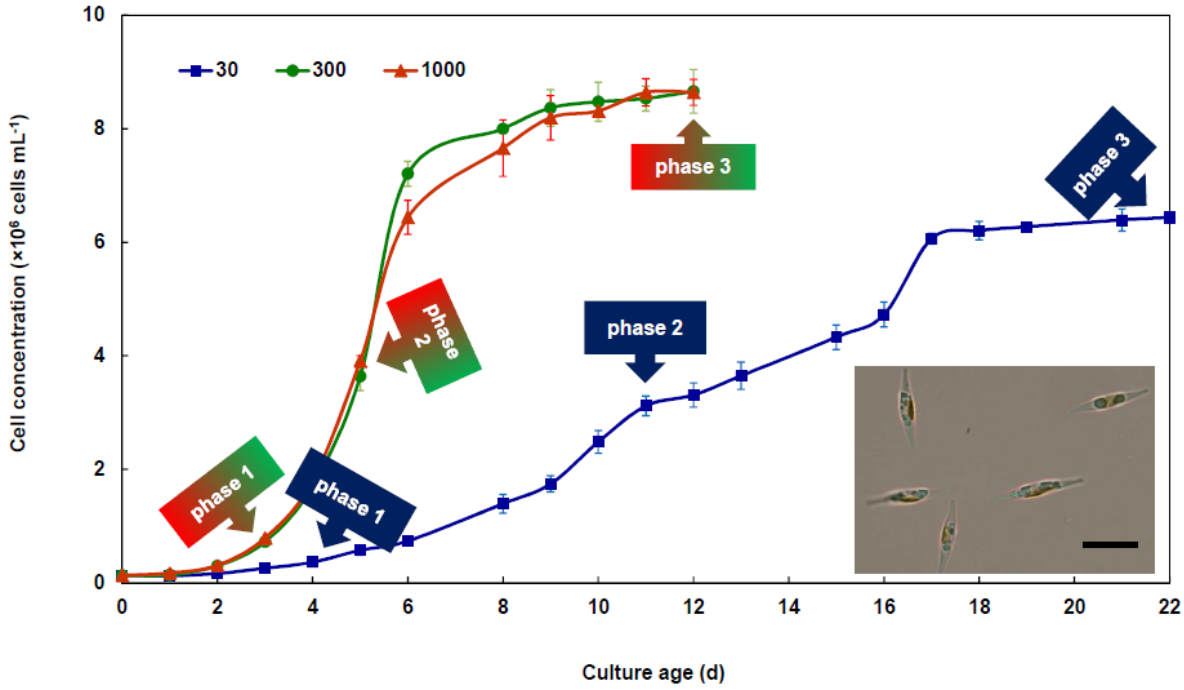

Figure 3.1. Growth of *Phaeodactylum tricornutum* under different light intensities.
Time course of cell density of cultures developing under 30 (LL), 300 (ML) and 1000 (HL) µmol m^{-2} s^{-1}. Each curve presents typical growth phases *i.e.* lag (phase 1), exponential (phase 2) and plateau (phase 3). The sampling time in each phase is indicated using arrows.
The insert presents a light microscopy picture of *P. tricornutum* grown under ML. The bar indicates 10 µm.

Supplemental data 3.2: Cellular pigment quota

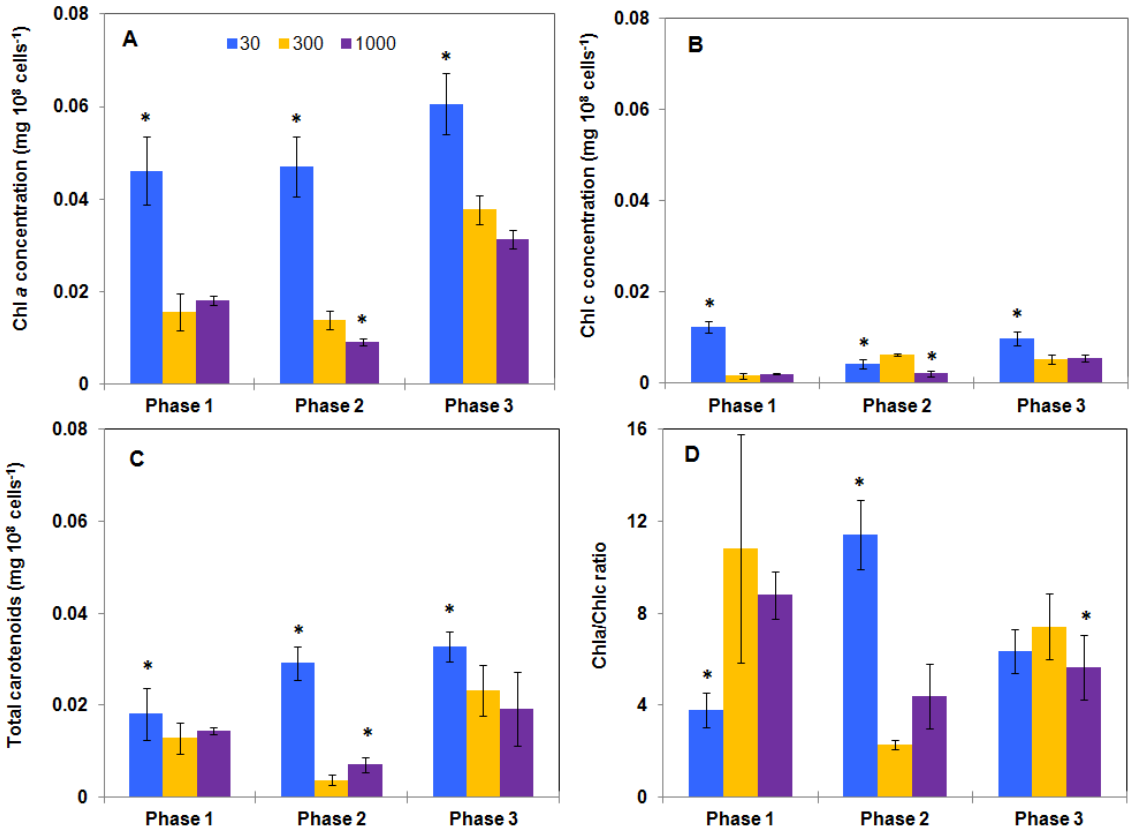

Figure 3.2. Pigments content per cell in *Phaeodactylum tricornutum* grown under different light intensities.

Changing photon flux densities altered pigment concentrations. The time-course of Chl *a* and total carotenoids accumulations were very similar under ML and HL: both decreased during the transition between phase 1 to phase 2 and significantly increased in phase 3. Under LL, the level of individual pigments increased from phase 1 to phase 3 except Chl c that first decreased and then increased. During phase 1 and phase 3, Chl c content was higher under LL than under ML or HL. Under LL, the ratio increased from phase 1 to phase 2 and then decreased until phase 3 is reached. At the end of phase 3 the ratio was similar for all conditions. Interestingly, total carotenoids mostly followed the Chl *a*/Chl c ratio except during phase 2 to phase 3 transition under LL.

Data are mean values ± SE (n = 3) and error bars represent SD. Means followed by asterisks are significantly different from the corresponding value for ML (p<0.05).

Supplemental data 3.3: Net photosynthesis and respiratory activities

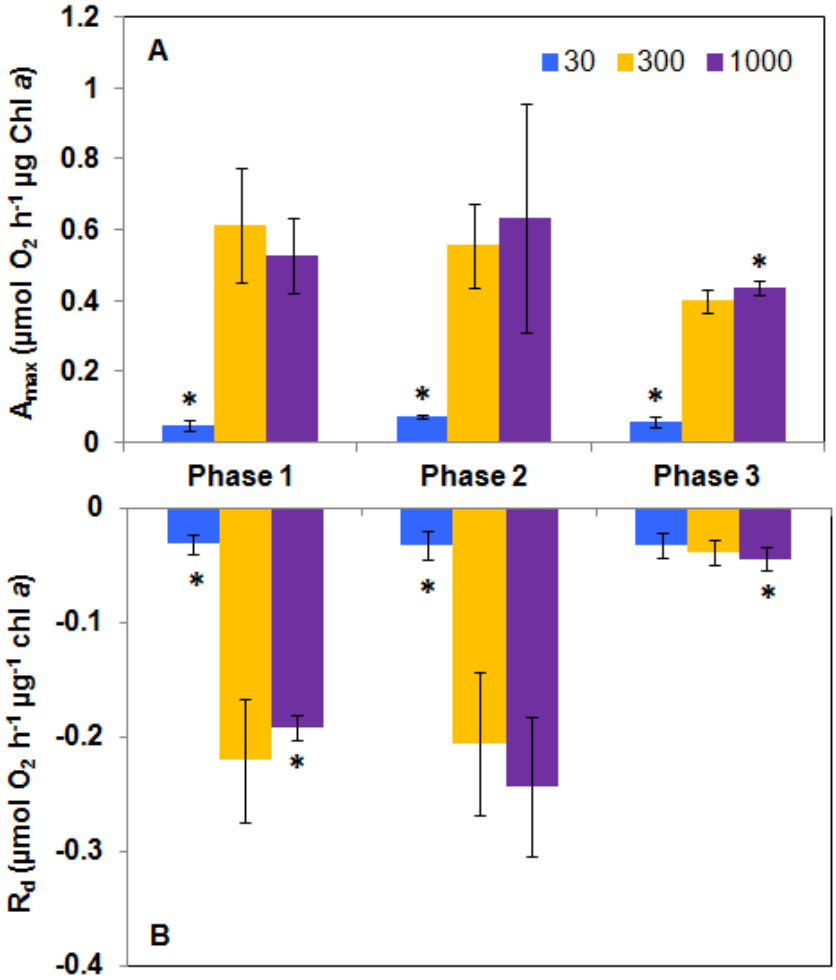

Figure 3.3. Impact of growth phase and photon flux density on net photosynthesis (A_{max}) and respiration (R_d) activities in *Phaeodactylum tricornutum.*
A_{max} and R_d were higher under ML and HL than under LL except during phase 3. However, when taken individually, neither R_d nor A_{max} were significantly affected by the value of the photon flux density during phase 1 and phase 2. During phase 3, Rd strongly decreased whereas A_{max} decreased by circa 20% only. Values represent the mean ± SE (n = 3) and error bars represent SD. Means followed by different letters and asterisks are significantly different in each light intensity and each growth phase, respectively (p<0.05).

Supplemental data 3.4: Kinetic of Chl *a* fluorescence Management of the incoming light energy

Figure 3.4 displays Chl fluorescence induction kinetics of *P. tricornutum* cells recorded under different light conditions. Comparison of the curves clearly indicated the differences between Fs levels. The F_0, F_M, F'_0, F'_M, F''_0 and F''_M were used to quantify parameters (Table 3.4) describing how the photosynthetic apparatus was managing the absorbed energy. They are briefly described below. For a comprehensive description, the reader is referred to Roháček et al. (2008, 2014).

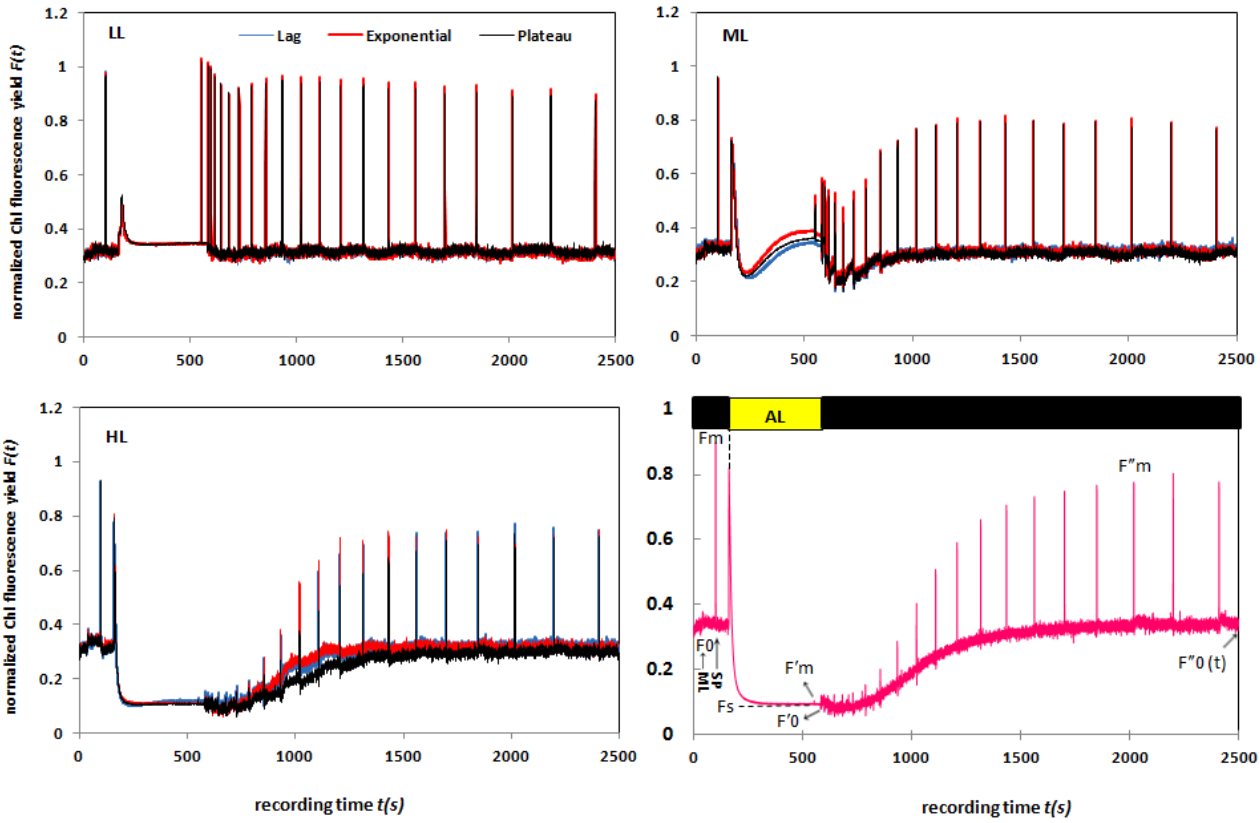

Figure 3.4. Chl fluorescence induction kinetics of *P. tricornutum* under LL, ML and HL. F_0: minimal fluorescence yield of dark-adapted sample with all PS II centers open; F_M: maximal fluorescence yield of dark-adapted sample with all PS II centers closed; F'_M: maximal fluorescence yield of illuminated sample with all PS II centers closed; F'_0: minimal fluorescence yield of illuminated sample with all PS II centers open (measured immediately after acclimation to light); AL: actinic light; ML: modulated light; SP: saturation pulse serving for transient full closure of PS II centers.

Table 3.4. Commonly fluorescence parameters used throughout the text for quantification of the photochemical (Φ_{P0}, qP, Φ_P, Φ_{II}) and non-photochemical (qN, q0, NPQ) processes (Equations according to Roháček et al. 2008)**.**

***Photochemical quenching parameters*:**	
Φ_{P0} Maximum quantum yield of PSII	$F_V/F_M = (F_M-F_o)/F_M$
Φ_{II} Photochemical efficiency of PSII	$(F'_M-F_S)/F'_M$
qP Photochemical quenching	$(F'_M-F_S)/(F'_M-F'_o)$
1-qP Degree of PSII reaction centre closure	$(F_S-F'_o)/(F'_M-F'_o)$
***Non-photochemical quenching parameters*:**	
NPQ Non-photochemical quenching	$(F_M-F'_M)/F'_M$
q_0 Relative change of minimum Chlorophyll F	$F_o-F'_o/F_o$
q_N Non-photochemical quenching of variable Chlorophyll F	$F_V-F'_V/F_V$

Maximum quantum yield of PSII photochemistry (Φ_{P0}): it quantifies the maximum photochemical efficiency of PSII in a dark-adapted state and is serve as a proxy of the fitness of the photosynthetic apparatus.
Effective quantum yield of photochemical energy conversion in PSII (ΦII): it quantifies efficiency of photochemical processes during conversion of the excitation energy by actually open PSII reaction centers.
Photochemical quenching of variable Chlorophyll fluorescence (qP): it quantifies the actual photochemical capacity of PSII and is proportional to the fraction of PSII reaction centers being actually in the open state under actinic irradiation.
Degree of PSII reaction centre closure (1-qP): it quantifies the proportion of centers that are closed and sometimes termed to "excitation pressure" on PSII (Maxwell and Johnson, 2000).
Non-photochemical chlorophyll fluorescence quenching (NPQ, qN): it reflects the excess radiation converted to heat during the actinic irradiation. Its extent correlates mostly to diatoxanthin formation. NPQ calculation differs from that of qN in the fact that the former relies on maximum fluorescence levels whereas the later relies on the variable fluorescence (see Supplemental Table 3.4; Roháček et al. 2008).
Relative change of minimum Chlorophyll fluorescence (q0): it is linked to processes of the non-photochemical nature activated in thylakoid membranes under the actinic irradiation.
qN analyses were performed as explained in Roháček et al. (2014). From the mechanism point of view, qNi relies on the dissipation of the proton gradient (ΔpH relaxation) and diatoxanthin epoxidation. qNf seems to be related to a fast conformational changes

occurring within the thylakoid membranes in the vicinity of the PSII complexes, whereas qNs could be related to photoinhibition and/or partial dissipation of the pH gradient (Roháček et al. 2014).

References

Roháček K., Soukupová J. & Barták M. (2008). Chlorophyll fluorescence: a wonderful tool to study plant physiology and plant stress. Plant Cell CompartmentsSelected Topics. Research Signpost, Kerala, India. 41–104.

Rohácek K., Bertrand M., Moreau B., Jacquette J., Caplat C., Morant-Manceau A. & Schoefs B. (2014). Relaxation of the non-photochemical Chlorophyll fluorescence quenching in diatoms: kinetics, components and mechanisms. Phil. Trans. R. Soc. 369: (1640), 20130241.

Maxwell K. & Johnson G.N. (2000). Chlorophyll fluorescence: a practical guide. J. Exp. Bot. 51: 659–668.

Supplemental data 3.5: PhotosynthesisIrradiance curve

To determine the optimal and stress-related photon flux densities in *P. tricornutum* the variations of gross photosynthesis activity as a function of the incoming photon flux density was measured using an oxygen electrode using LL, ML or HL adapted cells (see section 'Photosynthetic and Respiratory Activity, PI-curve' in Material and method section). Figure 3.5. presents the variations obtained with ML adapted *P. tricornutum* cells. Similar curves were obtained with the diatoms adapted to LL or HL (data not shown).

PI-curves were fitted according to the model of Eilers & Peeters (1988) using the CurveExpert. From these data, the following parameters were calculated:

α^B parameter: it is defined as the initial slope of the PI-curve. This parameter is usually considered as proportional to the efficiency in which microalgae harvest light (Eilers & Peeters, 1988, Nguyen-Deroche et al. 2012).

P^B_{max} parameter: it is defined as the asymptotic value of PI-curve. It reflects the maximal gross photosynthetic activity (Eilers & Peeters, 1988, Nguyen-Deroche et al. 2012).

E_k parameter: it is defined as the irradiance corresponding to the intercept between α^B and P^B_{max}. It defines the irradiance levels for which photosynthesis starts to be saturating (Eilers & Peeters, 1988, Nguyen-Deroche et al. 2012).

Light compensation irradiance (*Lci*): it is defined as the irradiance level for which the rate of oxygen production through photosynthesis exactly matches the rate of oxygen consumption through respiration.

The values obtained for the several LL, ML and HL adapted cells parameters are compared in Table 3.5. The value of E_k for the diatoms adapted to ML is very close to 300 µmol m^{-2} s^{-1}. It also indicates that the irradiances choosen as LL and HL provides stress conditions to the diatoms.

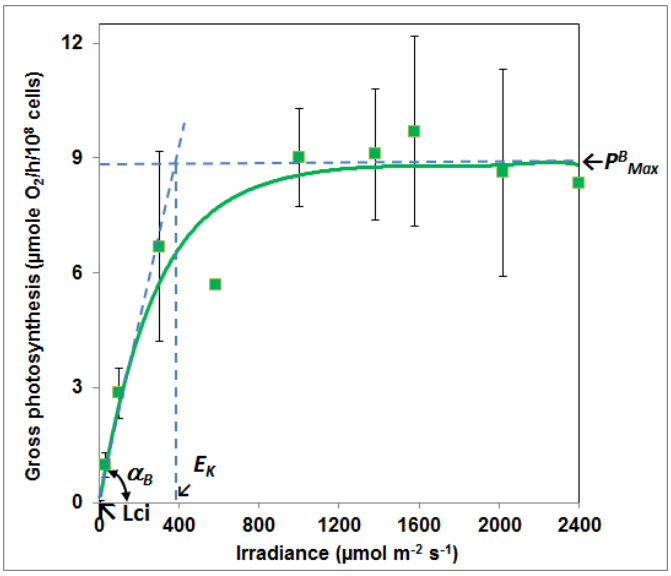

Figure 3.5. PI-curve recorded in *Phaeodactylum tricornutum* adapted to ML.
Diatom cells were grown under ML as explained in the Material and method section (experiment strategy and sampling'). The mean experimental points (n = 15) and the fitting curve are indicated in green. The dashed lines indicate the values of α^B, P^B_{max}, E_k and Lci.

Table 3.5. Parameters of PI-curves in *Phaeodactylum tricornutum* grown under LL, ML and HL. PI-curves were fitted according to the model of Eilers & Peeters (1988) using the CurveExpert software. Significant different data are indicated with different superscript letters (Tukey Test, *p≤0.05*). Mean values ± SE (n = 3–5).

Irradiance (µmol m^{-2} s^{-1})	**30**	**300**	**1000**
α^B (µmol O_2 h^{-1} μg^{-1} Chl *a*)	0.0006 ± 0.0004*	0.0021 ± 0.0005	0.0013 ± 0.0002
P^B_{max} (µmol O_2 h^{-1} μg^{-1} Chl *a*)	0.173 ± 0.035*	0.825 ± 0.159	0.582 ± 0.055*
E_K (µmol m^{-2} s^{-1})	176.87 ± 21.98*	374.49 ± 38.30	440.79 ± 38.30*
Lci (µmol m^{-2} s^{-1})	0	14	14

References

Eilers P.H.C. & Peeters J.C.H (1988). A model for the relationship between light intensity and the rate of photosynthesis in phytoplankton. Ecol. Model. 42: 199–215.

Nguyen-Deroche T.L.N., Caruso A., Trung Le T., Viet Bui T.V., Schoefs B., Tremblin G. & Morant-Manceau A. (2012). Zinc affects differently growth, photosynthesis, antioxidant enzyme activities and phytochelatin synthase expression of four Marine Diatoms. Sci. World J. 15.

Supplemental data 3.6: List of enzymes and related genes

Table 3.6. Name and sequences of the primers used , ID and localization List of the enzymes and of their corresponding gene/isogene(s), protein ID (http://genome.jgi.doe.gov/Phatr2/Phatr2.home.html) **and primers.**

Enzyme	Gene abreviation	Protein ID	Compartment	Primer-F (5'-3')	Primer-R (5'-3')
Pyruvate phosphate dikinase	PPDK	21988	plastid	CAGCGGGTTGAGCAAGACAT	TCATACCAGGCATGGAAATGG
Phosphoenolpyruvate carboxylase	PEPC1	51136	plastid	AATTGCCCAAGCTGGGTTTC	ATGACGTAGGCTCCCAAACAA
	PEPC2	27976	mitochondria	GCGACTCACATCAAGCATCAG	GTCTTCGCCGCAAGGAAAC
Malate dehydrogenase	MDH	51297	mitochondria	CAACCGCTCTCGATGCTTCT	TGTGACTGAGATCCGCAGCTA
Malate synthase	MS	54478	peroxisome	GGGCGGTATGAGTGCATCA	AGCTGTCACTTCGCGCAACT
Phosphoenolpyruvate carboxykinase	PEPCK	55018	mitochondria	GCCGAATACGGTGACACATTT	CTTCGGTCTCGGATCCCTTAT
Phosphoglycolate phosphatase	PGP	48026	plastid	ACCTGGCACCAATCATTTGG	CGGTAAACCACACCGTCACA
Pyruvate carboxylase	PYC1	30519	mitochondria	TTTCGACCGCTGGCATTTAT	GCGACTGGAGACTTGCTGGTA
	PYC2	49339	plastid	GGAAAATCCCGAGCGAGACT	GGAGTATCCAATGCCGTCCAT
Sedoheptulose-1,7-biphosphatase	SBP	56467	cytosol	GGAGCGGCAGGAGGATTAC	GGCGAGAGCTTCGTACGATT
Hydroxypyruvate reductase/glycerate	HPR	56499	mitochondria	GATCTCCGGCCTCGTGATT	GGAGGCTTCTCGGACTGAAA
Glyceraldehyde-3-phosphate dehydrogenase	GAPC1	22122	plastid	AGCCGACTACGTCTGCGAAT	GGGTGCCGAGTAGATGACCTT
	GAPDH	23598	cytosol	TGTGAGTCCGCTGCCTATCTC	CGTCGACGGTAAAGGATTGG
	GapC4 (TPI/GapC3)	32747/25308	mitochondria	TCCTCCATGGACGTGGTTTC	TGAGACCCTCCTTGAGTCCAA
6-phosphogluconate dehydrogenase	6PGDH	45333	cytosol	CTCAGCAAGCCTCGGAAAGT	AATTCGCTGATCGCTTCGAT
Oxoglutarate/malate transporter	OMT1	8990	mitochondria	ATTACCTCAATCAACGCCGAAA	GGCGAGCGCATAGATGAGA
Pyruvate kinase	PK1	22404	plastid	CGGATGTGTTGGCAAAGACA	AACCGCTGCCACTGTTGTTT
	PK2	49098	cytosol	GTAACGGCCACACAGATGCTT	AGTCCGTGCCGTCCAAGAC
	PK3	56445	cytosol	ATTGAATCGGGCATGAATGTG	TGTTTTGTGCAGCCTGACGTA
	PK4a/PK4b	45997/27502	cytosol	ATTTCGTCCGGGCTTGAGT	TGCCCAACAGCAATCCACTA

	PK5	49002	mitochondria	TGCAGCTACACCGTTCTATAATTCC	CGTACGGCTTCAGCTCTCAGA
	PK6	56172	mitochondria	CCTCCACTCGTCTCGGCATA	TGCAACTGTCGGGCTAACTTG
Bicarbonate transporter	SLV4_1	45656	plastid	GCCCAGCCGTTGACAATC	CAGCATCTTCGCCAATTGTG
	SLV4_2	32359	plastid	CGGTGCTCTGGATCGGAATA	ACCAAGTGCAAGGATGATGGTT
	SLV4_3	54405	membrane	TGGTTGCCTCCATTCTGATCT	TGAGTCGGCGTGATGCTATC
Triose phosphate isomerase	TPI_1	18228	plastid	ACCTGCCGTCAGATTTTGGT	CTGACGCTTCCTCCGTAAAGA
	TPI_2	50738	plastid	GGGTAGTCTTTGGCGAAACG	GATTCGGATTCGCCAATGC
Fructose-1,6-bisphosphatase	FBP	23247	cytosol	GCGATTGCGACCTCCTGTAA	CGTCGCCGGTTGAGTTG
	FBPC1	42886	plastid	ACATTGGGCTCTGGAGTCGAT	AAATGGGTCCAGAGGAAGGAA
	FBPC2	42456	plastid	GTGACGCTGACGCGCTTTA	TTGCCTTACAGGCCGTATCG
	FBPC3	31451	plastid	TTTGGGTATCCTGGCGACAA	ACAATCCACCCGCCTGTTC
	FBPC4	54279	plastid	AGCACCCGCTGTCGATTC	AAACCGGCTCAACGTAATGG
Glucose-phosphate isomerase	GPI_3	56512	plastid	CCACGCAACGGTCAATCTT	CGAAACGAGCTGTGGTCGAT
	GPI_1	23924	cytosol	TCAGCAAGGCGACATGGAA	GGTGCCAGGTTCACCGAATA
	GPI	53878	cytosol	AGCGCAGCAGCACATTCAT	CGGGCTGTGCAAAAAAGTTT
Fructose-bisphosphatase aldolase	Fba3	29014	cytosol	CGGATCGGTCGCTTTGG	AGTGGTCGGAATGAAGGATGA
	Fba4	42447	cytosol	GGACGAGAATCATTACGAGTAAAGC	GCGGTCCATCGTATCTTCAAA
	FbaC1	825	plastid	TGGTTGCCCTGGTTTGATG	CTTCGGAGAGATCCAACATGTG
	FbaC2	22993	plastid	ACCGGACAAGCCCAACAAG	TAGGTCGGCGTACGATTTGC
	FbaC5	51289	plastid	TGACGTTCTGACCGATGCA	GCCAGAGCACCAGGTTTCAC
Carbonic anhydrase	CA1	35370	secreted	GACACTTCCGGTACTATTTGGAGAA	GTCGCTGTAGTTGGCATCGA
	CA2	44526	secreted	CATACCATTGACGGTTTCAACACT	AGGTTGCGACTTTTTTGACGAA
	CA3	55029	secreted	CGCTTACAGTTCCAGGTGTATCG	TCGGCTCCCGAGAAATTG
	CA6	54251	secreted	TCGCAGTGGTGGTTCCTTTC	CATATGCAATTCGCCATCGT
	CA7	42574	secreted	AGCAAAGGTTTCCCGGATTG	GTGTGACTTCGGCGTCGTATC
	bCA4 (PtCA1)	42406	plastid	ACGTTATCGTCTGTGGTCACTATGA	CGGATGTTACGGAGCCAGAT
	bCA5 (PtCA2)	45443	secreted	CGTCGATTTGAACGTCATTGA	CCGCCATCCTTGTAGCTTTC
Phosphoglycerate mutase	PGAM_1	42857	plastid	CCGTCTGAGAACGAGGTTGTG	CGGGTACGCTGCCCATAC
	PGAM_2	43253	mitochondria	CAAGACAGTTATGGTGGCAGATTC	CCAAGGCATCCTCCATCTTC
	PGAM_3	43812	plastid	GATTGCGACCACCAGAAAGG	GTTGACGTGCCGAAAAAGGA
	PGAM_4	51298	plastid	AGGCGTTCCGCTCGTTTAC	GTCCTGATAACGGCGCAATC
	PGAM_5	26201	mitochondria	AAGCCTGCCGATTCCTCTCT	TTGCATGCTTGCACAGAATTT
	PGAM_6	33839	mitochondria	CCGCGGTACAATGGCTTT	CAAAATGGTACAACGCGTTCA
	PGAM_7	35164	mitochondria	CTGGACCAACGTCGGTCTTT	CGATCGAGTACCCGTGCAA

Glycine decarboxylase	GDCP	22187	mitochondria	CGTATTGCTTTGGAGGATTCG	GGACGATCCCACTTCTCATTG
	GDCT_1	56477	mitochondria	TCGAAACGCGAAGCAATCT	GGGAGCGTACCAGGATGGA
	GDCH	32847	mitochondria	TTCATTTGACAAAGGCGATAGC	TCGACGACAGTTCCAGAGATTG
NAD Malic enzyme	ME1	56501	mitochondria	TCGTATTATGAACATCCATTTGCA	TCGAGCATGACGTTCTTACGAA
Glycolate dehydrogenase/glycolate oxidase	GOX1	22568	peroxisome	GATGCCTTTGCTCGCTGGTA	CCGGCATACTGAGTCCTTGTC
	GOX2	50804	mitochondria	CAAGGACGCGTATTCCGAAT	TGTGACGTCCTGGCCAAAG
RubisCo small subunit	rbcS	ABK20640	plastid	TGCTTACGGTACTGAAAGTTGTGTT	AAGCAATACGACGACCTTCAAGT
RubisCo large subunit	rbcL	AAF07200	plastid	TTGGGCGCGTGATAATGA	AAATAACACGGAAGTTGATACCATGA
3-deoxy-7-phosphoheptulonate synthase	AroA	24353	plastid	CACGCCTGGAATTTGGACTT	GAAACGGAGCGACTCGTCAA
3-dehydroquinate synthase	AroB	20809	plastid	CTTTGAGTGGCAGGAGGATCA	AAGATCGCGTAATGGCGAAA
Shikimate/quinate 5-dehydrogenase / 3-dehydroquinate dehydratase	AT3G*	45535	cytosol	GGCAGAGTCCCGTTATTCGA	CGCGCATTGCTGAAACAAT
Shikimate kinase	SK*	49363	plastid	ATCGAAAGAGCAACAGGAATGAC	GTCCAAAACTTGCGCTTCCA
3-phosphoshikimate 1-carboxyvinyltransferase	EPSP*	18246	plastid	TCCCTGGTTCCAAATCTCTGA	CAAATGTCGTCGGAATCCAA
chorismate synthase	AT1G*	43429	plastid	TTGAGAGTGGAGACGGCTTTG	GGTCTCGGGATCCACGTAGA
Acetyl-CoA carboxylase	ACC1	54926	Plastid	CATGTCCGAGGCGATTGG	TTACTGTTCGCACACCCATAGC
	ACC2	55209	plastid	ACGGAAGCACATCCAATAACG	TCTCCGGCAGCAAAATGTATC
Pyruvate dehydrogenase	PDH1	20360	mitochondrial precursor	CAGGTTCACACTTACCGCTTCA	CGCCCACGCCTTTTCTT
	PDHA1	55035	mitochondrial precursor	TGGCGGGCTTGATTCTGA	CGGCTCGTCGTTCTCACA
	PDHB	20183	mitochondrial precursor	ACGCGACCATTATCTCCTTCA	TTCCACGGATACGCCTTTTT
Glycosyl transferase	BGS1	55327	cytosol	CCTTTGCCAACGACCATTCT	GGTGACCATAGTGGAGACGGATA

Supplemental data 3.7: An integrated model for central carbon metabolism in *Phaeodactylum tricornutum*

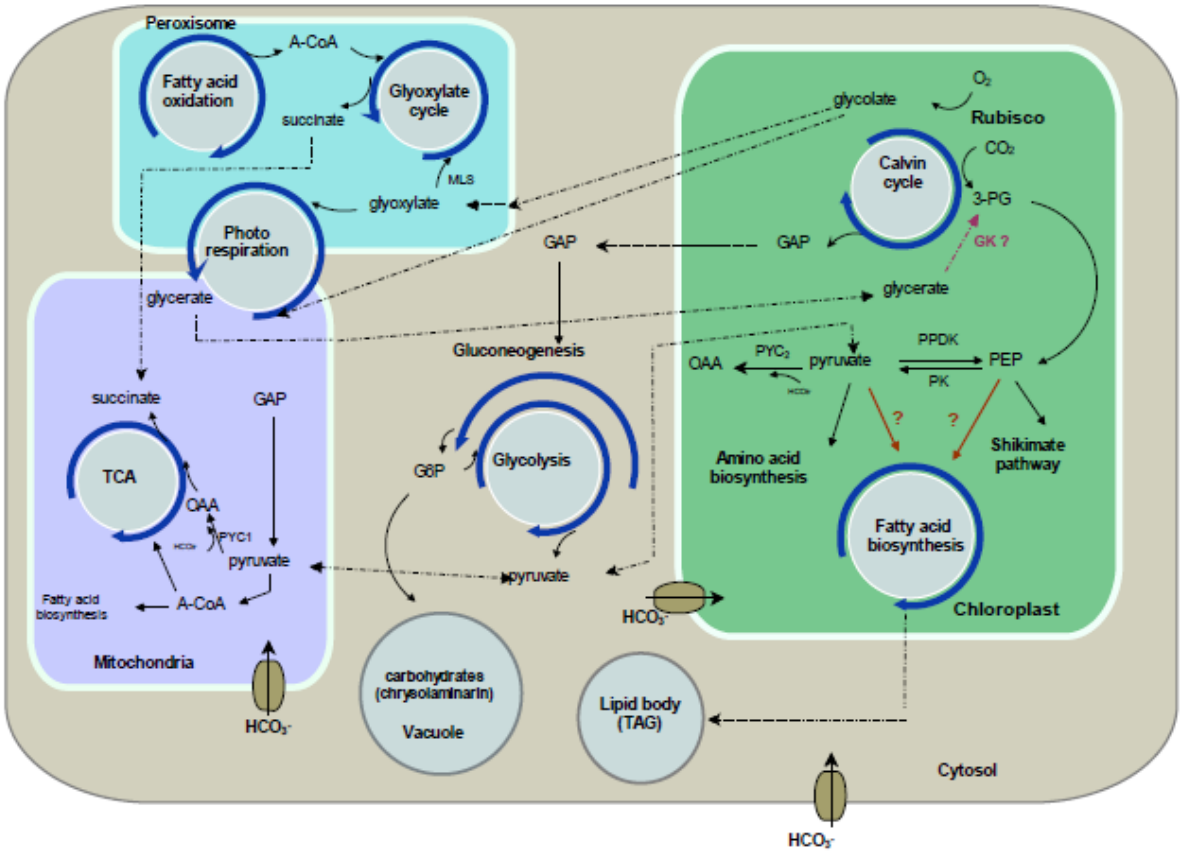

Figure 3.7. Simplified overview of central carbon metabolism and photorespiration in *Phaeodactylum tricornutum*.

3PG: 3-phospho-D-glycerate; GAP: D-glyceraldehyde-3-phosphate; PEP: phosphoenolpyruvate; OAA: oxaloacetate; A-CoA: acetyl-CoA; G6P: D-glucose-6-phosphate. For the full name of the genes, see the Supplemental Table 3.6.

Supplemental data 3.8: Heatmap of up or down-regulated genes under different light intensities

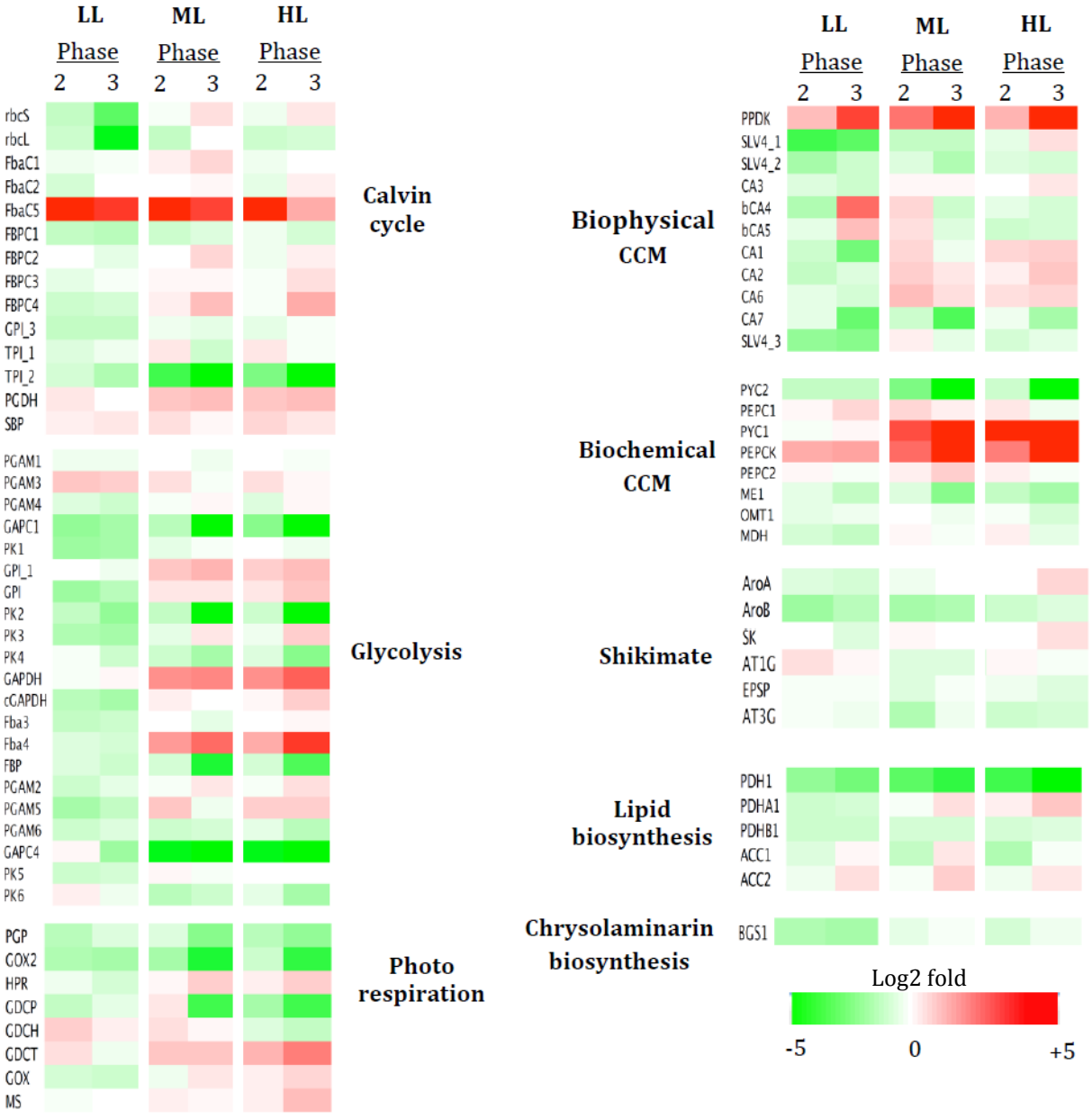

Figure 3.8. Dysregulated heatmap showing the expression pattern of 74 genes related to 8 pathways, with the greatest differences in expression (red: high, green: low). Columns represent relative (to phase 1) changes in the expression of genes in phase 2 or phase 3 under low light (LL) medium light (ML) and high light (HL).

Conclusion of part 1

The availability of the *Phaeodactylum tricornutum* genome database (Bowler et al. 2008) allowed the building of a new cellular model of the carbon metabolism (Figure 3.7). This model has been used to envision the capability of the diatom to respond to different light intensities. This enabled the investigation to assess not only lipid accumulation processes but also competing pathways with lipid synthesis. In this study, in most cases, the enzymes acting within the same pathway had the same directionality indicating a coordinated gene regulation and directed control. Results were both anticipated and surprising.

Generally, diatom cells could adapt to different light conditions in efficient ways to keep cell growth, processes and regulation. Growh rate and generation time under LL was less than ML and HL that showed the intensity of light was a limiting factor for cell mitosis frequency under LL. Anyway, with either fast or slow growth rate, cells faced C depletion in the medium and it was mostly responsible to reach plateau phase, while there was no N deficiency. Both elements are used to synthesize lipids, proteins or carbohydrates. Interestingly, in different growth phase and under different light intensities, strategy of the cells varied according to the accumulation of these molecules. For instance, lipid proportion was higher under LL phase 1, while under ML and HL it was very low. Also, cell C content (Q_C) under LL was either close or higher than ML and HL, while C uptake was lower. We concluded that because of low cell division rate (as a consequence of low light energy) under LL, the need of C import inside cells was lower then under the two other lights. Consequently more C was available in the cell environment and could be used for lipid accumulation, while fast cell division under ML and HL, require energy and most of the C are used to generate ATP to maintain growth rate. Lipid proportion increased under ML during phase 2 and 3, compare to LL and HL. Carbohydrates and proteins were the most abundant type of compounds under LL and HL, respectively.

In most cases, enzymes of the different pathways had coordinated gene regulation. In each growth phase, some genes/isogenes were the most responsible to direct the synthesis of intermediates to the final target, *i.e.* secondary compounds. For instance under LL phase 1, up-regulation of GAPDH, GAPC1 (key enzyme for lipid synthesis), PGAM1, PGAM4 and PK1 oriented the direction of pathways toward lipid synthesis, while these genes were mostly downexpressed under ML and HL (Figure 3.9). The activity of these genes varied by aging the culture, according to the growth condition, and they are up-regulated under ML in phase 2, resulting an increase in lipid synthesis in this condition. Of course many interactions between enzymes activity in different pathways and growth condition participate to orient carbon to different pathways including lipid synthesis. Indeed, it has been reported that CO_2 concentration affects metabolic and gene regulation, suggesting that exposing the cells to elevated CO_2 first

causes a shift in regulation of genes, and then a metabolic rearrangement (Hennon et al. 2015). In the study performed on the diatom *Thalassiosira pseudonana*, this organism rapidly responded to the increase of CO_2 by down expression of genes required for energy producing metabolic pathways, including photosynthesis and respiration, suggesting a general reduction in metabolism under high CO_2 (Hennon et al. 2015).

In our case, *P. tricornutm* faced CO_2 depletion condition by aging the culture and an up-regulation of some genes encoding enzymes involved in carbon concentration mechanism (CCM), including PYC1 and PEPCK was observed in phase 2 and even higher in phase 3 under ML and HL (Supplemental Figure 3.8). These results seemed complementary from those obtained with *T. pseudonanna* (Hennon et al. 2015).

The complexity of the interactions many enzymes and genes working in a huge network composed by related but different interacting pathways makes difficult to draw very precised conclusions without complementary 'omics' approaches such as proteomics and metabolomics. Interestingly but surprisingly, we observed a common point in all light levels that was orientation of mRNA transcription toward the synthesis of pyruvate and in some cases in the reverse direction to PEP. Pyruvate is a marshal point for the synthesis of high value molecules including lipids, proteins, carbohydrates, *etc*. PEP is the intermediate feeding this marshall point and serve also as a key intermediate to the synthesis of aromatic compounds such as aromatic amino acids. Our results confirm the previous conclusion about the existence of a pyruvate hub in microalgae (Smith et al. 2012; Shtaida et al. 2015) and also shows that reorientation of carbon metabolism might occur according to the environmental condition. For instance, under HL phase 3, in addition of carbon direction to pyruvate, reorientation of carbon toward PEP synthesis was also observed, parallelly with up-regulation of genes encoding enzymes of the shikimate pathway including AroA, AroB and SK that shows activation of this pathway. As in each light condition, PEP is even more synthesized by aging the cells; it seems that reorientation of carbon to PEP is mostly active when carbon availability is limiting in environment. This conclusion opens a very interesting avenue for microalga biotechnology aiming to produce secondary compounds. We believe that the results presented here are complementary of the few available data about the global responses of diatoms (Allen et al. 2008; Valuenzela et al. 2012, Fernie et al. 2012; Marchetti, et al. 2012; Shrestha et al. 2012) to environmental or biotic factors, including the response to light. These information are needed to better understand the activity and the regulation of enzymes and intermediates participating along the routes and, to go further, to determine a model in diatom from capturing CO_2 to the synthesis of high value molecules, such as fatty acids, proteins, chrysolaminarin through the reorientation of the carbon metabolism toward the production of secondary metabolites.

Physiological and molecular data showed that the impact of ML and HL on diatom cells were similar but quite different from LL. This conclusion may seem contradictory

but ultimately predictable because the sampling plan favored the comparison of samples in the same physiological state. It is a very important point in this work because (i) it validates a *posteriori*, the experimental hypothesis that at the chosen sampling times, the cells were in similar physiological states independently of the growth light intensity and (ii) it gives guarantee to the modifications that have been observed at the molecular level, *i.e.* they are mostly reflecting the impact of the light intensity on the cells and are just not due to cells being in completely different physiological states. To strengthen the aspect 'comparison of cells in the same physiological status', this experiment could have been performed using a set of photobiorectors, each of them working in a definite condition corresponding to those existing when algae were sampled. Unfortunately, such a possibility did not exist in our lab and anyway, it would have been a very much timeconsuming experiments. Neverthless, we would recommend the use of such a culture method if complementary experiments have to be realized.

References

Allen A., Laroche J., Maheswari U., Lommer M., Schauer N., Lopez P., Finazzi G., Fernie A. & Bowler C. (2008). Wholecell response of the pennate diatom *Phaeodactylum tricornutum* to iron starvation. Proc Natl Acad Sci. U.S.A. 105: 10438–10443.

Bowler C., Allen A.E. et al. (2008). The *Phaeodactylum* genome reveals the evolutionary history of diatom genomes. Nature 456: 239–244.

Hennon G M., Ashworth J., Groussman R.D., Berthiaume C., Morales R.L., Baliga N.S., Orellana M.V. & Armbrust E.V. (2015). Diatom acclimation to elevated CO2 via cAMP signalling and coordinated gene expression. Nat. Clim. Change 5: 761–765.

Fernie A.R., Obata T., Allen A.E., Araujo W.L. & Bowler C. (2012). Leveraging metabolomics for functional investigations in sequenced marine diatoms. Trends Plant Sci. 17: 395–403.

Marchetti A., Schruth D.M., Durkin C.A., Parker M.S., Kodner R.B., Berthiaume C.T., Morales R., Allen A.E. & Armbrust E.V. (2012). Comparative metatranscriptomics identifies molecular bases for the physiological responses of phytoplankton to varying iron availability. Proc. Natl. Acad. Sci. 109: E317–E325.

Shrestha R.P., Tesson B., NordenKrichmar T., Federowicz S., Hildebrand M. & Allen A.E. (2012). Whole transcriptome analysis of the silicon response of the diatom *Thalassiosira pseudonana.* BMC Genomics 13: 499.

Shtaida N., KhozinGoldberg I. & Boussiba S. (2015). The role of pyruvate hub enzymes in supplying carbon precursors for fatty acid synthesis in photosynthetic microalgae. Photosynth. Res. 116.

Smith S.R., Abbriano R.M. & Hildebrand M. (2012). Comparative analysis of diatom genomes reveals substantial differences in the organization of carbon partitioning pathways. Algal Res. 1: 216.

Valenzuela J., Mazurie A., Carlson R.P., Gerlach R., Cooksey K.E., Peyton B.M. & Fields M.W. (2012). Potential role of multiple carbon fixation pathways during lipid accumulation in *Phaeodactylum tricornutum*. Biotechnol. Biofuels. 5: 40.

Part II

The impact of light and mycorrhizal endosymbiosis in secondary compound regulation of land plant (*Mentha* sp.)

Plants are nonmotile organisms that have to constantly deal with changes in a wide range of abiotic and biotic factors in their immediate environment on a seasonal as well as daily basis. Along evolution, plants have acquired several defense mechanisms to cope with modifications of their abiotic environment such as light and/or with modifications of their biotic environment such as the colonization of their root by a symbiotic fungus. Both types of stress can induce carbon metabolism reorientation.

To better understand the mechanisms underlying this phenomenon, I first collected mint accessions in different regions of Iran, including warm and cold climates and determined their ability to be mycorrhized in their natural environment (Chapter 5). Then the capacity of light intensity and quality to modify the growth, development and EO production of the collected accession was tested using growth chamber equipped with different LED panels or fluorescent tubes. A comparison with plants grown in the field was also performed (Chapter 7). To determine whether abiotic and biotic stress can be combined to enhance EO production, mycorrhized plants were grown under different monochromatic and white lights delivered by LED panel. The results are presented in chapter 8. Chapter 6, which reviews the effects of monochromatic irradiation on growth and reorientation of carbon metabolism toward the production of secondary compounds in land plants and algae, serves as introduction for chapters 7 and 8.

Chapter 4

Isoprenoid biosynthesis in higher plants and green algae under normal and light stress conditions

Parisa Heydarizadeh[a,b], Justine Marchand[a], Mohammad R. Sabzalian[b], Martine Bertrand[c] and Benoît Schoefs[a*]

[a] MicroMar, Mer Molécules Santé, LUNAM, IUMLFR 3473 CNRS, University of Le Mans, Le Mans, France
[b] Department of Agronomy and Plant Breeding, College of Agriculture, Isfahan University of Technology, Isfahan, Iran
[c] MiMeTox, Microorganisms Metals and Toxicity INTECHMER – CNAM, BP324, F50103 Cherbourg Cedex, France.

* Corresponding author
email: benoit.schoefs@univ-lemans.fr
Tel: +33 2 43 83 37 72
fax: +33 2 43 83 39 17

Handbook of Plant and Crop stress (2014). Pessarakli, M. (Ed.).

4.1 Abstract

The isoprenoids, also called terpenoids, encompass more than 40 000 structures and consist of the largest class of metabolites in photosynthetic organisms. In bacteria and higher plants, the isoprenoid building units are formed through two pathways: the mevalonate pathway, which is localized in the cytosol and operates through the participation of six key enzymes and the 2-C-methyl-D-erythritol-4-phosphate pathway, which is localized in plastids and requires eight consecutive enzymes. The mevalonate pathway in single cell organisms of green algae, such as *Chlorella*, *Scenedesmus* and *Trebouxia* has been lost. Sesquiterpenes, triterpenes and homoterpenes are synthesized *via* the mevalonate pathway, while carotenoids, phytol, chlorophyll side chain, gibberellins, lutein, essential oil and abscisic acid are synthesized *via* the 2-C-methyl-D-erythritol-4-phosphate pathway. Well-known isoprenoids including menthol and carotenoids are synthesized by condensation of the two active isoprenoid C_5-units: IPP and DMAPP. (-)-Menthol biosynthesis requires eight enzymatic steps and all of the genes from GPP to menthol have been identified and characterized, except for isopulegone isomerase. So far, more than 20 different carotenogenesis enzymes have been cloned

from various organisms. The genes for almost all the enzymes, from the early steps of the isoprenoid pathway to the predominant xanthophylls, have been cloned. Almost all of isoprenoids are important for ameliorating abiotic stresses. They may increase the tolerance of leaves to transiently high temperatures and may also quench ozone and ROS levels inside leaves. Stress conditions may shift significant increase or decrease in enzymes activity in each pathway. Menthofuran is considered a stress metabolite in menthol biosynthesis pathway, catalyzed by menthofuran synthase from pulegone. The level of menthofuran and pulegone should be reduced to improve essential oil quality. Lycopene is an important intermediate in carotenogenesis pathway. In addition, this pathway involves two key enzymes, phytoene synthase and β-carotene hydroxylase. Most of the enzymes and genes related to carotenogenesis pathway have been identified in cyanobacteria and higher plants, but some of them are not found especially in algal species. Increase in isoprenoids yield and improvement in their composition could be attained by transgenic manipulation and to reach to this goal, it is necessary to understand metabolite trafficking and secretion processes.

4.2 Abbreviations

DOXP	1-deoxy-D-xylulose 5-phosphate
MEP	2-C-methyl-D-erythritol-4-phosphate
CDPME	4-diphosphocytidyl-2-C-methylerythritol
CDPME2P	4-diphosphocytidyl-2-C-methyl-D-erythritol-2-phosphate
MEcPP	2-C-methyl-D-erythritol 2,4-cyclopyrophosphate
HMBPP	(E)-4-Hydroxy-3-methyl-but-2-enyl pyrophosphate
GA3P	glyceraldehyde-3-phosphate
DXS	DOXP synthase
DXR	DOXP reductoisomerase
CMS	CDP-ME synthase
CMK	CDP-ME kinase
MCS	ME-cPP synthase
HDS	HMBPP synthase
IDS	IPP/DMAPP synthase
IDI	Isopentenyl/dimethylallyl diphosphate isomerase
IPP	isopentenyl diphosphate
DMAPP	dimethylallyl diphosphate
GPP	geranyl diphosphate
FPP	farnesyl diphosphate
GGPP	geranylgeranyl diphosphate/pyrophosphate
AC	acetyl-CoA
AAC	acetoacetyl-CoA

HMGCoA	3-hydroxy-3-methyl-glutaryl-CoA
MVA	mevalonate
MVP	mevalonate-5-phosphate
MVPP	mevalonate-5-pyrophosphate
AACT	AAC thiolase
HMGS	HMG-CoA synthase
HMGR	HMG-CoA reductase
MVK	mevalonate kinase
PMK	phosphomevalonate kinase
MVD	mevalonate diphosphate decarboxylase
TPP	thiamine diphosphate

4.3 Introduction

Based on their function, plant metabolites are classified into two groups: (1) primary metabolites such as carbohydrates, sterols, carotenoids, growth regulators, the polyprenol substituents of dolichols, quinines, and proteins participating in nutrition and essential metabolic processes within the plants and (2) secondary metabolites including substances in chemical defenses against herbivores and pathogens, which influence on ecological interactions between plants and their environment (Chappell 1995, 2002; Croteau et al. 2000). Secondary metabolites of the isoprenoid group constitute the most diverse family of natural products present in all living organisms, which to date have more than 40,000 identified compounds (Bohlmann & Keeling 2008; Dudareva et al. 2013). In addition, this family of compounds constitutes the most abundant biogenic volatile organic compounds in plants. The rate of emission in these compounds is estimated to be more than 1×10^{12} kg per year and has important role in plant growth, development, and general metabolism (Croteau et al. 2000; Guenther et al. 2006; Bohlmann & Keeling, 2008; Xing et al. 2010). The isoprenoid compounds consist of hemiterpenes (C5; *e.g*. isoprene), monoterpenes (C10; *e.g*. menthol), sesquiterpenes (C15; *e.g*. farnesol, bisabolol), diterpenes (C20; *e.g*. camphorene, taxol, ginkgolides), triterpenes (C_{30}; *e.g*. oleandric acid), tetraterpenes (C_{40}; *e.g.* lutein, β-carotene and secondary carotenoids such as astaxanthin), and polyterpenes $(C5H8)_n$ (Lichtenthaler 2010). They may be lipophilic or hydrophilic, volatile or nonvolatile, cyclic or acyclic, and chiral or achiral (Bohlmann & Keeling 2008). They serve in a variety of different functions in basic and specialized metabolism and they have a variety of roles in mediating antagonistic and beneficial interactions among organisms. They protect many species of plants, animals, and microorganisms against predators, pathogens, competitors, and environmental stresses (Gershenzon & Dudareva, 2007; Lohr et al. 2012).

For many years, it was accepted that in all organisms, isoprenoids are synthesized through the MVA pathway, and a few years ago, an alternative pathway for the

biosynthesis of IPP (and DMAPP) was identified. This novel pathway, known as the MEP pathway, is widely distributed in nature and is present even in most eubacteria (Rodríguez-Concepción & Boronat, 2013). Depending on the biotic and abiotic stress factor(s), either the MVA or the MEP pathway contributes to the biosynthesis of specific isoprenoids (Lohr et al. 2012). Almost all biotic and abiotic stress factors are able to affect isoprenoid biosynthesis and emission. Because abiotic stresses inhibit photosynthesis and volatile isoprenoids are mainly formed by the carbon directly derived from photosynthetic carbon metabolism, a concurrent negative effect of abiotic stresses on photosynthesis and isoprenoids emission would be expected. However, abiotic stresses could also stimulate biosynthesis and emission of constitutive isoprenoids (Fineschi & Loreto, 2012). The primary aim of the present chapter is to review and compare the occurrence, variation, and function of isoprenoid and carotenoid biosynthesis pathways in higher plants and green algae species under normal and light-stressed conditions and finding the key genes and enzymes associated with their biosynthesis.

4.4 Biosynthesis of isoprenoids

4.4.1 Toward GPP Biosynthesis

Despite their diversity, isoprenoids derive from the condensation of the five-carbon compounds IPP and its allylic isomer, DMAPP (Mahmoud & Croteau, 2001; Vranová et al. 2013; Xiang et al. 2013). The biosynthesis of IPP was first investigated by Konrad Bloch and Feodor Lynen in 1958 using animals and yeast as models (Spurgeon & Porter, 1981; Lichtenthaler et al. 1997; Lichtenthaler 1999), indicating that IPP and DMAPP are biosynthetically derived from MVA, a six-carbon compound. Actually, MVA is a cytosolic pathway (Figure 4.1), which starts with three acetyl-CoA and produces IPP for sterols, triterpenes, sesquiterpenes, polyterpenes, dolichol, brassinosteroids, and isoprenyl groups (Sauret-Güeto et al. 2006; Gunatilaka 2012). This pathway operates through the participation of six key enzymes and requires three ATP and two NADPH molecules to reach to the end products, IPP and its isomer DMAPP (Lichtenthaler 2010). The related enzymes have been found in higher plants (Bach et al. 1999), animals (Rodwell et al. 2000), archaea, fungi (Lombard & Moreira, 2011), and bacteria (Miziorko 2011; Takaichi 2011). Despite the fact that terrestrial plants and green algae have a common evolutionary ancestry (Delaux et al. 2013), it is accepted that the MVA pathway is generally absent in the common ancestor, Chlorophyta. In higher plants and green algae, however, the pathway has not been fully identified yet in detail (Grauvogel & Petersen, 2007; Lohr et al. 2012).

In 1990s, an alternative MVA-independent pathway was detected by labeling experimental material using 13C-labeled glucose isotopomers in plants and bacteria (Flesch & Rohmer, 1988; Rohmer et al. 1993) and the first proof for the presence of MEP pathway was obtained (Schwarz & Arigoni, 1999; Zhao et al. 2013). This detection

demonstrated that there are two isoprenoid biosynthesis pathways in cyanobacteria, higher plants, several green algae (Chlorophyceae has only the MEP pathway), and some bacteria (Lichtenthaler et al. 1997; Zeidler et al. 1997; Lichtenthaler 1998, 1999, 2010; Disch et al. 1998). The two pathways are localized in different compartments: the classical acetate/MVA pathway is in the cytosol and the MEP pathway in plastids. The two pathways are linked through exchange of metabolic precursors across the plastid envelopes, and it has been demonstrated that the transport of isoprenoid constituents proceeds exclusively in the chloroplast-to-cytosol direction, the reverse direction occurring at extremely slow rates (Vickers et al. 2009; Lichtenthaler 2010).

The non-mevalonate pathway occurs in plastids and requires eight consecutive enzymes to produce IPP and DMAPP, universal basic blocks for isoprenoid biosynthesis. This pathway is initiated by a head-to-head condensation of GA-3P and pyruvate (carbon 2 and 3) to DOXP that is catalyzed by DXS and is already known as an intermediate not only for the biosynthesis of IPP and DMAPP but also for thiamin and pyridoxol biosynthesis (Julliard & Douce, 1991; Julliard 1992). The gene encoding DXS, *dxs*, have been isolated from *Escherichia coli* (Sprenger et al. 1997; Lois et al. 1998), *Chlamydomonas* (Lichtenthaler 1999), and various plant species including *Mentha piperita*, *Arabidopsis thaliana*, and *Catharanthus roseus* (Bouvier et al. 1998; Lange et al. 1998) but were absent in animals and yeast genomes (Rodríguez-Concepción & Boronat, 2002; Shanker Dubey et al. 2003). Actually, the DXS enzyme seems to be coded by two or three genes in *A. thaliana* (Araki et al. 2000), *Zea mays* (Cordoba et al. 2009, 2011), *Oryza sativa* (Kim et al. 2005), *Medicago truncatula* (Walter et al. 2000, 2002), *Ginkgo biloba* (Kim et al. 2006), and *Pinus densiflora* (Kim et al. 2009). The enzyme requires thiamine diphosphate and divalent cations such as Mg_2^+ or Mn_2^+ for its activity (Bouvier et al. 1998; Lange et al. 1998; Estévez et al. 2000; Lois et al. 2000; Shanker Dubey et al. 2003). Several experiments have reported that DXS plays a critical role in the synthesis of IPP and DMAPP (Lois et al. 2000; Gong et al. 2006; Morris et al. 2006).

Increasing or decreasing the level of different final isoprenoid products (between twofold and sevenfold) including chlorophyll, carotenoids, tocopherols, and ABA in transgenic plants expressing higher (overexpression) or lower (antisense) DXS levels supports the rate-limiting function of DXS enzyme in this pathway in plants and shows accumulation of numerous isoprenoid products in the cell (Lois et al. 2000; Estévez et al. 2001; Shanker Dubey et al. 2003; Gong et al. 2006; Morris et al. 2006).

In the second step of the pathway, DOXP is converted to MEP by DXR in the presence of NADPH. DXR is the key enzyme of the pathway and has also rate-limiting roles in IPP and DMAPP biosynthesis (Veau et al. 2000; Mahmoud & Croteau, 2001; Carretero-Paulet et al. 2006). In transgenic peppermint (*M. piperita*), overexpressing DXR led to an increase in essential oil monoterpenes in leaf tissues compared to the wild type (Mahmoud & Croteau, 2001; Shanker Dubey et al. 2003). The related gene, *ispC* (formerly designated *yaeM* or *dxr*), was first isolated from *E. coli* (Takahashi et al. 1998). Homologous proteins have been also reported from plants, algae, bacteria, and the protozoa, *Plasmodium falciparum* (Lange & Croteau, 1999a; Eisenreich et al. 2004;

Matsuzaki et al. 2008). The enzyme uses Mg_2^+ or Mn_2^+ as cofactor and is inhibited by fosmidomycin (FSM), an herbicidal substance that inhibits plant carotenoid, phytol, and isoprenoid biosynthesis (White 1978; Zeidler et al. 1998; Lange & Croteau, 1999a; Fellermeier et al. 1999; Lichtenthaler 2000; Eisenreich et al. 2004). The final result is the bleached phenotype and the failure of seedling establishment (Zeidler et al. 1998; Carretero-Paulet et al. 2002, 2006).

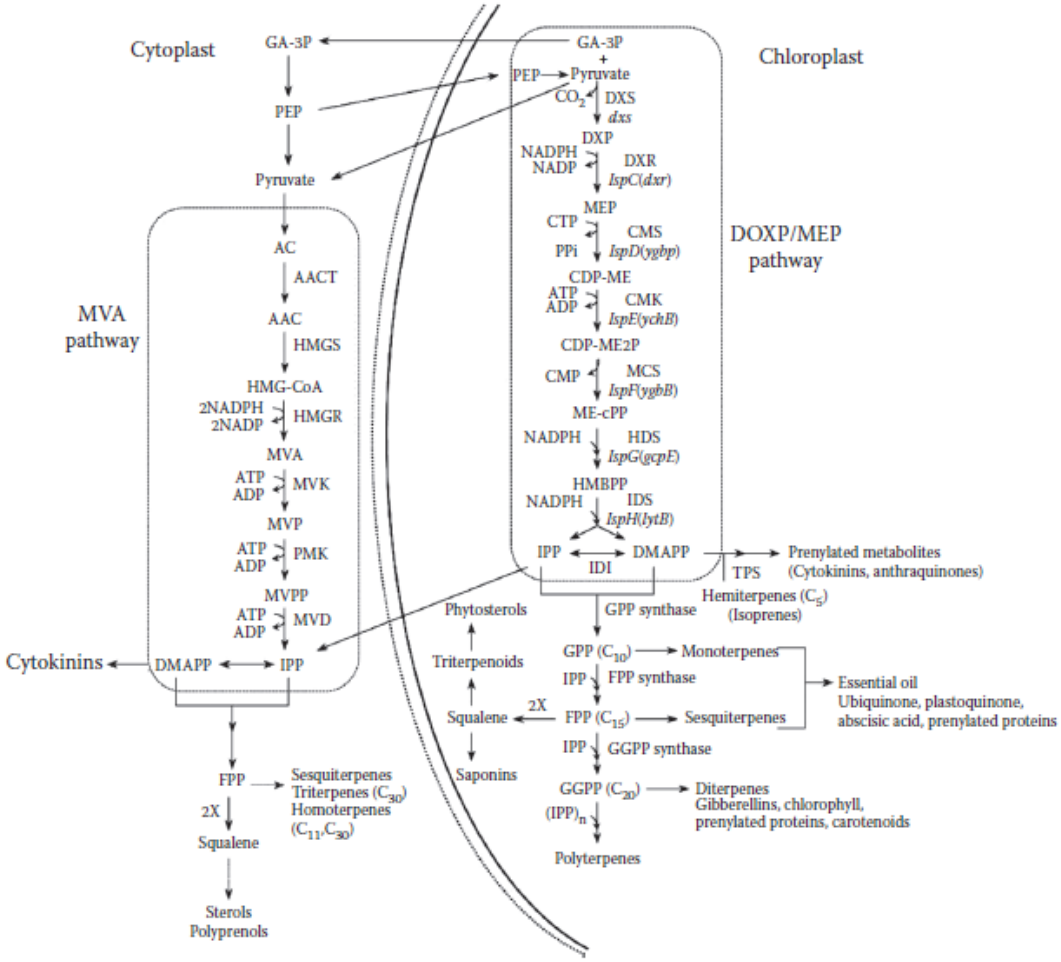

Figure 4.1. Metabolic pathways of the two independent isoprenoid biosynthesis pathways in the plant cell. (Adapted from Lichtenthaler, H.K., Annu. Rev. Plant Physiol. Plant Mol. Biol., 50, 47, 1999.)

Treatment of unicellular green alga, *Dunaliella salina*, with FSM resulted in the suppression of biosynthesis of C5 units, carotenoids, β-carotene, and chlorophyll. There is less information regarding whether the isoprenoid pathway in other algae can be influenced by selective inhibitors, such as mevinolin and FSM, or not (Paniagua-Michel et al. 2009).

The further step in the pathway contains the conversion of MEP to CDP-ME by CMS in the presence of cytidine triphosphate (CTP). The enzyme has essential role for IPP and DMAPP biosynthesis (Herz et al. 2000). The gene encoding the enzyme in *E. coli* was named *ygbP* and later was renamed as *ispD* (Eisenreich et al. 2004). In plants, the related gene was first cloned from *A. thaliana* (Rohdich et al. 2000a; Shanker Dubey et al. 2003). The similar enzyme in *E. coli* uses Mg_2^+, Mn_2^+, and CO_2^+ ions as cofactor, whereas the plant enzyme usually uses Ni_2^+ ions (Eisenreicha et al. 2004). In *Arabidopsis*, the enzyme requires a divalent cation, preferably Mg_2^+ (Rohdich et al. 2000a).

The next step of the pathway is the phosphorylation of the 2-hydroxyl group of CDP-ME into CDP-ME2P by the CMK enzyme in the presence of adenosine triphosphate (ATP). In isolated chromoplast of *Capsicum annuum*, 14C-labeled CDP-ME (the substrate for CMK) was efficiently converted into carotenoids, suggesting the possible role of the enzyme in carotenoid biosynthesis (Shanker Dubey et al. 2003). CMK requires Mg_2^+ as cofactor (Eisenreich et al. 2004).

The fifth step of the pathway is the formation of ME-cPP under the release of CMP. The reaction is catalyzed by MCS. The gene encoding such enzyme in *E. coli* was named *ygbB* (renamed as *ispF*) and has many putative orthologues in eubacteria as well as in *A. thaliana* (Herz et al. 2000), which require Mn_2^+ or Mg_2^+ as cofactor (Eisenreich et al. 2004). The sixth step in the pathway is the conversion of ME-cPP to HMBPP in the presence of NADPH (Rodríguez-Concepción & Boronat, 2002; Shanker Dubey et al. 2003) by the enzyme HDS (Rodríguez-Concepción & Boronat, 2002). The *E. coli* gene coding HDS annotated as *gcpE* (*ispG*) is conserved in plants, algae, and eubacteria but is absent in archaebacteria, yeast, and animal genomes (Rodríguez-Concepción & Boronat, 2002; Matsuzaki et al. 2008). The terminal step is the conversion of HMBPP into a 5:1 mixture of IPP and its isomer, DMAPP. The *lytB* gene (renamed as *ispH*) appears to encode the IDS (Rodríguez-Concepción et al. 2000, 2002) and causes the branching in which IPP and DMAPP are generated sequentially and this biochemical activity is an important difference between MVA and non-MVA pathways (Figure 4.1) (Charon et al. 2000; Rodríguez-Concepción et al. 2000, 2002).

In general, the chromosomal replacement study has revealed that in the MEP pathway, (1) the *dxs* gene has the highest impact among other isoprenoid genes on carotenoid production, (2) the *IPi* gene plays a significant role in the isoprenoid biosynthesis, (3) the *ispD* and *ispF* genes appear to form an operon, (4) CMS and MCS are rate-limiting enzymes in the isoprenoid flux, and (5) there are no rate limitations for *ispE*, *ispG*, and *ispH* genes (Das et al. 2007). In *Arabidopsis* and other plants (with some exceptions such as rubber trees), the transcript levels of all genes from the MEP pathway accumulate upon the exposure to light and during the development of the first true leaves of seedlings (Guevara-García et al. 2005; Hsieh et al. 2008). This positive regulation by light provides an advantage during early seedling development, which may elevate the demand for the photosynthetic pigments derived from the pathway (Schoefs et al. 1998; Cordoba et al. 2009).

A pivotal enzyme in monoterpene metabolism is GPPS, a member of the short-chain prenyl-transferase family catalyzing the head-to-tail condensation of one IPP and one DAMPP molecules to give rise to GPP. Supply of GPP is critical for terpenoid yield; therefore, studies on the regulation of genes in GPP biosynthesis assume central importance (Rohmer 1993; Croteau et al. 2005; Paniagua-Michel 2009; Clastre et al. 2011; Lohr et al. 2012; Paniagua-Michel et al. 2012). GGPPS is a central intermediate in the synthesis of plastidic isoprenoids such as monoterpenes and carotenoids. Other terpenes contain a 15-carbon and 20-carbon backbone synthesized by FPP synthase and GGPP synthase (GGPPS), yielding FPP and GGPP, respectively. FPP and GGPP are key substrates for several important branch-point enzymes. In plants, FPP and GGPP are required for the first committed step in the biosynthesis of sesquiterpenes and diterpenes, respectively. Geranylgeranyl diphosphate synthase catalyzes the condensation of three molecules of IPP and one molecule of DMAPP to produce GGPP, a 20-carbon molecule in the carotenoid pathway. Pairwise condensation of FPP and GGPP provides triisoprenoid (C_{30}) and tetraisoprenoid (C_{40}) biosynthesis. On the other hand, assembly of an undefined number of C5 precursors yields polyisoprenoids (Bohlmann & Keeling, 2008; Gonzales-Vigil et al. 2012). In land plants and green algae, collectively termed Viridiplantae (Latin name for *green plants*), currently, it is clear that the biosynthesis of monoterpenes appears to be localized in plastids. In recent years, our understanding of the numerous facets of isoprenoid metabolism in land plants has been rapidly increasing, while knowledge on the metabolic network of isoprenoids in algae still lags behind (Lohr et al. 2012).

4.4.2 From GPP to menthol biosynthesis

Terrestrial plants and marine algae produce a variety of secondary metabolites, including monoterpenes. The algal monoterpenes present several highly unusual characteristics, nearly always halogenated, and they possess ring structures quite unusual. There are a few reports suggesting monoterpene emission in algae, and a limited number of field studies suggest that these compounds play a role in the defense of marine algae (Bonsang et al. 1992; Milne et al. 1995; McKay et al. 1996; Wise 2003). Yassaa et al. (2008) have provided the first evidence for marine production of monoterpenes in nine algae species consisting of coccolithophorids, *Emiliania huxleyi*; diatoms, *Chaetoceros neogracilis*, *Chaetoceros debilis*, *Fragilariopsis kerguelensis*, *Phaeodactylum tricornutum*, and *Skeletonema costatum*; chlorophyte, *D. tertiolecta*; and cyanobacteria, *Synechococcus* and *Trichodesmium*. Among the phytoplanktons sampled, green algae species, *D. tertiolecta*, was the strongest emitter of monoterpenes followed by *P. tricornutum*, and nine monoterpenes were identified, namely, (−)-/(+)-pinene, myrcene, (+)-camphene, (−)-sabinene, (+)-3-carene, (−)-pinene, (−)-limonene, and p-ocimene. So far, it is not known that emissions by algal cells are a response to biotic (*e.g.* defense against predation) or abiotic (*e.g*. temperature, injury) stresses (Yassaa et al. 2008).

In many types of terrestrial plants, monoisoprenoids are the primary volatile constituents of the essential oils. In the genus *Mentha*, the peppermint (*M. piperita* L.) produces almost exclusively monoterpenes bearing an oxygen function at position C_3 such as (−)- or l-menthol, whereas spearmint types such as native spearmint (*M. spicata* L.) and Scotch spearmint (*M. gentilis* var. *cardiaca*) produce almost exclusively monoterpenes bearing an oxygen function at position C6, typified by carvone (Lawrence 1981). The biosynthesis of (−)-menthol has been studied by Croteau and coworkers for more than two decades, and the results were used as a model for biochemical and molecular genetic characterization of monoisoprenoid and essential oil biosynthesis (Croteau et al. 2005). Recently, the main and characteristic component of *M. piperita* essential oil, the monoisoprenoid (−)-menthol, was investigated, and cDNAs have been identified and characterized for all enzymes from GPP to (−)-menthol (Figure 4.2), except for isopulegone isomerase (Turner et al. 2012).

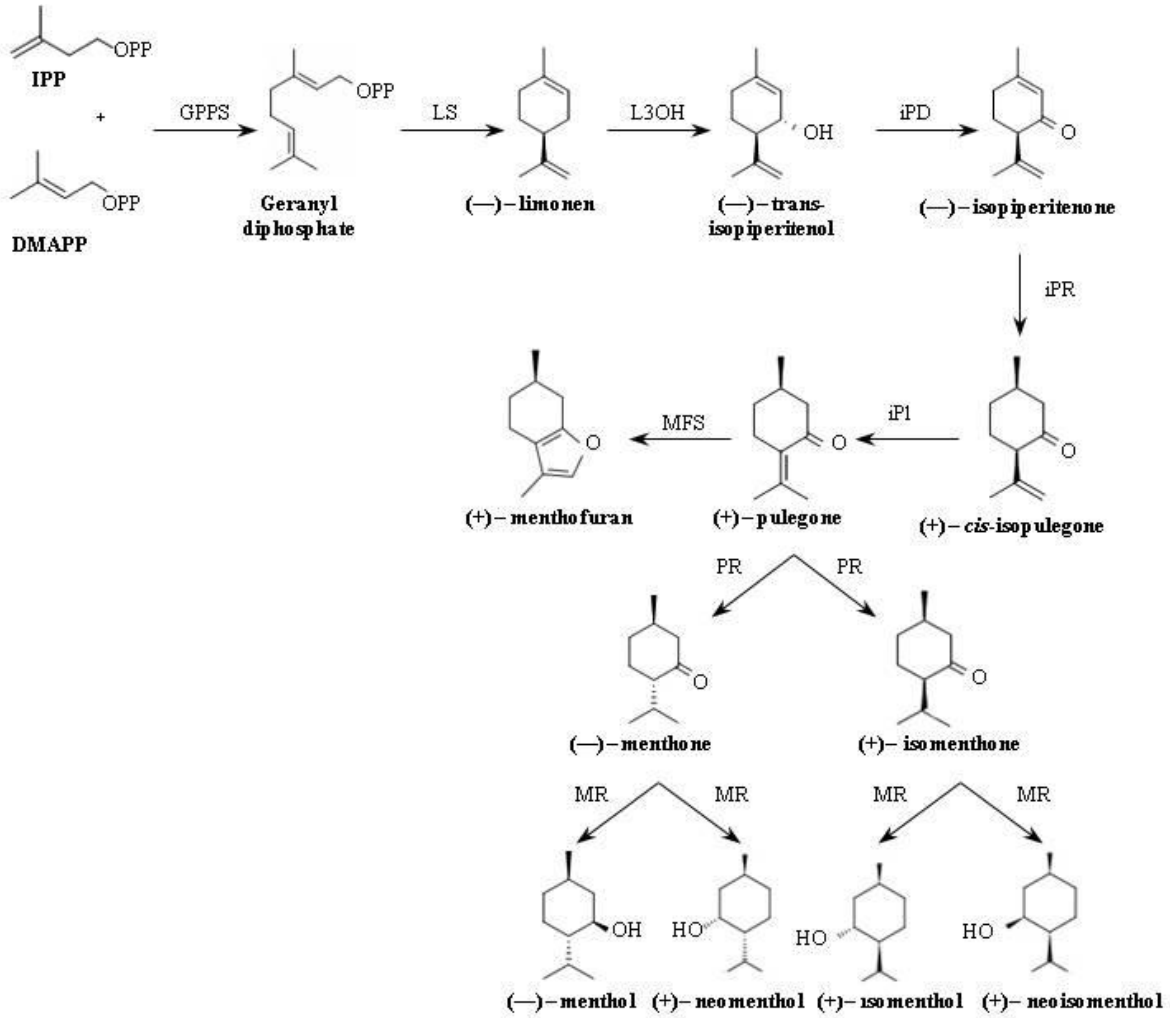

Figure 4.2. Metabolic pathway leading to the synthesis of (−)-menthol and related monoisoprenoids in *Mentha*.

The biosynthesis of (−)-menthol from primary metabolism requires eight enzymatic steps and proceeds from GPP. The first committed reaction catalyzes the cyclization of GPP to (−)-limonene by the first committed enzyme of the pathway, (−)-LS, a typical monoterpene cyclase. (−)-Limonene serves as olefinic precursor of essential oil terpenes of both peppermint and spearmint. The subsequent step, (−)-L3OH, using O_2 and NADPH, catalyzes the allylic hydroxylation of (−)-limonene at the three positions to form (−)-*trans*-isopiperitenol. Biosynthetic investigations have demonstrated that (−)-limonene undergoes cytochrome-mediated hydroxylation at C_3 to yield (−)-*trans*-isopiperitenol (peppermint) or at C6 to yield (−)-*trans*-carveol (spearmint) (Lupien et al. 1999). Typically, carvone accumulates in spearmint and superior oils of peppermint containing high quantities of menthol, moderate amounts of menthone, and low levels of pulegone and menthofuran. The remaining enzymes responsible for the subsequent redox transformations of isopiperitenol to menthol is present in both peppermint and spearmint species; however, carveol is a poor substrate in these processes (Croteau et al. 1991). In a study by Mahmoud et al. (2004), overexpression of *L3OH* gene resulted in a substantial increase in the limonene content (up to 80% of the essential oil compared to about 2% of the oil in wild-type peppermint) in the essential oil, without influence on oil yield,but simultaneously resulted in a decrease in (−)-menthol yield. According to this result, limonene does not impose a negative feedback suggesting that pathway engineering can be employed to significantly alter essential oil composition without adverse metabolic consequences in peppermint.

For the next step of the pathway, (−)-*trans*-isopiperitenol is converted to (−)-isopiperitenone by (−)-*trans*-isopiperitenol dehydrogenase (iPD) that oxidizes the hydroxyl group on the three positions using NAD^+ followed by (−)-isopiperitenone reductase (iPR) that catalyzes the reaction with reduction of the double bond between carbons 1 and 2 using NADPH to form (+)-*cis*-isopulegone. It has been reported that (+)-*cis*-isopulegone is the key intermediate in the conversion of (−)-isopiperitenone to (+)-pulegone (Park et al. 1993).

The next step of the pathway is isomerization of the remaining double bond to form (+)-pulegone by (+)-*cis*-iPI and then (+)-PR (isopiperitenone reductase) reduces this double bond using NADPH to form (−)-menthone. At the terminal step of the pathway, (−)-MR (menthone reductase) reduces the carbonyl group using NADPH to form (−)-menthol and (+)-neoisomenthol by (−)-MMR (menthone-menthol reductase) and to (+)-neomenthol and (+)-isomenthol by (−)-MNR (menthone-neomenthol reductase). The latter three monoterpenol isomers are minor constituents of peppermint oil (Croteau et al. 2005). The related enzymes are localized in different parts of the cell. GPPS and LS are localized in the leucoplasts (Turner et al. 1999, Turner and Croteau 2004), limonene 6-hydroxylase (of spearmint) is localized in the endoplasmic reticulum, iPD is found to be mitochondrial, and PR is localized in the cytosol (Turner and Croteau 2004). Both MMR and iPR are also localized in the cytoplasm and nucleoplasm of the secretory cells of peltate glandular trichomes (Turner et al. 2012). There is possibility to alter the composition and volume production of monoterpene and essential oil quality through

transgenic manipulations (Mahmoud & Croteau, 2001, 2003; Croteau et al. 2005; Wildung & Croteau, 2005; Bohlmann & Keeling, 2008).

4.4.3 Carotenoids

Carotenoids are C_{40} natural fat-soluble, yellow, orange, or sometimes red, isoprenoid pigments and essential components of the photosynthetic apparatus that serve two functions: light harvesting (accessory pigments) or photoprotection of the chlorophyll *a* molecules in the photosynthetic reaction centers against photo oxidation (Lichtenthaler 2012; Ruiz-Sola & Rodríguez-Concepción, 2012; Xiumin et al. 2012). There are over 750 known structurally defined carotenes that have been identified so far. Carotenoids are also formed in several non-green and nonphotosynthetic organisms, such as yeast, bacteria, and molds, to protect them against damage by light and oxygen (Lichtenthaler 2012; Ruiz-Sola & Rodríguez-Concepción, 2012). They can be synthesized from carotenoid pathway by most organisms except for the animal kingdom that are generally unable to synthesis the components (Moran & Jarvik, 2010; Takaichi, 2011; Lichtenthaler 2012). So far, little is known about the mechanisms that regulate carotenoid biosynthesis (Meier et al. 2011). High carotenoid levels are found in the chloroplasts of photosynthetic tissues, but the highest amounts of carotenoids are found in chromoplasts. Besides chromoplasts, all other plastid types synthesize carotenoids but the level of carotenoid accumulation varies widely among different plastid types (Ruiz-Sola & Rodríguez-Concepción, 2012). Unlike chromoplasts that show highly diverse carotenoids, depending on the organ, species, and genetic variely, chloroplasts have a remarkably similar carotenoid composition in all plants, with lutein (45% of the total), β-carotene (25%–30%), violaxanthin (10%–15%), and neoxanthin (10%–15%) as the most abundant carotenoids (Britton 1993). Photosynthetic reaction centers are enriched in carotene (β-carotene), whereas xanthophylls are most abundant in the light-harvesting processes (Ruiz-Sola & Rodríguez-Concepción, 2012).

Many different types of carotenoids are extracted from higher plants and algal species. The largest structural variety of carotenoids is encountered in marine environments produced by microscopic and macroscopic algae (Liaaen-Jensen 1991; Mimouni et al. 2012). Approximately, 30 types of carotenoids participate in photosynthesis (*primary carotenoids*) and others are functional carotenogenesis intermediates (*secondary carotenoids*).

4.4.4 From GPP to secondary carotenoids

The main carotenoid biosynthetic pathway was elucidated in the latter half of the twentieth century using biochemical (from the 1960s) and molecular (from the 1980s) approaches. Major advances in the identification of genes and enzymes of the pathway have been made from the 1990s (Ruiz-Sola & Rodríguez-Concepción, 2012). In

terrestrial plants, most of the carotenogenesis pathways and functionally related enzymes are known, but little is known among algae (Takaichi 2011).

In the large group of green algae, the carotenoid biosynthesis is more complex. Like higher plants, the more advanced evolutionary group of green algae, such as *Charales* and *Zygnematales*, possesses both MVA and MEP pathways. In contrast, often single-cell organisms of green algae, such as *Chlorella*, *Scenedesmus*, and *Trebouxia*, represent carotenoid and sterol biosynthesis *via* the MEP pathway, and the MVA pathway is lost (Lichtenthaler 2010). Despite the importance of these taxa, *Haematococcus pluvialis* (astaxanthin biosynthesis) and *Dunaliella* sp. (β-carotene biosynthesis), for the commercial production, most of the studies on secondary carotenoid pathway have been performed by these organisms (Das et al. 2007; Lemoine & Schoefs, 2010; Moulin et al. 2010).

The first committed step in carotenoid biosynthesis is a head-to-head condensation of the two C20 molecules of GGPP by phytoene synthase (PSY) (CrtB, Psy, Pys) to form phytoene (Figure 4.1). GGPP is also the precursor for several other groups of metabolites, including chlorophyll and tocopherol. PSY is a major rate-controlling carotenoid enzyme at unknown plastid sites, either in plastoglobuli or in stroma and thylakoid membranes (Shumskaya et al. 2012). The green algae *Ostreococcus* and *Micromonas* possess two orthologous copies of the PSY genes, possibly indicating an ancient gene duplication event. In contrast, higher plants possess only one class of the PSY gene and the other gene copy is lost (Tran et al. 2009). For the next step in the pathway, phytoene undergoes four sequential reactions to form lycopene (Farré et al. 2010; Walter & Strack, 2011). This route requires three enzymes including phytoene desaturase (PDS) (CrtP, Pds), ζ-carotene desaturase (CrtQ, Zds), and *cis*-carotene isomerase (CrtH, CrtISO). In higher plants and green algae, α-carotene, β-carotene, and their derivatives are derived from lycopene (Figure 4.3).

In the next step, the carotenoid pathway has branches at the cyclization reaction to produce carotenoids with either two β-rings (such as β-carotene and its derivatives) or one ε- and one β-ring (such as α-carotene and lutein) (Figure 4.3). Inability of the lycopene ε-cyclase enzyme (LCYe) to add two ε-rings to the symmetrical lycopene is the cause of the absence of a branch leading to carotenoids with two ε-rings in most plants (except lettuce) (Cunningham 2002). Plants contain two CrtL lycopene cyclases (LCYs), lycopene ε-cyclase (CrtL-e, LCYe) and lycopene β-cyclase (CrtL-b, LCYB), that form enzymatic products of α-carotene and β-carotene. Lutein and zeaxanthin are generated by the hydroxylation of these two carotenoids, respectively. Their function is light harvesting within the antenna of photosystems I and II (PSI and PSII) (Sheen 1991; Bradbury et al. 2012).

In the absence of stress, hydroxyl groups are introduced into β-carotene to produce zeaxanthin by β-carotene hydrolase (CrtR, CrtR-b, BCH), and zeaxanthin epoxidase (Zep, NPQ) is responsible for producing violaxanthin through antheraxanthin, in both higher plants and algae. Epoxidases, such as violaxanthin and zeaxanthin, are more common among algal carotenoids (Liaaen-Jensen 1991). The first Zep cDNA was identified from

tobacco (*Nicotiana plumbaginifolia*) and was named as ABA2 (Marin et al. 1996). Under light stress and with the development of a high-pH gradient across the thylakoids, the reaction is different, and the two steps of mono-de-epoxidation reactions of the violaxanthin into zeaxanthin with antheraxanthin as an intermediate are catalyzed by violaxanthin de-epoxidase (Vde) in order to dissipate the excess energy in the form of heat from excited chlorophylls (Takaichi 2011). The first sequenced cDNA of Vde was obtained from romaine lettuce (*Lactuca sativa* L.), and the homologous genes were sequenced in the genome of diatoms *Thalassiosira pseudonana* and *P. tricornutum*. So far, most of the carotenogenesis enzymes and genes have been found in cyanobacteria (Takaichi & Mochimaru, 2007), diatoms (Bertrand 2010), green algae (Lemoine & Schoefs, 2010; Moulin et al. 2010), and higher plants (Frommolt et al. 2008); however, in algal species, some of them have not been found yet (Takaichi 2011). It seems that higher plants and algae have common carotenogenesis pathways, and all of the enzymes and genes related to this pathway are presented in Table 4.1 (for confirmed genes and enzymes in cyanobacteria and algae, see Takaichi 2011). No counterpart of the neoxanthin synthase (*Nsy*) was reported in *A. thaliana* (Cunningham 2002).

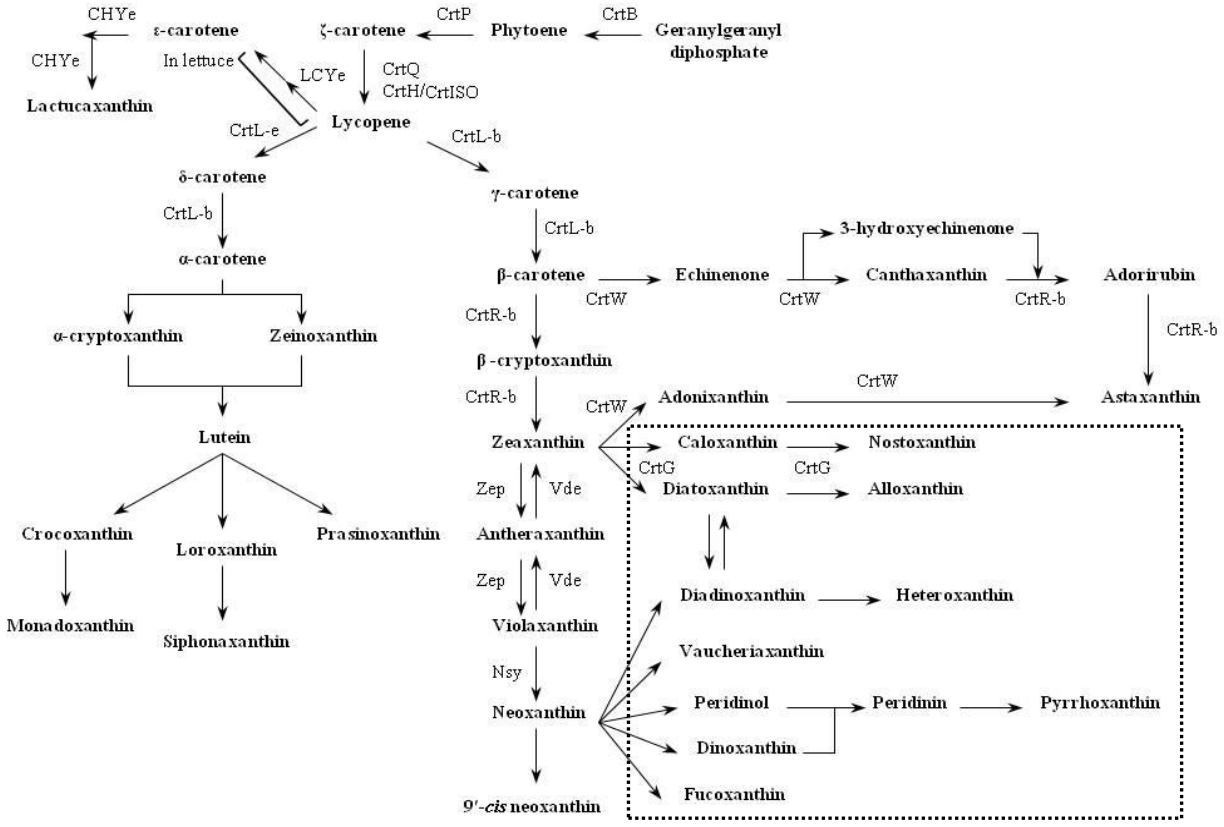

Figure 4.3. Carotenogenesis scheme and confirmed enzymes in higher plants and green algae. The dashed part of graph could be synthesized only in some algae.

Major carotenoids in most species of the class of the green algae, Chlorophyta (Prasinophyceae, Chlorophyceae, Ulvophyceae, Trebouxiophyceae, Charophyceae), and land plants consist of β-carotene, violaxanthin, and neoxanthin (Takaichi 2011). Some carotenoids are found only in some classes or divisions of higher plants and algae, and for this reason, they are used as chemotaxonomic markers (Rowan 1989; Liaaen-Jensen 1990). In this respect, green algae including Euglenophyta, Chlorarachniophyta, and Chlorophyta contain the same carotenoids, such as lutein, β-carotene, 9-*cis* neoxanthin, and violaxanthin (Takaichi 2011). For comparison, tomato (*Lycopersicon esculentum* Mill.) contains prolycopene, ζ-carotene, β-carotene, or δ-carotene, and carrot (*Daucus carota* L.) contains xanthophylls, ζ-carotene, β-carotene, δ-carotene, and lycopene (MacKinney & Jenkins, 1949; Buishand & Gabelman, 1980; Ronen et al. 2000).

Carotenoid content pattern can change during the life cycle of plants and algae. The unicellular green alga *H. pluvialis*, the most suitable source of astaxanthin (of the most important diterpenes), accumulates this antioxidant (up to 4% by dry weight) in response to various environmental stress conditions such as high light intensities, nitrogen limitation, and salt stress in extraplastidic lipid globules as a secondary carotenoids (Boussiba et al. 1999; Boussiba 2000; Grünewald et al. 2001; Schoefs et al. 2001; Lemoine & Schoefs, 2010; Moulin et al. 2010). The massive accumulation of astaxanthin occurs during cyst cell formation, whereas in green vegetative phase and without stress condition, zeaxanthin accumulation occurs (Vidhyavathi et al. 2008). In red pepper (*Ca. annuum* L.) when ripening is started, chloroplast pigments, lutein, and neoxanthin are decreased, whereas β-carotene and antheraxanthin are increased (Hornero-Mendez et al. 2000).

4.5 Isoprenoid protection against diverse stresses

Almost all of isoprenoids have the ability to increase the tolerance of leaves to transiently high temperatures and light stress, and they may also quench ozone and ROS levels inside the leaves (Loreto & Velikova, 2001; Sharkey et al. 2001; Behnke et al. 2007; Loreto & Fares, 2007; Vickers et al. 2009; Lohr et al. 2012). They also reduce the formation of nitric oxide in the mesophyll and could modulate the signaling of defense-induced biosynthetic pathways (Velikova et al. 2005). Among the 100,000 chemical products that are known to be produced by plants, at least 1700 of these are known to be volatile isoprenoids. Two of the most important functions of volatile isoprenoids are protections of plant tissues from thermal and oxidative stresses (Behnke et al. 2007; Loivamäki et al. 2007; Spinelli et al. 2011). There are key dissipation processes and mechanisms for the resistance to excess energy and the other environmental stresses, which are mediated by a particular group of carotenoids. Monoterpene emission is equivalent to 1%–2% of photosynthetic carbon fixation (Sharkey & Yeh, 2001). Some enzymes positioned at key points in metabolic pathways are ideal candidates for regulation, as their activity can affect the output of the entire pathways. These enzymes typically share two characteristics: they catalyze (1) reactions far from equilibrium and

(2) early committed steps in the pathways. For instance, in menthol pathway and during stressful conditions, an important diversion from the pathway to menthol is the transformation of (+)-pulegone to menthofuran catalyzed by menthofuran synthase (MFS), and because of this, it is considered as a *stress metabolite* (Croteau et al. 2005). Together, menthofuran and (+)-pulegone are described as an *off* odor and accumulate to high levels (15%–20% of the oil) under stress conditions (Croteau et al. 2005; Rios-Estepa et al. 2008). Some carotenoids play similar role(s) during the stress.

4.5.1 Light stress

Menthol and carotenoid biosynthesis involve a series of enzymes that mainly starts from MEP pathway and each alteration in the pathway flux should be observable at the level of products (Mahmoud & Croteau, 2001; Paniagua-Michel et al. 2012). Comparative expression analysis of the MEP pathway genes under various growing conditions shows that transcript accumulation of these genes in plants is modulated by multiple external signals and in a coordinated manner. One signal that impacts strongly the transcript accumulation of several genes in the MEP pathways is light (Cordoba et al. 2009). Studies show that light stress can increase expression of some genes in MEP pathway. For instance, *dxs* is more expressed under light stress (Kawoosa et al. 2010; Meier et al. 2011). UV-B irradiation may induce upregulation of *dxs*, *gpps*, *fpps*, and *Ipi* genes that are necessary for menthol and carotenoid biosynthesis (Dolzhenko et al. 2010; Lemoine & Schoefs, 2010). Vidhyavathi et al. (2008) also reported that the expression of carotenogenic genes, *PSY*, *PDS*, *LCY*, β-carotene ketolase (*BKT*), and β-carotene hydroxylase (*CHY*) were upregulated in green algae, *H. pluvialis*, under nutrient stress and higher light intensity, and astaxanthin content as a stress metabolite was increased. It is also believed that most plants respond to high light conditions with a 1.4–2-fold increase of xanthophyll cycle carotenoids (violaxanthin, zeaxanthin, neoxanthin), an enhanced operation of the xanthophyll cycle, and an increase of β-carotene levels (Lichtenthaler 2007; Lemoine & Schoefs, 2010).

4.5.1.1 Light stress and menthol biosynthesis

Light quality is an important factor for essential oil production. Menthol biosynthesis in peppermint can be decreased by supplementary blue light (450 nm) because of shifting the carbon flow to (+)-menthofuran production (Maffei & Scannerini, 1999). In addition to visible light, one of the unavoidable stress factors in natural condition of photosynthetic organisms is the exposure to UV-B radiation (280–320 nm). However, isoprenoid production is induced by UV radiation, but not always supplementary UV-B leads to increased isoprenoid production (Dolzhenko et al. 2010). Maffei and Scannerini (2000) reported that additional UV-B light has negative effect on essential oil quality with positive effect on high amounts of (+)-menthofuran. In addition, UV-A radiation (360 nm) affects the composition of peppermint oil by increasing (+)-menthofuran

Table 4.1. Enzymes and genes related to isoprenoid pathways (MEP, menthol biosynthesis, carotenogenesis) whose functions have been confirmed in higher plants and green algae (continued).

pathway	Enzyme name	Gene/ Synonm genes	Plant species	references	Green algae species	references
MEP	DOXP synthase (DXS)	*dxs*	*A.rabidopsis thaliana*	Araki et al (2000), Estévez et al (2000)	*Botryococcus braunii*	Daisuke et al (2012)
			Mentha piperita	Lange et al (1998)	*Dunaliella* sp	Hermin Pancasakti (2008)
			Medicago truncatula	Walter et al (2002)	*Ostreococcus lucimarinus*	Matsuzaki et al (2008)
			Capsicum annuum	Bouvier et al (1998)	*Chlamydomonas reinhardtii*	Matsuzaki et al (2008)
			Catharanthus roseus	Chahed et al (2000)	*Ostreococcus tauri*	Frommolt et al (2008)
			Lycopersicon esculentum	Lois et al (2000)	*Volvov carteri*	Frommolt et al (2008)
			Oryza sativa	Matsuzaki et al (2008)		
			Picea abies	Phillips et al (2007)		
			Zea mays	Walter et al (2000)		
			Ginkgo biloba	Kim et al 2006		
MEP	DOXP reductoisomerase (DXR)	*ispC (dxr)*	*Arabidopsis thaliana*	Carretero-Paulet et al (2002), Schwender et al (1999)	*Ostreococcus lucimarinus*	Matsuzaki et al (2008)
			Mentha piperita	Lange & Croteau (1999a), Mahmoud and Croteau (2001)	*Ostreococcus tauri*	Frommolt et al (2008)
			Oryza sativa	Matsuzaki et al (2008)	*Chlamydomonas reinhardtii*	Matsuzaki et al (2008)
			Hevea brasiliensis		*Volvov carteri*	Frommolt et al (2008)
MEP	CDP-ME synthase (CMS)	*ispD (ygbP)*	*Arabidopsis thaliana*	Rohdich et al (2000a)	*Ostreococcus lucimarinus*	Matsuzaki et al (2008)
			Capsicum	Luttgen et al (2000)	*Ostreococcus tauri*	Frommolt et al (2008)

			annuum			
			Oryza sativa	Matsuzaki et al (2008)	*Chlamydomonas reinhardtii*	Matsuzaki et al (2008)
					Volvox carteri	Frommolt et al (2008)
MEP	CDP-ME kinase (CMK)	*ispE (ychB)*	*Mentha piperita*	Lange & Croteau (1999b)	*Ostreococcus lucimarinus*	Matsuzaki et al (2008)
			Arabidopsis thaliana	Frommolt et al (2008)	*Ostreococcus tauri*	Frommolt et al (2008)
			Lycopersicon esculentum	Rohdich et al (2000b)	*Chlamydomonas reinhardtii*	Matsuzaki et al (2008)
			Oryza sativa	Matsuzaki et al (2008)	*Volvox carteri*	Frommolt et al (2008)
			Triticum aestivum	Frommolt et al (2008)		
			Hordeum vulgare	Frommolt et al (2008)		
			Populous trichocarpa	Frommolt et al (2008)		
MEP	ME-CP synthase (MCS)	*ispF (ygbB), MDS*	*Mentha ×piperita*	Dolzhenko et al (2010)	*Ostreococcus lucimarinus*	Matsuzaki et al (2008)
			Catharanthus roseus	Veau et al (2000)	*Ostreococcus tauri*	Frommolt et al (2008)
			Capsicum annuum	Fellermeier et al (2001), Herz et al (2000)	*Chlamydomonas reinhardtii*	Matsuzaki et al (2008)
			Narcissus pseudonarcissus	Fellermeier et al (1999)		
			Oryza sativa	Matsuzaki et al (2008)		
MEP	HMBPP synthase (HDS)	*ispG (gcpE)*	*Arabidopsis thaliana*	Hecht et al (2001)	*Ostreococcus lucimarinus*	Matsuzaki et al (2008)
			Oryza sativa	Matsuzaki et al (2008)	*Chlamydomonas reinhardtii*	Matsuzaki et al (2008)
MEP	HMBPP reductase (IDS/HDR)	*ispH (lytB)*	*Capsicum annuum*	Adam et al (2002)	*Ostreococcus lucimarinus*	Matsuzaki et al (2008)
			Oryza sativa	Matsuzaki et al (2008)		
			Ginkgo biloba	Kim et al (2008)		
			Pinus taeda	Kim et al (2008)		
MEP	Isopentenyl	*IPi*	*Arabidopsis*	Cunningham (2002)	*Chlamydomonas*	Frommolt et al (2008)

	diphosphate isomerase (IDI)		*thaliana*		*reinhardtii*	
					Ostreococcus lucimarinus	Frommolt et al (2008)
					Ostreococcus tauri	Frommolt et al (2008)
Menthol biosynthesis	(-)-limonene synthase	*LS/LC, TPS, FES*	*Menthe spicata, Mentha×piperita*	Colby et al (1993), Alonso et al (1992)		
			Arabidopsis thaliana, Picea abies	Bohlmann et al (2000), Martin et al (2004)		
			Ocimum basilicum	Iijima et al (2004)		
Menthol biosynthesi	(-)-limonene-3-hydroxylase	*L3OH, ER, PM, GI*	*Menthe spicata, Menth ×piperita*	*Turner & Croteau (2004)*		
			Mentha×piperita	Lupien et al (1999)		
			Perilla frutescens	Mau et al (2010)		
Menthol biosynthesi	(-)-*transe* isopiperitenol dehydrogenase	*IPD/ISPD*	*Mentha×piperita, M. spicata*	*Turner & Croteau (2004),* Ringer et al (2005)		
Menthol biosynthesi	(-)-isopiperitenone reductase	*ISPR*	*Mentha×piperita, M.spicata*	Ringer et al (2003, 2005)		
			Arabidopsis thaliana	Ringer et al (2005)		
Menthol biosynthesi	(+)-*cis* isopulegone isomerase	*IPL*	*Mentha×piperita*	Bohlmann & Keeling (2008)		
Menthol biosynthesi	(+)-menthofuran synthesis	*MFS*	*Mentha×piperita*	*Mahmoud &Croteau (2003)*		
Menthol biosynthesi	(+)pulegone reductase	*PR*	*Mentha×piperita*	Ringer et al (2003)		
Menthol biosynthesi	(-)-menthone reductase	*MR, MMR, MNR*	*Mentha×piperita, M. spicata*	Bohlmann & Keeling (2008), Davis et al (2005), Ringer et al (2005)		
			Arabidopsis thaliana	Ringer et al (2005)		
carotenogenesis	Geranylgeranyl	*CrtE, ggps*	*Arabidopsis*	Cunningham (2002)		

	pyrophosphate synthase		*thaliana*			
carotenogenesis	Phytoene synthase	*PSY, PYS, crtB*	*Arabidopsis thaliana*	Frommolt et al (2008)	*Chlamydomonas reinhardtii*	McCarthy et al (2004)
			Triticum aestivum	Frommolt et al (2008)	*Haematococcus pluvialis* NIES-144	Steinbrenner & Linden (2003)
			Hordeum vulgare	Frommolt et al (2008)	*Ostreococcus lucimarinus*	Frommolt et al (2008)
			Populous trichocarpa	Frommolt et al (2008)	*Ostreococcus tauri*	Frommolt et al (2008)
			Lycopersicon esculentum	Frommolt et al (2008)	*Volvov carteri*	Frommolt et al (2008)
			Oryza sativa	Frommolt et al (2008)		
carotenogenesis	Phytoene desaturase	*PDS, crtP, CRTI*	*Arabidopsis thaliana*	Cunningham (2002	*Chlamydomonas reinhardtii*	Vila et al (2008)
			Lycopersicon esculentum Mill.	Cunningham (2002	*Chlorella zofingiensis* ATCC 30412	Liu et al (2010)
					Haematococcus pluvialis (SAG 19-a)	Vidhyavathi et al (2008)
carotenogenesis	ζ-carotene desaturase	*ZDS, crtQ*	*Arabidopsis thaliana*	Cunningham (2002		
			Zea mays	Isaacson (2004)		
carotenogenesis	Lycopene β-cyclase	*CrtL-b, crtL, lcy-b*	*Solanum lycopersicum*	Ronen et al (1999)		
			Arabidopsis thaliana	Cunningham (2002	*Dunaliella salina* CCAP 19/30	Ramos et al (2008)
					Haematococcus pluvialis NIES-144	Steinbrenner & Linden (2003)
carotenogenesis	Carotene isomerase	*CrtH/CrtISO*	*Arabidopsis thaliana*	Cunningham (2002		
carotenogenesis	Lycopene ε-cyclase	*CrtL-e, LCYe*	*Solanum lycopersicum*	Ronen et al (1999)		
			Arabidopsis thaliana	Fiore et al (2012)		
			Lactuca sativa romaine	*Cunningham & Gantt (2001)*		

carotenogenesis	β-carotene hydroxylase	*CrtR-b,CrtR, BCH, CHY, CHYB*	*Arabidopsis thaliana*	Cunningham (2002	*Haematococcus pluvialis* NIES-144	Lindeh (1999), Steinbrenner & Linden (2001)
carotenogenesis	β-carotene ketolase	*CrtW, BKT*			*Haematococcus pluvialis* NIES-144	Steinbrenner & Linden (2001)
					Haematococcus pluvialis strain 34/7	Lotan & Hirschberg (1995)
					Chlorella zofingiensis ATCC 30412	Huang et al (2006)
carotenogenesis	Zeaxanthin epoxidase	*Zep, npq, ABA*	*Arabidopsis thaliana*	Cunningham (2002	*Chlamydomonas reinhardti*i	Baroli et al (2003)
			Nicotiana plumbaginifolia	Marin et al 1996	*Ostreococcus lucimarinus*	Frommolt et al (2008)
			Capsicum annuum	Hieber et al 2000	*Ostreococcus tauri*	Frommolt et al (2008)
			Lycopersicon esculentum	Hieber et al 2000		
			Prunus armeniaca	Hieber et al 2000		
carotenogenesis	Violaxanthin de-epoxidase	*vde*	*Arabidopsis thaliana*	Cunningham (2002	*Mantoniella squamata*	Goss (2003)
					Ostreococcus lucimarinus	Frommolt et al (2008)
					Ostreococcus tauri	Frommolt et al (2008)
carotenogenesis	β-carotene 2-hydroxylase	*crtG*				
carotenogenesis	Neoxanthin synthase	*Nsy*				

content. UV-B irradiation may induce upregulation of *ipI* and *MR*-genes and also can downregulate the expression of *L3OH* and *TPS* genes (Dolzhenko et al. 2010).

4.5.1.2 Light stress and carotenogenesis

In plants, the xanthophyll cycle (the reversible interconversion of two carotenoids, violaxanthin and zeaxanthin) has a key photoprotective role to enhance tolerance to high light but also to other stress conditions, such as nitrogen starvation, which has not been reported previously (Cousoab et al. 2012). The accumulation of β-carotene and zeaxanthin at high photon flux densities has been reported in *A. thaliana*. In this plant, overexpression of the *chyb* gene that encodes CHY, an enzyme in the zeaxanthin biosynthetic pathway, causes a specific twofold increase in the size of the xanthophyll cycle pool. The plants are more tolerant to conditions of high light and high temperature than other organisms. Their stress protection is probably due to the function of zeaxanthin in preventing oxidative damage of membranes (Davison et al. 2002).

In *Chlamydomonas reinhardtii*, the high increase in the transcript levels of the cytochrome-dependent CHY and ε-carotene hydroxylase in response to high light suggests an important role of these enzymes in regulation of xanthophyll synthesis upon light stress (Depka et al. 1998; Cousoab et al. 2012). In *Chlorella*, high-irradiance stress did not increase mRNA levels of neither lycopene β-cyclase gene (*lcy-b*) nor lycopene ε-cyclase gene (*lcy-e*), whereas the transcript levels of *psy*, *pds*, *chyB*, and *bkt* genes were enhanced. Nevertheless, the synthesis of the secondary carotenoids astaxanthin, canthaxanthin, and zeaxanthin was triggered, and the levels of the primary carotenoids α-carotene, lutein, violaxanthin, and β-carotene were decreased (Cordero et al. 2012). In higher plants, LCY plays as key role under high light stress and assists in preventing ROS-dependent damage of DNA, proteins, carbohydrates, and lipids by reducing accumulation of β-carotene-5,6-epoxide (Bradbury et al. 2012).

In green algae, in addition of lycopene as an important intermediate, the carotenogenesis pathway involves two key enzymes, PSY (PSY/CrtB) and CHY (CrtR-b/CHYB). The application of high light intensities in *H. pluvialis* caused a transient increase in CHY mRNA and consequently astaxanthin accumulation (Steinbrenner and Linden 2001). Carotenogenic genes expression in *H. pluvialis* including PSY, PDS, LCY, BKT, and CHY is upregulated under high light (Steinbrenner & Linden, 2001, Vidhyavathi et al. 2008). In the study of Pirastru et al. (2012), *Scenedesmus* sp. was tolerant to the long-term (40 days) high light stress condition due to the production of secondary carotenoids, such as astaxanthin and canthaxanthin. The biosynthesis of these secondary carotenoids was highly induced after the deterioration of PSII complexes when chlorophyll synthesis and cell division were inhibited. In the other study, exposure of *Chlorococcum* to high irradiance caused an increase in the amount of xanthophyll-cycle pigments and in the carotenoid/chlorophyll ratio. As a result of exposure to stress conditions, cell division was completely stopped, although an

increase in the biomass dry weight could be detected due to an increase in the cell size (Masojídek et al. 2000).

Dunaliella sp. was exposed to high light intensity (4000 μmol m^{-2} s^{-1}) for 2 h and it lost its carotenoid and chlorophyll content up to 20% and 15%, respectively. In contrast, zeaxanthin was increased by approximately 200% (Young & Britton, 1990). In this respect, it seems that carotenes (such as α- and β-carotene) are more sensitive to photobleaching than xanthophylls (such as lutein, zeaxanthin, neoxanthin, violaxanthin, and α- and β-cryptoxanthin), and sensitivity of chlorophyll is ranged between carotenes and xanthophylls (Siems et al. 2002). In the other report by Chang et al. (2013), *Ch. reinhardtii* was exposed to high light (3000 μmol m^{-2} s^{-1}), and carotenoid content was slightly reduced during the first 30 min of illumination and strongly diminished after 60 min. The expression of the transcripts of enzymes involved in carotenoid biosynthesis, including PSY, PDS, and lycopene ε-cyclase (LCYE), initially increased and then decreased. These results suggest that to ameliorate the stress, a reduction in the degree of carotenoid breakdown occurs by activation of *de novo* carotenoid synthesis.

4.6 Genetic engineering

Harnessing the powers of plant, algal, and microbial systems for economically valuable isoprenoid production requires extensive research and completely understanding their biosynthesis and genomics, as well as the effect of environmental and stress conditions. Metabolic engineering could enhance plant adaptation to climate change and improve food security and nutritional value. For instance, in transgenic peppermint, by downregulation of the *MFS* gene, lower amount of menthofuran and (+)-pulegone in the oil was produced. This led to an increase in the isoprenoid flux through PR and ultimately more (−)-menthol content (Mahmoud and Croteau 2003). Increasing the other enzymes involved in carotenogenesis pathway, CHY and PSY, has also an important role during stress conditions, such as light stress. Discovery of differential gene products like PSY or CHYB locations linked to activity and isozyme type advances the engineering potential for modifying carotenoid biosynthesis (Shumskaya et al. 2012).

In the recent years, all the genes of menthol biosynthesis pathway have been isolated, cloned, and characterized, but there are still several enzymes such as iPD, iPR, iPI, PR, and MR that need to be explored for their metabolic engineering potential (Dolzhenko et al. 2010). On the other hand, for carotenoid biosynthetic pathway, the catalytic steps have been described, although, the regulatory mechanisms that control carotenoid accumulation remain poorly understood (Lee et al. 2012). With genetic engineering or genetic modification, it is possible to manipulate the characteristics and functions of the original genes of each pathway in organisms. The objective of this process is to introduce new physiological and physical features or characteristics, change the patterns of production, and boost the yield of metabolites including isoprenoid synthesis in plants and microorganisms.

4.7 Conclusion

In conclusion, the MEP pathway of plastid IPP and isoprenoid biosynthesis is well established with its seven main enzymes and corresponding genes, but all of the enzymes and genes related to the pathway and also the physiological roles of isoprenoids are not entirely clear (Sharkey & Yeh, 2001; León & Cordoba, 2013). The regulatory mechanisms employed by plants and algae to adjust the amount and composition of isoprenoids are being revealed. Many of the developmental and regulatory aspects of menthol biosynthesis are known in the *Mentha* genus. Recently, many new carotenoids synthesis genes have been isolated (Cheng 2006). Much of what has been learned about the carotenoid pathway in higher plants has come from *Arabidopsis* and tomato and in green algae has come from *H. pluvialis* and *Dunaliella* sp. (Cunningham 2002; Lemoine & Schoefs, 2010; Moulin et al. 2010).

In the aspect of human life, isoprenoids, as the great chemical derivatives of plants and algae, are utilized in industrial and chemical materials and could potentially even become as biofuel sources. Discovering the biosynthesis of the most important isoprenoids and identifying the role of related enzymes in plants and algae species is critically important to achieve modification of each pathway and product *via* plant metabolic engineering and biochemical engineering of plant and microbial systems. The performance of metabolically engineered higher plants and green algae species toward essential oil or carotenoid production is encouraging, and in some cases, their production capacity has either reached to the maximum or exceeded the production by native species. For instance, when the mutant of unicellular green alga, *Ch. reinhardtii*, was exposed to nutritional stress (N starvation), after 48 h, the carotenoid content was increased 30-fold, whereas in wild type, the carotenoid content was increased 15-fold, demonstrating that genetic manipulation can enhance carotenoid production (Wang et al. 2009). In tomato fruits, overexpression of lycopene β-cyclase enzyme (LCYB) increased both β-carotene and total carotenoids (Cunningham 2002). It is important to develop technologies that will produce isoprene in a cost-effective, environmentally friendly way and utilizing renewable sources. Modification of the MEP pathway and its related pathways in plants and microorganisms is necessary for the future production of chloroplast isoprenoids such as β-carotene (provitamin A) and α-tocopherol (vitamin E).

4.8 Acknowledgments

The authors thank the French Ministry for Education and Scientific Research and the University of Le Mans for financial supports. PH is very grateful to Pres LUNAM (programme: Structuration des coopérations inter nationales des laboratoires par la mobilité internationale des doctorants) and the Collège doctoral of the University of Le Mans (programme: Aide à la cotutelle internationale de thèse) for their financial supports.

4.9 References

Adam P., Hecht S., Eisenreich W., Kaiser J., Gräwert T., Arigoni D., Bacher A. & Rohdich F. (2002). Biosynthesis of terpenes: Studies on 1-hydroxy-2-methyl-2-(E)-butenyl-4-diphosphate reductase. Proc. Natl. Acad. Sci. USA 99: 12108–12113.

Alonso W.R., Rajaonarivony J.I., Gershenzon J. & Croteau R. (1992). Purification of 4*S*-limonene synthase, a monoterpene cyclase from the glandular trichomes of peppermint (*Mentha* × *piperita*) and spearmint (*Mentha spicata*). J. Biol. Chem. 267: 7582–7587.

Araki N., Kusumi K., Masamoto K., Niwa Y. & Iba K. (2000). Temperature-sensitive *Arabidopsis* mutant defective in 1-deoxy-*D*-xylulose 5-phosphate synthase within the plastid non-mevalonate pathway of isoprenoid biosynthesis. Physiol. Plantarum 108: 19–24.

Bach T.J., Boronat A.J., Campos N.J., Ferrer A.J. & Vollack K.U.J. (1999). Mevalonate biosynthesis in plants. Crit. Rev. Biochem. Mol. Biol. 34: 107–122.

Baroli I., Do A.D., Yamane T. & Niyogi K.K. (2003). Zeaxanthin accumulation in the absence of a functional xanthophyll cycle protects *Chlamydomonas reinhardtii* from photooxidative stress. Plant Cell 15: 992–1008.

Behnke K., Ehlting B., Teuber M., Bauerfeind M., Louis S., Hänsch R., Polle A., Bohlmann J. & Schnitzler J.P. (2007). Transgenic, non-isoprene emitting poplars don't like it hot. Plant J. 51: 485–499.

Bertrand M. (2010). Carotenoid biosynthesis in diatoms. Photosynth. Res. 106: 89–102.

Bohlmann J. & Keeling C.I. (2008). Isoprenoid biomaterials. Plant J. 54: 656–669.

Bohlmann J., Martin D., Oldham N.J. & Gershenzon J. (2000). Isoprenoid secondary metabolism in *Arabidopsis thaliana*: cDNA cloning, characterization, and functional expression of a myrcene/(*E*)-beta-ocimene synthase. Arch. Biochem. Biophys. 375: 261–269.

Bonsang B., Polle C. & Lambert G. (1992). Evidence for marine production of isoprene. Geophys. Res. Lett. 19: 1129–1132.

Boussiba S. (2000). Carotenogenesis in the green alga *Haematococcus pluvialis*: Cellular physiology and stress response. Physiol. Plantarum 108: 111–117.

Boussiba S., Wang B., Yuan P.P., Zarka A. & Chen F. (1999). Changes in pigments profile in the green alga *Haematococcus pluvialis* exposed to environmental stresses. Biotechnol. Lett. 21: 601–604.

Bouvier F., d'Harlingue A., Suire C., Backhaus R.A. & Camara B. (1998). Dedicated roles of plastid transketolase during the early onset of isoprenoid biogenesis in pepper fruits. Plant Physiol. 117: 1423–1431.

Bradbury L.M.T., Shumskaya M., Tzfadia O., Wu S.B., Kennelly E.J. & Wurtzel E.T. (2012). Lycopene cyclase paralog CruP protects against reactive oxygen species in oxygenic photosynthetic organisms. Proc. Natl. Acad. Sci. USA 109: 1888–1897.

Britton G. (1993). Carotenoids in chloroplasts pigment-protein complexes. In Pigment-Protein Complexes in Plastids: Synthesis and Assembly. Sundqvist C. & M. Ryberg (Eds). 447–483. San Diego, CA: Academic Press.

Buishand J.G. & Gabelman W.H. (1980). Studies on the inheritance of root color and carotenoid content in red × yellow and red × white crosses of carrot, *Daucus carota* L. Euphytica 29: 241–260.

Carretero-Paulet L., Ahumada I., Cunillera N., Rodríguez-Concepción M., Ferrer A., Boronat A & Campos N. (2002). Expression and molecular analysis of the *Arabidopsis DXR* gene encoding 1-deoxy-*D*-xylulose-5-phosphate reductoisomerase, the first committed enzyme of the 2-*C*-methyl-derythritol-4-phosphate pathway. Plant Physiol. 129: 1581–1591.

Carretero-Paulet L., Cairó A., Botella-Pavía P., Besumbes O., Campos N., Boronat A. & Rodríguez-Concepción M. (2006). Enhanced flux through the methylerythritol 4-phosphate pathway in *Arabidopsis* plants overexpressing deoxyxylulose 5-phosphate reductoisomerase. Plant Mol. Biol. 62: 683–695.

Chahed K., Oudin A., Guivarc'h N., Hamdi S., Chénieux J.C., Rideau M. & Clastre M. (2000). 1-Deoxy-*D*-xylulose 5-phosphate synthase from periwinkle: cDNA identification and induced

gene expression in terpenoid indole alkaloid-producing cells. Plant Physiol. Biochem. 38: 559–566.
Chang H.L., Kang C.Y. & Lee T.M. (2013). Hydrogen peroxide production protects *Chlamydomonas reinhardtii* against light-induced cell death by preventing singlet oxygen accumulation through enhanced carotenoid synthesis. J. Plant Physiol. 20: S0176–S1617.
Chappell J. (1995). Biochemistry and molecular biology of the isoprenoid biosynthetic pathway in plants*. Annu. Rev. Plant Physiol. Plant Mol. Biol.* 46: 521–547.
Chappell J. (2002). The genetics and molecular genetics of terpene and sterol origami. Curr. Opin. Plant Biol. 5: 151–157.
Charon L., Hoeffler J.F., Pale-Grosdemange C. Lois L., Campos N., Boronat A. & Rohmer M. (2000). Deuterium labeled isotopomers of 2-C-methyl-d-erythritol as tools for the elucidation of the 2-C-methyl-*D*-erythritol 4-phosphate (MEP) pathway for isoprenoid synthesis. Biochem. J. 346: 737–742.
Cheng Q. (2006). Structural diversity and functional novelty of new carotenoid biosynthesis genes. J. Ind. Microbiol. Biotechnol. 33: 552–555.
Clastre M., Papon N., Courdavault V., Giglioli-Guivarch N., St-Pierre B. & Simkin A.J. (2011). Subcellular evidence for the involvement of peroxisomes in plant isoprenoid biosynthesis. Plant Signal. Behav. 6: 2044–2046.
Colby S.M., Alonso W.R., Katahira E.J., McGarvey D.J. & Croteau R. (1993). 4*S*-limonene synthase from the oil glands of spearmint (*Mentha spicata*). cDNA isolation, characterization, and bacterial expression of the catalytically active monoterpene cyclase. J. Biol. Chem. 268: 23016–23024.
Cordero B.F., Couso I., Leon R., Rodriguez H. & Vargas M.A. (2012). Isolation and characterization of a lycopene ε-cyclase gene of *Chlorella* (Chromochloris) *zofingiensis*. Regulation of the carotenogenic pathway by nitrogen and light. Mar. Drugs 10: 2069–2088.
Cordoba E., Porta H., Arroyo A., San Román C., Medina L., Rodríguez-Concepción M. & León P. (2011). Functional characterization of the three genes encoding 1-deoxy-D-xylulose 5-phosphate synthase in maize. J. Exp. Bot. 62: 2023–2038.
Cordoba E., Salmi M. & León P. (2009). Unraveling the regulatory mechanisms that modulate the MEP pathway in higher plants. J. Exp. Bot. 60: 2933–2943.
Cousoab I., Vilaa M., Vigaraa J., Cordero B.F., Vargas M.Á., Rodríguez H. & León R. (2012). Synthesis of carotenoids and regulation of the carotenoid biosynthesis pathway in response to high light stress in the unicellular microalga *Chlamydomonas reinhardtii.* Eur. J. Phycol. 47: 223–232.
Croteau R., Karp F., Wagschal K.C., Satterwhite D.M., Hyatt D.C. & Skotland C.B. (1991). Biochemical characterization of a spearmint mutant that resembles peppermint in monoterpene content. Plant Physiol. 96: 744–752.
Croteau R., Kutchan T.M. & Lewis N.C. (2000). Natural products (secondary metabolites). In Biochemistry and Molecular Biology of Plants. Buchanan B., Gruissem W. & Jones R. (Eds.). 1250–1268. Rockville, MD: American Society of Plant Biologists.
Croteau R.B., Davis E.M., Ringer K.L. & Wildung M.R. (2005). (−)-Menthol biosynthesis and molecular genetics. Naturwissenschaften 92: 562–577.
Cunningham F.X. (2002). Regulation of carotenoid synthesis and accumulation in plants. Pure Appl. Chem. 74: 1409–1417.
Cunningham F.X. & Gantt E. (2001). One ring or two? Determination of ring number in carotenoids by lycopene epsilon-cyclases. Proc. Natl. Acad. Sci. USA. 98: 2905–2910.
Daisuke M., Holger J.K., Yohei S., Yusuke F., Koremitsu S., Tomohisa K., Shigeki M. & Shigeru O. (2012). The single cellular green microalga Botryococcus braunii, race B possesses three distinct 1-deoxy-*D*-xylulose 5-phosphate synthases. Plant Sci. 185–186: 309–320.
Das A., Yoon S.H., Lee S.H., Kim J.Y., Oh D.K. & Kim S.W. (2007). An update on microbial carotenoid production: Application of recent metabolic engineering tools. Appl. Microbiol. Biotechnol. 77: 505–512.

Davis E.M., Ringer K.L., McConkey M.E. & Croteau R. (2005). Monoterpene metabolism. Cloning, expression, and characterization of menthone reductases from peppermint. Plant Physiol. 137: 873–881.

Davison P.A., Hunter C.N. & Horton P. (2002). Overexpression of β-carotene hydroxylase enhances stress tolerance in *Arabidopsis*. Nature 418: 203–206.

Delaux P.M., Séjalon-Delmas N., Bécard G. & Ane J.M. (2013). Evolution of the plant–microbe symbiotic "toolkit". Trends Plant Sci. 18: 298–304.

Depka B., Jahns P. & Trebst A. (1998). β-Carotene to zeaxanthin conversion in the rapid turnover of the D1 protein of photosystem II. FEBS Lett. 424: 267–270.

Disch A., Schwender J., Müller C., Lichtenthaler H.K. & Rohmer M. (1998). Distribution of the mevalonate and glyceraldehydes phosphate/pyruvate pathways for isoprenoid biosynthesis in unicellular algae and the cyanobacterium *Synechocystis* PCC 6714. Biochem. J. 333: 381–388.

Dolzhenko Y., Bertea C.M., Occhipinti A., Bossi S. & Maffei M.E. (2010). UV-B modulates the interplay between terpenoids and flavonoids in peppermint (*Mentha* × *piperita* L.). J. Photochem. Photobiol.

Dudareva N., Klempien A., Muhlemann J.K. & Kaplan I. (2013). Biosynthesis, function and metabolic engineering of plant volatile organic compounds. New Phytol. 198: 16–32.

Eisenreich W., Bacher A., Arigoni D. & Rohdich F. (2004). Biosynthesis of isoprenoids *via* the non-mevalonate pathway. Cell Mol. Life Sci. 61: 1401–1426.

Estévez J.M., Cantero A., Reindl A., Reichler S. & Leon P. (2001). 1-Deoxy-*D*-xylulose 5-phosphate synthase, a limiting enzyme for plastidic isoprenoid biosynthesis. J. Biol. Chem. 276: 22901–22909.

Estévez J.M., Cantero A., Romero C., Kawaide H., Jiménez L.F., Kuzuyama T., Seto H., Kamiya Y. & León, P. (2000). Analysis of the expression of *CLA1*, a gene that encodes the 1-deoxyxylulose 5-phosphate synthase of the 2-*C*-methyl-*D*-erythritol-4-phosphate pathway in *Arabidopsis.* Plant Physiol. 124: 95–103.

Farré G., Sanahuja G., Naqvi S., Bai C., Capell T., Zhu C. & Christou P. (2010). Travel advice on the road to carotenoids in plants. Plant Sci. 179: 28–48.

Fellermeier M., Kis K., Sagner S., Maier U., Bacher A. & Zenk M.H. (1999). Cell-free conversion of 1-deoxy-*D*-xylulose 5-phosphate and 2-*C*-methyl-*D*-erythritol 4-phosphate into β-carotene in higher plants and its inhibition by fosmidomycin. Tetrahedron Lett. 40: 2743–2746.

Fellermeier M., Raschke M. et al. (2001). Studies on the nonmevalonate pathway of terpene biosynthesis. The role of 2*C*-methyl-*D*-erythritol 2, 4-cyclodiphosphate in plants. Eur. J. Biochem. 268: 6302–6310.

Fineschi S. & Loreto F. (2012). Leaf volatile isoprenoids: An important defensive armament in forest tree species. J. Biogeosci. Forest. 5: 13–17.

Fiore A., Dall'Osto L., Cazzaniga S., Diretto G., Giuliano G. & Bassi R. (2012). A quadruple mutant of *Arabidopsis* reveals a β-carotene hydroxylation activity for LUT1/CYP97C1 and a regulatory role of xanthophylls on determination of the PSI/PSII ratio. BMC Plant Biol. 12: 50.

Flesch G. & Rohmer M. (1988). Prokaryotic hopanoids: The biosynthesis of the bacteriohopan skeleton. Eur. J. Biochem. 175: 405–411.

Frommolt R., Werner S., Paulsen H. Goss R., Wilhelm C., Zauner S., Maier U.G., Grossman A.R., Bhattacharya. D & Lohr M. (2008). Ancient recruitment by chromists of green algal genes encoding enzymes for carotenoid biosynthesis. Mol. Biol. Evol. 25: 2653–2667.

Gershenzon J. & Dudareva N. (2007). The function of terpene natural products in the natural world. Nat. Chem. Biol. 3: 408–414.

Gong Y.F., Liao Z.H., Guo B.H., Sun X.F. & Tang K.X. (2006). Molecular cloning and expression profile analysis of *Ginkgo biloba DXS* gene encoding 1-deoxy-*D*-xylulose 5-phosphate synthase, the first committed enzyme of the 2-*C*-methyl-*D*-erythritol 4-phosphate pathway. Planta Med. 72: 329–335.

Gonzales-Vigil E., Hufnagel D.E., Kim J., Last R.L. & Barry C.S. (2012). Evolution of TPS20-related terpene synthases influences chemical diversity in the glandular trichomes of the wild tomato relative *Solanum habrochaites*. Plant J. 71: 921–935.

Goss R. (2003). Substrate specificity of the violaxanthin de-epoxidase of the primitive green alga *Mantoniella squamata* (Prasinophyceae). Planta 217: 801–812.

Grauvogel C. & Petersen J. (2007). Isoprenoid biosynthesis authenticates the classification of the green alga *Mesostigma viride* as an ancient streptophyte. Gene 396: 125–133.

Grünewald K., Hirschberg J. & Hagen C. (2001). Ketocarotenoid biosynthesis outside of plastids in the unicellular green alga *Haematococcus pluvialis*. J. Biol. Chem. 276: 6023–6029.

Guenther A., Karl T., Harley P., Wiedinmyer C., Palmer P.I. & Geron C. (2006). Estimates of global terrestrial isoprene emissions using MEGAN (Model of Emissions of Gases and Aerosols from Nature). Atmos. Chem. Phys. 6: 3181–3210.

Guevara-García A.A., San Roman C., Arroyo A., Cortés M.E., Gutiérrez-Nava M.L. & León P. (2005). The characterization of the *Arabidopsis clb6* mutant illustrates the importance of post-transcriptional regulation of the methyl-*D*-erythritol 4-phosphate pathway. Plant Cell 17: 628–643.

Gunatilaka A.L. (2012). Plant natural products. In Natural Products in Chemical Biology. Civjan N. (Ed.). Hoboken, NJ: John Wiley & Sons, Inc.

Hecht S., Eisenreich W., Adam P., Amslinger S., Kis K., Bacher A., Arigoni D. & Rohdich F.

(2001). Studies on the nonmevalonate pathway to terpenes: The role of the GcpE (IspG) protein. Proc. Natl. Acad. Sci. USA. 98: 14837–14842.

Hermin Pancasakti K. (2008). Microbiological and ecophysiological characterization of green algae *Dunaliella* sp. for improvement of carotenoid production. Nat Indonesia 10: 66–69.

Herz S., Wungsintaweekul J. et al. (2000). Biosynthesis of isoprenoids: YgbB protein converts 4-diphosphocytidyl-2*C*-methyl-*D*-erythritol2-phosphate to 2*C*-methyl-*D*-erythritol2, 4-cyclodiphosphate. Proc. Natl. Acad. Sci. USA. 97: 2486–2490.

Hieber A.D., Bugos R.C. & Yamamoto H.Y. (2000). Plant lipocalins: Violaxanthin de-epoxidase and zeaxanthin epoxidase. Biochim. Biophys. Acta 1482: 84–91.

Hornero-Mendez D., Gomez-Ladron de Guevara R. & Minguez-Mosquera M.I. (2000). Carotenoid biosynthesis changes in five red pepper (*Capsicum annuum* L.) cultivars during ripening. Cultivar selection for breeding. J. Agric. Food Chem. 48: 3857–3864.

Hsieh M.H., Chang C.Y., Hsu S.J. & Chen J.J. (2008). Chloroplast localization of methylerythritol 4-phosphate pathway enzymes and regulation of mitochondrial genes in *ispD* and *ispE* albino mutants in *Arabidopsis*. Plant Mol. Biol. 66: 663–673.

Huang J.C., Wang Y., Sandmann G. & Chen F. (2006). Isolation and characterization of a carotenoid oxygenase gene from *Chlorella zofingiensis* (Chlorophyta). Appl. Microbiol. Biotechnol. 71: 473–479.

Iijima Y., Davidovich-Rikanati R., Fridman E., Gang D.R., Bar E., Lewinsohn E. & Pichersky E. (2004). The biochemical and molecular basis for the divergent patterns in the biosynthesis of terpenes and phenylpropenes in the peltate glands of three cultivars of basil. Plant Physiol. 136: 3724–3736.

Isaacson T., Ohad I., Beyer P. & Hirschberg J. (2004). Analysis *in vitro* of the enzyme CRTISO establishes a poly-*cis*-carotenoid biosynthesis pathway in plants. Plant Physiol. 136: 4246–4255.

Julliard J.H. (1992). Biosynthesis of the pyridoxal ring (vitamin B6) in higher plant chloroplasts and its relationship with the biosynthesis of the thiazole ring (vitamin B1). C. R. Acad. Sci. Ser. III 314: 285–290.

Julliard J.H. & Douce R. (1991). Biosynthesis of the thiazole moiety of thiamin (vitamin B1) in higher plant chloroplasts. Proc. Natl. Acad. Sci. USA. 88: 2042–2045.

Kawoosa T., Singh H., Kumar A., Sharma S.K., Devi K., Dutt S., Kumar Vats S., Sharma M., Singh Ahuja P. & Kumar S. (2010). Light and temperature regulated terpene biosynthesis: Hepatoprotective monoterpene picroside accumulation in *Picrorhiza kurrooa.* Funct. Integr. Genomics 10: 393–404.

Kim B.R., Kim S.U. & Chang Y.J. (2005). Differential expression of three 1-deoxy-D-xylulose-5-phosphate synthase genes in rice. Biotechnol. Lett. 27: 997–1001.
Kim S.M., Kuzuyama T., Chang Y.J., Song K.S. & Kim S.U. (2006). Identification of class 2 1-deoxy-*D*-xylulose 5-phosphate synthase and 1-deoxy-*D*-xylulose 5-phosphate reductoisomerase genes from *Ginkgo biloba* and their transcription in embryo culture with respect to ginkgolide biosynthesis. Planta Med. 72: 234–240.
Kim S.M., Kuzuyama T., Kobayashi A., Sando T., Chang Y.J. & Kim S.U. (2008). 1-Hydroxy-2-methyl-2-(E)-butenyl 4-diphosphate reductase (IDS) is encoded by multicopy genes in gymnosperms *Ginkgo biloba* and *Pinus taeda*. Planta 227: 287–298.
Kim Y.B., Kim S.M., Kang M.K., Kuzuyama T., Lee J.K., Park S.C., Shin S.C & Kim S.U. (2009). Regulation of resin acid synthesis in Pinus densiflora by differential transcription of genes encoding multiple 1-deoxy-*D*-xylulose 5-phosphate synthase and 1-hydroxy-2-methyl-2-(*E*)-butenyl 4-diphosphate reductase genes. Tree Physiol. 29: 737–749.
Lange B.M. & Croteau R. (1999a). Isoprenoid biosynthesis *via* a mevalonate-independent pathway in plants: Cloning and heterologous expression of 1-deoxy-*D*-xylulose-5-phosphate reductoisomerase from peppermint. Arch. Biochem. Biophys. 365: 170–174.
Lange B.M. & Croteau R. (1999b). Isopentenyl diphosphate biosynthesis *via* a mevalonate-independent pathway: Isopentenyl monophosphate kinase catalyses the terminal enzymatic step. Proc. Natl. Acad. Sci. USA. 96: 13714–13719.
Lange B.M., Wildung M.R., McCaskill D. & Croteau R. (1998). A family of transketolases that directs isoprenoid biosynthesis *via* a mevalonate independent pathway. Proc. Natl. Acad. Sci. USA. 95: 2100–2104.
Lawrence B.M. (1981). Monoterpene interrelationships in the *Mentha* genus: A biosynthetic discussion. In *Essential Oils*, Mookherjee B.D. & Mussinan C.J. (Eds.). 1–81. Wheaton, IL: Allured Publishing.
Lee J.M., Joung J.G., McQuinn R., Chung M.Y., Fei Z., Tieman D., Klee H. & Giovannoni J. (2012). Combined transcriptome, genetic diversity and metabolite profiling in tomato fruit reveals that the ethylene response factor SlERF6 plays an important role in ripening and carotenoid accumulation. Plant J. 70: 191–204.
Lemoine Y. & Schoefs B. (2010). Secondary ketocarotenoid astaxanthin biosynthesis in algae: A multifunctional response to stress. Photosynth. Res. 106: 155–177.
León P. & Cordoba E. (2013). Understanding the mechanisms that modulate the MEP pathway in higher plants. In Isoprenoid Synthesis in Plants and Microorganisms: New Concepts and Experimental Approaches. Bach T.J. & Rohmer M. (Eds.). 457–464. New York: Springer.
Liaaen-Jensen S. (1990). Marine carotenoids. New J. Chem. 14: 747–759.
Liaaen-Jensen S. (1991). Marine carotenoids: Recent progress. Pure Appl. Chem. 63: 1–12.
Lichtenthaler H.K. (1998). The plant's 1-deoxy-*D*-xylulose-5-phospate pathway for biosynthesis of isoprenoids. Fett/Lipi. 100: 128–138.
Lichtenthaler H.K. (1999). The 1-deoxy-*D*-xylulose-5-phosphate pathway of isoprenoid biosynthesis in plants. Annu. Rev. Plant Physiol. Plant Mol. Biol. 50: 47–65.
Lichtenthaler H.K. (2000). Non-mevalonate isoprenoid biosynthesis: Enzymes, genes and inhibitors. Biochem. Soc. Trans. 28: 785–789.
Lichtenthaler H.K. (2007). Biosynthesis, accumulation and emission of carotenoids, α-tocopherol, plastoquinone, and isoprene in leaves under high photosynthetic irradiance. Photosynth. Res. 92: 163–179.
Lichtenthaler H.K. (2010). The non-mevalonate DOXP/MEP (deoxyxylulose 5-phosphate/methyl erythritol 4-phosphate) pathway of chloroplast isoprenoid and pigment biosynthesis. in the chloroplast: basic and applications. Rebeiz C.A. et al. (Eds.). 95–118. Dordrecht, the Netherlands: Springer.
Lichtenthaler H.K. (2012). Biosynthesis, localization and concentration of carotenoids in plants and algae. In Photosynthesis: Plastid Biology, Energy Conversion and Carbon Assimilation. Eaton-Rye J.J., Tripathy B.D. & Sharkey T.D. (Eds.). 95–112. Dordrecht, the Netherlands; Heidelberg, Germany; London, U.K.; New York: Springer.

Lichtenthaler H.K., Rohmer M. & Schwender J. (1997). Two independent biochemical pathways for isopentenyl diphosphate biosynthesis in higher plants. Physiol. Plant. 101: 643–652.
Linden H. (1999). Carotenoid hydroxylase from *Haematococcus pluvialis*: cDNA sequence, regulation and functional complementation. Biochem. Biophys. Acta 1446: 203–212.
Liu J., Zhong Y., Sun Z., Huang J., Sandmann G. & Chen F. (2010). One amino acid substitution in phytoene desaturase makes *Chlorella zofingiensis* resistant to norflurazon and enhances the biosynthesis of astaxanthin. Planta 232: 61–67.
Lohr M., Schwender J. & Polle J.E. (2012). Isoprenoid biosynthesis in eukaryotic phototrophs: A spotlight on algae. Plant Sci. 185–186: 9–22.
Lois L.M., Campos N., Putra S.R., Danielsen K., Rohmer M. & Boronat A. (1998). Cloning and characterization of a gene from *Escherichia coli* encoding a transketolase-like enzyme that catalyzes the synthesis of *D*-1-deoxyxylulose 5-phosphate, a common precursor for isoprenoid, thiamin, and pyridoxol biosynthesis. Proc. Natl. Acad. Sci. USA. 95: 2105–2110.
Lois L.M., Rodriguez-Concepcion M., Gallego F., Campos N. & Boronat A. (2000). carotenoid biosynthesis during tomato fruit development: Regulatory role of 1-deoxy-*D*-xylulose-5-phosphate synthase. Plant J. 22: 503–513.
Loivamäki M., Gilmer F., Fischbach R.J. Sörgel, C., Bachl, A., Walter, A., & Schnitzler, J. P (2007). Arabidopsis, a model to study biological functions of isoprene emission. Plant *Physiol*. 144:1066–1078.
Lombard J. & Moreira D. (2011). Origins and early evolution of the mevalonate pathway of isoprenoid biosynthesis in the three domains of life. Mol. Biol. Evol. 28: 87–99.
Loreto F & Fares S. (2007). Is ozone flux inside leaves only a damage indicator? Clues from volatile isoprenoid studies. Plant Physiol. 143: 1096–1100.
Loreto F. & Velikova V. (2001). Isoprene produced by leaves protects the photosynthetic apparatus against ozone damage, quenches ozone products, and reduces lipid peroxidation of cellular membranes. Plant Physiol. 127: 1781–1787.
Lotan T. & Hirschberg J. (1995). Cloning and expression in *Escherichia coli* of the gene encoding β-*C*-4-oxygenase, that converts β-carotene to the ketocarotenoid canthaxanthin in *Haematococcus pluvialis*. FEBS Lett. 364: 125–128.
Lupien S., Karp F., Wildung M. & Croteau R. (1999). Regiospecific cytochrome P450 limonene hydroxylases from mint (*Mentha*) species: cDNA isolation, characterization, and functional expression of (−)-4*S*-limonene-3-hydroxylase and (−)-4*S*-limonene-6-hydroxylase. Arch. Biochem. Biophys. 368: 181–192.
Luttgen H., Rohdich F. et al. (2000). Biosynthesis of isoprenoids: YchB protein of *Escherichia coli* phosphorylates the 2-hydroxy group of 4-diphosphocytidyl-2 *C*-methyl-*D*-erythritol. Proc. Natl. Acad. Sci. USA. 97: 1062–1067.
MacKinney G. & Jenkins J.A. (1949). Inheritance of carotenoid differences in *Lycopersicon esculentum* strains. Proc. Natl. Acad. Sci. USA. 35: 284–291.
Maffei M. & Scannerini S. (1999). Photomorphogenic and chemical responses to blue light in *Mentha piperita*. J. Essent. Oil Res. 11: 730–738.
Maffei M. & Scannerini S. (2000). UV-B effect on photomorphogenesis and essential oil composition in peppermint (*Mentha piperita* L). J. Essent. Oil. Res. 12: 523–529.
Mahmoud S.S. & Croteau R.B. (2001). Metabolic engineering of essential oil yield and composition in mint by altering expression of deoxyxylulose phosphate reductoisomerase and menthofuran synthase. Proc. Natl. Acad. Sci. USA. 98: 8915–8920.
Mahmoud S.S. & Croteau R.B. (2003). Menthofuran regulates essential oil biosynthesis in peppermint by controlling a downstream monoterpene reductase. Proc. Natl. Acad. Sci. USA. 100: 14481–14486.
Mahmoud S.S., Williams M. & Croteau R. (2004). Cosuppression of limonene-3-hydroxylase in peppermint promotes accumulation of limonene in the essential oil. Phytochemistry 65: 547–554.
Marin E., Nussaume L., Quesada A., Gonneau M., Sotta B., Hugueney P., Frey A. & Marion-Poll A. (1996). Molecular identification of zeaxanthin epoxidase of *Nicotiana plumbaginifolia*, a gene

involved in abscisic acid biosynthesis and corresponding to the ABA locus of *Arabidopsis thaliana*. Eur. Mol. Biol. Org. J. 15: 2331–2342.
Martin D.M., Fäldt J. & Bohlmann J. (2004). Functional characterization of nine Norway Spruce *TPS* genes and evolution of gymnosperm terpene synthases of the TPS-d subfamily. Plant Physiol. 135: 1908–1927.
Masojídek J.J., Torzillo G., Kopecký J., Koblížek M., Nidiaci L., Komenda J., Lukavská. A. & Sacchi A. (2000). Changes in chlorophyll fluorescence quenching and pigment composition in the green alga *Chlorococcum* sp. grown under nitrogen deficiency and salinity stress. J. Appl. Phycol. 12: 417–426.
Matsuzaki M., Kuroiwa H., Kuroiwa T., Kita K. & Nozaki H. (2008). A cryptic algal group unveiled: A plastid biosynthesis pathway in the oyster parasite *Perkinsus marinus.* Mol. Biol. Evol. 25: 1167–1179.
Mau C.J., Karp F., Ito M., Honda G. & Croteau R.B. (2010). A candidate cDNA clone for (−)-limonene-7-hydroxylase from *Perilla frutescens*. Phytochemistry 71: 373–379.
McCarthy S. S., M. C. Kobayashi, and K. K. Niyogi. 2004. White mutants of *Chlamydomonas reinhardtii* are defective in phytoene synthase. Genetics 168: 1249–1257.
McKay W.A., Turner M.F., Jones B.M.R. & Halliwell C.M. (1996). Emissions of hydrocarbons from marine phytoplankton -some results from controlled laboratory experiments. Atmos. Environ. 30: 2583–2593.
Meier S., Tzfadia O., Vallabhaneni R., Gehring C. & Wurtze E.T. (2011). A transcriptional analysis of carotenoid, chlorophyll and plastidial isoprenoid biosynthesis genes during development and osmotic stress responses in *Arabidopsis thaliana.* BMC Syst. Biol. 5: 77.
Milne P.J., Riemer D.D., Zika R.G. & Brand L.E. (1995). Measurement of vertical distribution of isoprene in surface seawater, its chemical fate, and its emission from several phytoplankton monocultures. Mar. Chem. 48: 237–244.
Mimouni V., Ulmann L. & Pasquet V. (2012). The potential of microalgae for the production of bioactive molecules of pharmaceutical interest. Curr. Pharm. Biotechnol. 13: 2733–2750.
Miziorko H.M. (2011). Enzymes of the mevalonate pathway of isoprenoid biosynthesis. Arch. Biochem. Biophys. 505: 131–143.
Moran N.A. & Jarvik T. (2010). Lateral transfer of genes from fungi underlies carotenoid production in aphids. Science 328: 624–627.
Morris W.L., Ducreux L.J., Hedden P., Millam S. & Taylor M.A. (2006). Overexpression of a bacterial 1-deoxy-D-xylulose 5-phosphate synthase gene in potato tubers perturbs the isoprenoid metabolic network: Implications for the control of the tuber life cycle. J. Exp. Bot. 57: 3007–3018.
Moulin P., Lemoine Y. & Schoefs B. (2010). Modification of the carotenoid metabolism in plastids: A response to stress conditions. In Handbook of Plant and Crop Stress. Pessarakli M. (Ed.). 407–433. Boca Raton, FL: CRC Press.
Paniagua-Michel J., Capa-Robles W., Olmos-Soto J. & Gutierrez-Millan L.E. (2009). The carotenogenesis pathway *via* the isoprenoid-β-carotene interference approach in a new strain of *Dunaliella salina* isolated from Baja California Mexico. Mar. Drugs 7: 45–56.
Paniagua-Michel J., Olmos-Soto J. & Acosta Ruiz M. (2012). Pathways of carotenoid biosynthesis in bacteria and microalgae. Methods Mol. Biol. 892: 1–12.
Park S.H., Chae Y.A., Lee H.J. & Kim S.U. (1993). Menthol biosynthesis pathway in *Mentha piperita* suspension cells. J. Korean Agric. Chem. Soc. 36: 358–363.
Phillips M.A., Walter M.H. et al. (2007). Functional identification and different expression of 1-deoxy-D-xyloluse 5-phosphate synthase in induced terpenoid resin formation of Norway spruce (*Picea abies*). Plant Mol. Biol. 65: 243–257.
Pirastru L., Darwish M., Chu F.L., Perreault F., Sirois L., Sleno L. & Popovic R. (2012). Carotenoid production and change of photosynthetic functions in *Scenedesmus* sp. exposed to nitrogen limitation and acetate treatment. J. Appl. Phycol. 24: 117–124.

Ramos A., Coesel S., Marques A., Rodrigues M., Baumgartner A., Noronha J., Rauter A., Brenig B. & Varela J. (2008). Isolation and characterization of a stress-inducible *Dunaliella salina Lyc*-β gene encoding a functional lycopene β-cyclase. Appl. Microbiol. Biotechnol. 79: 819–828.

Ringer K.L., Davis E.M. & Croteau R. (2005). Monoterpene metabolism. Cloning, expression, and characterization of (−)-isopiperitenol/(−)-carveol dehydrogenase of peppermint and spearmint. Plant Physiol. 137: 863–872.

Ringer K.L., McConkey M.E., Davis E.M., Rushing G.W. & Croteau R. (2003). Monoterpene double-bond reductases of the (−)-menthol biosynthetic pathway: Isolation and characterization of cDNAs encoding (−)-isopiperitenone reductase and (+)-pulegone reductase of peppermint. Arch. Biochem. Biophys.

Rios-Estepa R., Turner G.W., Lee J.M., Croteau R.B. & Lange B.M. (2008). A systems biology approach identifies the biochemical mechanisms regulating monoterpenoid essential oil composition in peppermint. Proc. Natl. Acad. Sci. USA. 105: 2818–2823.

Rodríguez-Concepción M. & Boronat A. (2002). Elucidation of the methylerythritol phosphate pathway for isoprenoid biosynthesis in bacteria and plastids. A metabolic milestone achieved through genomics. Plant Physiol. 130: 1079–1089.

Rodríguez-Concepción M. & Boronat A. (2013). Isoprenoid biosynthesis in prokaryotic organisms. In *Isoprenoid Synthesis in Plants and Microorganisms*. Bach T.J. & Rohmer M. (Eds.). 1–16. New York; Heidelberg, Germany; Dordrecht, the Netherlands; London, U.K.: Springer.

Rodríguez-Concepción M., Campos N., Lois L.M., Maldonado C., Hoeffler J.F., Grosdemange-Billiard C., Rohmer M. & Boronat A. (2000). Genetic evidence of branching in the isoprenoid pathway for the production of isopentenyl diphosphate and dimethylallyl diphosphate in *Escherichia coli*. FEBS Lett. 473: 328–332.

Rodwell V.W., Beach M.J. et al. (2000). 3-Hydroxy-3-methylglutaryl-CoA reductase. Methods Enzymol. 324: 259–280.

Rohdich F., Wungsintaweekul J., Eisenreich W., Richter G., Schuhr C.A., Hecht S., Zenk M.H. & Bacher A. (2000a). Biosynthesis of isoprenoids: 4-Diphosphocytidyl-2-*C*-methyl-*D*-erythritol synthase of *Arabidopsis thaliana.* Proc. Natl. Acad. Sci. USA. 97: 6451–6456.

Rohdich F., Wungsintaweekul J., Luttgen H., Fischer M., Eisenreich W., Schuhr C.A., Fellermeier M., Schramek N., Zenk M.H. & Bacher A. (2000b). Biosynthesis of isoprenoids: 4-Diphosphocytidyl-2-*C*-methyl-*D*-erythritol kinase from tomato. Proc. Natl. Acad. Sci. USA. 97: 8251–8256.

Rohmer M. (1993). The discovery of a mevalonate-independent pathway for isoprenoid biosynthesis in bacteria, algae and higher plants. Nat. Prod. Rep. 16: 565–574.

Rohmer M., Knani M., Simonin P., Sutter B. & Sahm H. (1993). Isoprenoid biosynthesis in bacteria: A novel pathway for early steps leading to isopentenyl diphosphate. Biochem. J. 295: 517–524.

Ronen G., Carmel-Goren L., Zamir D. & Hirschberg J. (2000). An alternative pathway to β-carotene formation in plant chromoplasts discovered by map-based cloning of *Beta* and *old-gold* color mutations in tomato. Proc. Natl. Acad. Sci. USA. 97: 11102–11107.

Ronen G., Cohen M., Zamir D. & Hirschberg J. (1999). Regulation of carotenoid biosynthesis during tomato fruit development: Expression of the gene for lycopene epsilon-cyclase is down-regulated during ripening and is elevated in the mutant Delta. Plant J. 17: 341–351.

Rowan K.S. (1989). Photosynthetic Pigments of Algae. Cambridge, U.K.: Cambridge University Press.

Ruiz-Sola M.Á. & Rodríguez-Concepción M. (2012). Carotenoid biosynthesis in *Arabidopsis*: A colorful pathway. Arabidopsis Book 10: e0158.

Sauret-Güeto S., Botella-Pavía P., Flores-Pérez U., Martínez-García J.F., San Román C., León P., Boronat A. & Rodríguez-Concepción M. (2006). Plastid cues posttranscriptionally regulate the accumulation of key enzymes of the methylerythritol phosphate pathway in *Arabidopsis*. Plant Physiol. 141: 75–84.

Schoefs B., Bertrand M. & Lemoine Y. (1998). Changes in the photosynthetic pigments in bean leaves during the first photoperiod of greening and the subsequent dark-phase. Comparison between old (10-d-old) leaves and young (2-d-old) leaves. Photosynth. Res. 57: 203–213.

Schoefs B., Rmiki N., Rachidi J. & Lemoine Y. (2001). Astaxanthin synthesis in *Haematococcus pluvialis* requires a cytochrome P450-dependent hydroxylase and an active synthesis of fatty acids. FEBS Lett. 500: 125–128.

Schwarz M.K. & Arigoni D. (1999). Ginkgolide biosynthesis. In *Comprehensive Natural Product Chemistry*. Cane D.E. (Ed.). 340–367. Oxford, U.K.: Pergamon.

Schwender J., Muller C., Zeidler J. & Lichtenthaler H.K. (1999). Cloning and heterologous expression of a cDNA encoding 1-deoxy-*D*-xylulose-5-phosphate reductoisomerase of *Arabidopsis thaliana*. FEBS Lett. 455: 140–144.

Shanker Dubey V., Bhalla R. & Luthra R. (2003). An overview of the non-mevalonate pathway for isoprenoid biosynthesis in plants. J. Biosci. 28: 637–646.

Sharkey T.D., Chen X.Y. & Yeh S. (2001). Isoprene increases thermotolerance of fosmidomycin-fed leaves. Plant Physiol. 125: 2001–2006.

Sharkey T.D. & Yeh S. (2001). Isoprene emission from plants. Annu. Rev. Plant Physiol. Plant Mol. Biol. 52: 407–436.

Sheen J. (1991). Molecular mechanisms underlying the differential expression of maize pyruvate, orthophosphate dikinase genes. Plant Cell 3: 225–245.

Shumskaya M., Bradbury L.M.T., Monaco R.R. & Wurtzel E.T. (2012). Plastid localization of the key carotenoid enzyme phytoene synthase is altered by isozyme, allelic variation, and activity. Plant Cell 24: 3725–3741.

Siems W.G., Sommerburg O. & Van Kuijk F.J.G.M.(2002). Oxidative breakdown of carotenoids and biological effects of their metabolites. In Handbook of Antioxidants. Cadenas E. & Packer L. (Eds). 117–145. New York: Marcel Dekker.

Spinelli F., Cellini A., Marchetti L., Mudigere K. & Piovene C. (2011). Emission and function of volatile organic compounds in response to abiotic stress. In Abiotic Stress in Plants-Mechanisms and Adaptations. Shanker A. & Venkateswarlu B. (Eds). 367–395. Rijeka, Croatia: InTech.

Sprenger G.A., Schoerken U. et al. (1997). Identification of a thiamin-dependent synthase in Escherichia coli required for the formation of the 1-deoxy-D-xylulose 5-phosphate precursor to isoprenoids, thiamin, and pyridoxol. Proc. Natl. Acad. Sci. USA. 94: 12857–12862.

Spurgeon S.L. & J. Porter W. (1981). Introduction. In Biosynthesis of Isoprenoid Compounds. Porter J.W. & Spurgeon S.L. (Eds). 1–46. New York, Wiley.

Steinbrenner J. & Linden H. (2001). Regulation of two carotenoid biosynthesis genes coding for phytoene synthase and carotenoid hydroxylase during stress-induced astaxanthin formation in the green alga *Haematococcus pluvialis*. Plant Physiol. 125: 810–817.

Steinbrenner J. & Linden H. (2003). Light induction of carotenoid biosynthesis genes in the green alga *Haematococcus pluvialis*: Regulation by photosynthetic redox control. Plant Mol. Biol. 52: 343–356.

Takahashi S., Kuzuyama T., Watanabe H. & Seto H. (1998). A 1-deoxy-D-xylulose 5-phosphate reductoisomerase catalyzing the formation of 2-C-methyl-D-erythritol 4-phosphate in an alternative nonmevalonate pathway for isoprenoid biosynthesis. Proc. Natl. Acad. Sci. USA 95: 9879–9884.

Takaichi S. (2011). Carotenoids in algae: Distributions, biosyntheses and functions. Mar. Drugs 9: 1101–1118.

Takaichi S. & Mochimaru M. (2007). Carotenoids and carotenogenesis in cyanobacteria: Unique ketocarotenoids and carotenoid glycosides. Cell. Mol. Life Sci. 64: 2607–2619.

Tran D., Haven J., Qiu W.G. & Polle J.E. (2009). An update on carotenoid biosynthesis in algae: Phylogenetic evidence for the existence of two classes of phytoene synthase. Planta 229: 723–729.

Turner G., Gershenzon J., Nielson E.E., Froehlich J.E. & Croteau R. (1999). Limonene synthase, the enzyme responsible for monoterpene biosynthesis in peppermint, is localized to leucoplasts of oil gland secretory cells. Plant Physiol. 120: 879–886.

Turner G.W. & Croteau R. (2004). Organization of monoterpene biosynthesis in *Mentha*. Immuno cytochemical localizations of geranyl diphosphate synthase, limonene-6-hydroxylase, isopiperitenol dehydrogenase, and pulegone reductase. Plant Physiol. 136: 4215–4227.

Turner G.W., Davis E.M. & Croteau R.B. (2012). Immunocytochemical localization of short-chain family reductases involved in menthol biosynthesis in peppermint. Planta 235: 1185–1195.

Veau B., Courtois M., Oudin A., Chenieux J.C., Rideau M. & Clastre M. (2000). Cloning and expression of cDNAs encoding two enzymes of the MEP pathway in *Catharanthus roseus*. Biochem. Biophys. Acta 1517: 159–163.

Velikova V., Pinelli P., Pasqualini S., Reale L., Ferranti F. & Loreto F. (2005). Isoprene decreases the concentration of nitric oxide in leaves exposed to elevated ozone. New Phytol. 166: 419–425.

Vickers C.E., Gershenzon J., Lerdau M.T. & Loreto F. (2009). A unified mechanism of action for volatile isoprenoids in plant abiotic stress. Nat. Chem. Biol. 5: 283–291.

Vidhyavathi R., Venkatachalam L., Sarada R. & Ravishankar G.A. (2008). Regulation of carotenoid biosynthetic genes expression and carotenoid accumulation in the green alga *Haematococcus pluvialis* under nutrient stress conditions. J. Exp. Bot. 59: 1409–1418.

Vila M., Couso I. & León R. (2008). Carotenoid content in mutants of the chlorophyte Chlamydomonas reinhardtii with low expression levels of phytoene desaturase. Process Biochem. 43: 1147–1152.

Vranová E., Coman D. & Gruissem W. (2013). Network analysis of the MVA and MEP pathways for isoprenoid synthesis. Annu. Rev. Plant Biol. 64: 665–700.

Walter M.H., Fester T. & Strack D. (2000). Arbuscular mycorrhizal fungi induce the non-mevalonate methylerythritol phosphate pathway of isoprenoid biosynthesis correlated with accumulation of the yellow pigment and the other apocarotenoids. Plant J. 21: 571–578.

Walter M.H., Hans J. & Strack D. (2002). Two distantly related genes encoding 1-deoxy-D-xylulose 5-phosphate synthases: Differential regulation in shoots and apocarotenoid-accumulating mycorrhizal roots. Plant J. 31: 243–254.

Walter M.H. & Strack D. (2011). Carotenoids and their cleavage products: Biosynthesis and functions. Nat. Prod. Rep. 28: 663–692.

Wang Z.T., Ullrich N., Joo S., Waffenschmidt S. & Goodenough U. (2009). Algal lipid bodies: Stress induction, purification, and biochemical characterization in wild-type and starchless Chlamydomonas reinhardtii. Eukaryot. Cell 8: 1856–1868.

White R.H. (1978). Stable isotope studies on the biosynthesis of the thiazole moiety of thiamin in Escherichia coli. Biochemistry 17: 3833–3840.

Wildung M.R. & Croteau R.B. (2005). Genetic engineering of peppermint for improved essential oil composition and yield. Transgenic Res. 14: 365–372.

Wise M.L. (2003). Monoterpene biosynthesis in marine algae. Phycologia 42: 370–377.

Xiang S., Usunow G., Lange G., Busch M & Tong L. (2013). 1-Deoxy-d-xylulose 5-phosphate synthase (DXS), a crucial enzyme for isoprenoids biosynthesis. In isoprenoid synthesis in plants and microorganisms. Bach T.J. & Rohmer M. (Eds.). 17–28. New York; Heidelberg, Germany; Dordrecht, the Netherlands; London, U.K.: Springer.

Xing S., Miao J., et al. (2010). Disruption of the 1-deoxy-D-xylulose-5-phosphate reductoisomerase (DXR) gene results in albino, dwarf and defects in trichome initiation and stomata closure in Arabidopsis. Cell Res. 20: 688–700.

Xiumin F.U., Kong W., et al. (2012). Plastid structure and carotenogenic gene expression in red- and white-fleshed loquat (*Eriobotrya japonica*) fruits. J. Exp. Bot. 63: 341–354.

Yassaa N., Peeken I., et al. (2008). Evidence for marine production of monoterpenes. Environ. Chem. 5: 391–401.

Young A. & Britton G. (1990). Photobleaching in the unicellular green alga Dunaliella parva. Photosynth. Res. 25: 129–136.

Zeidler J.G., Lichtenthaler H.K., May H.U. & Lichtenthaler F.W. (1997). Is isoprene emitted by plants synthesized via the novel isopentenyl pyrophosphate pathway? Z. Naturforsch. 52c: 15–23.

Zeidler J.G., Schwender J., Muller C., Weidemeyer J., Beck E., Jomaa H. & Lichtenthaler H.K. (1998). Inhibition of the non-mevalonate 1-deoxy-D-xylulose-5-phosphate pathway of plant isoprenoid biosynthesis by fosmidomycin. Z. Naturforsch. 53c: 980–986.

Zhao L., Chang W., Xiao Y., Liu H. & Liu P. (2013). Methylerythritol phosphate pathway of isoprenoid biosynthesis. Annu. Rev. Biochem. 82: 497–530.

Chapter

5

Mycorrhizal infection, essential oil content and morpho-phenological characteristics variability in three mint species

Parisa Heydarizadeh[a,b], Morteza Zahedi[a*], Mohammad R. Sabzalian[a], Ehsan Ataii[a]

[a] MicroMar, Mer Molécules Santé, LUNAM, IUML-FR 3473 CNRS, University of Le Mans, Le Mans, France
[b] Department of Agronomy and Plant Breeding, College of Agriculture, Isfahan University of Technology, Isfahan, Iran

* Corresponding author
email: mzahedi@cc.iut.ac.ir
Tel: +98 31 13 91 34 54
fax: +98 31 13 91 22 54.

Scientia Horticulturae (2013). 153: 136–142.

5.1 Abstract

This study investigated the natural variation of arbuscular mycorrhizal associations and variation in morpho-phenological characteristics and essential oil content of 40 accessions of *Mentha* species including *Mentha spicata* L., *Mentha piperita* L. and *Mentha longifolia* (L.) Hudson collected from 13 provinces of Iran. The colonization by Arbuscular Mycorrhizal Fungi (AMF) was naturally found in 38 accessions ranged from 1.4 to 71.8% of infection. There was a significant variation between and within species in terms of essential oil content differing from 0.30 to 3.33% beyond the previously reported range. Accessions collected from colder climate conditions exhibited significantly higher oil content than those from warmer conditions. *M. longifolia* had significantly higher oil content than the other two species. A high variation in fresh weight and leaf water content was also observed and higher mean values were obtained in accessions of *M. piperita* and *M. longifolia*, respectively. A dendrogram generated using the UPGMA algorithm classified the 40 accessions into four distinctive groups based on the species and discriminating characteristics. The high variability in naturally mycorrhizal infection, essential oil content and morphophenological characteristics suggests the possibility of improving mint accessions for horticultural and medicinal uses through selection in breeding programs.

5.2 Introduction

Mint has been exploited for essential oil production and herbage yield in a variety of applications including pharmaceutical, ornamental, food and vegetable uses and for confectionery and cosmetics industries (Zeinali et al. 2004). For each purpose, a great number of clones and species should be evaluated before selec-tion for high levels of essential oil and vegetable yield, based on a well-developed method to choose between and within the species (Mirzaie-Nodoushan et al. 2001). To date, little attention has been given to the evaluation of diverse mint collections and the factors affecting oil content and production of edible tissues. Arbuscular mycorrhizal fungi (AMF) are ubiquitous soil inha-bitants forming the largest group symbiotically associated with agricultural crops (Smith & Read, 1997). They help plant species to uptake water and nutrients and make physiological changes to increase growth and productivity of host plants (Gupta & Janardhanan, 1991; Bethlenfalvay & Linderman, 1992).

Today, AMF are important components of rhizosphere microbial communities in natural ecosystems as well as they are exten-sively used as biofertilizers in agroecosystems (Smith & Read, 1997). Although mycorrhizal detection and investigations of their impacts on medicinal plants have rarely been conducted, they have been observed to be associated with medicinal and aromatic plants (Gupta et al. 1995). The symbiotic AMF can also induce changes in the accumulation of secondary metabolites, including phenolics in roots and aerial parts and also essential oil of host plants (Devi & Reddy, 2002; Rojas-Andrade et al. 2003; Yao et al. 2003; Copetta et al. 2006; Toussaint et al. 2007).

The recognition of the status of mycorrhizal association and its variation in medicinal and aromatic plants is, therefore, of particular concern to improve the quantity of pharmaceutical substances. In *Mentha* species, little is known about the distribution and nat-urally infection of AMF and their effects on either the production of essential oil or plant secondary metabolic pathways; though, there are reports that AMF could affect genetic variation of mint (Van der Heijden et al. 1998). In *Mentha arvensis* L. Gupta et al. (2002) reported that mycorrhizal inoculation significantly increased oil content and yield compared to non-mycorrhizal plants. Freitas et al. (2004) also observed that inoculation with AMF led to an increase of 89% in the essential oil and menthol contents of M. arvensis plants.

In *Mentha piperita*, Mucciarelli et al. (2003) observed that coloniza-tion by a non-mycorrhizal fungus increased essential oil content and altered the oil composition. Yet, no attempts have been made to investigate the variability of AMF colonization among *Mentha* species and to reveal the adaptation of plant-fungus accessions to different climatic conditions in a diverse genetic population. Three economically important *Mentha* species including *Mentha spicata*, *Mentha longifolia* and *Mentha piperita* have an extensive geographical range in Iran which in turn may bring about a sig-nificant genetic variation in these species for breeding mint in terms of important characteristics. For this purpose, collection and evaluation of diversity in plant germplasm is a prerequisite. On the other hand, environmental factors including the relation-ship between mint plant

and mycorrhizal colonization may also affect the morpho-phenological and physiological characteristics. This means that any report on genetic variation of mint should include the infection status of plant with mycorrhiza. The objectives of this study were, therefore, to survey the variation of morpho-phenological, and essential oil content and their relations in a broad mint germplasm collected from 13 provinces of Iran and investigate the effect of climate conditions of collected samples on different characteristics. The variation of AMF infection was also reported in genotypes of three *Mentha* species collected from various regions.

5.3 Material and methods

5.3.1 Plant material

A total of 28 accessions of *M. spicata* (spear mint) (which is the prevalent species of mint in Iran), 6 accessions of *M. longifolia* (horsemint) and 6 accessions of *M. piperita* (pepper mint) were collected from their natural habitats in 13 provinces of Iran (Figure 5.1) (Heydarizadeh et al. 2013). The collection strategy was to survey all environmental conditions that we categorized them into two groups; colder and warmer areas based on annual temperature. It is worth mentioning that colder areas have relatively higher precipitation compared to warmer areas. In each province, the most common accessions of species were collected with whole soil around, bagged and transferred to laboratory. A sample of plant roots including 20 rootlets originating from rhizomes and stolons and from each accession was immediately taken and the soil was then removed from the surface of the roots under running tap water.

No.	Province	Temperature (°C)	Rainfall (mm)	Climate
1	Western Azerbaijan	11.5 ±1.86	404	
2	Hamadan	11.3±1.83	328	
3	Kermanshah	14.3±1.54	427	
4	Lorestan	17.2±1.55	409	
5	Alborz	14.9±1.62	248	
6	Ghazvin	14.0±1.83	351	
7	Northern Khorasan	16.1±1.24	253	
8	Khozestan	25.3±1.37	161	
9	Markazi	21.9±1.97	192	
10	Esfahan	20.3±1.43	120	
11	Yazd	19.1±1.57	125	
12	Fars	23.5±1.32	195	
13	Razavi Korasan	19.1±1.92	174	

Figure 5.1. Collection sites map of 40 mint accessions (*). and colder and warmer areas, respectively.

After washing, root samples were prepared for determination of percent colonization by arbuscular mycorrhizae using the modified staining method of Phillips & Hayman (1970) as described below.

5.3.2 Morpho-phenological characteristics analysis

To evaluate the variation of morpho-phenological characteristics and essential oil content in the same condition, the accessions were transplanted into a bare field (not planted before) located at Isfahan University of Technology, Isfahan, Iran (latitude 35◦44'N, longitude 51◦10'E, altitude 1320 m) and allowed to grow during 2009–2010. Field plots were 1.5 m long and 1.5 m wide arranged in a randomized complete block design with three replications. Between and within row spacing was 50 and 20 cm, respectively. In each row, 5 plants with the same size were cultured. The soil was a clay-loam type, well drained, with a pH of 6.8 fertilized with 60 kg N/ha and 30 kg P/ha before planting. Weeds were manually eliminated and plants were irrigated twice a week. Days to full flowering were calculated since initiation of regrowth on March 20. Then after, plants were cut at crown level; fresh weight per plant was immediately measured. Plants were oven-dried in 70 ◦C for 48 h and dry weight per plant was also recorded in each plot. The number of branches on the main stem, plant height, the number of flowers per plant, flower length, leaf length and width were also determined based on 10 measurements for each accession in each plot. The average values were used for data analysis. Leaves were removed from 5 plants and their leaf areas were measured using a leaf area meter (Model LI-3 100, LI-COR, Inc., Lincoln, NE). After desiccation, leaf water content was calculated according this formula:

leaf water content = [(leaf fresh weight − leaf dry weight) / leaf fresh weight] × 100

5.3.3 Mycorrhizal colonization assessments

The washed roots were cut into ~1-cm pieces, cleared in 10% KOH (24 h) and then rinsed in water. The materials were next acidified in 5% lactic acid (24 h) and the samples were again rinsed in water. The roots were stained with 0.05% aniline blue in 80% lactic acid (24 h) and finally stored in 80% lactic acid (Phillips & Hayman, 1970).

The percentage of root fungal colonization was estimated according to the gridline intersect method (Giovannetti and Mosse, 1980). Twenty root pieces (20 cm) mounted on slides (10×10) in glycerol:lactic acid (5:1) were examined at 800× and 1000× magnifications using a Nikon BH-2 light microscope containing an ocular crosshair eyepiece. Intersections between roots and crosshairs were observed for presence or absence of AMF (any arbuscules, vesicles and hyphae) and the percent incidence of infection over total intersections was calculated from the presence of colonized cells.

∗ Vesicle length, Vesicle width and hyphea diameter were measured by a mini camera and WinRHIZO Tron software.

*Colonization (%) = (number of infected roots / totall number of crossing roots) × 100
Accordingly percent of colonization in figure 4.2 (as an example) is : (88/147) × 100 = 59.86

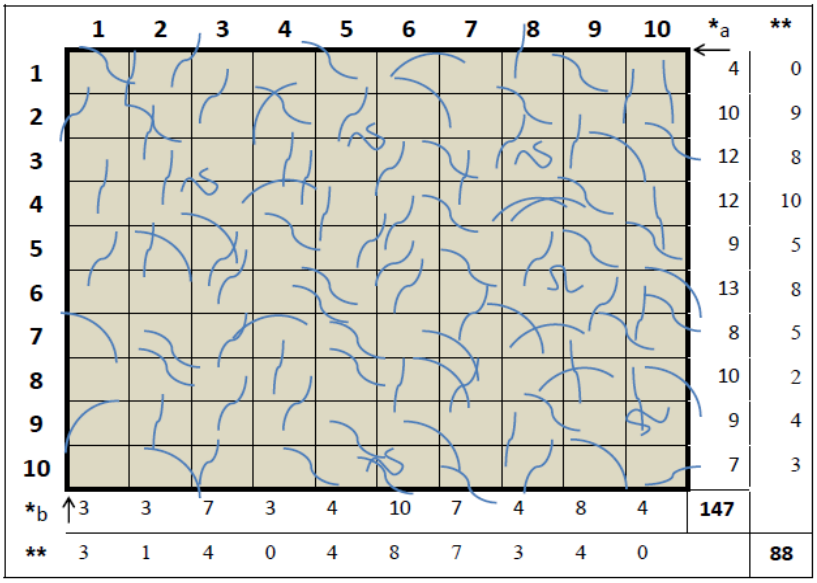

Figure 5.2. Assessement of mychorrhizal colonization. *: number of roots crossing horizontal (a) and vertical (b) lines, **: mychorrhizal infected roots (vesicule, arbuscule, hypha, coil, spore) in crossing roots.

5.3.4 Essential oil isolation

A sample of 100 g of fresh leaves taken from each accession was shade dried and ground by using an electric grinder. The fine powder was mixed with 500 ml distilled water and submit-ted to hydro-distillation for 6 h using a Clevenger-type 5 apparatus (British Pharmacopoeia, 1980). The essential oil fraction was col-lected, weighted and calculated as percentage of sample dry weight. 2.5.

5.3.5 Statistical analysis

Quantitative analyses of morpho-phenological characteristics were performed by one-way analysis of variance (ANOVA) using SAS software package (version 9.0) and based on unbalanced completely randomized design. Fungal colonization percentages were arcsine transformed to ensure data normality before anal-ysis. Accessions were assigned as random samples and the mean squares of three mint species were tested

∗ This part, including figure 4.2, is not in the manuscript and has been added in the content of thesis.

against the pooled mean squares of accessions within species. Also, mean squares of accessions in each species were tested against mean squares of replications within each accession. The differences among species and accessions were compared by least significant difference (LSD) test using SAS statistical software (SAS Inc. NC). Pearson cor-relation coefficients were employed in order to determine the degree of association between morphophenological characteris-tics and essential oil content. According to geographical similarity, the accessions of three species were divided into two collection-site conditions of colder and warmer to determine the effect of geographical conditions on essential oil content and its relation to other characteristics. A cluster analysis of the data was also performed to classify the most similar accessions based on the morpho-phenological characteristics and oil content according to Ward's method (Ward, 1963) and to establish the structure and degree of association among mint accessions using SPSS software (Version 10.0, SPSS Inc., Chicago, USA).

5.4 Results

5.4.1 Mycorrhizal colonization assessment

All accessions except for two collected from Qazvin and Esfahan provinces were colonized by AMF (Table 5.1). Mycorrhizal infection ranged from 1.4 to 71.8% in *M. spicata*, from 0.0 to 50.0% in *M. longifolia* and from 0.0 to 44.4% in *M. piperita*. There was higher mycorrhizal colonization in *M. spicata* with an average of 30.3% (±4.2) compared to 18.9% (±7.9) and 24.1% (±7.6) in *M. piperita* and *M. longifolia*, respectively but the differences among the coloniza-tion rates were not statistically significant. The highest and lowest rates of colonization were found in two accessions of *M. spicata* collected from Ahvaz and Meibod regions, respectively. Extraradical hyphae forming appressorium (hyphodium), hyphal coils and arbuscules were observed in root tissues of all mycorrhizal genotypes (Figure 5.3).

5.4.2 Morpho-phenological characteristics assessment of mint species

Among recorded characteristics, the number of flowers per plant was the most variable characteristic based on the coefficient of variation (CV) which was 120.56% followed by leaf area and inflo-rescence length (CVs were 54.27 and 47.49%, respectively). The minimum variability was also obtained for leaf length and days to flowering (CV = 15.16% and 15.04%, respectively). The more the CV, the greater variability in the characteristic and therefore, higher CV could show the heterogeneity in the population needed for selec-tion in breeding programs. Among accessions, the yield of shoot fresh weight ranged from 6.68 (Semirom) to 40.04 g (Kermanshah) and for shoot dry weight it ranged from 4.13 (Bojnourd) to 17.23 g (Esfahan4). On average, accessions from *M. piperita* presented remarkably higher mean val-ues in terms of shoot fresh weight compared to those from *M. spicata* and *M. longifolia*. However, no

significant differences were found among species regarding shoot dry weight. Leaf water con-tent ranged from 25.91 (Yazd) to 69.16% (Kashan3) both belonging to *M. spicata* (Table 5.1). On average, *M. longifolia* had significantly higher water content than the other two species. Esfahan4 accession from *M. spicata* had the highest number of flowers per plant (137.9) while, the lowest number (10.4) belonged to Kabootarabad accession from M. piperita. The number of branches and leaf area per plant were not significantly different among species. However, the Khorramabad accession was char-acterized by the highest branch number as a potential for leaf production associated

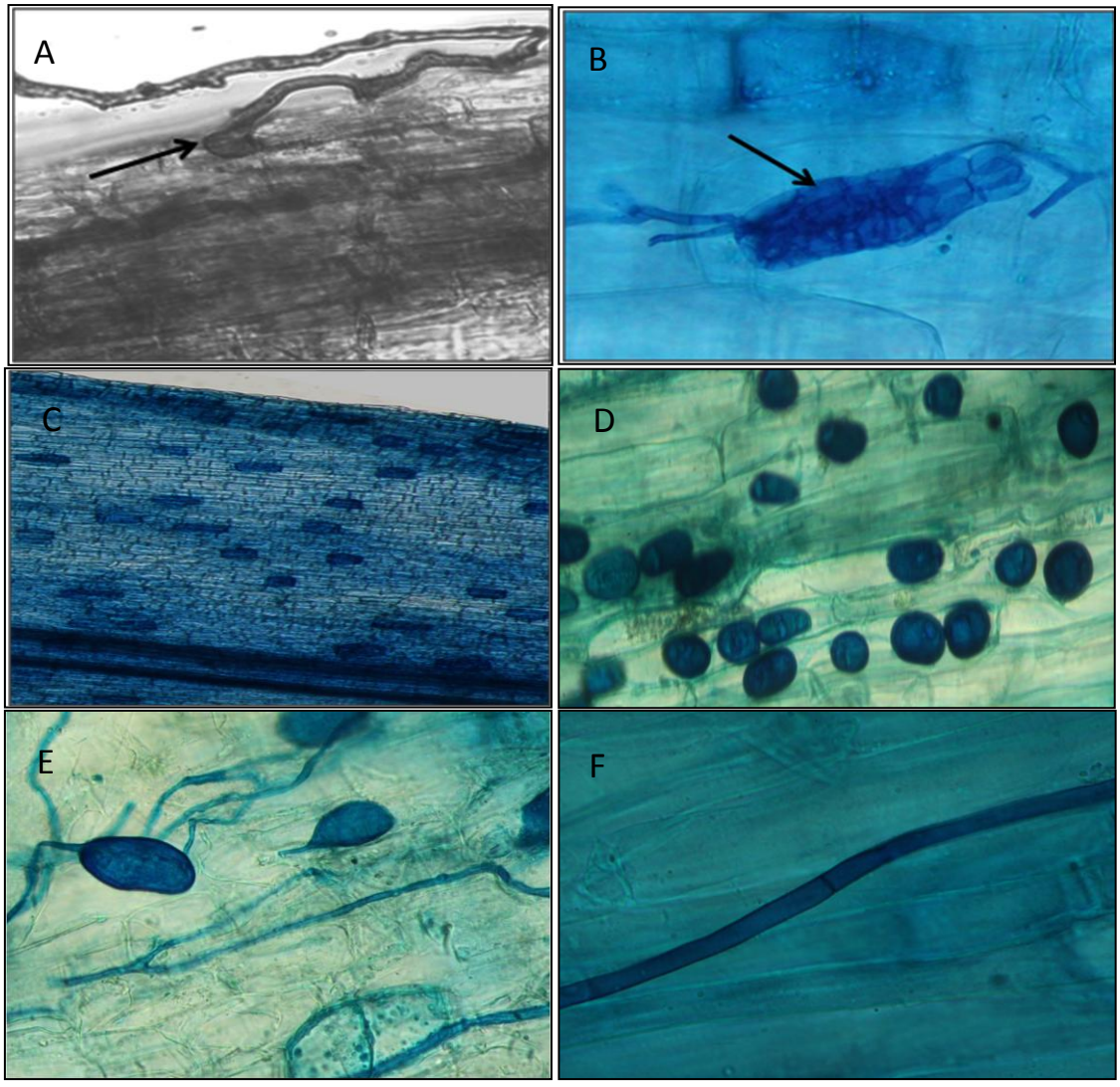

∗**Figure 5.3. Arbuscular mycorrhizal fungi compartment visible under light microscope**. A: apressorium; B: irregular hyphae coil; C: arbuscules inside cortex cells; D, E: vesicles; F: hyphae

∗ This has been added in the content of thesis

with high leaf area in the range of obtained data from all accessions. The tall and early flowering accessions were from M. longifolia where Karaj was the tallest (77.7 cm) and Simirom was the earliest (80 days to flowering). Meanwhile, acces-sion Esfahan3 from *M. spicata* and accession Tabas from *M. piperita* were the shortest (22.4 cm) and latest (162 days to flowering), respectively (Table 5.1). The phenotypic correlations between different characters (Table 5.2) showed that mint fresh herb yield was positively corre-lated with leaf length and the number of flowers per plant (r = 0.36* and 0.32*, respectively).

Shoot dry weight was also positively cor-related with the number of flowers per plant (r = 0.61**). Therefore, an increase in flower formation is in correspondence with an increase in shoot fresh and dry weight. Moreover, a significant positive correlation (r = 0.46**) was found between fresh weight and days to flowering implying that late flowering mint plants have higher herb yield.

5.4.3 Essential oil content

The essential oil content was one of the most variable charac-teristics (CV = 61.09%) and it ranged from 0.30% (in Yazd accession from *M. spicata*) to 3.33% (in Hamadan accession from *M. longifolia*) over all tested accessions. There was only significant difference between *M. longifolia* and *M. spicata* in terms of essential oil content (Table 5.1). Considering variation within each species, the essential oil content in accessions belonging to *M. spicata* ranged from 0.30 to 1.45% with an average of 0.80% whereas, in M. longifolia and *M. piperita* it ranged from 0.63 to 3.33% and 0.69 to 1.60% with an average of 1.25 and 1.00%, respectively. No significant correlations were observed between oil content and morpho-phenological char-acters. Lawrence (1989) and Kokkini et al. (1995) suggested that the variability in essential oil content within *M. spicata* could have mainly been resulted from the impact of environmental factors. To test this conclusion, the data of our study were first splited into two data sets based on annual temperature (colder and warmer) of collection regions while colder areas have higher annual rainfall. Within each data set, correlations were then evaluated between leaf oil content and the other characteristics (Table 5.3). There were no significant correlations, but the mean oil content of accessions collected from colder region was higher than that of accessions collected from warmer area.

Table 5.1. Means and coefficient of variation of mycorrhizal colonization, morphophenological characteristics and essential oil content in 40 mint genotypes.

No	Species	Province	Region	Colonization (%)	Days to flowering	Height (cm)	Leaf length (cm)	Leaf width (cm)	Flower length(cm)	Branch number	Flower/plant	Leaf area (cm^2)	Leaf water (%)	Fresh weight(g/plant)	Dry weight (g/plant)	Oil content (%)
1	*Mentha*	W. Azerbaijan	Mahabad	24.0	123	51.0	2.97	2.02	3.93	15.4	32.9	5.65	43.73	15.71	10.47	0.62
2	*spicata*	Khozestan	Ahvaz	71.8	109	49.0	2.97	2.06	4.37	20.1	60.4	5.93	33.38	15.91	8.95	1.03
3		Khozestan	Abadan	6.7	127	57.0	2.83	1.85	4.29	29.3	15.5	4.09	59.26	7.83	4.30	0.67
4		N. Khorasan	Bojnourd1	44.1	100	59.0	2.83	1.31	3.34	20.1	13.3	2.33	57.50	10.13	4.13	0.98
5		N. Khorasan	Bojnourd2	7.4	99	47.0	2.97	1.96	4.10	21.1	19.6	6.92	56.22	16.67	6.67	1.45
6		Razavi Korasan	Neishabour	9.3	108	52.0	2.71	1.11	5.04	24.3	14.1	2.48	51.58	10.74	6.04	1.30
7		Markazi	Mahallat	7.1	106	43.2	2.29	0.98	5.65	17.0	31.6	2.91	49.43	12.28	6.25	0.37
8		Hamadan	Hamadan	42.0	108	40.6	2.80	1.90	4.56	19.6	22.0	4.31	64.83	22.23	8.15	0.78
9		Esfahan	Kashan1	7.5	98	39.6	2.37	1.74	6.94	21.2	22.1	3.59	47.71	12.08	5.22	0.49
10		Es114	Kashan2	34.3	83	39.1	2.60	1.64	9.63	22.0	29.5	4.08	62.82	9.29	5.36	1.23
11		Esf115	Kashan3	64.2	99	47.4	2.49	1.68	6.22	16.0	24.1	5.57	69.16	16.99	7.22	0.71
12		Esfahan	Kashan4	28.8	103	38.9	2.42	1.52	7.80	16.0	25.2	3.84	38.19	13.79	6.59	0.45
13		Esfahan	Kashan5	20.0	87	41.4	2.67	1.60	5.68	21.2	22.1	4.01	47.92	12.05	6.70	0.75
14		Esfahan	Khoor&Biabanak1	68.7	98	39.4	2.19	1.38	4.83	11.3	31.4	2.47	56.76	11.20	4.89	0.82
15		Esfahan	Khoor&Biabanak2	27.1	108	46.2	2.25	1.55	5.39	23.0	30.6	3.68	37.36	15.0	9.39	0.84
16		Es41	Esfahan1	41.5	98	44.6	2.65	1.53	4.56	20.3	86.6	3.23	55.31	26.22	13.54	1.05
17		Esfahan	Esfahan2	27.3	123	50.0	2.41	1.08	6.19	29.1	91.0	2.60	40.91	16.88	8.93	1.03
18		Esfahan	Esfahan3	30.6	82	22.4	2.11	1.0	5.99	17.0	19.1	1.53	42.77	12.57	5.84	1.36
19		Es113	Esfahan4	29.5	103	45.8	2.33	0.84	3.60	31.5	137.9	2.93	57.45	39.42	17.23	0.88
20		Esfahan	Esfahan5	64.9	93	32.7	1.98	0.85	4.89	21.6	80.8	1.86	48.60	20.07	11.49	0.65
21		Lorestan	Khorramabad	8.6	108	45.7	2.80	1.79	3.95	39.5	19.1	8.86	62.57	20.06	8.26	0.93
22		Yazd	Yazd	28.1	103	34.9	2.70	1.83	4.29	18.0	25.3	5.21	25.91	11.58	6.63	0.30
23		Yazd	Dehbala	6.8	99	48.0	2.39	1.10	4.69	18.1	31.2	2.42	44.46	14.74	6.90	0.53
24		Yazd	Nasrabad	42.3	100	36.8	2.67	1.18	3.56	11.4	19.3	3.37	42.74	9.05	4.61	0.38
25		Yazd	Meibod	1.4	98	39.4	2.70	1.15	3.67	13.6	15.4	3.0	39.30	18.6	5.74	0.63
26		Fars	Shiraz	28.4	123	38.6	3.0	1.56	5.27	23.3	18.9	4.79	38.14	15.47	5.79	0.77
27		Kermanshah	Kermanshah A	25.3	133	41.0	2.67	1.26	4.57	21.9	22.1	2.74	60.00	17.35	9.72	0.74
28		Kermanshah	Kermanshah K	49.2	108	37.8	2.55	1.63	2.99	26.6	18.7	4.52	48.72	15.81	5.81	0.70
	Mean ± SE			**30.3±4.2^{a*}**	**104.38 ±2.34^{a}**	**43.16±1.42^{b}**	**2.58±0.05^{b}**	**1.47±0.07^{a}**	**5.00±0.27^{a}**	**21.05±1.16^{a}**	**34.99±5.56^{a}**	**3.89±0.31^{a}**	**49.38±1.99^{b}**	**15.70±1.19^{b}**	**7.53±0.56^{a}**	**0.80±0.06^{b}**
29	*Mentha*	Alborz	Karaj	30.4	108	77.7	2.73	1.54	8.56	26.0	22.6	4.91	61.37	9.68	5.20	0.63
30	*longifolia*	Hamadan	Hamadan	50.0	108	59.7	2.26	1.26	4.04	15.6	19.4	3.65	66.06	11.60	8.08	3.33
31		Esfahan	Esfahan	33.9	87	59.5	2.59	1.07	6.28	15.3	35.6	3.32	66.89	17.16	11.31	1.11
32		Esfahan	Kashan	20.0	99	49.7	2.51	0.91	5.72	17.4	52.7	2.15	68.63	12.33	7.27	0.82
33		Esfahan	Semirom	0.0	80	33.6	1.69	0.71	4.01	13.3	20.0	1.33	67.55	6.68	4.37	0.80
34		W. Azerbaijan	Mahabad	10.5	108	56.1	2.72	1.37	4.80	13.5	23.2	4.48	52.21	10.72	4.94	0.81
	Mean ± SE			**24.1±7.6^{a}**	**98.33±4.98^{a}**	**56.05±5.88^{a}**	**2.42±0.16^{b}**	**1.14±0.13^{b}**	**5.57±0.7^{a}**	**16.85±1.93^{a}**	**28.92±5.33^{ab}**	**3.31±0.56^{a}**	**63.79±2.53^{a}**	**11.36±1.41^{b}**	**6.86±1.07^{a}**	**1.25±0.26^{a}**
35	*Mentha*	Esfahan	Kashan	25.7	142	49.2	2.81	1.71	4.03	17.6	21.4	4.13	46.26	26.58	10.14	0.69
36	*piperita*	Esfahan	Esfahan	44.4	153	47.0	3.02	1.78	4.65	18.6	21.0	3.60	30.34	17.39	5.95	1.40
37		Esfahan	Kabootarabad	5.5	157	42.5	3.06	1.51	3.71	19.8	10.4	5.25	33.83	23.42	11.20	1.60
38		Kermanshah	Kermanshah	35.3	149	50.9	3.20	1.82	4.85	12.4	15.7	4.53	34.61	40.04	11.94	0.99
39		Ghazvin	Ghazvin	0.0	157	52.1	3.04	1.83	4.11	24.1	15.9	5.65	53.96	23.05	7.47	0.66
40		Yazd	Tabas	2.6	162	52.1	3.12	1.95	4.77	35.3	19.8	5.88	39.30	32.89	11.23	0.65
	Mean ± SE			**18.9±7.9^{a}**	**153.33±2.88^{b}**	**48.97±1.52^{ab}**	**3.04±0.05^{a}**	**1.77±0.06^{a}**	**4.35±0.19^{b}**	**21.30±3.20^{a}**	**17.38±1.72^{b}**	**4.84±0.37^{a}**	**39.72±3.63^{c}**	**27.23±3.29^{a}**	**9.66±.0.98^{a}**	**1.00±0.17^{ab}**
	CV%			71.60	15.04	26.17	15.16	32.35	47.49	42.94	120.56	54.27	27.77	39.19	43.06	61.09

*Means with the same letters within columns are not significantly different ($p \leq 5\%$)

Table 5.2. Relationship among different traits based on correlation coefficients (r) between morphophenological characters and oil content of 40 mint genotypes.

Traits	DF	HT	LL	LD	FL	BN	FP	LA	LW	FW	DW	OC
DF	1											
HT	0.28	1										
LL	0.67**	0.38*	1									
LD	0.46**	0.19	0.71**	1								
FL	0.47**	0.03	0.35*	0.14	1							
BN	0.25	0.19	0.21	0.21	0.10	1						
FP	0.25	0.05	0.34*	0.37*	0.17	0.26	1					
LA	0.37*	0.25	0.65**	0.79**	0.08	0.40*	0.25	1				
LW	0.40*	0.28	0.32*	0.27	0.32*	0.06	0.11	0.10	1			
FW	0.46**	0.03	0.36*	0.17	0.43**	0.27	0.32*	0.23	0.19	1		
DW	0.52**	0.06	0.11	0.01	0.20	0.24	0.61**	0.09	0.07	0.82**	1	
OC	0.04	0.20	0.01	0.06	0.15	0.04	0.06	0.00	0.19	0.00	0.11	1

**, * Significant at 1% and 5% levels of probability, respectively,

DF: Days to flowering; HT: Height; LL: Leaf length; LD: Leaf width; FL: Flower length; BN: Branch number; FP: Flower/plant; LA: Leaf area; LW: Leaf water; FW: Fresh weight; DW: Dry weight; and OC: Oil content.

Table 5.3. Mean comparison of fungal colonization percentage and oil content and phenotypic correlation coefficients (r) between essential oil content with morphophenological characteristics categorized based on mint species and collection region.

Category	Group	Fungal colonization (%)	Oil content (%)	DF	HT	LL	LD	FL	BN	FP	LA	LW	FW	DW
Species	*M. spicata*	30.3$^{a\xi}$	0.80^{b}	0.19	0.13	0.14	0.02	0.11	0.30	0.11	0.05	0.31	0.12	0.10
	M. piperita	18.9^{b}	1.00^{ab}	0.09	0.90*	0.16	0.71*	0.45	0.41	0.64	0.35	0.76*	0.40	0.11
	M. longifolia	24.1^{ab}	1.25^{a}	0.31	0.08	0.19	0.13	0.46	0.21	0.30	0.08	0.22	0.15	0.35
Region	Colder area	27.11^{a}	1.15^{a}	0.05	0.21	0.19	0.07	0.12	0.21	0.19	0.06	0.35	0.07	0.09
	Warmer area	27.87^{a}	0.82^{b}	0.13	0.12	0.22	0.04	0.12	0.18	0.01	0.04	0.02	0.17	0.24

$^{\xi}$ Means with the same letters in each category are not significantly different ($p \leq 5\%$).* Significant at 5% level of probability,

DF: Days to flowering; HT: Height; LL: Leaf length; LD: Leaf width; FL: Flower length; BN: Branch number; FP: Flower/plant; LA: Leaf area; LW: Leaf water; FW: Fresh weight; DW: Dry weight; and OC: Oil content.

5.4.4 Cluster analysis

The dendrogram illustrated four different clusters (Figure. 5.4). Cluster I comprises eight accessions of *M. spicata* and four out of six accessions of *M. longifolia* including that collected from Hamadan having the highest essential oil content (3.33%). Cluster II and III covered the most accessions of *M. spicata* plus two remaining accessions of *M. longifolia* with lower essential oil content than accessions categorized in cluster I. Four accessions of cluster III, which were all collected from Esfahan province, had higher herb fresh weight and number of flowers per plant compared to acces-sions of cluster II. Cluster IV included all accessions of *M. piperita* as well as four accessions of *M. spicata*. Cluster analysis showed relative distinctness of three mint species in terms of morpho-phenological characteristics but it did not differentiate accessions based on collection sites.

5.5 Discussion and conclusions

5.5.1 Discussion

The results revealed a high variation among mint accessions in regard to abundance of mycorrhizal colonization that may come from variability of mint genotypes or may be due to the effect of environmental conditions of natural habitats. These may also show that mint could have mycorrhizal infection up to 70% that in turn it could guarantee nutrient availability in potentially high levels of environmental uncertainty. The level of root infection by mycorrhizal species could deter-mine the extent of positive effects of mycorrhiza on growth parameters of myccorhizal dependent plant species (Graham et al. 1991; Copetta et al. 2006). Zubek & Błaszkowski (2009) showed that the level of root colonization by AM fungi was low in some medicinal plants. Therefore, the effects of these associated micro-organisms on medicinal properties of infected plants are expected to be insignificant if they are mycorrhizal dependent species. The existence of high variation in naturally occurring mycorrhizal colonization up to 71.8% in this study indicates that mint might be also a highly mycorrhizal associated plant under natural soil conditions. However, there is little information avail-able on dependency of mint species to mycorrhizal infection. This could be determined by the evaluation of difference in mint growth parameters under mycorrhizal and non-mycorrhizal conditions (Graham et al. 1991). Gupta et al. (2002) reported that the effect of inoculation with Glomus fasciculatum, on growth and oil yield of menthol mint (*M. arvensis*) was more pronounced only in one out of three tested cultivars. Karagiannidisa et al. (2011) also showed the difference among three Glomus species naturally infecting *Mentha viridis* on plant essential oil percentage. Therefore, the positive effect of this study was wider than those reported in the previous works. The herb yield of mint acces-sions evaluated by Zeinali et al. (2004) had variability with a range from 8.1 to 15.9 g per plant. Mirzaie-Nodoushan et al. (2001) iden-tified days to flowering among

accessions of four mint species from 103 to 130 and Zeinali et al. (2004) reported a range from 83 to 100 days among 12 mint landraces. In comparison, the herb yield and days to flowering in our study ranged from 6.7 to 40.0 g and 80 to 162 days, respectively. These differences might be related to the utilization of a far more number of mint accessions in this work taken from the sites having unlike environmental conditions.

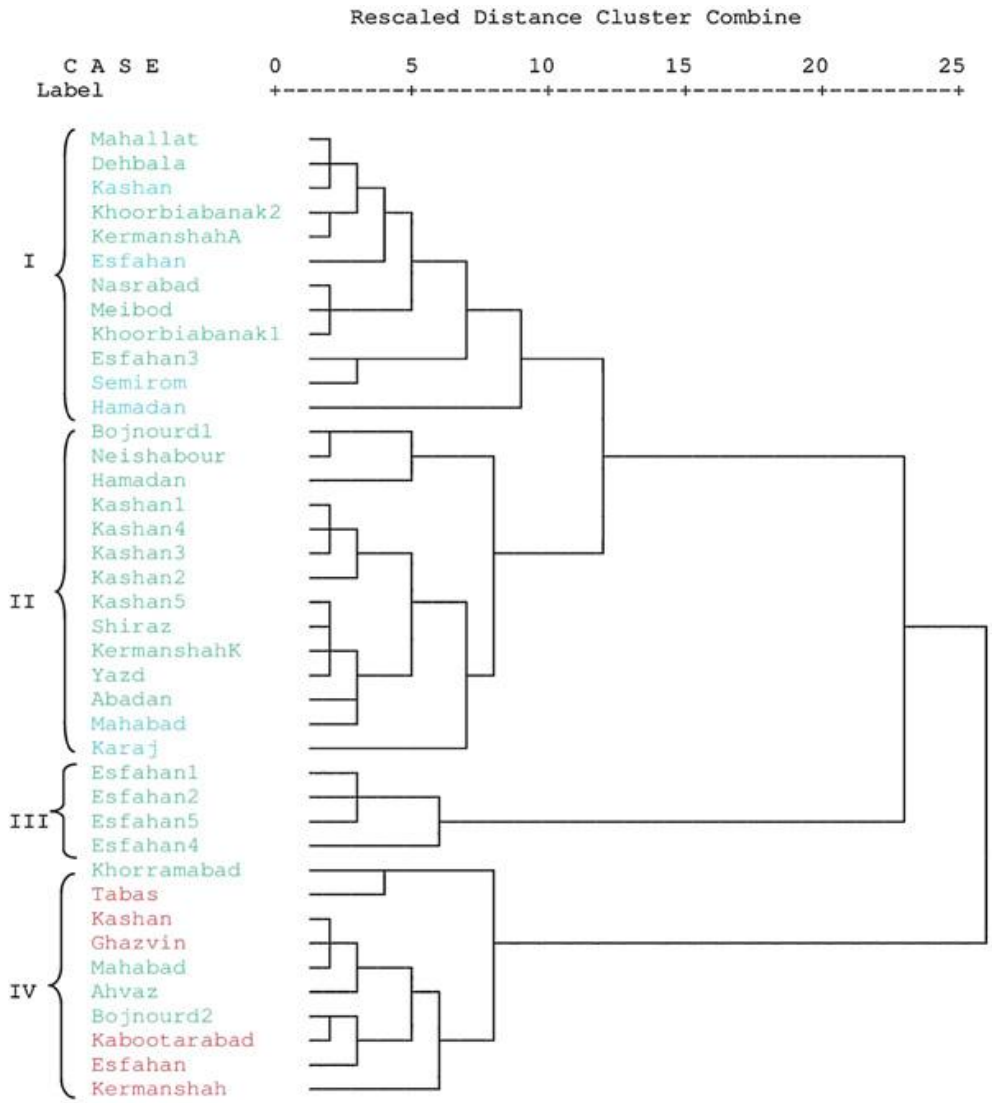

Figure. 5.4. Dendrogram generated from cluster analysis of 40 accessions of mint based on morpho-phenological characteristics and essential oil content using Ward clus-tering procedure. Green color represents *M. spicata*, blue represents *M. longifolia* and red represents *M. piperita.* (For interpretation of the references to color in figure legend, the reader is referred to the web version of the article.)

Among mint morpho-phenological characteristics, higher fresh weight and water content are impor-tant in particular for fresh uses and our results showed that simultaneous selection for both is possible since no significant negative correlation was found between the two characteristics (Table 5.2). This study showed high variability of essential oil content in *M. spicata*. Elmasta et al. (2006) also reported that the essential oil content ranged from 1.2 to 2.2% in *M. spicata*, overlapping with the range of data obtained in this study (0.30 to 1.45%). Our results also showed high potential of *M. longifolia* and *M. piperita* for essen-tial oil production. The essential oil content of mint populations previously reported from Iran ranged from 0.43 to 2.10% (Mirzaie-Nodoushan et al. 2001; Zeinali et al. 2004.) while, the essential oil content of the two extreme accessions in this study, Yazd (*M. spicata*) and Hamadan (*M. longifolia*), was respectively less (0.30%) and more (3.33%) than reported range. There is no available infor-mation in the references for a highly essential oil-rich accession of *M. longifolia* as it was identified (accession Hamadan) in the present study. Such an outstanding accession could be multiplied and introduced to growers and could also be used for mint breeding programs.

There was no significant correlation between oil content and morpho-phenological characteristics in the 40 tested accessions of mint. Maffei et al. (1994) also reported that the correlation was not significant between leaf area and oil productivity in peppermint. However, in the study of Mirzaie-Nodoushan et al. (2001) using only 12 accessions of Mentha species, leaf essential oil content had positive correlation with leaf and stem length and negative correlation with days to flowering. In this study, the mean oil content of accessions collected from colder regions was higher than that of accessions collected from warmer areas (Table 5.3). This result may confirm the main role of environmental factors in determining the variation of mint oil content as a quantitative inherited char-acteristic. This also points out that water stress in warmer regions may have strongly depressed the variation of mint species with high essential oil percentage.Cluster analysis could almost differentiate accessions of three mint species into four different clusters based on plant morpho-phenological characteristics particularly herb fresh weight, the number of flowers per plant and essen-tial oil content. This shows that Mentha species have significant distinctive characteristics in terms of some morpho-phenological characteristics and essential oil content. However, the results from cluster analysis could not discriminate the accessions based on the two collection-site conditions of colder and warmer areas. This means that variation of mint characteristics, except for leaf oil content, has not been significantly affected by environmental conditions.

5.5.2 Conclusion

A high variation was observed in mycorrhizal colonization of mint accessions of three *Mentha* species collected from different natural conditions. This may provide high adaptability of mint accessions to resource-limited growing situations; however, the

effect of natural variation of AMF colonization on mint physiologi-cal and morpho-phenological characteristics is remained unknown. Cluster analysis could almost separate three mint species based on the variation of morpho-phenological characters and essential oil content but it did not differentiate the two collection sites. We did not find any strong correlation between morpho-phenological characteristics and essential oil content. Therefore, selection for morpho-phenological characteristics may not be potentially suit-able for improving oil content of mint genotypes in breeding programs. Although essential oil content was significantly affected by mint species, the effects of environmental conditions was more pronounced. An accession with outstanding essential oil content was identified in M. longifolia that may provide an opportunity for its propagation and distribution among growers for horticultural and medicinal purposes.

5.6 Acknowledgment

The authors thank Dr. Hossein Zeinali, Isfahan Agricultural Research Center, for providing of some accessions and Dr. Aghafakhr Mirlohi, Isfahan University of Technology, for critical review of this manuscript before submission.

5.7 References

Bethlenfalvay G.J. & Linderman R.G. (1992). Mycorrhizae in Sustainable Agriculture. ASA Special Publication 54, USA. British Pharmacopoeia, 1980. H. M. S. Office. 2, London, 109-110.

Copetta A., Lingua G. & Berta G. (2006). Effects of three AM fungi on growth, distribution of glandular hairs, and essential oil production in *Ocimum basilicum* L. var. Genovese. Mycorrhiza 16: 485–494.

Devi M.C. & Reddy M.N. (2002). Phenolic acid metabolism of groundnut (*Arachis hypogaea* L.) plants inoculated with VAM fungus and Rhizobium. Plant Growth Regul. 37: 151–156.

Elmasta M., Dermirtas I., Isildak O. & Aboul-Enein H.Y. (2006). Antioxidant activity of Scarvone isolated from spearmint (*Mentha spicata* L Fam. Lamiaceae). J. Liq. Chromatogr. Relat. Technol. 29: 1465–1475.

Freitas M.S.M., Martins M.A. & Vieira I.J.C. (2004). Producão e qualidade de óleos essenciais de *Mentha arvensis* em resposta a inoculacão de fungos micorrízicos arbusculares. Pesq. Agropec. Bras. 39: 887–894.

Giovannetti M. & Mosse B. (1980). An evaluation of techniques for measuring vesicular-arbuscular mycorrhizal infection in roots. New Phytol. 84: 227–230.

Graham J.H., Eissenstat D.M. & Drouillard D.L. (1991). On the relationship between a plant's mycorrhizal dependency and rate of vesicular-arbuscular mycorrhizal colonization. Funct. Ecol. 5: 773–779.

Gupta M.L. & Janardhanan K.K. (1991). Mycorrhizal association of Glomus aggregatum with palmarosa enhances growth and biomass. Plant Soil 131: 261–263.

Gupta M.L., MohanKumar V. & Janardhanan K.K. (1995). Distribution of VA-mycorrhizal fungi in medicinal and aromatic plants. Kavaka 23: 29–33.

Gupta M.L., Prasad A., Ram M. & Kumar S. (2002). Effect of the vesicular-arbuscular mycorrhizal (VAM) fungus *Glomus fasciculatum* on the essential oil yield related characters and nutrient acquisition in the crops of different cultivars of menthol mint (*Mentha arvensis*) under field conditions. Bioresour. Technol. 81: 77–79.

Karagiannidisa N., Thomidisa T., Lazarib D., Panou-Filotheoua E. & Karagiannidoua C. (2011). Effect of three Greek arbuscular mycorrhizal fungi in improving the growth, nutrient concentration, and production of essential oils of oregano and mint plants. Sci. Hort. 129: 329–334.

Kokkini S., Karousou R. & Lanaras T. (1995). Essential oils of spearmint (Carvone-rich) plants from the island of Crete (Greece). Biochem. Syst. Ecol. 23: 425–430.

Lawrence B.M. (1989). Labiatae oils-mother nature's chemical factory. In: Proc. 11th Int. Congr. Essential oils, fragrance and favours, Nov. 11–16, New Delhi, India.

Maffei M., Mucciarelli M. & Scannerini S. (1994). Are leaf area index (LAI) and flowering related to oil productivity in peppermint? Flavour Fragr. J. 9: 119–124.

Mirzaie-Nodoushan H., Rezaie M.B. & Jaimand K. (2001). Path analysis of the essential oil-related characters in *Mentha* spp. Flavour Fragr. J. 16: 340–343.

Mucciarelli M., Scannerini S., Bertea C. & Maffei M. (2003). *In vitro* and in vivo peppermint (*Mentha piperita*) growth promotion by nonmycorrhizal fungal col-onization. New Phytol. 158: 579–591.

Phillips J. & Hayman D.S. (1970). Improved procedures for clearing roots and staining parasitic and vesicular-arbuscular mycorrhizal fungi for rapid assessment of infection. Trans. Br. Mycol. Soc. 55: 158–161.

Rojas-Andrade R., Cerda-Garcia-Rojas C.M., Frias-Hernandez J.T., Dendooven L., Olalde-Portugal V. & Ramos-Valdivia A.C. (2003). Changes in the concentration of trigonelline in a semi-arid leguminous plant (*Prosopis laevigata*) induced by an arbuscular mycorrhizal fungus during the presymbiotic phase. Mycorrhiza 13: 49–52.

Smith S.E. & Read D.J. (1997). Mycorrhizal Symbiosis. San Diego CA., Toussaint J.P., Smith F.A. & Smith S.E. (Eds.). (2007), 2nd ed. Academic Press. Arbuscular mycorrhizal fungi can induce the production of phytochemicals in sweet basil irrespective of phosphorus nutrition. Mycorrhiza 17: 291–297.

Van der Heijden M.G.A., Klironomos J.N., Ursic M., Moutoglis P., Streitwolf-Engel R., Boller T., Wiemken A. & Sanders I.R. (1998). Mycorrhizal fungal diversity deter-mines plant biodiversity, ecosystem variability and productivity. Nature 396: 69–72.

Ward J.H.J. (1963). Hierarchical grouping to optimize an objective function. J. Am. Stat. Assoc. 58: 236–244.

Yao M.K., Desilets H., Charles M.T., Boulanger R. & Tweddell R.J. (2003). Effect of myc-orrhization on the accumulation of rishitin and solavetivone in potato plantlets challenged with Rhizoctonia solani. Mycorrhiza 13: 333–336.

Zeinali H., Arzani A. & Razmjoo K. (2004). Morphological and essential oil content diversity of Iranian mints (*Mentha* spp.). Iran J. Sci. Technol. Trans. A. 28: 1–9.

Zubek S. & Błaszkowski J. (2009). Medicinal plants as hosts of arbuscular mycorrhizal fungi and dark septate endophytes. Phytochem. Rev. 8: 571–580.

Chapter 6

Photosynthesis under artificial light: the shift in primary and secondary metabolism

Eva Darko[a], Parisa Heydarizadeh[b,c], Benoit Schoefs[b], Mohammad R. Sabzalian[c*]

[a] Agricultural Institute, Centre for Agricultural Research, Hungarian Academy of Sciences, Martonvásár, Hungary
[b] MicroMar, Mer Molécules Santé, IUML - FR 3473 CNRS, Faculté des Sciences et Techniques, University of Le Mans, Le Mans, France
[c] College of Agriculture, Department of Agronomy and Plant Breeding, Isfahan University of Technology, Isfahan 84156-83111, Iran

* Corresponding author
email: sabzalian@cc.iut.ac.ir
Tel: +98 31 13 91 34 52
fax: +98 31 13 91 22 54.

Philosophical Transactions of the Royal Society B (2014). 369(1640): 20130243.

6.1 Abstract

Providing an adequate quantity and quality of food for the escalating human population under changing climatic conditions is currently a great challenge. In outdoor cultures, sunlight provides energy (through photosynthesis) for photosynthetic organisms. They also use light quality to sense and respond to their environment. To increase the production capacity, controlled growing systems using artificial lighting have been taken into consideration. Recent development of light-emitting diode (LED) technologies presents an enormous potential for improving plant growth and making systems more sustainable. This review uses selected examples to show how LED can mimic natural light to ensure the growth and development of photosynthetic organisms, and how changes in intensity and wavelength can manipulate the plant metabolism with the aim to produce functionalized foods.

6.2 Introduction

The rising population, climate changes, land use competition for food, feed, fuel and fibre production as well as the increasing demand for valuable natural compounds all reinforce the need for artificial growing systems such as greenhouses, soilless systems and vertical gardening, even in spacecrafts and space stations. Most of these growing systems require the application of additional, at least supplementary, light sources to ensure plant growth. Because these sources are heat dissipaters requiring cooling, artificial systems are frequently at odds with the demand for sustainability in industrial processes. In terms of both economics and sustainability, new lighting technologies such as lightemitting diodes (LEDs) thus were necessary to be developed (Massa et al. 2006; Sheng et al. 2013). Above all technological properties, LEDs should be compatible with the photosynthesis and light-signalling requirements of plants, which are tightly linked with the two main characteristics of light: wavelength and fluence.

Being mostly immobile, photosynthetic organisms must adapt to their biotic and abiotic environments that they sense through different types of receptors, including photoreceptors (Cheng et al. 2004). The pigment moiety of photoreceptors allows the receptor to extract from the incoming natural white light the specific information related to the intensity of the environmental light constraints. This information is used to develop the adequate response (Cheng et al. 2004)

Photosynthesis is a photobiochemical process using light energy to produce ATP and NADPH, ultimately consumed in the assembly of carbon atoms in organic molecules. Functionally, photons are harvested by protein–chlorophyll (Chl)–carotenoid complexes (that form the light harvesting antenna of photosystems) and then transferred to the photosystem reaction centre, where electrons are generated; these processes take place in the chloroplast (Solymosi & Keresztes, 2012). If lighting is too weak, photosynthesis cannot work efficiently and etiolation symptoms appear (Solymosi & Schoefs, 2010). However, excessive light generates oxygen radicals and causes photoinhibition. Both phenomena strongly limit primary productivity (Barber & Andersson, 1992).

Photosynthetic processes are often modified in plants grown under artificial lighting, because lamps do not usually mimic the spectrum and energy of sunlight. Agronomically, new lighting technologies such as LEDs have the potential to cover fluence and wavelength requirements of plants, while allowing specific wavelengths to be enriched, thus supplying the light quantity and quality essential for different phases of growth. The biomass and metabolic products of cultivated plants can therefore be modified.

This review gives a brief summary of the types of artificial lighting available for growing photosynthetic organisms. The capacity of LEDs to mimic the effects of natural light in terms of energy and information, thus ensuring the growth and development of photosynthetic organisms, and the potential for manipulating the plant metabolism to produce functionalized foods through changes in the intensity and wavelength are also reviewed here using selected examples.

6.3 Artificial light sources for photosynthesis

Artificial lighting should provide plants with energy and information required for development. For this purpose, fluorescent lamps, particularly those having enhanced blue and red spectra (*i.e.* cool fluorescent white lamps), are widely used in growth chambers, together with additional light sources to achieve the sustained photosynthetic photon fluence necessary for high productivity (Massa et al. 2006; Yeh & Chung, 2009). However, the spectrum and intensity of fluorescent lights are not stable over a long time.

High intensity discharge (HID) lamps, such as metal halide and high-pressure sodium lamps, have relatively high fluence (max. 200 lumens per watt) and high photosynthetically active radiations (PARs) efficiency (max. 40%), and are typically used in greenhouses and plant growth rooms. The drawbacks including elevated arc to fire energy requirement, the high operational temperature preventing placement close to the canopy and the spectral distribution (high proportion of green–yellow region, significant ultraviolet radiation and altered red:far-red ratio), which may shift according to the input power, strongly limit their use and innovation (Martineau et al. 2012).

Among artificial lighting systems, LEDs present the maximum PAR efficiency (80–100%, see supplemental Table 6.1). LEDs emitting blue, green, yellow, orange, red and far red are available and can be combined to provide either high fluence (over full sunlight, if desired), or special light wavelength characteristics, thanks to their narrow-bandwidth light spectrum (Bula et al. 1991). The high efficiency, low operating temperature and small size enable LEDs to be used in pulsed lighting and be placed close to the leaves in interlighting and intracanopy irradiation (Yeh & Chung, 2009). Their long life expectancy and ease of control make them ideal for greenhouses in use all year round (Yeh & Chung, 2009). The LED technology is predicted to replace fluorescent and HID lamps in horticultural systems and to revolutionize controlled growth environments.

6.4. Changing light intensity and quality

From the biological point of view, the main questions about LEDs are related to their ability to mimic and enhance the beneficial effects of natural light while avoiding the adverse influence. Below, selected examples are used to provide a short review on useful properties of LED lights in these aspects.

6.4.1 Light-emitting diode light(s) can sustain normal plant growth

Pioneer experiments on plant growth under red LEDs on lettuce were reported by Bula et al. (1991). Martineau et al. (2012) calculated that the amounts of dry matter per mole of artificial lighting gained by lettuce grown using red (650 nm) LEDs or highpressure sodium lamps were identical, and Chang et al. (2011) calculated that the maximum photon utilization efficiency for growth of the green alga Chlamydomonas

reinhardtii under red LEDs is centred at 674 nm. Lettuce grown under red LEDs presented hypocotyls and cotyledons that were elongated, a phenomenon known to be phytochrome-dependent. Under red LEDs illumination, phytochrome stimulation is especially high as far red light is not provided. Hypocotyl elongation could be prevented by adding at least 15 mmol m^{-2} s^{-1} of blue light (Hoenecke et al. 1992). Although a complete demonstration was not provided, one can hypothesize that the supplemented blue light activated cryptochrome, a blue-light photoreceptor that mediates reduction of hypocotyl length (Ahmad et al. 2002).

The efficiency of red (650–665 nm) LEDs on plant growth is easy to understand because these wavelengths perfectly fit with the absorption peak of chlorophylls (Schoefs, 2002) and phytochrome, while the supplemented blue light introduced the idea that growth under natural light could be mimicked using blue and red LEDs. In addition to providing a better excitation of the different types of photoreceptors, the blue + red combination allowed a higher photosynthetic activity than that under either monochromatic light (Sabzalian et al. 2014). Some authors attributed this effect to a higher nitrogen content of the bluelight-supplemented plants, whereas others suggested a better stomatal opening, thus providingmore CO_2 for photosynthesis.

It is well established that stomata opening is controlled by blue light photoreceptors (Schwartz & Zeiger, 1984). This is possibly reflected in the increase of shoot dry matter with increasing levels of blue light (Goins et al. 1998). The supplementation of blue and red LEDs could also be complemented with green LED. Illumination with more than 50% of green LED light caused a reduction in plant growth, whereas treatments containing up to 24% green light enhanced growth for some species (Kim et al. 2006). Recently, LEDs have been successfully tested for their ability to allow the growth of agronomically important crops, fruit and flower plants, and even trees [Sabzalian et al. 2014; Astolfi et al. 2012). Table 6.1 shows the parameter changes in selected taxa exposed to different wavelengths of LEDs compared with the other light sources.

6.4.2 Chloroplast differentiation and de-differentiation

In the absence of light or under deep shade conditions, plants develop etiolation symptoms, such as the absence of Chl, reduced leaf size and hypocotyl elongation (Solymosi & Schoefs, 2010). When the plants are exposed to light, chloroplast differentiation involves the accumulation of proteins, lipids and photosynthetic pigments (Biswal et al. 2003). The kinetics of Chl accumulation present a lag phase under white LED light, which is eliminated when plants are grown under blue LED (460–475 nm) but not in red LED light (650–665 nm) (Wua et al. 2007). Interestingly, similar Chl amounts were reached, regardless of the LED colour. In contrast to Chl, red LED-irradiated pea leaves contained higher levels of β-carotene than those grown under blue or white LED light (Wua et al. 2007). The light intensity is also important in Chl synthesis. For instance, Tripathy & Brown (1995) showed that wheat seedlings accumulated Chl under red LED light at 100 μmol m^{-2} s^{-1}, but not at 500 μmol m^{-2} s^{-1}.

This inhibition of Chl accumulation under high fluence red LED light could be avoided by the supplementation of blue light (30 µmol m^{-2} s^{-1}). Although no demonstration of the effect was provided by the authors, the absence of Chl accumulation under high fluence red light could result from a fast photodestruction of the newly formed Chl molecules (Franck et al. 1995). Interestingly, re-etiolation provides adequate conditions for the production of white asparagus, chicory or seakale (Péron, 1990). In tea leaves, the re-etiolation increases the content of volatiles (aroma), especially volatile phenylpropanoids/benzenoids and several amino acids, including L-phenylalanine (Yang et al. 2012), suggesting the activation of a plastid-located shikimate pathway (Brillouet et al. 2012).

6.4.3 High fluence light-emitting diode triggers production of secondary compounds

Photosynthetic organisms exposed to high light develop short- and long-term response mechanisms to reduce stress effects. Some of these mechanisms are the specific topic of other papers included in this special issue (xanthophylls cycle (Dall'Osto et al. 2014), non-photochemical quenching (Roháček et al. 2014), re-oxidation of the reduction equivalents through photorespiration, the malate valve and the action of antioxidants (Heyno et al. 2014)).

This section is dedicated to the metabolic shifts triggered by high light stress. They are used in repairing mechanisms (Long et al. 1994), shielding (Lee & Gould, 2002), reactive oxygen species (ROS) quenching (Lee & Gould, 2002) or the production of storage compounds (Lemoine & Schoefs, 2010). The synthesis of the metabolites takes place in plastids (terpenoids (Lemoine & Schoefs, 2010)) or involves them (phenylpropanoids (Brillouet et al. 2013)). Typical examples are medicinal plants and herbs of pharmaceutical importance such as mint (*Mentha* sp.) (Sabzalian et al. 2014) and jewel orchid (*Anoectohilus* sp.) (Ma et al. 2010). However, a decrease in secondary metabolites, flavonoids and phenolics, was also observed with increasing irradiance in the medicinal plant cat's whiskers (Orthosiphon stamineus) (Ibrahim & Jaafar, 2012), indicating that the light irradiance may have negative consequences on secondary metabolite production.

In higher plants, it has been documented that depending on species and growing conditions, the secondary metabolites and pigments in the flavonoid family accumulate under photoinhibitory conditions at cell level (Chan et al. 2010), although the mechanistic aspects of LED light effects are not well understood.

The high fluence effect of LED light has been studied more in photosynthetic microorganisms, partly because they present huge biotechnological and economic potential (biofuels, pharmaceuticals, food additives and cosmetics) (Chan et al. 2010). For instance, Wang et al. (2007) assessed the economic efficiency of energy converted to biomass in microalga (Spirulina platensis) culture under different LED monochromatic lights as grams of biomass per litre per dollar.

Table 6.1. The effects of LEDs on plants' growth parameters and metabolism compared with conventional lights: selected examples. HPS, high-pressure sodium; CFL, compact fluorescent light; PPFD, photosynthetic photon flux density; DW, dry weight; FW, fresh weight.

taxa	parameter	LEDs value (bold)/wavelength (nm)/intensity (PPFD)	conventional (HPS, CFL) value (bold)/ type/intensity (PPFD)
Lactuca sativa var.	dry mass ($gmol^{-1}$ $m^{-2)}$ wet mass	**0.45**/650/319	**0.46**/HPS, Na/642
capital	($gmol^{-1}$ m^{-2})	**7.21**	**8.18**
Raphanus sativus	productivity (gcm^{-2} day^{-1})	**0.14**/455 + 640 + 660 + 735/ 9 + 120 + 9.4 + 3	**0.9**/HPS/250
var. Saxa			
Cucumis sativus	fruit FW (g)	**976**/HPS + 445/400 + 16	**735**/HPS, Na/510
L. 'Bodega'	DW (g)	**47.5**	**34**
Lycopersicon	fruit DW (g)	**54.8**	**39.15**
esculentum 'trust'	plant DW (g)	**113**	**136**
Dendranthema	plantlet growth:	/440;650;440 + 650;	/CFL/50
grandiflorum		650 + 720/50	
Kitam 'Cheonsu'	FW (mg per plantlet)	**361;446;750;498**	**713**
plantlets	net photosynthesis (Pn, $\mu mol\ CO_2\ m^{-2}\ s^{-1}$)	**0.75;1.95;4.6;2.2**	**3.4**
Lactuca sativa cv.	metabolite ($mg\ g^{-1}$ FW):	/640; 455 + 640 + 735/200	/HPS, Son-T Agro/200
Grand rapids	carbohydrates	**8;10**	**2**
	nitrates	**0.8;1.0**	**1.4**
	C vit (mg %)	**7;5**	**10**
Petroselinum crispum	carbohydrates	**42.5;23**	**35**
cv. Moss curled	nitrates	**non-evaluable**	**non-evaluable**
	C vit	**145;140**	**130**
Majorana hortensis	carbohydrates	**13;12**	**8**
Moench.	nitrates	**0.6;0,5**	**1.25**
	C vit	**19;19**	**20**
Brassica oleracea		/730;640;525;440;400/253,	not used
cv. 'Winterbor'	lutein ($mg\ 100\ g^{-1}$ FM)	**6.9;11.2;7.8;9.8;8.1**	
	glucosinolate ($mg\ 100\ g^{-1}$ DM)	**21.7;32.0;0.8;ND;ND**	
Petunia hybrid cv.	volatile molecules	/660;755/50	CFL/50
Mitchell diploid	($nmol\ kg^{-1}$):		
	benzylalcohol	**0.23;0.2**	**0.015;**
	2-phenylethanol	**0.25;0.17**	**0.02;**
	phenylacetaldehyde	**4.5;4.0**	**2;**
Fragaria x ananassa		/455;660;755/50	
cv. Strawberry	methyl butyrate	**1.8;2.1;3.0**	**1.8;**
festival	ethyl caproate	**ND;0.5;0.2**	**1.9**
Panax ginseng	metabolites phenolic acids ($\mu g\ g^{-1}$ DW):	/465;630/24	CFL/24
	vanilic acid	**41;27**	**0.33**
	coumaric acid	**314;186**	**76**
	ferulic acid	**586;313**	**319**
Mentha sp.	essential oil (% of DW)	/660;470/500	/sunlight/1800
M. spicata		**4.34;5.03**	**0.66**
M. piperita		**7.00;3.11**	**1.40**
M longifolia		**4.37;3.19**	**3.33**

The data showed that at the light intensity of 1500–3000 μmol m^{-2} s^{-1}, red LEDs consumed the least power and yielded the highest economic efficiency when emitted at the same intensity compared with blue LEDs (up to 110 versus lower than 10 g per litre per dollar, respectively). However, such a high fluence is not always requested. For instance, in the green microalga Dunaliella salina, light stress to drive the accumulation of β-carotene was within the range of 170–255 μmol m^{-2} s^{-1} using LEDs, whereas 1000 μmol m^{-2} s^{-1} photon flux was needed using conventional lights such as fluorescent lamps and high-pressure sodium lamps (Lamers et al. 2010). Additional red or blue (470 nm) LED light caused stress whereby the xanthophylls cycle was activated. The additional blue light was less stressful than the red light (Fu et al. 2013). Katsuda et al. (2004) reported that red LED light allowed the growth of the green alga Haematococcus pluvialis, whereas blue LED light enhanced astaxanthin production. More recently, Katsuda et al. (2008) showed that in mixotrophic growing conditions, flashing LED light (8 μmol photon m^{-2} s^{-1}) triggered similar astaxanthin concentration to continuous LED light (12 μmol photon m^{-2} s^{-1}).

Such low light requirement suggests the involvement of photoreceptors. A putative transduction mechanism of the blue light signal would involve major carotenoids in D. salina. Signalling of secondary carotenoidsynthesis involves chloroplast-generated ROS (Lee & Gould, 2002). Much more investigation is needed to understand the impact of LED light on primary and secondary metabolism of photosynthetic organisms.

6.4.4 Modification of the metabolism through supplemental monochromatic lighting

The effect of supplemental blue and/or red LED light is not limited to growing and developmental properties. They also increase the antioxidant content of vegetables. For instance, red (658–660 nm) LED light increased the phenolics concentration in lettuce leaves [48] and the anthocyanin content of red cabbage leaves (Wua et al. 2007). One can therefore imagine designing supplemental LED light treatments as pre- or post-harvesting processes to fashion raw materials. This would provide great commercial and production advantages. For instance, Colquhoun et al. (2013) used LED treatment to modify the synthesis of volatile compounds in flowers and fruits. In tomato, a red LED treatment (668 nm, 50 μmol photon m^{-2} s^{-1}) triggered a significant increase of 2-methyl-butanol and 3-methyl-1-butanol levels, whereas the amount of cis-3-hexanol was reducedwhen comparedwith the levels reachedwithwhite LED light. Because two of those three compounds are involved in the degree of tomato sweetness (Tieman et al. 2012), one can hypothesize that the LED treatment will impact the taste of the fruit. The mechanismof action of themonochromatic light has not been studied as yet, but one can assume that the red light affects terpenoid production in the chloroplast through phytochrome. Alternatively, specific ROS production could have the same action as shown in the case of secondary carotenoid synthesis (Lee & Gould, 2002).

6.5 Photosynthesis in the light of future advances

Food production relies on photosynthesis. Providing sufficient quantity and quality of food for nine billion people as predicted in 2050 is especially challenging under the constraints of global climate change. Controlled-environment agriculture (CEA) technologies, including greenhouse, hydroponics, aquacultures and aeroponic systems, as well as the vertical farming possibilities, provide alternative and complementary sources for crop production, particularly in areas with limited daylight (in northern latitudes) or adverse environmental conditions (droughts, floods, storms and saline soils) or in areas with limited space, such as cities and space stations (Massa et al. 2006; Yeh & Chung, 2009).

The advantages of CEA technologies, *i.e*. elevated crop yield per year (owing to shorter culture period under optimal environmental conditions and cultivation year round), greater growth area per m^2 (large plant density, multi-tier cultivation shelves), efficient nutrient andwater use, fewer crop losses and no pesticide application, make them efficient for crop production. In addition, these technologies may produce standard high-quality horticultural products. However, in contrast to outdoor agriculture, closed and indoor plant cultivations rely on novel light sources such as LEDs capable of stimulating plant growth while drastically reducing energy consumption.
LEDs represent an innovative artificial lighting source for plants, both as supplemental or sole-source lighting, not only owing to their intensity, spectral and energy advances, but also via the possibilities for targeted manipulation of metabolic responses in order to optimize plant productivity and quality. LEDs are now commercially applicable mainly for leafy greens, vegetables, herbs and pot flowers (Table 6.1).

A more complete references was also presented in the seventh International Symposium on Light in Horticultural Systems, held in Wageningen (http://www.acta hort.org/books /956).

The application of LEDs also has enormous potential for the processes that generate oxygen and purify water, in algal culture for producing feedstock, pharmaceuticals, fuels or dyes, and in plant tissue cultures for the micropropagation of, for example, strawberry or flowering plants (Nhut et al. 2000; Lian et al. 2002).

Research on the effects of LEDs on primary and secondary metabolism of plants and on how the direction and mixing of LEDs influence plant responses, coupled with advances in the dynamic modification of light quantity and quality in different phases of growth may contribute to the efficient utilization of LED lighting technologies in plant cultivation in closed environments (Figure 6.1).

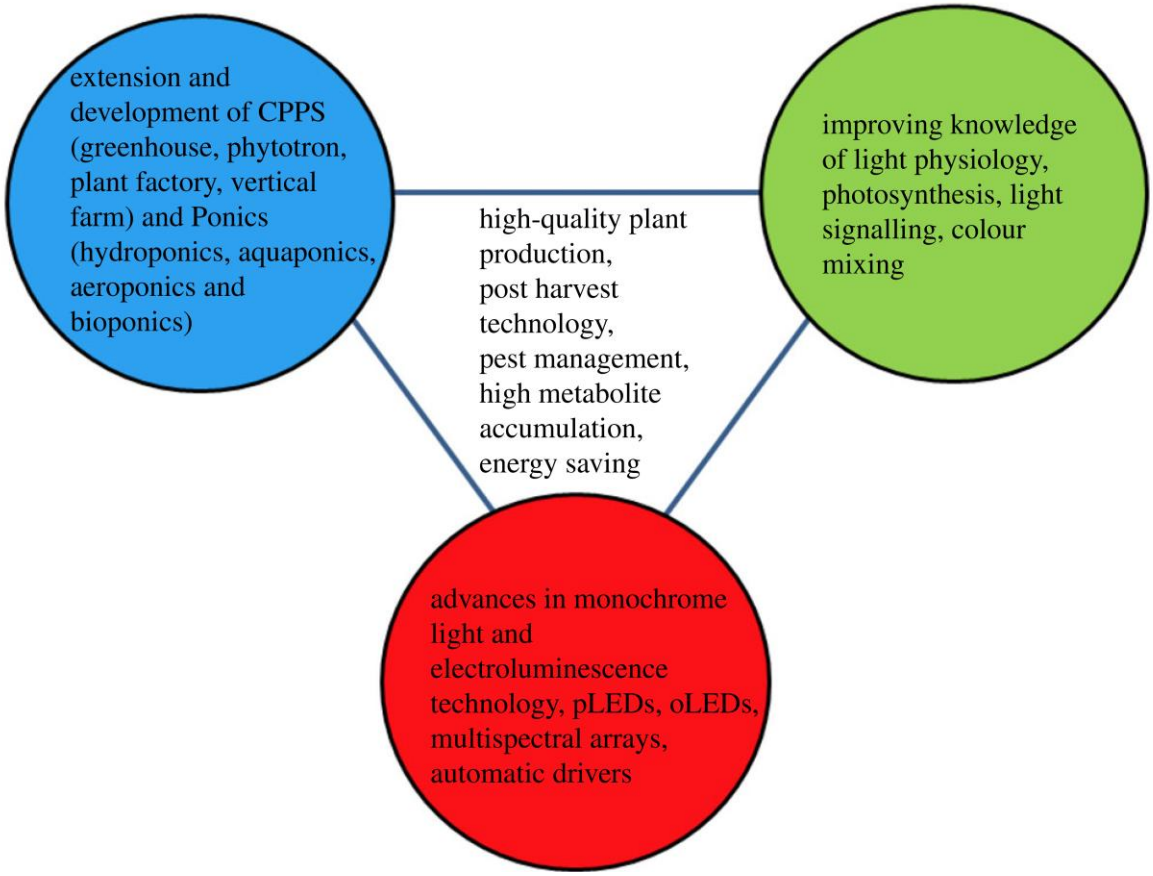

Figure 6.1. Trilateral connection of technological and physiological advances for improvement of plant production using LED lighting. CPPS, closed plant production systems; pLED, polymer light-emitting diode; oLED, organic light-emitting diode. (Online version in colour.)

The lighting industry needs to offer energy-efficient, ecologically sustainable lamps adapted to the changing requirements of consumers. LEDs equipped with driver chips could provide the additional benefits of operational flexibility, efficiency, reliability, controllability and intelligence for greenhouse lighting systems. However, the acceptance of solid-state LED lighting in niche applications in horticultural lighting will depend on improvements in conversion efficiency and light output per package of LED light and the cost of lumens per package. It is predicted that horticultural cultivation under controlled environmental conditions (horticulture industry) will expand in the near future, as was presented in the workshop on Challenges in Vertical Farming (http://challengesinverticalfarming.org/). The new technologies provide possibilities for economically efficient consumption of light energy for horticultural cultivation of crops both on Earth and in space in the near future, and may contribute to feeding the growing human population and maintaining outdoor (principally forest) ecosystems and thus to the protection of the Earth.

6.6 Acknowledgments

The authors acknowledge their institutes, Hungarian Academy of Sciences, University of Le Mans and Isfahan University of Technology. M.R.S. also thanks the Iranian National Elites Foundation for financial support of work on LED incubator construction and cultivation of horticultural and agronomic crops illuminated with LED lights. Funding statement. E.D. appreciates partial financial support from TA´ MOP (grant no. 4.2.2A-11/1/KONV-2012-0008).

6.7 References

Massa G.D., Emmerich J.C., Morrow R.C., Bourget C.M. & Mitchell C.A. (2006). Plant growth lighting for space life support: a review. Gravit. Space Biol. Bull. 19: 19–30.

Sheng C.X., Singh S., Gambetta A., Drori T., Tong M., Tretiak S. & Vardeny Z.V. (2013). Ultrafast intersystemextension crossing in platinum containing p-conjugated polymers with tunable spin–orbit coupling. Sci. Rep. 3: 2653.

Cheng M., Chory J. & Fankhauser C. (2004). Light signal transduction in higher plants. Annu. Rev. Genet. 38: 87–117.

Solymosi K. & Keresztes A. (2012). Plastid structure, diversification and interconversions II. Land plants. Curr. Chem. Biol. 18: 187–204.

Solymosi K. & Schoefs B. (2010). Etioplast and etiochloroplast formation under natural conditions: the dark side of chlorophyll biosynthesis in angiosperms. Photosynth. Res. 105: 143–166.

Barber J. & Andersson B. (1992). Too much good thing: light can be bad for photosynthesis. Trends Biochem. Sci. 17: 61–66.

Yeh N. & Chung J.P. (2009). High-brightness LEDs: energy efficient lighting sources and their potential in indoor plant cultivation. Renew. Sustain. Energy Rev. 13: 2175–2180.

Martineau V., Lefsrud M. & Naznin M. (2012). Comparison of light-emitting diode and highpressure sodium light treatments for hydroponics growth of Boston lettuce. HortScience 47: 477–482.

Bula R.J., Morrow R.C., Tibbitts T.W., Barta D.J., Ignatius R.W. & Martin T.S. (1991). Light emitting diodes as a radiation source for plants. HortScience 26: 203–205.

Chang R.L., Ghamsari L. et al. (2011). Metabolic network reconstruction of Chlamydomonas offers insight into light-driven algal metabolism. Mol. Syst. Biol. 7: 518.

Hoenecke M.E., Bula R.J. & Tibbitts T.W. (1992). Importance of 'blue' photon levels for lettuce seedlings grown under red-light-emitting diodes. HortScience 27: 427–430.

Ahmad M., Grancher N., Heil M., Blac R.C., Giovani B., Galland P. & Lardemer D. (2002). Action spectrum for cryptochrome-dependent hypocotyl growth inhibition in Arabidopsis. Plant Physiol. 129: 774–785.

Schoefs B. (2002). Chlorophyll and carotenoid analysis in food products. Properties of the pigments and methods of analysis. Trends Food Sci. Technol. 13: 361–371.

Sabzalian M.R., Heydarizadeh P., Zahedi M., Boroomand A., Agharokh M., Sahba M.R. & Schoefs B. (2014). High performance of vegetables, flowers and medicinal plants in a red–blue LED incubator for indoor plant production. Agron. Sustain. Dev. 34: 879–886

Schwartz A. & Zeiger E. (1984). Metabolic energy for stomatal opening: roles of photophosphorylation and oxidative phosphorylation. Planta 161: 129–136.

Goins G.D., Yorio N.C., Sanwo-Lewandowski M.M. & Brown C.S. (1998). Life cycle experiments with Arabidopsis under red light-emitting diodes (LEDs). Life Support Biosph. Sci. 5: 143–149.

Kim H.H., Wheeler R.M., Sager J.C., Goins G.D. & Norikane J.H. (2006). Evaluation of lettuce growth using supplemental green light with red and blue lightemitting diodes in a controlled environment: a review of research at Kennedy Space Center. Acta Hort. 711: 111–119.
Astolfi S., Marianello C., Grego S. & Bellarosa R. (2012). Preliminary investigation of LED lighting as growth light for seedlings from different tree species in growth chambers. Not. Bot. Horticult. Agrobot. 40: 31–38.
Tamulaitis G., Duchovskis P., Bliznikas Z., Breive K., Ulinskaite R., Brazaityte A., Novičkovas A. & Žukauskas A. (2005). High-power light-emitting diode based facility for plant cultivation. J. Phys. D, Appl. Phys. 38: 3182–3187.
Ménard C., Dorais M., Hovi T. & Gosselin A. (2006). Developmental and physiological responses of tomato and cucumber to additional blue light. Acta Hort. (ISHS) 711: 291–296.
Kim S.J., Hahn E.J., Heo J.W. & Paek K.Y. (2004). Effects of LEDs on net photosynthetic rate, growth and leaf stomata of Chrysanthemum plantlets *in vitro*. Sci. Horticult. 101: 143–151.
Urbonavičiūtė A., Samuolienė G., Brazaityté A., Ulinskaité R., Jankauskienė J., Duchovskis P. & Žukauskas A. (2008). The possibility to control the metabolism of green vegetables and sprouts using light emitting diode illumination. Sodininkyste ir Darz ininkyste 27: 83–92.
Lefsrud M.G., Kopsell D.A. & Sams C. (2008). Irradiance from distinct wave-length light-emitting diodes affect secondary metabolites in kale. HortScience 43: 2243–2244.
Colquhoun T.A., Schwieterman M.L. et al. (2013). Light modulation of volatile organic compounds from petunia flowers and select fruits. Postharvest Biol. Tech. 86: 37–44.
Park S.Y., Lee J.G., Cho H.S., Seong E.S., Kim H.Y., Yu C.Y. & Kim J.K. (2013) Metabolite profiling approach for assessing the effects of colored light-emitting diode lighting on the adventitious roots of ginseng (Panax ginseng C. A. Mayer). Plant Omics J. 6: 224–230.
Biswal U.C., Biswal B. & Raval M.K. (2003). Chloroplast biogenesis: from proplastid to gerontoplast. Dordrecht, The Netherlands: Kluwer Academic Publisher (Springer).
Wua M.C., Hou C.Y., Jiang C.M., Wang Y.T., Wang C.Y., Chen H.H. & Chang H.M. (2007). A novel approach of LED light radiation improves the antioxidant activity of pea seedlings. Food Chem. 101: 1753–1758.
Tripathy B.C. & Brown C.S. (1995). Root–shoot interaction in the greening of wheat seedlings grown under red light. Plant Physiol. 107: 407–411.
Franck F., Schoefs B., Barthe´lemy X., Mysliwa-Kurdziel B., Strzalka K. & Popovic R. (1995). Protection of native chlorophyll(ide) forms and of photosystem II against photodamage during early stages of chloroplast differentiation. Acta Physiol. Plant. 17: 123–132.
Péron J.Y. (1990). Seakale: a new vegetable produced as etiolated sprouts. In Advances in new crops. Janick J. & Simon J.E. (Eds.). 419–422. Portland, OR: Timber Press.
Yang Z., Kobayashi E. et al. (2012). Characterization of volatile and non-volatile metabolites in etiolated leaves of tea (Camellia sinensis) plants in the dark. Food Chem. 135: 2268–2276.
Brillouet J.M., Romieu C., Schoefs B., Solymosi K., Cheynier V., Fulcrand H., Verdeil J.L. & Conéjéro G. (2013). The tannosome is an organelle forming condensed tannins in the chlorophyllous organs of Tracheophyta. Ann. Bot. 112: 1003–1014.
Dall'Osto L., Cazzaniga S., Wada M. & Bassi R. (2014) On the origin of a slowly reversible fluorescence decay component in the Arabidopsis npq4 mutant. Phil. Trans. R. Soc. B 369, 20130221.
Roháček K., Bertrand M., Moreau B., Jacquette B., Caplat C., Morant-Manceau A. & Schoefs B. (2014). Relaxation of the non-photochemical chlorophyll fluorescence quenching in diatoms: kinetics, components and mechanisms. Phil. Trans. R. Soc. B. 369, 20130241.
Heyno E., Innocenti G., Lemaire S.D, Issakidis-Bourguet E. & Krieger-Liszkay A. (2014). Putative role of the malate valve enzyme NADP–malate dehydrogenase in H_2O_2 signalling in Arabidopsis. Phil. Trans. R. Soc. B. 369, 20130228.
Long S.P., Humphries S. & Falkowski P.G. (1994). Photoinhibition of photosynthesis in nature. Annu. Rev. Plant Physiol. Plant Mol. Biol. 45: 633–662.

Lee D.W. & Gould K.S. (2002). Why leaves turn red: pigments called anthocyanins probably protect leaves from light damage by direct shielding and by scavenging free radicals. Am. Sci. 90: 524–531.

Lemoine Y. & Schoefs B. (2010). Secondary ketocarotenoid astaxanthin biosynthesis in algae: a multifunctional response to stress. Photosynth. Res. 106: 155–177.

Ma Z., Sh L., Zhang M., Jiang S. & Xiao Y. (2010). Light intensity affects growth, photosynthetic capacity, and total flavonoid accumulation of Anoectohilus plants. HortScience 45: 863–867.

Ibrahim M.H. & Jaafar H.Z. (2012). Primary, secondary metabolites, H_2O_2, malondialdehyde and photosynthetic responses of Orthosiphon stimaneus Benth. to different irradiance levels. Molecules 17: 1159–1176.

Chan L.K., Koay S.S., Boey P.L. & Bhatt A. (2010). Effects of abiotic stress on biomass and anthocyanin production in cell cultures of Melastoma malabathricum. Biol. Res. 43: 127–135.

Mimouni V., Ulmann L., Pasquet V., Mathieu M., Picot L., Bougaran G., Cadoret J.P., Morant-Manceau A. & Schoefs B. (2012). The potential of microalgae for the production of bioactive molecules of pharmaceutical interest. Curr. Pharm. Biotechnol. 13: 2733–2750.

Wang C.Y., Fu C.C. & Liu Y.C. (2007). Effects of using lightemitting diodes on the cultivation of Spirulina platensis. Biochem. Eng. J. 37: 21–25.

Lamers P.P., van de Laak C.C., Kaasenbrood P.S., Lorier J., Janssen M., De Vos R.C., Bino R.J. & Wijffels R.H. (2010). Carotenoid and fatty acid metabolism in light-stressed Dunaliella salina. Biotechnol. Bioeng. 106: 638–648.

Fu W., Guðmundsson Ó., Paglia G., Herjólfsson G.Ó.S., Andrésson Palsson B. & Brynjólfsson S. (2013) Enhancement of carotenoid biosynthesis in the green microalga Dunaliella salina with lightemitting diodes and adaptive laboratory evolution. Appl. Microbiol. Biotechnol. 97: 2395–2403.

Katsuda T., Lababpour A., Shimahara K. & Katoh S. (2004). Astaxanthin production by *Haematococcus pluvialis* under illumination with LEDs. Enzyme Microb. Technol. 35, 81–86. (doi:10.1016/j.enzmictec.2004.03.016)

47. Katsuda T, Shiraishi H, Ishizu N, Ranjbar R, Katoh S. 2008 Effect of light intensity and frequency of flashing light from blue light emitting diodes on astaxanthin production by *Haematococcus pluvialis*. J. Biosci. Bioeng. 105: 216–220.

Li Q,. & Kubota C. (2009). Effects of supplemental light quality on growth and phytochemicals of baby leaf lettuce. Exp. Exp. Bot. 67: 59–64.

Tieman D., Bliss P. et al. (2012). The chemical interactionsunderlying tomato flavor preferences. Curr.Biol. 22: 1035–1039.

Nhut D.T., Takamura T., Watanabe H. & Tanaka M. (2000). Light emitting diodes (LEDs) as a radiation source for micropropagation of strawberry. In Transplant production in the 21st century. Kubota C. & Chun C. (Eds.). 114–118. Dordrecht, The Netherlands: Kluwer Academic Publishers.

Lian M.L., Murthy H.N. & Paek K.Y. (2002). Effects of light emitting diodes (LEDs) on the *in vitro* induction and growth of bulblets of Lilium oriental hybrid 'Pesaro'. Sci. Horticult. 94: 365–370.

6.8 Supplemental data

Supplemental data 6.1. Artificial light sources used in plant cultivation

Table 6.1. Properties of common artificial light sources used in plant cultivation.

Lighting Efficiency: is luminous efficacy of a light source which produces visible light. In SI system, luminous efficacy is described as lumens per watt (lm/W); *PAR*: Photosynthetically Active Radiations: designates the part of spectral radiation from 400 to 700 nanometers that photosynthetic organisms use in the process of photosynthesis; *Spectral specificity*: shows the dominant wave band (color) of light sources; *Lifespan*: is the average time that a light source is expected to have rated service life; *Energy cost*: the cost of electricity generated by different sources typically as Euro/kWh, or $/KWh; *Heat generation*: the conversion of electricity to heat instead of photosynthetic light; *Environmental*: environmentally friendly status.

Light Category	Type	Lighting Efficiency (lm/watt)	% PAR efficiency	Spectral specificity	Lifespan (10^3 hours)	Energy cost	Price of shopping	Heat generation	Environmental
Fluorescent	Compact Fluorescent	46-75	35-40	Polychromatic (white) 492–600 nm	8-1	Low	Inexpensive	Low	Negative
	Tubular Fluorescent	70-104	20-30	Polychromatic (white) 492–600 nm	15-24	Low	Inexpensive	Low	Negative
High intensity Discharge	Metal Halide	65-115	29-32	Bluish 400 - 500 nm	10-20	Very high	Expensive	Medium	Negative
	Low Pressure Sodium	100-200	15–29	Yellowish 570-590 nm	>24	High	Expensive	Medium	Negative
	High Pressure Sodium	100-110	30-35	Golden-yellowish 570-590 nm	>24	Very high	Expensive	Medium	Negative
Solid-State	Light-Emitting Diode	58-200	80-100	Monochrome	25>	Very low	Recently inexpensive	Very low	Positive

References

Halonen L., Tetri E. & Bhusal P. (2010) IEA Annex 45 – Guidebook on Energy Efficient Electric Lighting for Buildings. Halonen L., Tetri E. & Bhusal P. (Eds.). Aalto University. 376.

Liu Y.S. (2008). An overview of the development of major light sources: from light bulbs to solid state lighting, III-Nitride Devices and Nanoengineering. Taiwan. Imperial College Press. 1-18.

Sager J.C. & McFarlane J.C. (1997). Radiation. In Plant Growth Chamber Handbook. Langhans R.W. & Tibbitts T.W. (Eds.). Iowa State University. Iowa Agriculture and Home Economics Experiment Station Special Report. 99: 1-29.

Chapter 7

High performance of vegetables, flowers, and medicinal plants in a red-blue LED incubator for indoor plant production

Mohammad R. Sabzalian[a*], Parisa Heydarizadeh[a,b], Morteza Zahedi[a], Amin Boroomand[a], Mehran Agharokh[a], Mohammad R. Sahba[a], Benoît Schoefs[b]

[a] College of Agriculture, Department of Agronomy and Plant Breeding, Isfahan University of Technology, Isfahan 84156-83111, Iran
[b] MicroMar, Mer Mole´cules Sante´, IUML - FR 3473 CNRS, Faculte´ des Sciences et Techniques, University of Le Mans, Le Mans, France

* Corresponding author
email: sabzalian@cc.iut.ac.ir
Tel: +98 31 13 91 34 52
fax: +98 31 13 91 22 54.

Agronomy for sustainable development (2014). 34: 879-886.

7.1 Abstract

In urban agriculture, plant growth is limited by the availability of light. Light emitting diodes (LED) could provide specific quality and quantity of light overcoming existing limitations for normal plant growth. However, there have been very few investigations on the applications of LED in incubators and plant growth chambers. The devices fabricated in this study, were lighted with 100%red, 100%blue, 70%red+30 % blue, or 100 % white LED. We cultivated *Mentha piperita*, *Mentha spicata* and *Mentha longifolia*, lentil, basil, and four ornamentals to test the effect of various LED lights on plants productivity compared with field and greenhouse conditions. Our results show that 70/30 % red-blue LED light increased *Mentha* essential oil yield up to four times along with increases in plant photosynthesis and fresh weight compared with field condition. Also, *Mentha* growth under fluorescent light dramatically decreased compare to the ones grown under LED. The red-blue LED incubator also led to a better growth of lentil and basil and to higher flower buds and less days to flowering for pot flowers versus

greenhouse conditions. Our findings demonstrate that LED could improve economic characteristics of plant species by probably stimulating plant metabolism.

Keywords: Essential oil, Incubator, Light emitting diodes, *Mentha*, Pot flower, Vegetable.

7.2 Introduction

Food supply shortage due to increasing population, limited cultivated lands, serious droughts, floods, and storms as well as pest and disease outbreaks and climate changes, are forcing people to indoor and urban plant production (Yeh & Chung, 2009). With demanding world of low energy input and high plant quality output, the desired planting systems should be clean; safe and eco-friendly; and simultaneously, fast, economic, and profitable. Urban culture systems and vertical farming constitute responses to these challenges to make progress in efficiently production of crop plants and vegetables.

In the past, plant culture in controlled-environments had frequent constraints particularly commercially available light sources, which could not provide a stable level of radiant energy with high photosynthetic photon flux and a spectrum close to that of sunlight. These limitations for plants growth were evident, especially for those cultured inside phytotrons and small growth chambers (incubators) (Delepoulle et al. 2008). However, the recent application of light emitting diodes (LED) in different studies suggest that they are high intensity sources of visible radiation for growing horticultural and agronomic plants under closed conditions, dominantly illuminated by blue, red, red-blue, or white LED lights (Brown et al. 1995; Yanagi & Okamoto, 1997; Duong et al. 2002; Kurilcik et al. 2008). The recent decrease of both blue and red LED price together with the increase in their brightness has made LED light as an important alternative irradiation possibility, allowing better growth and production of plants and microorganisms (Table 7.1). For recent review, see Darko et al. (2014).

The invention of light emitting diodes (LED) could be considered as the next great innovation in lighting. The basic LED consists of a semiconductor diode, *i.e.* a chip of semiconductor material doped with impurities to create a junction emitting light wavelength, depending on the band gap energy of the materials that forms the junction (Yam & Hassan, 2005). They have been evolved from low-intensity signal indicators into powerful light sources (Yeh & Chung, 2009). They are suitable for many applications from street lighting to lighting greenhouses and illuminating urban agricultural system, which is now a growing high-tech industry. With high efficiency, long life expectancy, small physical dimensions, low operating temperatures, and ease of control, LED lights are, therefore, expected to be developed further and become a light source with considerable potential for high-power lighting, as used where plant production could be continued all year round.

Table 7.1. Examples of positive effects of LED lighting on plants and microorganisms productions.

Type of LED illumination	Effects	Plant/organism	Reference
Red -10% Blue fluorescent light	Higher shoot dry weight, higher seed yield	Wheat	Goins et al. 1997
Red-Blue	Higher shoot and root fresh weight	Micropropagated strawberry plants	Nhut et al. 2000
Red-Blue	Larger and higher bulblet fresh and dry weight	Lilium	Lian et al. 2002
Red-Blue	Improved flower induction, higher number of flower buds and open flowers	Cyclamen persicum	Heo et al. 2003
Blue	Higher carotenoid production	Thraustochytriumsp CHN-1	Yamaoka et al. 2004
Red-Blue	Higher leaf area and photosynthetic rate	Radish and Lettuce	Tamulaitis et al. 2005
Blue	Astaxanthin production	Haematococcus pluvialis	Katsuda et al. 2006
Red	Better growth	Spirulina platensis	Wang et al. 2007
Red	Higher antioxidant activity	pea	Wu et al. 2007
Red	Higher rooting percentage	grape	Poudel et al. 2008
Red-Blue	Economic production	Lettuce	Martineau et al. 2012
Red	Increase in volatile molecules	Petunia, Strawberry	Colquhoun et al. 2013

LED: Light Emitting Diode

For plant culture, in addition to their monochromatic bandwidth, LED lights present several advantages including (1) maintaining constant light output over years, (2) consuming low electricity, and (3) producing low heat radiation while emitting high light intensities (Yeh & Chung, 2009). The last property allows providing higher photosynthetic photon flux levels at least 500 µmol m^{-2} s^{-1} and higher ratio of light intensity to heat radiation compared with conventional lighting systems. This introduces LED as a promising lighting source for sustainable production in growth chambers and greenhouses.

To commercialize LED-equipped systems and to make them available to the market, they must be accompanied with sophisticated accessories to assist automatically controlling and adjusting light and probably other environmental parameters. One of these growing systems was constructed and reported for the first time by Folta et al. (2005) for plant research, which could control environmental growth factors; however, plant growth performance was not reported. In the present study, to investigate the suitability of such growth chambers, they were equipped with red-blue LED arrays (Figure 7.1) in order to (1) evaluate the potential of the chambers for high quality plant production and (2) determine the effects of LED light on the growth of some medicinal and ornamental plants as compared with those grown in field or greenhouse conditions.

7.3 Material and methods

7.3.1 Growth chamber construction

The growth chamber was 1.0 width×0.6 depth×1.5 m height surrounded by thick blocks of polyurethane foam (3 cm) for insulation (Figure 7.1). A linear temperature gradient of 26–44 °C could be produced by heat flow from the warm copper block to the cool copper block through the walls, floor, and lid of the chamber (each 1 cm thick). Temperature was measured with a digital thermometer accurate to 0.1°C (ATE040, Arvin Tajhiz Espadana Co., Iran).

7.3.2 Light control system

Four sets of the control unit (CU) were independently designed to support 120 LED lights in four growth cabinets. LED arrays (OSRAM, Germany), emitting white (380–760 nm), red (650–665 nm), blue (460–475 nm), and redblue (70 %:30 %) light were affixed to a ceramic and steel support to facilitate efficient heat transfer to the mounting substrate. All the LED lights were 1.0 W (0.25 A of input current) and were driven by a circuit consisted of a standard 2 A power supply delivering 110 VDC to a common bus feeding LED lights (Kaming, Taiwan) in series. Voltage to the arrays that is the illumination intensity was tuned via a selfmade potentiometer up to 500 µmol m^{-2} s^{-1} on each separate incubator at the plant leaf surface.

Figure 7.1. Constructed light emitting diode (LED) incubator with mint plants grown under irradiation platform. This growth chamber is in size of 1.0 width×0.6 depth×1.5 m height, equipped with microcontroller for setting the plant growth parameters of light, temperature and humidity to support plant superior growth.

The light intensity was also measured via a light meter (LI-250A, LI-COR Inc., USA) with a 2 π quantum sensor (LI-190, LI-COR Inc., USA) during the plants' growth. A 0.72 K Ω (50 W) power resistor was placed in the circuit as a current limiter. Input and output capacitors were also provided to improve transient response.

This configuration was repeated for each growth chamber. The CU was outfitted with two 100 mm 12 V fans, one facing into and one facing out of the CU. Each individual LED sheet was also outfitted with a heat sink to ensure adequate cooling. A microcontroller containing a logic control for setting the growth parameters was written in the assembly language of ASM51 (Arvin Tajhiz Espadana Co., Iran) and applied on each growth cabinet to adjust temperature, LED brightness, and light/dark duration (16/8 h). The cabinets were thereafter used to raise some vegetables and potted flowers, which are economically important, not previously reported to be studied under LED illumination and cultivable in indoor environments.

7.3.3 Mint growth evaluation

Five randomly selected rhizomes with the same size of three species of mint, *i.e*. *Mentha spicata* (spear mint), *Mentha piperita* (pepper mint), and *Mentha longifolia* (horse mint) were cultured in plastic pots (10×10 cm) filled with a loam soil amended with cow manure.Mints were collected from the natural habitats of Iran (Heydarizadeh et al. 2013) and planted in the research field (Isfahan University of Technology, Isfahan, Iran, 32° 40′N, 51° 40′E). Rhizomes were planted in pots 1-cm deep. Pots from each mint species were placed in four LED incubators and in the field with three replications.

Growth temperature was set at 25±2 °C similar to the outside average daily temperature. Pots were irrigated once a day with tap water (hardness 13, pH 7.5) and nourished with nutrient solution (1 g/L) containing the main nutritive elements (K, Ca, Mg, N, P, and S) once a week. Grown plants were photographed 60 days after planting, and net CO_2 assimilation was measured by a portable photosynthesis meter (LCi ADC Instruments, UK). The aboveground part of the plants was harvested, and fresh and dry weights were determined. Dried leaves were ground using an electric grinder. The fine powder was mixed with 500-mL distilled water and submitted to distillation for 6 h using a Clevenger-type 5 apparatus (British Pharmacopoeia 1980). The oil fraction was collected and weighted, and the percentage of essential oil was calculated based on dry weight unit. Plants grown in the field at the same time were treated similarly.

7.3.4 Green and potted flower cultivation

Basil (*Ocimum basilicum* L.) and lentil (Lens culinaris Medic) were seeds planted and seedlings of primula (*Primula vulgaris* Huds.), marigold (*Calendula officinalis* L.), treasure flower (*Gazania splendens* Moore), and stock plant (*Matthiola incana* (L.) R. Br.) were transplanted into the pots (10×10 cm) filled with horticultural soil. Pots were placed inside a red-blue LED incubator (light: 500 µmol m^{-2} s^{-1}; temperature: 25±2 °C; humidity: 60±5 %) and in a greenhouse (as a control) in three replications. Plants were grown to full vegetative growth (for basil and lentil) or full flowering stage (for potted flowers), photographed and compared with plants grown under the greenhouse condition (natural light: 235–1,800 µmol m^{-2} s^{-1}; temperature: 25±2 °C; humidity: 60±5 %), in terms of days to full growth/flowering, the number of flowers, and plant height.

7.3.5 Statistical analysis

Plant pots at three replications were arranged in growth cabinets considered as different environments. Data were analyzed, using the Statistical Analysis System (SAS Institute Inc. 1999) program package, according to completely randomized design, and the combined analysis was performed to compare the environments. After an analysis of variance (ANOVA), significant differences among means were determined by least

significant difference (LSD) test ($p<0.05$). Principle components analysis (PCA) was also performed using SPSS (SPSS Inc. Chicago IL.V. 17).

7.4 Results and discussion

7.4.1 LED light effects on plant growth

To determine the effectiveness of light emitting diodes (LED) irradiation in plant production, economically important plants such as mint, basil, lentil, marigold, primula, treasure flower, and stock plant were grown conventionally (in the greenhouse) or in cabinets equipped with red-blue (70:30 %) LED. Generally, the plants grown under LED light were as healthy as or healthier than those grown in the greenhouse (Figure 7.2). In this study, except for mint, only plant parameters mainly determining the price and marketability of the plants including days to flowering and full growth, dwarfness, and profuse flowering (Roh & Lawson, 1996; Singh 2006) were recorded. As reported in Table 7.2, plants grown under red-blue LED irradiation were significantly smaller in size. Okamoto et al. (1997) also found that stem length in lettuce was decreased significantly with an increase in blue light. Under LED irradiation, basil and lentil reached to full growth, and buds of potted flowers were opened significantly earlier than those raised in the greenhouse. The plants grown for flowering developed significantly more floral buds per plants (~twofold) and produced plenty of flowers (Table 7.2).

According to our knowledge about LED lighting effects on plants, it is difficult to detail the reasons for such effects but it could be suggested that the red irradiation in the absence of far-red light is continuously stimulating phytochromes, photoreceptors controlling node elongation (Schaer et al. 1983), floral transition (Boss et al. 2004), and flowering (Runkle & Heins, 2001). On the other hand, blue light inhibits cell growth, and blue light photoreceptors might regulate and change gene expression through which stem elongation is prohibited (Lin 2000; Banerjee & Batschauer, 2005).

In *Mentha* species, plant fresh weight was significantly higher in the field in *M. piperita*, while in *M. longifolia*, redblue LED had significantly higher values than the other environments including field. For *M. spicata*, there was no significant difference in this regard between red-blue LED incubator and field. However, plant dry weight was significantly greater in the field in all species (Table 7.3).

In the absence of red light, *i.e.* in the incubator with pure blue LED, the fresh growth was significantly lower when comparedwith pure red LED, except for *M. longifolia*, which did not show significant difference between the two lighting conditions (Table 7.3). In contrast, plant dry weight was not significantly different between the two pure colors incubators; however, both had lower values than that taken from red-blue LED cabinet. It has been reported that the spectral composition of red LED matches with the red absorbance area of chlorophylls a and b present in chloroplasts of higher plants (Schoefs 2002; Wang et al. 2007), nevertheless, it has been also reported that blue light has complementary effect. Although, red light may have higher contribution to the plant

Figure 7.2. Comparison of growth of peppermint, basil, and marigold under red-blue light emitting diode (LED) in incubator (a–c) and inside greenhouse (d–f). The plants grown under red-blue LED were as healthy as or even better than those grown in greenhouse in terms of productivity or the number of flowers.

Table 7.2. Mean (±SE) comparison of potted plants grown under LED incubator and greenhouse in terms of days to flowering/full growth, the number of flowers and height, indicating the superiority of red-blue LED incubator.

Plant	Species	Planting Source	Environment	Days to flowering/full growth	No. Flowers/pot	Height (cm)
Basil	*Ocimum basilicum*	Seed	Red-Blue LED incubator	25±2.1b*	----	23±5.6b
			Greenhouse	50±7.6a	----	47±8.9a
Lentil	*Lens culinars*	Seed	Red-Blue LED incubator	21±1.5b	----	19±2.5b
			Greenhouse	30±5.3a	----	28±4.3a
Primula	*Primula vulgaris*	Seedling	Red-Blue LED incubator	18±2.2b	20±4.4a	12±2.1b
			Greenhouse	40±6.3a	10±3.6b	20±5.5a
Marigold	*Calendula officinalis*	Seedling	Red-Blue LED incubator	20±1.5b	30±5.2a	16±1.8b
			Greenhouse	50±6.7a	15±6.3b	28±4.8a
Treasure flower	*Gazania splendens*	Seedling	Red-Blue LED incubator	37±2.6b	15±4.5a	18±2.3b
			Greenhouse	60±6.9a	7±2.1b	32±7.2a
Stock	*Matthiola incana*	Seedling	Red-Blue LED incubator	28±1.1b	45±4.5a	21±2.3b
			Greenhouse	58±8.5a	22±4.8b	36±6.4a

LED: light Emitting Diode and SE: Standard Error of means

*means followed by different letters in each column in each plant are significantly different according to LSD test ($p<0.05$)

Table 7.3. Mean comparisons of fresh and dry weight, height, water content, essential oil and photosynthetic rate of mint plants, sampled 60 days after planting, grown in different LED cabinets and field condition.

Incubator/ Environment	Mint species	Photosynthesis (µMol Co_2 m^{-2} s^{-1})	Height (cm)	Fresh weight (g/plant)	Dry weight (g/plant)	Dry weight (g) cm^{-1}	Water content (% of fresh weight)	Essential oil content (% of dry weight)
Red LED	*M. piperita*	14.28	20.8	16.73	2.24	0.11	86.61	7.00
	M. spicata	8.74	24.1	18.72	2.21	0.09	88.20	4.34
	M. longifolia	5.62	28.1	13.37	1.89	0.07	85.84	4.37
Blue LED	*M. piperita*	8.83	12.1	6.39	1.27	0.10	80.04	3.11
	M. spicata	4.96	12.7	6.24	1.24	0.10	80.10	5.03
	M. longifolia	3.21	16.2	10.27	1.95	0.12	81.02	3.19
Red-Blue LED	*M. piperita*	20.70	13.2	27.36	4.45	0.34	83.71	5.12
	M. spicata	16.17	14.5	25.89	4.17	0.29	83.89	2.60
	M. longifolia	6.48	19.4	36.99	6.10	0.31	83.50	4.86
White LED	*M. piperita*	15.27	23.5	16.03	2.67	0.11	83.33	2.34
	M. spicata	10.81	26.7	17.85	3.30	0.12	81.48	2.58
	M. longifolia	4.52	31.9	17.70	2.70	0.08	84.75	3.53
Field	*M. piperita*	18.89	52.1	32.90	11.23	0.22	65.87	1.40
	M. spicata	14.00	52.1	23.06	7.47	0.14	67.61	0.66
	M. longifolia	4.61	59.7	11.60	8.08	0.14	30.34	3.33
LSD* (0.05)	--------	2.08	5.65	3.31	1.06	0.03	5.31	0.59

LSD: Least Significant Difference; LED: Light Emitting Diode

*means having difference lower than LSD are not significantly different ($P<0.05$).

photosynthesis, our results indicate that neither pure red nor blue LED is enough to satisfy full growth of mint. Brown et al. (1995) compared pepper (*Capsicum annuum* L.) plants grown under red LED with similar plants grown under red LED plus blue light emitted from fluorescent lamps. Pepper biomass was reduced when plants were grown under red LED light without blue wavelengths, compared with those grown under supplemental blue lamps.

Therefore, it seems that plant species could not terminate their normal growth under pure red LED light (Yorio et al. 2001). The plants grown under white LED light displayed a significantly higher fresh weight than blue LED light (Table 7.3), but except for *M. longifolia*, there was no significant difference between white and red LED lights in this respect. White light is a combination of low intensities of red and blue lights and other low efficient light wavelengths, diluting the effect of red-blue light on the net photosynthesis. This may decrease the growth rate of plants illuminated by white light compared with red-blue LED lights.

Among LED lights, the maximum height belonged to the plants grown under white and red, whereas those grown under blue and red-blue were significantly shorter. However, plants grown in the field were taller than those raised under LED lights (Table 7.3). Light quality, especially blue and red wavelengths, controls the opening and closure of stomata (Shimazaki et al. 2007). This may change the amount of water in plant tissues, which in turn can affect plant size and height. As indicated in Table 7.3, the water content in plants grown in the LED cabinets fluctuated from 80.04 to 88.20 %, while the water content of plants raised in the field never exceeded 67.61 %. These data suggest that the shorter height of plants grown under LED compared with field was not related to water shortage. Instead, the constant solicitation of blue photoreceptors is likely the source of reduction of plant size. The results showed that red-blue LED light improved water content and fresh weight of mint plants as good as or even better than field condition. It is worth mentioning that high fresh weight and water content are the two important characteristics of mint for fresh uses.

Since the total biomass production of plants could be influenced by plant size as a function of light quality, the dry weight per each height unit was used as a proxy of yield index after 2 months. The lowest values of 0.08–0.12 g dry weight cm−1 were found under red and white LED irradiation and the highest values of 0.29–0.34 g dry weight cm−1 were observed under red-blue LED. The values obtained for the plants grown in the field were intermediate (Table 7.3). The spectral composition of blue (460–475 nm) and red (650–665 nm) LED fits well to the light absorption spectrum of carotenoids and chlorophyll pigments (Schoefs 2002). Therefore, it was determined whether the increase in dry weight per plant size unit is due to an increase in the photosynthetic activity of the plants.

To test this, the CO_2 fixation was first measured and then principle components analysis (PCA) was performed in order to understand the relation between photosynthesis rate and the other variables (Figure 7.3). Despite the fact that the values of photosynthesis greatly varied with species and light quality, the highest values were always found in *M.*

piperita and the lowest in *M. longifolia* (Table 7.3). The plot of depicting variables based on the two first principle components shows no particular trend between the photosynthetic activity and dry weight, suggesting that the strategy In utilization of fixed CO_2 is different, depending on the light source. However, there was high collinearity between dry weight per plant size and fresh weight with photosynthesis indicating that higher photosynthesis under LED is correlated with increase in fresh and specific dry weight.

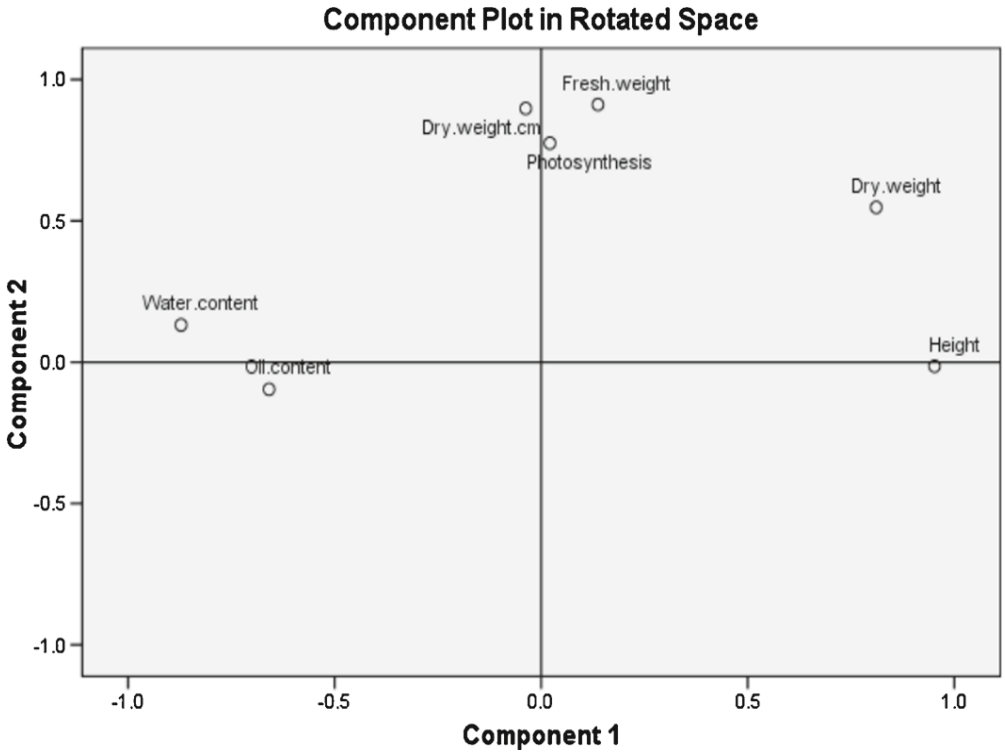

	Rotated Components	
Characteristic	1	2
Photosynthesis	0.021	0.775
Height	0.952	-0.014
Fresh Weight	0.137	0.912
Dry Weight	0.811	0.548
Dry Weight cm^{-1}	-0.038	0.898
Water content	-0.872	0.132
Oil Content	-0.659	-0.096
% of variance	45.29	31.05

Figure 7.3. The collinearity among mint characteristics using principle components analysis. The plot of principle components shows high trend between the photosynthetic activity with fresh weight and dry weight per plant size indicating that higher photosynthesis under LED is correlated with increase in fresh and specific dry weight.

7.4.2 LED light effects on mint essential oil

It has been well-established that light quality constitutes signals that can trigger metabolic modifications (Liu et al. 2004). To test this with LED light, three mint species grown in growth cabinets each equipped with red, blue, red-blue, or white LED were analyzed for their essential oil content. Our results demonstrated that mint plants of all three species grown under red or red-blue LED light accumulated dramatically higher essential oil content compared with those grown in the field. The maximum increase in oil content was fourfold higher in *M. piperita* grown under red LED light compared with the field. Under blue or white LED light, significant increases in essential oil content were also observed compared with the field except for *M. longifolia* (Table 7.3).

There is limited information on stimulation of the essential oil accumulation in plants with medicinal properties under LED lights. It seems that red LED may affect the metabolic pathways, leading to an increase in essential oil content. The positive effect of LED light on metabolic pathways has not been well-documented; however, there are possible hypotheses about the role of LED light on increasing biosynthesis of some metabolites. Liu et al. (2004) hypothesized that red LED light may repress the expression of negative regulator genes of pigmentation like LeCOP1-LIKE, resulting in plants with dark green leaves and elevated carotenoid levels. It has been also postulated that LED light could affect secretion or stability of or sensitivity to phytohormones, consistent with the improvement in morphogenesis and productivity of the plant in response to LED lighting (Tamulaitis et al. 2005). However, how these changes take place and affect essential oil accumulation is not yet known and warrant further investigations because of their high positive impact on economic extraction and value of essential oil from plants grown under LED lighting.

7.5 Conclusion

The development of human population mostly relies on plant species for nutrition, health, and other human activities. Due to environmental constraints and limited cultivated lands, it is critical to develop indoor systems, allowing significantly higher or at least similar production of yield than outdoor environments. To fulfill this demand, a LED incubator was constructed and evaluated in this study. It offers LED lighting regimes supporting complete plant growth and development.

The device provided conditions for a faster growth of mint, lentil and basil, and some ornamental plants in our experiments. LED lights were used because they do not include the drawbacks of traditional nondurable lamp systems. The results of this work demonstrated that the studied vegetables and potted flowers took benefits from LED lighting such as dwarfness and increased essential oil production. Among the LED light qualities, most of the beneficial effects were best obtained when red-blue illumination was applied. This conclusion agreed with those attained on the growth and morphogenesis of lettuce and radish in the previous research. LED lighting may provide

a novel tool and a new challenge for agricultural research and production alongside its influence on plant morphology and composition. LED lights could be easily integrated into incubators having control systems in which complex lighting programs are facilitated, including selected spectral composition over a growth period or the whole plant developmental stage for improving quality and economic yield of plant species.

7.6 Acknowledgments

The corresponding author would like to thank the Iranian National Elites Foundation and Isfahan University of Technology for the financial support of this research. BS also thanks the University of Le Mans for support. We would also like to express our appreciation to Mr. Ehsan Ataii for the assistance in conducting experiments and Prof. Aghafakhr Mirlohi for the critical review of the preliminary draft of this manuscript.

7.7 References

Banerjee R. & Batschauer A. (2005). Plant blue-light receptors. Planta 20: 498–502.

Boss P.K., Bastow R.M., Mylne J.S. & Dean C. (2004). Multiple pathways in the decision to flower: enabling, promoting, and resetting. Plant Cell 16: S18–S31.

British Pharmacopoeia, (1980) H. M. S. Office. 2, London, 109–110.

Brown C.S., Schuerger A.C. & Sager J.C. (1995). Growth and photomorphogenesis of pepper plants under red light-emitting diodes with supplemental blue or far-red lighting. JAmSocHortic Sci 120: 808–813.

Colquhoun T.A., Schwieterman M.L., Gilbert J.L., Jaworski EA., Langer K.M., Jones C.R., Rushing G.V., Hunter T.M., Olmstead J., Clark D. & Folta K.M. (2013). Light modulation of volatile organic compounds from petunia flowers and select fruits. Postharvest Biol. Technol. 86: 37–44.

Darko E., Heydarizadeh P., Schoefs B. & Sabzalian M.R. (2014). Photosynthesis under artificial light: the shift in primary and secondary metabolism. Phil Trans R Soc B. 20130243.

Delepoulle S., Renaud C. & Chelle M. (2008). Improving light position in a growth chamber through the use of a genetic algorithm. In: Plemenos D. & Miaoulis G. (Eds.). Artificial Intelligence Techniques for Computer Graphics Studies in Computational Intelligence, Springer, Berlin, Heidelberg, 67-82.

Duong T.N., Hong L.T.A., Watanabe H., Goi M. & Tanaka M. (2002). Growth of banana plantlets cultured *in vitro* under red and blue light-emitting diode (LED) irradiation source. Acta Hort. 575: 117–124.

Folta K.M., Koss L.L., McMorrow R., Kim H.H., Kenitz J.D., Wheeler R. & Sager J.C. (2005). Design and fabrication of adjustable red-green-blue LED light arrays for plant research. BMC Plant Biol. 5: 17.

Goins G.D., Yorio N.C., Sanwo M.M. & Brown C.S. (1997). Photomorphogenesis, photosynthesis, and seed yield of wheat plants grown under red lightemitting diodes (LEDs.) with and without supplemental blue lighting. J. Exp. Bot. 48:.1407–1413.

Heo J.W., Lee C.W., Murthy H.N. & Paek K.Y. (2003). Influence of light quality and photoperiod on flowering of Cyclamen persicum Mill. cv. 'Dixie White'. Plant Growth Regul. 40: 7–10.

Heydarizadeh P., Zahedi M., Sabzalian M.R. & Ataii E. (2013). Mycorrhizal infection, essential oil content and morpho-phenological characteristics variability in three mint species. Sci. Hortic. 153: 136–142.

Katsuda T., Shimahara K., Shiraishi H., Yamagami K., Ranjbar R. & Katoh S. (2006). Effect of flashing light fromblue light emitting diodes on cell growth and astaxanthin production of Haematococcus pluvialis. J. Biosci. Bioeng. 102: 442–446.
Kurilcik A., Miklusyte-Canova R., Dapkuniene S., Zilinskaite S., Kurilcik G., Tamulaitis G., Duchovskisand P. & Zukauskas A. (2008). *In vitro* culture of Chrysanthemum plantlets using light-emitting diodes. Cent. Eur. J. Biol. 2: 161–167.
Lian M.L., Murthy H.N. & Paek K.Y. (2002). Effects of light emitting diodes (LEDs) on the *in vitro* induction and growth of bulblets of Lilium oriental hybrid 'Pesaro'. Sci. Hortic. 94: 365–370.
Lin C. (2000). Plant blue-light receptors. Trends Plant Sci. 5: 337–342.
Liu Y., Roof S., Ye Z., Barry C., van Tuinen A. & Vrebalov J. (2004). Manipulation of light signal transduction as a means of modifying fruit nutritional quality in tomato. PNAS 101: 9897–9902.
Martineau V., Lefsrud M., Tahera Nazanin M. & Kopsell D.A. (2012). Comparison of light-emitting diode and high-pressure sodium light treatments for hydroponics growth of Boston lettuce. Hortscience 47: 477–482.
Nhut D.T., Takamura N.T., Watanabe H. & Tanaka M. (2000). Light emitting diodes (LEDs) as a radiation source for micropropagation of strawberry. In: Kubota C. & Chun C (Eds.). Transplant production in the 21st century, Kluwer Academic Publishers, Dordrecht, The Netherlands, 114–118.
Okamoto K., Yanagi T. & Kondo S. (1997). Growth and morphogenesis of lettuce seedlings raised under different combinations of red and blue light. Acta Horticult. 435: 149–157.
Poudel P.R., Kataoka I. & Mochioka R. (2008). Effect of red- and blue-lightemitting diodes on growth and morphogenesis of grapes. Plant Cell Tissue Organ Cult. 92: 147–153.
Roh M.S. & Lawson R.H. (1996). Requirements for new floral crops-perspectives for the United States of America. Acta Horticult. 454: 29–38.
Runkle E.S. & Heins R.D. (2001). Specific functions of red, far red, and blue light in flowering and stem extension of long-day plants. J. Am. Soc. Hortic. Sci. 126: 275–282.
SAS Institute, Inc (1999) SAS/STAT User's Guide. SAS Institute, Inc, Cary.
Schaer J.A., Mandoli D.F. & Briggs W.R. (1983). Phytochrome-mediated cellular photomorphogenesis. Plant Physiol. 72: 706–712.
Schoefs B. (2002). Chlorophyll and carotenoid analysis in food products. Properties of the pigments and methods of analysis. Trends Food Sci. Technol. 13: 361–371.
Shimazaki K., Doi M., Assmann S.M. & Kinoshita T. (2007). Light regulation of stomatal movement. Annu. Rev. Plant Biol. 58: 219–247.
Singh A.K. (2006). Flower crops: cultivation and management. New India Publishing Agency, Pitampuram.
Tamulaitis G., Duchovskis P., Bliznikas Z., Breive K., Ulinskaite R., Brazaityte A., Novickovas A. & Zukauskas A. (2005). Highpower light-emitting diode based facility for plant cultivation. J. Phys. D. Appl. Phys. 38: 3182–3187.
Wang C.Y., Fub C.C. & Liu Y.C. (2007). Effects of using light-emitting diodes on the cultivation of Spirulina platensis. Biochem. Eng. J. 37: 21–25.
Wu M.C., Hou C.Y., Jiang C.M., Wang Y.T., Wang C.Y., Chen H.H. & Chang H.M. (2007). Novel approach of LED light radiation improves the antioxidant activity of pea seedlings. Food Chem. 101: 1753–1758.
Yam F.K., Hassan Z. (2005). Innovative advances in LED technology. Microelectron J. 36: 129–137.
Yamaoka Y., Carmona M.L. & Oota S. (2004). Growth and carotenoid production of Thraustochytrium sp. CHN-1 cultured under super-bright red and blue light-emitting diodes. Biosci Biotechnol. Biochem. 68: 1594–1597.
Yanagi T. & Okamoto K. (1997). Utilization of super-bright light emitting diodes as an artificial light source for plant growth. Acta Horticult. 418: 223–228.
Yeh N. & Chung J.P. (2009). High-brightness LEDs-energy efficient lighting sources and their potential in indoor plant cultivation. Renew Sustain. Energ. Rev. 13: 2175–2180.

Yorio N.C., Goins G.D., Kagie H.R., Wheeler R.M. & Sager J.C. (2001). Improving spinach, radish, and lettuce growth under red lightemitting diodes (LEDs) with blue light supplementation. Hort sci. 36: 380–383.

Chapter 8

The effects of light and mycorrhizal symbiosis on growth parameters and essential oil of three mint species

8.1 Abstract

This experiment was conducted to evaluate the effects of light quality and mycorrhizal symbiosis on growth and essential oil of three mint species (*Mentha spicata*, *Mentha piperita* and *Mentha longifolia*). The genotypes were inoculated with three species of AMF including *Glomus clarum*, *G. mosseae* and *G. etunicatum*. The pots were placed inside LED incubators, containing red, blue, red+blue, white and fluorescent lights. Two different light intensity treatments including 150 and 500 µmol photon m^{-2} s^{-1} were applied. Morphological characteristics and essential oil content of plants in each condition were measured and compared. The highest shoot dry weight of plants grown under 150 µmol m^{-2} s^{-1} belonged to *M. spicata*. Under 500 µmol m^{-2} s^{-1}, there were no big differences of shoot fresh and dry weight among three species. Under 150 µmol m^{-2} s^{-1} *G. etunicatum* was the best species to increase mint dry weight, and white LED was the most effective light in this respect. Blue and red+blue LED increased shoot fresh and dry weight under 500 µmol m^{-2} s^{-1}. In general, mint vegetative growth was higher under 150 µmol m^{-2} s^{-1} and essential oil content increased in plants grown under 500 µmol m^{-2} s^{-1}. *M. piperita* and *M. longifolia* produced more essential oil especially under red and red+blue LED. Among three AMF species, *G. mosseae* stimulated essential oil content, especially in *M. piperita* and *M. longifolia*. In this study plant mycorrhization did not change dramatically growth and essential oil content compare to non-mycorrhizal plants.

8.2 Introduction

Light quality and quantity are among the most important required invironmentl factors for plant growth and developement (Furlan & Fortin, 1977; Ferguson & Menge, 1982). In indoor culture, supplemental lighting is used to increase the photosynthetic daily light integral (total amount of photosynthetically active light received in a day) in temperate climates and to extend the photoperiod to increase growth and hasten

development of horticultural crops (Suzuki et al. 2011). Semiconductor light-emitting diodes (LEDs) are the most recent and highligted candidates to reach this aim by increase photosynthesis and therefore crop growth in greenhouse and nursery environments (Girón González, 2012).

In addition of improve in lighting system for indoor culture, improvement of nutrient absorption can also lead to benefit the culture as much as possible. In this respect, arbuscular mycorrhizal fungi have been widely used in agriculture to improve the cultivation of many crops. Naturally, their associations are the predominant form of symbiosis in aromatic plants including *Mentha* species, with different colonization range (Karagiannidis et al. 2011; del Rosario Cappellari et al. 2015). In particular for mint, there are reports that root colonization by AM fungi improved growth, quality and quantity of essential oils and nutrient uptake, depending upon plant variety (Gupta et al. 2002; Karagiannidis et al. 2011; Adolfsson et al. 2015). Anyway, the effect of AM fungi on plants depends strongly on the extent of colonization (Copetta et al. 2006) and affect by the quality and quantity of light (Furlan & Fortin, 1977; Ferguson & Menge, 1982; Hayman, 1983).

In spite of the LEDs capacity to emit high intensity monochromic light at a wide range of spectrum, but the variation of light spectra used in plant research is still limited, including red, blue and to a lesser extend yellow (Pinho et al. 2007; Lee et al. 2010), green and far-red (Tamulaitis et al. 2005; Stutte et al. 2009; Ilieva et al. 2010; Johkan et al. 2012) independently or in mixed ratios. In addition, there is no report on the effect of LEDs on mycorrhizal colonization in aromatic plants. Therefore, the present study consists of a comparative analysis of the effects induced by three AM fungi under different LED light quality and quantity, on plant growth and essential oil production. This can help for comparing the benefits and drawbacks of different light quality and quantity, and the morphological and physiological responses of plants grown under them, to improve profitability and production of this plant.

8.3 Material and Methods

8.3.1 Mycorrhizal inoculation

In order to assess the effect of Arbuscular Mycorrhiza Fungi (AMF) on growth parameters and essential oil content of mint plant, three different species of the genus *Glomus* (obtained from Soil and Water Research Institute, Karaj, Iran) including *G. etunicatum, G. mosseae* and *G. clarum* were used separately for inoculation of three *Mentha* species including, *M. spicata* (Esfahan), *M. piperita* (Ghazvin), *M. longifolia* (Hamedan) (see Figure 5.1 in chapter 5).

Three randomly selected stolones with the same size (five-cm) of three species of mint were cultured in plastic pots (10×20 cm), two-third filled with a loam soil amended with compost. Inoculation was done by deposition of 10 g of soil inoculum (containing +

150 spores of AMF + root segments of *Sorghum bicolor* L.), right underneath the stolones, except for the uninoculated controls.

8.3.2 Growth chamber condition

Different light qualities (100% blue LED, 100% red LED, 70% red + 30% blue, white LED (Figure 8.1), warm white flourescent cabinet) and two light intensities (150 and 500 µmol m^{-2} s^{-1}) were used to set the experiment (temperature: 25±2 °C; humidity: 60±5 %; 16/8 light/dark duration). Incubated plants were placed in each cabinet in a randomized complete block design with three replications. Pots were irrigated once a day with tap water (hardness 13, pH 7.5) and after the first leaf appearance nourished twice a week with nutrient solution (Hoagland & Arnon 1950). The aboveground part of the plants was harvested 60 days after planting and fresh and dry weights, height, branch number and essential oil content were determined as explained before. Also, roots were collected for mycorrhizal colonization assessments, as explained before (see chapter 5, part 5.3.3).

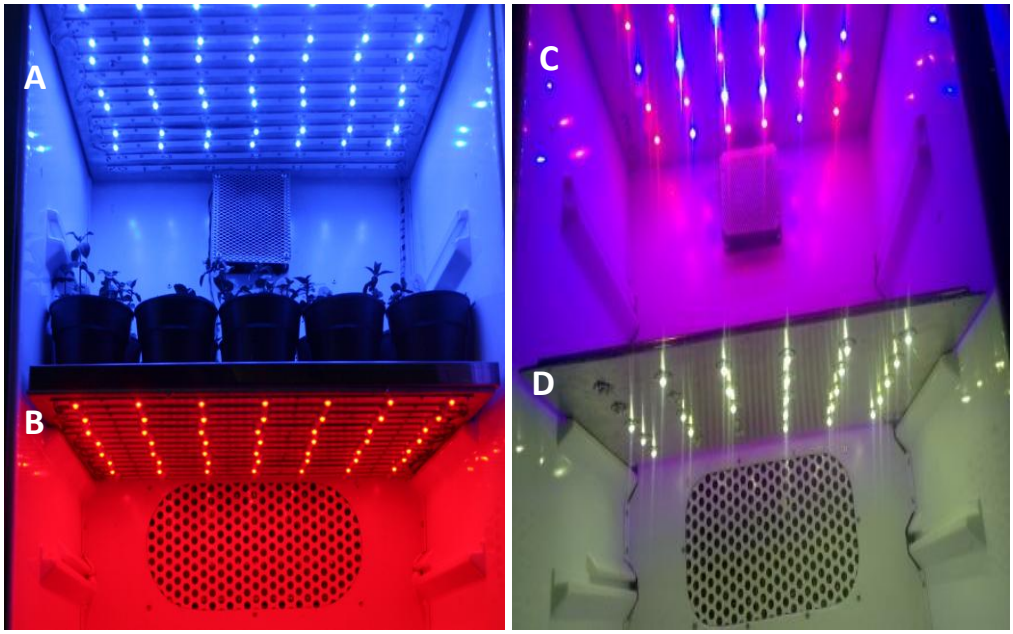

Figure 8.1. Cabinets with LED irradiations. (A) blue, (B) red, (C) 70% red + 30% blue, (D) white

8.3.3 Statistical analysis

Data were analyzed, using the Statistical Analysis System (SAS Institute Inc. 1999) as explained before (see chapter 5, part 5.3.5)

8.4 Results

8.4.1 Development of *Mentha* species and AMF under different light conditions

Two levels of light intensity (150 and 500 µmol m^{-2} s^{-1}) were applied to study the influence of light quality on fungal colonization and plant developement.

Growth under 150 µmol m^{-2} s^{-1}

Under low light intensity, *M. spicata* had the highest percentage of colonization with mycorrhiza (except under red LED) and also highest vegetative growth including height, branch number, fresh and dry weight, in all wavelengths, except under fluorescent illumination (Table 8.1). The results showed that *M. longifolia* could grow better under fluorescent incubator, compare to the two others. The lowest percentage of colonization belonged to *M. longifolia* under red LED.

Inoculation of *Mentha* species with mycorrhiza increased their vegetative growth compare to non-mycorrhizal plants and *G. etunicatum* was the most effective mycorrhizal genotype to increase fresh weight (27.5, 13.5 and 14.1 g/plant) and dry weight (4.61, 2.43 and 2.34 g/plant) in *M. spicata*, *M. longifolia* and *M. piperita*, respectively (Table 8.2). In non-mycorrhizal plants these value decreased for fresh weight (14.1, 7.74 and 8.43 g/plant) and dry weight (2.49, 1.48 and 1.45 g/plant) in *M. spicata*, *M. longifolia* and *M. piperita,* respectively.

The positive effects of *G. etunicatum* to increase fresh and dry weight were also observed with the interaction effects between wavelengths and mycorrhizal genotypes (Table 8.3). The most percentage of AMF colonization belonged to *G. etunicatum* in all light conditions mostly under white LED (75.6 %), while the less colonization was also observed under white LED but with the symbiosis of *G. mosseae* (4.34 %).

In general, by taking to account all the interaction between lights, plants and AMF, the results releaved that blue, red+blue and white LED stimulated the colonization and *G. etunicatum* had the highest colonization rate (49.8%) (Table 8.4). In general, *M. spicata* had the highest height, branch number, fresh and dry weight, while the lowest belonged to *M. piperita*. White light significantly increased height, branch number, fresh and dry weight and blue light was the most effective light after white, to increase these traits.

Growth under 500 µmol m^{-2} s^{-1}

The same trend was observed for the mycorrhizal colonization under different light conditions, compare to low light (Table 8.1). *M. spicata* had the highest colonization under blue (34.8 %), red + blue (26 %) and white LED (21.0 %), while *M. piperita* had the highest colonization under red LED (30.3 %) and fluorescent (19.2 %). The less percent of colonization observed under red LED in *M. longifolia* (7.17 %). Under blue LED the highest growth characteristics belonged to *M. longifolia* and under other light conditions they vried and did not follow this rythem. For instance, fresh weight under red LED belonged to *M. spicata* (15.4 %) and under red + blue and white LED belonged to *M. piperita* (16.3, 11.2 %, respectively) and under fluorescent belonged to *M. longifolia* (11.8 %).

Under high light, interaction effects between *Mentha* species and mycorrhizal genotypes showed increase of growth in the plants inoculated with mycorrhiza compare to non-mycorrhizal plants, as it was the case also under low light (Table 8.2). *G. etunicatum* effectively increased height (except in *M. piperita*), fresh weight (14.7, 12.7 and 11.9 g/plant) and dry weight (2.51, 2.45 and 1.96 g/plant) in *M. spicata*, *M. longifolia* and *M. piperita*, respectively.

G. etunicatum had more colonization with plant species in all light conditions, compare to the two other mycorrhiza (Table 8.3) and the highest colonization abtained under white LED (54.5 %). Colonization of *G. clarum* in plants remained weak under different lights (between 9.28-20.6 %), while *G. mosseae* had lower colonization than *G. clarum* in some conditions including red LED (13.0 %) and white LED (8.86 %). The positive effects of *G. etunicatum* to increase fresh and dry weight were observed under red + blue, white and fluorescent light. Surprisingly, under blue LED, non-mycorrhizal plants had fresh and dry weight as high as inoculated plants with *G. clarum*.

In general, the highest colonization was observed in *M. spicata* (23.1%) and blue, red + blue and white LED were the most effective lights to increase colonization percentage (Table 8.4). *G. etunicatum* had the highest colonization (41.4%). White light stimulated branch number in *Mentha* species, while the plants under red light had the lowest number of branch. *M.piperita* had the highest height and branch number (Table 8.4). Ioculation of plants with *G. etunicatum* increased height, fresh and dry weight, as well as under 150 µmol m^{-2} s^{-1}. Red+blue was the most effective lights to increase fresh and dry weight in plants.

Comparison between two light intensities releaved that vegetative growth of *Mentha* species was higher under 150 µmol m^{-2} s^{-1}. We observed that fungal colonization, height and fresh weight were significantly higher under low light intensity compare to high light (Table 8.4). In this respect the traites increased by 13.3, 53 and 10.9 %, respectively. Branch number was higher under high light (44.5 %) and there was no significant difference in dry weight between two light intensities.

8.4.2 Essential oil content under different lights

In both low light and high light intensities plants behaved differently under different vawelenghts and none of them could produce detectable essential oil under fluorescent light (Table 8.1). Blue LED increased essential oil content in *M. spicata*, while red and white lights increased oil content mostly in *M. piperita*. This result was observed under low and high light conditions.

The most essential oil content in *M. longifolia* and *M. piperita* achieved with inoculation by *G. etunicatum* under both low light (3.38 and 5.41 %) and high light (2.66 and 4.28 %), respectively (Table 8.2).

Interaction between light and mycorrhizal genotypes shwod that *G. mosseae* significantly increased essential oil content in all wavelengths and both light intensities (Table 8.3). Plants grown under fluorescent remained weak with undetectable essential oil production (Table 8.4 and figure 8.1).

In general, by comparison of interactions between experimental components, *i.e.* light, *Mentha* species and mycorrhizal genotypes, we observed that essential oil content was higher under 500 µmol m^{-2} s^{-1}, around 37.1 %, compare to 150 µmol m^{-2} s^{-1} (Table 8.4). There was no significant defferences between *Mentha* species for essential oil production under low light, while *M. longifolia* and *M. piperita* produced more essential oil under high light intensity. Red LED was the best wavelength and *G. mosseae* was the best mycorrhizal genotype to increase essential oil. Generally, the production of non-mycorrhizal plants did not differ with the plant inoculated with *G. clarum* and *G. etunicatum*.

8.5. Discussion

The inoculated plants displayed a higher vegetative growth compare to control (non-inoculated plants), under two light intensities (Table 8.4). Studies about arbuscular mycorrhizal (AM) fungi with aromatic plants interaction have shown increases in plant growth and esential oil production (Copetta et al. 2006; Khaosaad et al. 2006; Zeng et al. 2013; del Rosario Cappellari et al. 2015). The effects of mycorrhization by *Glomus* species in increase of height, fresh and dry weight in aromatic plants including *M. arvensis* (Gupta et al. 2002), *M. spicata* (Bagheri et al. 2015), *M. piperita* (del Rosario Cappellari et al. 2015), *Ocimum basilicum* (Zolfaghari et al. 2013), *Glycyrrhiza glabra* L. (Yadav et al. 2013), *Origanum majoranum (*Devi & Reddy, 2002) has been reported.

Anyway they are some conflicts between several studies that show different plant species may have different responses to the same light wavelenght. For instance, in the study performed by Okamoto et al. (1997) on lettuce, plant height significantly decreased under blue LED, while in another study plant height of *Perilla frutescens* (from Lamiaceae family) increased under blue LED compare to red, red + blue LED and white fluorescent light (Ogawa et al. 2012). The decrease of height can be due to the inhibition effects of blue light on cell growth and also blue light photoreceptors might regulate and

change gene expression through which stem elongation is prohibited (as it is described in chapter 7; see also Huché-Thélier et al. 2016).

Mycorrhization leads to increase plant growth based on three main functions of the AM fungi: (i) stimulation of plant development by impacting the phytohormone balance; (ii) enhancement of plant fitness by increasing resistance or tolerance to biotic and abiotic stress; and (iii) improvement of plant nutrition by supplying mineral nutrients, particularly inorganic phosphate (Smith & Read, 2008, Adolfsson et al. 2015). It seems that allocation of primary production differs depending on the growth condition, plant species and AM fungal species (Kaschuk et al. 2009; Adolfsson et al. 2015).

Inoculated plants grown under 150 μmol m^{-2} s^{-1} had higher height, percent of colonization and fresh weight compare to the plants grown under 500 μmol m^{-2} s^{-1} (Table 8.4). The response of plants to colonization by AMF depends mainly on the host plant and fungal species, as well as environmental conditions, such as light intensity, nutrient levels, temperature, *etc.* (Smith & Smith 1996). There is no report about the effect of different LED quality and quantity on mycorrhizal colonization and growth parameters of higher plants. Increasing the intensity of fluorescent lamps, stimulated growth in onion (Hayman, 1974). Colonization of Sudan grass, inoculated by *Glomus fasciculatum,* as measured by root infection and sporulation, increased with increasing light intensity (Ferguson & Menge, 1982).

According to the results of this study, each genotype of mycorrhiza was more effective in some conditions and by changing the light intensity or wavelength the efficiency of mycorrhiza could decrease. In addition to environmental condition and plant species, the importance of AM fungal species is also important for plant production (Kaschuk et al. 2009). For instance in our study, in some conditions, non-mycorrhizal plants had better growth than inoculated plants (Table 8.4). One reason might be related to the condition of our experiments that plants did not face water deficiency, while mycorrhizal fungi are more effective under drought, for host plant (Augé et al. 2015; Ruiz-Lozano et al. 2015).

LEDs stimulated plants growth and essential oil production more than fluorescent light. Indeed, Positive effects of different LED quality on plant production has been reported in several studies (Avercheva et al. 2012; Ogawa, et al. 2012; Dayani et al. 2016). Essential oil content of mycorrhizal plants increased under 500 compare to 150. It has been reported that isoprenoids are key components of the antioxidant defense system of plants facing severe excess light stress (Brunetti et al. 2015). Red LED stimulated essential oil production more than the other LED lights.

There is no information on stimulation of the essential oil accumulation in mycorrhizal plants with medicinal properties under LED lights. For more details on the effect of red light on essential oil production of plants see chapter 7, part 7.4.2.

Table 8.1. Mean comparison of light (quality and quantity) and *Mentha* species on morphophenological characteristics and essential oil content.

Light quality		150 µmol m^{-2} s^{-1}						500 µmol m^{-2} s^{-1}					
	Mentha species	Colonization (%)	Height (cm)	Branch number	Dry weight (g/plant)	Fresh weight (g/plant)	Essential oil content (%)	Colonization (%)	Height (cm)	Branch number	Dry weight (g/plant)	Fresh weight (g/plant)	Essential oil content (%)
Blue	*M.spicata*	41.8^{a}	52.7^{a}	11.2^{a}	3.89^{a}	20.4^{a}	2.46^{a}	34.8^{a}	14.8^{c}	7.83^{b}	2.30^{ab}	11.8^{b}	3.71^{a}
	M.longifolia	14.9^{b}	25.4^{c}	2.66^{c}	1.68^{c}	8.67^{c}	2.24^{b}	11.9^{c}	36.1^{a}	11.0^{a}	2.80^{a}	15.4^{a}	3.65^{b}
	M.piperita	13.5^{bc}	45.0^{b}	5.0^{b}	2.35^{b}	12.5^{b}	1.95^{c}	18.6^{b}	16.4^{b}	1.91^{c}	1.58^{c}	7.64^{c}	3.29^{c}
Red	*M.spicata*	15.5^{b}	51.5^{a}	10.3^{a}	2.08^{a}	16.6^{a}	2.33^{b}	15.3^{b}	19.7^{c}	7.33^{a}	2.00^{ab}	15.4^{a}	3.51^{b}
	M.longifolia	9.36^{c}	30.2^{c}	2.41^{b}	0.89^{c}	7.03^{c}	2.12^{c}	7.17^{c}	27.9^{b}	4.29^{b}	1.60^{c}	9.26^{c}	3.41^{c}
	M.piperita	34.0^{a}	47.4^{b}	2.16^{b}	1.05^{b}	8.17^{b}	3.34^{a}	30.3^{a}	33.7^{a}	4.50^{b}	2.67^{a}	14.3^{b}	4.92^{a}
Red+Blue	*M.spicata*	36.3^{a}	45.7^{a}	5.08^{a}	3.42^{a}	21.0^{a}	1.90^{b}	26.0^{a}	21.5^{c}	10.3^{b}	2.92^{a}	15.8^{b}	3.01^{b}
	M.longifolia	18.1^{b}	24.7^{c}	3.41^{b}	1.78^{b}	10.9^{b}	2.64^{a}	13.8^{c}	28.8^{b}	13.2^{a}	2.31^{ab}	13.4^{c}	4.12^{a}
	M.piperita	15.8^{c}	36.7^{b}	5.33^{a}	1.95^{b}	21.2^{a}	1.61^{c}	16.7^{b}	33.7^{a}	5.66^{c}	2.00^{b}	16.3^{a}	2.67^{c}
White	*M.spicata*	25.8^{a}	63.7^{a}	10.4^{a}	4.93^{a}	29.3^{a}	1.61^{c}	21.0^{a}	25.1^{a}	9.66^{b}	2.00^{ab}	10.1^{b}	2.78^{bc}
	M.longifolia	15.8^{c}	30.4^{c}	4.25^{b}	1.53^{c}	9.35^{c}	1.74^{b}	13.9^{c}	18.8^{c}	19.6^{a}	1.45^{c}	8.09^{c}	2.85^{b}
	M.piperita	24.2^{ab}	49.7^{b}	10.2^{a}	2.51^{b}	49.7^{b}	1.88^{a}	19.6^{b}	24.2^{ab}	4.41^{c}	2.22^{a}	11.2^{a}	3.08^{a}
Fluorescent	*M.spicata*	22.1^{a}	24.4^{c}	1.75^{b}	1.67^{b}	24.4^{c}	—	18.1^{b}	24.4^{c}	6.33^{b}	1.80^{b}	7.68^{b}	—
	M.longifolia	16.9^{c}	33.1^{a}	2.41^{a}	2.62^{a}	33.1^{a}	—	15.4^{c}	33.1^{a}	10.6^{a}	2.87^{a}	11.8^{a}	—
	M.piperita	21.0^{ab}	29.0^{b}	1.95^{b}	1.03^{bc}	29.0^{b}	—	19.2^{a}	29.0^{b}	2.70^{c}	1.00^{c}	4.10^{c}	—

*means followed by different letters in each column in each plant are significantly different according to LSD test ($p<0.05$)

Table 8.2. Mean comparison of *Mentha* species and mycorrhizal genotypes under different light intensities on morphophenological characteristics and essential oil content.

Mentha species	150 µmol m^{-2} s^{-1}							500 µmol m^{-2} s^{-1}					
	Mycorrhiza species	Colonization (%)	Height (cm)	Branch number	Dry weight (g/plant)	Fresh weight (g/plant)	Essential oil content (%)	Colonization (%)	Height (cm)	Branch number	Dry weight (g/plant)	Fresh weight (g/plant)	Essential oil content (%)
M.spicata	*G.clarum*	18.2^{c}	44.7^{c}	12.5^{a}	2.33^{c}	14.0^{c}	1.50^{bc}	16.3^{c}	22.0^{b}	9.49^{a}	1.99^{b}	11.7^{b}	2.45^{b}
	G.etunicatum	55.5^{a}	55.7^{a}	2.53^{c}	4.61^{a}	27.5^{a}	1.62^{b}	40.9^{a}	27.4^{a}	9.26^{ab}	2.51^{a}	14.7^{a}	2.62^{a}
	G.mosseae	39.5^{b}	41.9^{d}	4.13^{b}	3.36^{b}	19.7^{b}	3.59^{a}	35.0^{b}	18.7^{c}	7.20^{c}	1.87^{b}	11.3^{b}	2.25^{c}
	Control	0.0^{d}	48.0^{b}	1.86^{d}	2.49^{c}	14.1^{c}	1.59^{b}	0.0^{d}	16.3^{d}	7.26^{c}	1.50^{bc}	10.9^{c}	2.69^{a}
M.longifolia	*G.clarum*	8.89^{c}	28.4^{bc}	6.86^{a}	1.10^{c}	6.12^{d}	1.75^{c}	8.10^{c}	24.5^{cd}	11.6^{b}	2.05^{ab}	11.2^{b}	2.77^{c}
	G.etunicatum	36.4^{a}	29.1^{b}	1.86^{c}	2.43^{a}	13.5^{a}	1.94^{b}	29.9^{a}	33.2^{a}	9.63^{c}	2.45^{a}	12.7^{a}	3.15^{b}
	G.mosseae	14.6^{b}	26.5^{c}	2.13^{b}	1.79^{b}	10.0^{b}	3.38^{a}	11.7^{b}	31.5^{ab}	11.4^{b}	1.43^{b}	10.7^{c}	5.41^{a}
	Control	0.0^{d}	31.0^{a}	1.26^{cd}	1.48^{bc}	7.74^{c}	1.67^{c}	0.0^{d}	26.7^{c}	14.2^{a}	1.31^{b}	11.7^{ab}	2.70^{c}
M.piperita	*G.clarum*	20.3^{b}	36.9^{c}	12.9^{a}	1.26^{bc}	7.14^{d}	1.87^{c}	20.0^{b}	28.4^{a}	3.86^{b}	1.37^{ab}	9.58^{bc}	2.98^{d}
	G.etunicatum	57.6^{a}	43.8^{ab}	2.80^{b}	2.34^{a}	14.1^{a}	1.89^{c}	53.2^{a}	25.7^{c}	4.66^{a}	1.96^{a}	11.9^{a}	3.11^{c}
	G.mosseae	8.91^{c}	45.8^{a}	2.40^{b}	2.05^{ab}	12.2^{b}	2.66^{a}	10.3^{c}	27.9^{ab}	3.66^{b}	1.50^{ab}	11.3^{ab}	4.28^{a}
	Control	0.0^{d}	42.2^{b}	1.63^{c}	1.45^{b}	8.43^{c}	2.36^{b}	0.0^{d}	27.6^{ab}	3.16^{c}	1.00^{b}	10.2^{b}	3.59^{b}

*means followed by different letters in each column in each plant are significantly different according to LSD test ($p<0.05$)

Table 8.3. Mean comparison of light (quality and quantity) and mycorrhizal genotypes on morphophenological characteristics and essential oil content.

Light quality		150 µmol m^{-2} s^{-1}						500 µmol m^{-2} s^{-1}					
	Mycorrhiza species	Colonization (%)	Height (cm)	Branch number	Dry weight (g/plant)	Fresh weight (g/plant)	Essential oil content (%)	Colonization (%)	Height (cm)	Branch number	Dry weight (g/plant)	Fresh weight (g/plant)	Essential oil content (%)
Blue	*G.clarum*	13.6^{c}	33.8^{d}	20.1^{a}	1.61^{c}	8.28^{c}	1.57^{d}	17.5^{c}	20.5^{bc}	7.11^{b}	2.65^{a}	12.6^{a}	2.58^{d}
	G.etunicatum	45.0^{a}	43.3^{b}	2.33^{b}	3.12^{a}	16.5^{a}	1.88^{b}	36.6^{a}	24.6^{ab}	4.33^{c}	1.81^{c}	9.75^{c}	3.13^{b}
	G.mosseae	35.0^{b}	38.4^{c}	1.11^{cd}	3.21^{a}	16.9^{a}	3.78^{a}	32.9^{b}	25.0^{a}	9.22^{a}	2.47^{ab}	11.6^{b}	5.81^{a}
	Control	0.0^{d}	48.7^{a}	1.66^{c}	2.61^{b}	13.8^{b}	1.63^{c}	0.0^{d}	19.6^{c}	7.0^{b}	2.70^{a}	12.5^{a}	2.68^{c}
Red	*G.clarum*	21.6^{c}	44.1^{b}	14.3^{a}	1.16^{b}	9.21^{b}	1.96^{cd}	20.6^{c}	22.6^{d}	6.88^{a}	2.00^{b}	12.8^{c}	3.00^{d}
	G.etunicatum	31.8^{a}	50.7^{a}	1.77^{c}	2.39^{a}	18.8^{a}	2.02^{c}	27.6^{a}	25.8^{c}	6.27^{a}	2.32^{b}	14.9^{b}	3.32^{c}
	G.mosseae	25.0^{b}	38.1^{c}	2.66^{b}	0.99^{c}	7.72^{b}	4.12^{a}	22.2^{b}	28.1^{b}	5.22^{b}	3.50^{a}	16.2^{a}	6.06^{a}
	Control	0.0^{d}	39.3^{c}	1.11^{cd}	0.82^{c}	6.63^{d}	2.29^{b}	0.0^{d}	31.6^{a}	3.11^{c}	0.98^{c}	8.03^{d}	3.41^{b}
Red+Blue	*G.clarum*	18.0^{c}	27.8^{d}	9.33^{a}	1.49^{c}	9.16^{c}	1.89^{b}	14.2^{b}	28.0^{b}	11.2^{b}	1.98^{b}	12.3^{c}	3.05^{b}
	G.etunicatum	54.8^{a}	42.2^{a}	3.77^{b}	3.84^{a}	23.6^{a}	1.78^{c}	48.3^{a}	34.4^{a}	13.1^{a}	2.98^{a}	18.9^{a}	2.80^{d}
	G.mosseae	20.8^{b}	39.3^{b}	3.77^{b}	2.69^{b}	16.6^{b}	2.71^{a}	13.0^{c}	26.4^{c}	4.55^{d}	2.07^{b}	12.3^{c}	4.29^{a}
	Control	0.0^{d}	37.4^{c}	1.55^{c}	1.52^{c}	9.44^{c}	1.82^{bc}	0.0^{d}	23.4^{d}	10.0^{c}	2.54^{ab}	17.3^{b}	2.93^{c}
White	*G.clarum*	7.75^{b}	46.1^{c}	24.5^{a}	2.12^{b}	13.0^{c}	1.40^{d}	9.28^{b}	21.9^{bc}	11.1^{bc}	1.97^{a}	10.0^{b}	2.30^{d}
	G.etunicatum	75.6^{a}	48.1^{b}	2.44^{c}	3.77^{a}	23.5^{a}	1.58^{c}	54.5^{a}	28.8^{a}	7.55^{c}	2.00^{a}	11.6^{a}	2.61^{c}
	G.mosseae	4.34^{c}	44.4^{d}	4.44^{b}	3.87^{a}	22.5^{c}	2.23^{a}	8.86^{b}	20.7^{b}	14.2^{a}	1.95^{a}	10.2^{b}	3.76^{a}
	Control	0.0^{d}	53.1^{a}	1.77^{d}	2.20^{b}	13.1^{c}	1.75^{b}	0.0^{d}	19.4^{c}	12.0^{b}	0.98^{b}	7.37^{c}	2.96^{b}
Fluorescent	*G.clarum*	18.1^{c}	31.7^{a}	2.22^{a}	1.43^{bc}	5.85^{c}	—	12.5^{c}	31.7^{a}	5.33^{b}	1.50^{c}	6.41^{c}	—
	G.etunicatum	41.9^{a}	30.1^{ab}	1.66^{b}	2.52^{a}	10.3^{a}	—	39.9^{a}	30.1^{ab}	8.0^{a}	2.70^{a}	10.3^{a}	—
	G.mosseae	20.0^{b}	29.9^{bc}	2.44^{a}	1.26^{c}	5.18^{c}	—	17.9^{b}	29.9^{b}	3.88^{c}	1.24^{d}	5.18^{d}	—
	Control	0.0^{d}	23.6^{c}	1.83^{b}	1.88^{b}	7.59^{b}	—	0.0^{d}	23.6^{c}	8.94^{a}	2.03^{b}	9.48^{b}	—

*means followed by different letters in each column in each plant are significantly different according to LSD test ($p<0.05$)

Table 8.4. Mean comparison of light quality and quantity, mint species and mycorrhizal genotypes on morphophenological characteristics and essential oil content.

		150 µmol m^{-2} s^{-1}						500 µmol m^{-2} s^{-1}					
		Colonization (%)	Height (cm)	Branch number	Dry weight (g/plant)	Fresh weight (g/plant)	Essential oil content (%)	Colonization (%)	Height (cm)	Branch number	Dry weight (g/plant)	Fresh weight (g/plant)	Essential oil content (%)
Genotype	*M.spicata*	28.3^{a}	47.6^{a}	7.76^{a}	3.20^{a}	18.8^{a}	2.07^{a}	23.1^{a}	21.1^{c}	8.30^{b}	2.20^{a}	12.2^{a}	3.25^{b}
	M.longifolia	21.7^{b}	42.2^{b}	4.94^{b}	1.77^{b}	10.5^{b}	2.19 ^{a}	20.9^{b}	27.4^{b}	3.84^{c}	2.20^{a}	10.7^{b}	3.51 ^{a}
	M.piperita	15.0^{c}	28.8^{c}	3.03^{c}	1.70^{b}	9.36^{c}	2.19 ^{a}	12.4^{c}	28.9^{a}	11.7^{a}	1.89^{b}	11.6^{a}	3.49 ^{a}
Light quality	Blue	23.4^{a}	41.0^{b}	6.30^{b}	2.64^{b}	13.9^{b}	2.22^{b}	23.4^{a}	22.5^{b}	6.91^{c}	2.40^{a}	11.6^{c}	3.55^{b}
	Red	19.6^{b}	43.0^{b}	4.97^{c}	1.34^{e}	10.6^{c}	2.60^{a}	19.6^{b}	27.0^{a}	5.37^{d}	2.20^{ab}	13.0^{b}	3.95^{a}
	Blue+Red	23.4^{a}	36.7^{c}	4.61^{c}	2.38^{c}	14.7^{b}	2.05^{c}	23.4^{a}	28.0^{a}	9.72^{b}	2.39^{a}	15.2^{a}	3.27^{c}
	White	21.9^{a}	47.9^{a}	8.30^{a}	2.99^{a}	18.0^{a}	1.74^{d}	21.9^{a}	22.7^{b}	11.2^{a}	1.72^{bc}	9.81^{d}	2.91^{d}
	Fluorescent	20.0^{b}	28.8^{d}	2.04^{d}	1.77^{d}	7.24^{d}	0.0^{e}	20.0^{b}	28.8^{a}	6.54^{cd}	1.86^{b}	7.85^{e}	0.0^{e}
Mycorrhiza	*G.clarum*	15.8^{c}	36.7^{d}	4.1^{a}	1.56^{d}	9.10^{d}	1.70^{b}	14.8^{c}	25.0^{bc}	8.33^{a}	2.02^{b}	10.8^{b}	2.73^{c}
	G.etunicatum	49.8^{a}	42.9^{a}	2.40^{c}	3.12^{a}	18.4^{a}	1.81^{b}	41.4^{a}	28.7^{a}	7.85^{ab}	2.36^{a}	13.1^{a}	2.96^{bc}
	G.mosseae	21.0^{b}	38.0^{c}	2.88^{b}	2.40^{b}	14.0^{b}	3.21^{a}	19.0^{b}	26.0^{b}	7.42^{b}	2.24^{ab}	11.1^{b}	4.98^{a}
	Control	0.0^{d}	40.4^{b}	1.58^{d}	1.81^{c}	10.1^{c}	1.87^{b}	0.0^{d}	23.5^{c}	8.21^{a}	1.84^{c}	10.9^{b}	3.0^{b}
	Mean	**21.7±3.2^{a}**	**39.5±1.8^{a}**	**4.41±1.0^{b}**	**2.22±0.1^{a}**	**12.9±1.1^{a}**	**1.97±0.2^{b}**	**18.8±2.7^{b}**	**25.8±0.8^{b}**	**7.95±0.6^{a}**	**2.11±0.1^{a}**	**11.5±0.5^{b}**	**3.13±0.3^{a}**

*means followed by different letters in each column in each plant are significantly different according to LSD test ($p<0.05$)

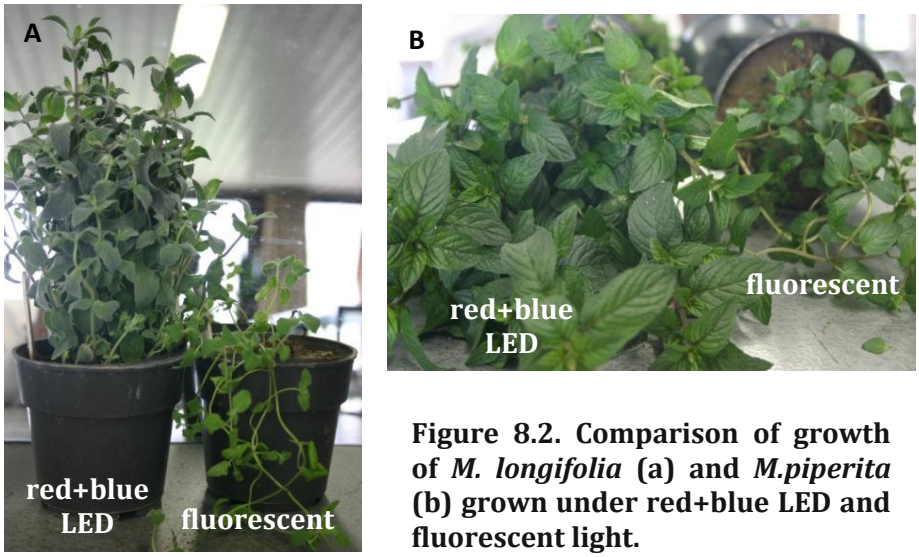

Figure 8.2. Comparison of growth of *M. longifolia* (a) and *M.piperita* (b) grown under red+blue LED and fluorescent light.

8.6 Acknowledgment

The authors are grateful to D.r. Morteza Zahedi, D.r. Mohammad Reza Sabzalian, Mr. Ehsan Ataii and Isfahan University of Technology (IUT) for their support.

8.7 References

Adolfsson L., Solymosi K., Andersson M.X., Keresztes Á., Uddling J., Schoefs B. & Spetea C. (2015). Mycorrhiza symbiosis increases the surface for sunlight capture in *Medicago truncatula* for better photosynthetic production. PLoS One 10: e0115314.

Augé R.M., Toler H.D. & Saxton A.M. (2015). Arbuscular mycorrhizal symbiosis alters stomatal conductance of host plants more under drought than under amply watered conditions: a metaanalysis. Mycorrhiza 25: 1324.

Avercheva O., Bykova E., Taranov E., Bassarskaya E., Zhigalova T. & Choob V. (2012). Growing with LED lighting of different spectral quality affects morphogenesis and production of lettuce plants. Proceedings of the VII-th international symposium on light in horticultural systems. Wageningen, the Netherlands. 109.

Bagheri S., Davazdahemami S. & Moghadam J.M. (2015). Variation in Growth Characteristics, Nutrient Uptake, and Essential Oil Content in Three Mycorrhizal Genotypes of *Mentha spicata* L. Int. J. Sci. Res. Knowledge 3: 067076.

Brunetti C., Guidi L., Sebastiani F. & Tattini M. (2015). Isoprenoids and phenylpropanoids are key components of the antioxidant defense system of plants facing severe excess light stress. Environ. Exper. Bot.

Copetta A., Lingua G. & Berta G. (2006). Effects of three AM fungi on growth, distribution of glandular hairs, and essential oil production in *Ocimum basilicum* L. var. Genovese. Mycorrhiza 16: 485–494.

Dayani S., Heydarizadeh P. & Sabzalian M.R. (2016). Efficiency of Light emitting diodes for the future photosynthesis. In Handbook of Plant and Crop Stress. Pessarakli M. (Ed.). (under Press).
del Rosario Cappellari L., Santoro M.V., Reinoso H., Travaglia C., Giordano W. & Banchio E. (2015). Anatomical, morphological, and phytochemical effects of inoculation with plant growthpromoting rhizobacteria on peppermint (Mentha piperita). J. chem. Ecol. 41: 149158.
Devi M.C. & Reddy M.N. **(**2002). Phenolic acid metabolism of groundnut (*Arachis hypogaea* L.) plants inoculated with VAM fungus and Rhizobium. Plant Growth Regul. 37: 151–156.
Ferguson J.J. & Menge J.A. (1982). The influence of light intensity and artifically extended photoperiod upon infection and sporulation of *Glomus fasciculatus* on sudan grass and on root exudation of sudan grass. New Phytol. 92: 183191.
Furlan V. & Fortin J.A. (1977). Effects of light intensity on the formation of vesiculararbuscular endomycorrhizas on *Allium cepa* by *Gigaspora calospora*. New Phytol. 79: 335340.
Girón González E. (2012). LEDs for general and horticultural lighting. AALTO University. School of Electrical Engineering.
Gupta M.L., Prasad A., Ram M. & Kumar S. (2002). Effect of the vesicular–arbuscular mycorrhizal (VAM) fungus Glomus fasciculatum on the essential oil yield related characters and nutrient acquisition in the crops of different cultivars of menthol mint (*Mentha arvensis*) under field conditions. Bioresour. Technol. 81: 77–79.
Hayman D.S. (1974). Plant growth responses to vesicular arbuscular mycorrhiz. New Phtol. 73: 7180.
Hayman D.S. (1983). The physiology of vesiculararbuscular endomycorrhizal symbiosis. Can. J. Bot. 61: 944963.
Hoagland D.R. & Arnon D.I. (1950). The water culture method for growing plants without soil. Calif. Agr. Expt. Sta. Circ. 347: 132.
Huché-Thélier L., Crespel L., Le Gourrierec J., Morel P., Sakr S. & Leduc N. (2016). Light signaling and plant responses to blue and UV radiations-Perspectives for applications in horticulture. Environ. Exp. Bot. 121: 22-38.
Ilieva I., Ivanova T., Naydenov Y., Dandolov I. & Stefanov D. (2010). Plant experiments with Light emitting diode module in Svet space greenhouse. Adv. Space Res. 46: 840845.
Johkan M., Shoji K., Goto F., Hahida S. & Yoshihara T. (2012). Effect of green light wavelength and intensity on photomorphogenesis and photosynthesis in *Lactuca sativa*. Environ. Exp. Bot. 75: 128133.
Karagiannidis N., Thomidis T., Lazari D., PanouFilotheou E. & Karagiannidou C. (2011). Effect of three Greek arbuscular mycorrhizal fungi in improving the growth, nutrient concentration, and production of essential oils of oregano and mint plants. Sci. Hort. 129: 329334.
Kaschuk G, Kuyper T.W., Leffelaar P.A., Hungria M. & Giller K.E. (2009). Are the rates of photosynthesis stimulated by the carbon sink strength of rhizobial and arbuscular mycorrhizal symbioses? Soil Biol. Biochem. 41: 1233–1244.
Khaosaad T., Vierheiling H., Nell M., ZitterlEglsser K. & Novak J. (2006). Arbuscular mycorrhiza alter the concentration of essential oils in oregano (Origanum sp., Lamiaceae). Mycorrhiza 16: 443–446.
Lee N.Y., Lee M.J., Kim Y.K., Park J.C., Park H.K., Choi J.S., Hyun J.N., Kim K.J., Park K.H. & Ko J.K. (2010). Effect of light emitting diode radiation on antioxidant activity of barley leaf. J. Korean Soc. Appl. Biol. Chem. 53: 685690.
Okamoto K., Yanagi T. & Kondo S. (1997). Growth and morphogenesis of lettuce seedlings raised under different combinations of red and blue light. Acta Horticult. 435: 149–157.
Ogawa E., Tonsho I., Watanabe H., OhashiKaneko K., Ono E., Amaki W. & Goto E. (2012). Changes of aromatic compound contents in perilla and rocket grown under various wavelengths of LED light conditions. Book of Abstracts, 7th International Symposium on Light in Horticultural Systems, ISHS Lightsym,Wageningen, Netherland.

Pinho P., Särkkä L., Tetri E., Tahvonen R. & Halonen L. (2007). Evaluation of lettuce growth under multispectralcomponent supplemental solid state lighting in greenhouse enviroment. Int. Rev. Elec. Eng. 2.

Ruiz-Lozano J.M., Aroca R., Zamarreño Á.M., Molina S., Andreo-Jiménez B., Porcel R., García-Mina J.M., Ruyter-Spira C. & López-Ráez J.A. (2015). Arbuscular mycorrhizal symbiosis induces strigolactone biosynthesis under drought and improves drought tolerance in lettuce and tomato. Plant cell environ.

Smith S.E. & Read D.J. (2008). Mycorrhizal symbiosis. Cambridge UK: Academic Press.

Smith F.A. & Smith S.E. (1996). Mutualism and parasitism: Diversity in function and structure in the arbuscular (VA) mycorrhizal symbiosis. Adv. Bot. Res. 22: 1–43.

Stutte G.W., Edney S. & Skerritt T. (2009). Photoregulation of bioprotectant content of red leaf lettuce with Light emitting diodes. HortScience. 44: 7982.

Suzuki K., Yasuba K. & Takaichi M. (2011). Effect of the supplemental lighting on the growth of young plants in second nursery in tomato. Acta Hort. 907: 269330.

Tamulaitis G., Duchovskis P., Bliznikas Z., Breive K., Ulinskaite R., Brazaityte A., Novičkovas A. & Žukauskas A. (2005). Highpower Light emitting diode based facility for plant cultivation. J. Phys. D Appl. Phys. 38: 3182.

Yadav K., Aggarwal A. & Singh N. (2013). Arbuscular mycorrhizal fungi induced acclimatization and growth enhancement of *Glycyrrhiza glabra* L.: A potential medicinal plant. Agric Res. 2: 4347.

Zeng Y., Gu L.P., Che D.B., Hao Z.P.,Wang J.Y., Huang L.Q., Yang G., Cui X.M., Yang L., Wu Z.X., Chen M.L. & Zhang Y. (2013). Arbuscular mycorrhizal symbiosys and active ingredients of medicinal plants: current research status and prospectives. Mycorrhiza 23: 253–265.

Zolfaghari M., Nazeri V., Sefidkon F. & Rejali F. (2013). Effect of arbuscular mycorrhizal fungi on plant growth and essential oil content and composition of *Ocimum basilicum* L. Iran. J. Plant Physiol. 3: 643650.

Conclusion of part 2

Regardless the climate and the place of harvesting, the mint accessions were moderately mycorrhized suggesting that the abiotic component of the environment had not a crucial influence on this process. This conclusion is important because it allows the extrapolation of our data to other accessions not studied here.

The study of monochromatic lights delivered by LEDs on growth and EO production in *Mentha* species revealed differential impact on the different accessions. Regardless light intensity, the highest EO production was obtained under red LED light while under this lighting condition, CO_2 fixation, and therefore growth, was similar to that obtained with white light or sunlight. Interestingly, red+blue lighting gave worse results in terms of EO production when compared to red light and dry weight when compared to sunlight while CO_2 fixation was the highest.

The study of the interactions between lighting conditions and mycorrhization on the different accessions, revealed that under low light intensity *M. spicata* had the highest growth regardless the light wavelengths but under high light the highest growth depended on the lighting wavelength for the *Mentha* accessions. Regarding the possibility to combine abiotic and biotic stress to enhance either growth or EO production, we found that *G. mosseae* was the only mycorrhizal genotype triggering an increase of EO production (compared to nonmycorrhizal plants), and this independantly of the light intensity. However, light intensity appears as an important factor in the control of EO production. Indeed, we found that high light increased EO production in *Mentha* accessions more than low light. This result suggests that the additional photons 'inform' the plants about the need to increase EO production through a mechanism that remains so far elusive. We can however hypothesize that red light triggers a carbon reorientation probably through *de novo* expression of genes involved in the carbon metabolism. We have seen in part one that many of the enzymes involved in this metabolism are coded by isogenes, for which expression was dependant of environmental factors. Alternatively, red light could enhance expression of genes encoding key enzymes of the terpenoid pathway, thus enhancing the flux of carbon into this pathway. Another possibility would reside in a direct activation of already present enzymes by red light. Altogether, our results demonstrate that the interaction between biotic and abiotic environmental factors may strongly impacts growth and development of plants.

Chapter

9

General conclusion and perspective

In this sudy, the main aim was to investigate the effects of different lighting or illumination conditions (including quality and quantity) on the reorientation of the carbon metabolism toward the production of secondary metabolites in unicellular and multicellular organisms. Accordingly, we set up two main experiments on diatom (*P. tricornutum*) and land plant (*Mentha* sp.). In diatom we used molecular, biochemical and physiological approaches to obtain new information on the studied processes in *P. tricornutum* cells grown under different fluorescent intensities. In land plants, morphological, biochemical and physiological approaches have been used to characterize the impact of AM and/or monochromatic and polychromatic lights delivered by LED on growth, development and EO production of different *Mentha* species, originally collected in the natural environment in Iran.

Our results showed that the impact of different light intensities on cell development, physiology and gene regulation of *P. tricornutum* depends on growth phases *i.e*. the cell physiological state. Low photon abundance was a limiting factor for growth, and in all light conditions C-deficiency was mostly responsible for the occurrence of plateau phase in the cultures.

Because cell physiology is affected by growth conditions, all the measurements performed in the same physiological states. This allowed us to conclude that the obtained results are just related to the impact of light and are mostly independent of the physiological states of cells. Accordingly, physiological and molecular data showed that the effects of ML and HL on diatom cells were similar but quite different from LL. One of the main results of this study was the orientation of carbon mostly toward pyruvate formation and in some cases (mostly in HL phase 3) to PEP formation. In this study pyruvate was highlighted as a hub intermediate that is used to synthesis high value molecules including lipids and proteins. Lipid production was higher under LL phase 1 but in phase 2 and 3 the relative amount of chrysolaminarin was higher compare to ML and HL. Lipid production increases under ML in phase 2 and 3, while protein amount was higher under HL compare to LL and ML.

PEP is also an important intermediate to form aromatic compounds, including amino acids *via* the shikimate pathway. This pathway was activated mostly under HL phase 3, compare to ML. It is difficult to firmly conclude and interpret this result without a quantification of aromatic compouds. The measurement of the products of this pathway

may help us to find better correlation between enzyme activity and aromatic amino acids synthesis.

We suggest to continue the study of *P. tricornutum* by: (1) using bioreactor technology to avoid controlling the CO_2 limitation and study more deeply molecular biology and biochemistry of diatom cells in the same physiological state under stress conditions (2) focusing more deeply on fatty acid biosynthesis and chrysolaminarin pathways using a more global approach of the gene/isogenes of different enzymes to understand better the compensation of target genes toward desired products, (3) qualify lipid classes in cells grown under the three light conditios to estimate the percentage of saturated and unsaturated fatty acids. This type of information is of importance in the frame of algal biotechnology because the type of lipid production would condition the type of usage of the produced lipids (biofuels, nutrition, cosmetic *etc*), (4) visualize the intracellular lipid bodies and also cell size in different growth phases to determine if the increase in lipid synthesis could be correlated to the cell size, the size and/or number of lipid bodies, (5) measurement of terpenoid content of diatom cells to conclude better the activation of shikimate pathway with the results of gene expression of related enzymes and (6) growing diatom cells under different LED wavelengths and intensities to compare the results with what we obtained using fluorescent light and with other organisms such as land plants.

The results of the effect of various LED lights on plants productivity revealed that red+blue and red LED illuminations stimulated vegetative growth and essential oil production, respectively, more than the other light tested. Plant growth under fluorescent light remained weak without producing detectable essential oil. We concluded that LED could improve economic characteristics of *Mentha* species through metabolic stimulation(s).

In our culture conditions, mycorrhization changed the reaction of plants to different LED wavelenghts. These changes were also depending on the light intensities (150 or 500 µmol m^{-2} s^{-1}). Interestingly, under these two light intensities, red light (650–665 nm) was the most effective to stimulate essential oil synthesis in mycorrhizal plants. The reactions of mycorrhizal plants differed under two light intensities in term of vegetative growth. Under 150 µmol m^{-2} s^{-1} white LED and under 500 µmol m^{-2} s^{-1} red and red+blue LED were the most affective lights to estimulate plant vegetative growth. Indeed, plants vegetative growth was higher under 150 µmol m^{-2} s^{-1} while EO synthesis increased under 500 µmol m^{-2} s^{-1}, showing that light intensity also triggers the reorientation of the carbon metabolism toward the production of secondary metabolites in mint, clealry, blue and red photoreceptors seemed involved. At present it is however difficult to conclude further on their nature and their involvement in the light intensity control on the reorientation. This is essentially due to the fact that the effects of both light quality and quantity look species dependent and that there are nowhere elese reports on mint (see also Huchier-Thélier et al. 2016).

In this study, *G. mosseae* stimulated EO content, and red LED stimulated mycorrhizal colonization more than the other lights. We conclude that in this experiment red LED

was the most stressful condition for *Mentha* species, because of the most essential oil synthesis and most AMF colonization under this light.

Some questions required to be answered to understand the role of light quality and quantity on EO production: (1) is increasing the EO related to increase of primary metabolites synthesis followed by more pomping of glucose inside secretory cells of PGT? (2) is the expression of genes/isogenes in MEP pathways of secretory cells related to the light quality and/or quantity or their expression is independent of light? (3) what is the relation between light quality or quantity with isoprenoid pathway activation? and (4) what are the photoreceptor(s) involved and in case of several how do they cooperate?

Further steps for answering these questions could be (1) a study of monoterpenoid pathway inside trichomes at the level of enzymes, from MEP pathway to EO synthesis. (2) focus on the most effective and the less effective lights to see the changes in gene expression of the pathways. In this respect red LED and fluorescent can be the first candidates, because of their most and less stimulation effects, respectively, on EO synthesis. (3) the same studies at the level of enzymes on inoculated plants with *G. mosseae* to understand if the fungus affects the expression of genes encoding key enzymes in monoterpenoid pathway or they have indirect effects, such as supporting the plant for more primary production by different ways including exploratory capacity for mineral nutrients or increasing the level of phytohormons such as abscisic acid, auxins, gibberellins, cytokinins, *etc*, (4) test the activity of phytochrome and blue-light receptors using reduced adequate irradiations and (5) analysis of EO components to see which wavelength can estimulate production of oil with better quality.

To summarize all, in this study we handled two very different organisms - a unicellular diatom and a multicellular land plant - and studied how light was regulating the reorientation of the carbon metabolism toward the production of secondary metabolites. For technical reasons, lack of enough scientific data and time constrains, it was not possible to study each model with similar tools and details. Nevertheless, one main conclusion of this study is that the metabolism of both models is arranged and reorganized under stress conditions in such a way that pyruvate, a platform molecule serving for the synthesis of secondary metabolites such as terpenoids and lipids. This conclusion seems to be a general feature in microalgae because accumulation of terpenoids was found in other types of algae (*e.g.*, green algae: Tocquin et al. 2012; Kopecky et al. 2000; haptophytes: Bougaran et al. 2012; Guihéneuf et al. 2015; red algae: Khotimchenko & Yakovleva, 2005) but surely should also be modulated because mint taxons are very sensitive to lighting modifications and seem not able to react to light stress (*e.g.*, Kopecky et al. 2000). During this work we obtained elements suggesting that the metabolism of *P. tricornutum* might be flexible as we could observe over-expression of gene leading to the production of aromatic compounds. Such flexibility seems to have been lost in land plants.

Another finding of this work is that the pathway activated would partly depend on the physiological state of the cell. This probably is also the case for the secretory cells of

PGT and their production is also modulated by the environmental conditions: light quality and mycorrhizal fungus. The impact of these factors on marine microalgae is only started and already similar features can be found. For instance, in the *Isochrysis,* blue light irradiation, combined to change in the dilution ratio increased the production of lipids (Marchetti et al. 2013). A careful check of the references indicates that the effects of monochromatic light on microalgae are species dependent (Darko et al. 2014). Beside the well known fungus-microalga symbiosis forming aerian lichens, for which the association seemed obligatory, the only reported optional symbiosis between an eukaryotic microalga (Chlamydomonas) and a fungus (Alternaria) is artificial and requires the presence of a bacterium (Azotobacter) (Lőrincz et al. 2010). In this association, the chlorophyll quota is higher than in the control cultures and a reduced excretion of amino acids. The increase of chlorophyll quota was also frequently reported when land plants are colonized by mycorrhizal fungus (Valentine et al. 2001; Rai et al. 2008). Unfortunately, no additional studies; for instance including light effects, have been conducted so far. Altogether, the results and the reasoning presented here suggest the existence of a unity in the response to light quality and quantity in photosynthetic organisms.

References

Bougaran G., Rouxel C., Dubois N., Kaas R., Grouas S., Lukomska E., Coz J.R.L. & Cadoret J.P. (2012). Enhancement of neutral lipid productivity in the microalga *Isochrysis* affinis *Galbana* (T-Iso) by a mutation-selection procedure. Biotechnol. Bioeng. 109: 2737-2745.

Darko E., Heydarizadeh P., Schoefs B. & Sabzalian M.R. (2014). Photosynthesis under artificial light: the shift in primary and secondary metabolism. Phil. Trans. R. Soc. B. 20130243.

Guihéneuf F., Mimouni V., Tremblin G. & Ulmann L. (2015). Light intensity regulates LC-PUFA incorporation into lipids of Pavlova lutheri and the final desaturase and elongase activities involved in their biosynthesis. J. Agr. Food Chem. 63: 1261-1267.

Huché-Thélier L., Crespel L., Le Gourrierec J., Morel P., Sakr S. & Leduc N. (2016). Light signaling and plant responses to blue and UV radiations—Perspectives for applications in horticulture. Environ. Exp. Bot. 121: 22-38.

Kopecky J., Schoefs B., Loest K., Stys D. & Pulz O. (2000). Microalgae as a source for secondary carotenoid production: a screening study. Arch. Hydrobiol. Suppl. Algol. Stud. 133: 153-168.

Khotimchenko S.V. & Yakovleva I.M. (2005). Lipid composition of the red alga Tichocarpus crinitus exposed to different levels of photon irradiance. Phytochem. 66: 73-79.

Marchetti J., Bougaran G., Jauffrais T., Lefebvre S., Rouxel C., SaintJean B., Lukomska E., Robert R. & Cadoret J.P. (2013). Effects of blue light on the biochemical composition and photosynthetic activity of *Isochrysis* sp.(Tiso). J. Appl. Phycol. 25: 109119.

Lőrincz Z., Preininger É., Kósa A., Pónyi T., Nyitrai P., Sarkadi L., Kovács G.M., Böddi B., & Gyurján I. (2010). Artificial tripartite symbiosis involving a green alga (Chlamydomonas), a bacterium (Azotobacter) and a fungus (Alternaria): morphological and physiological characterization. Folia Microbiol. 55: 393-400.

Rai M.K., Shende S. & Strasser R.J. (2008). JIP test for fast fluorescence transients as a rapid and sensitive technique in assessing the effectiveness of arbuscular mycorrhizal fungi in *Zea mays*: Analysis of chlorophyll *a* fluorescence. Plant Biosyst. 142: 191–198.

Tocquin P., Fratamico A. & Franck F. (2012). Screening for a low-cost *Haematococcus pluvialis* medium reveals an unexpected impact of a low N/P ratio on vegetative growth. J. Appl. Phycol. 24 : 365-373.

Valentine A.J., Osborne B.A. & Mitchell D.T. (2001). Interactions between phosphorus supply and total nutrient availability on mycorrhizal colonization, growth and photosynthesis of cucumber. Sci. Hortic. 88: 177–189.

Thèse de Doctorat

Parisa HEYDARIZADEH

Régulation de la synthèse des composés secondaires par les organismes photosynthétiques en condition de stress

Regulation of the synthesis of secondary compounds by photosynthetic organisms in response to stress

Résumé

En condition de stress, les organismes photosynthétiques réorientent leur métabolisme vers la production de métabolites d'intérêt. Cette thèse vise à fournir de nouvelles informations sur ces processus chez les algues et les plantes supérieures.

La 1ère partie est consacrée aux effets de 3 éclairements différents sur le métabolisme du carbone de la diatomée *Phaeodactylum tricornutum*. L'impact d'un éclairement supérieur à 300 µmol photons m^{-2} s^{-1} (ML) est tout à fait différent de celui obtenu pour un éclairement de 30 µmol photons m^{-2} s^{-1} tant au niveau physiologique que moléculaire. Dans nos conditions, la carence en carbone constitue la cause principale de l'apparition de la phase stationnaire. La synthèse des lipides est plus élevée sous un éclairement inférieur à ML. En revanche, la synthèse des protéines et de chrysolaminarine augmente respectivement sous fort et faible éclairements. Les changements d'expression génique suggèrent que la conversion réversible du phospho*énol*-pyruvate en pyruvate constitue une étape clé de l'orientation des intermédiaires dans les différentes voies de biosynthèse des molécules d'intérêt. L'état physiologique des cellules doit être considéré pour la comparaison d'échantillons.

La 2ème partie du mémoire est consacrée aux effets de la quantité et de la qualité de la lumière délivrée par des LED (bleu, rouge, 70% de lumière rouge+30% de bleu et blanc) sur la régulation de la synthèse de métabolites secondaires chez 3 espèces de menthe prélevées dans la nature. La qualité de la lumière influence la stratégie d'utilisation du carbone par les plantes. Par exemple, la lumière rouge stimule le mieux la production de la synthèse de l'huile essentielle chez la menthe alors que le taux de fixation du carbone est similaire à celui trouvé dans les autres conditions d'illumination. *Glomus mossae* est le seul champignon mycorhizien à arbuscules à induire une augmentation supplémentaire de la production d'huile essentielle.

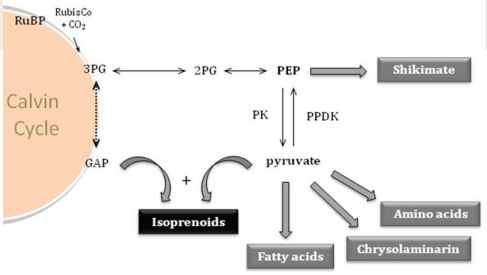

Abstract

Under stress, photosynthetic organisms reoriente their metabolism toward the production of high added value molecules. Regarding the importance of this process, it is surprising that the processes on which the reorientation relies are still not better understood. This thesis aims to provide new information regarding these processes. The 1st part of this thesis is dedicated to the effects of 3 different light intensities on the carbon metabolism of the diatom *Phaeodactylum tricornutum*. The impact of light intensities higher than 300 µmol photons m^{-2} s^{-1} (ML) were different from those obtained with 30 µmol photons m^{-2} s^{-1} at the physiological and molecular levels. Carbon deficiency was responsible for the occurrence of plateau phase in cultures. Except lag phase, lipid synthesis was higher under ML In contrast, protein and chrysolaminarin syntheses increased under 1000 and 30 µmol photons m^{-2} s^{-1}, respectively. Gene expression modifications suggest that the reversible conversion between phospho*enol*pyruvate and pyruvate constitutes a key step for the orientation of intermediates to either high value molecules biosynthetic pathways. The physiological state of the cells should be taken into consideration when samples comparison is considered.

The 2nd part of the report is dedicated to the effects of light quantity and quality (blue, red, 70% red+30% blue and white light delivered by LED) on the regulation of essential oil synthesis in 3 *Mentha* species collected in nature. The light quality impacts the strategy of carbon utilization by the plant. Typically, red light was the most effective for stimulating the production of essential oil in *Mentha* sp. while carbon fixation capacity was similar to that found in other ligthing conditions. Regardless the light intensity, *Glomus mossae* was the only arbuscular mycorrhizal fungus able to enhance additionally essential oil production

Key Words

***Phaeodactylum*, *Mentha*, light intensity, LED, secondary metabolism, transcriptomics**

Mots clés

***Phaeodactylum*, *Mentha*, intensité de l'éclairement, LED, métabolisme secondaire, transcriptomique**